JOHANN WOLFGANG GOETHE
UNIVERSITÄT
FRANKFURT AM MAIN

Humanized mice as preclinical model for HIV infections

Dissertation
zur Erlangung des Doktorgrades
der Naturwissenschaften

vorgelegt beim Fachbereich Biochemie, Chemie und Pharmazie
der Johann Wolfgang Goethe - Universität
in Frankfurt am Main

von
Sarah Manon Büchner
aus Schwedt/Oder

Frankfurt am Main 2014
(D30)

Vom Fachbereich Biochemie, Chemie und Pharmazie (14) der Johann Wolfgang Goethe - Universität als Dissertation angenommen.

Dekan: _____

Gutachter: _____

Datum der Disputation: _____

Eidesstattliche Erklärung

Hiermit erkläre ich, dass ich die vorliegende Arbeit: „*Humanized mice as preclinical model for HIV infections*“ selbständig verfasst habe und keine anderen als die angegebenen Quellen und Hilfsmittel verwendet wurden.

Frankfurt, den 25.02.2014 _____

Sarah Büchner

Teile dieser Arbeit sind bereits in internationalen Fachzeitschriften veröffentlicht worden.

Büchner SM, **Sliva K**, **Bonig H**, **Völker I**, **Waibler Z**, **Kirberg J**, **Schnierle BS**. Delayed onset of graft-versus-host disease in immunodeficient human leucocyte antigen-DQ8 transgenic, murine major histocompatibility complex class II-deficient mice repopulated by human peripheral blood mononuclear cells.
Clin Exp Immunol. 2013 Aug; 173(2):355-64. doi: 10.1111/cei.12121

Table of contents

Zusammenfassung

Das Humane Immundefizienz Virus (HIV) ist ein Virus, welches zur Familie der Retroviren und zur Gattung der Lentiviren gehört. Es wurde 1983 von Luc Montagnier und Françoise Barré-Sinoussi vom Institut Pasteur in Paris als Erreger der erworbenen Immunschwäche (*acquired immunodeficiency syndrom*, AIDS) identifiziert. Bisher sind zwei verschiedene Arten von HI-Viren bekannt, die als HIV-1 und HIV-2 bezeichnet werden und dieselben Übertragungswege sowie Krankheitssymptome aufzeigen. Während HIV-1 das am weitesten in der Welt verbreitetste Virus ist, beschränkt sich die Ausbreitung von HIV-2 bislang nur auf die Region Westafrika.
HIV infiziert ausschließlich humane Zellen wie z.B. T-Zellen, Dendritische Zellen oder Makrophagen, welche den CD4-Rezeptor auf der Oberfläche tragen. Durch die Bindung des HIV-Glykoproteins gp120 an den CD4-Rezeptor humaner Zellen wird der Eintritt des Virus in die Wirtzelle vorbereitet. Neben den CD4-Rezeptoren sind die Chemokin-Rezeptoren CXCR4 (hauptsächlich auf T-Zellen) und CCR5 (hauptsächlich auf Monozyten) am Eintrittsprozess beteiligt. HI - Viren, welche CD4 Zellen ausschließlich über CXCR4 infizieren bezeichnet man als X4-trophe Viren. Als R5-trophe Viren werden solche bezeichnet, die CD4-Zellen ausschließlich über CCR5 infizieren. X4R5 Mischformen sind möglich. Die unterschiedliche Ausprägung dieser Rezeptoren beeinflusst die Übertragungswahrscheinlichkeit und den Verlauf der HIV-Infektion.

Die präklinische Entwicklung und das Testen von neuen Medikamenten oder Impfstoffen gegen HIV sind mit besonderen Schwierigkeiten verbunden. Vor allem ist dies dem Fehlen von geeigneten Tiermodellen geschuldet, mit welchen eine HIV-Infektion im Menschen simuliert werden kann. Sehr aufwendige Infektionsstudien wurden bislang in Affen gemacht, jedoch können deren Ergebnisse nur bedingt auf den Menschen übertragen werden. Ebenfalls genutzt wurden genmodifizierte Mäuse, welche den humanen CD4-Rezeptor bzw. Korezeptoren sowie das HIV-Genom exprimieren, aber diese Modelle waren aufgrund ihrer unvollständigen HIV Replikation für die Forschung nicht nutzbar. Im Gegensatz dazu stellt die

Entwicklung von „humanisierten Mäusen“ ein kleines Tiermodell dar, welches sich bereits in der HIV Forschung bewährt hat.

Historisch gesehen war die *scid* Maus der erste Mausstamm, der für die Etablierung von humanisierten Mäusen genutzt wurde. In der *scid* Maus führt eine autosomal rezessive Mutation des Gens, welches für die V(D)J Rekombination verantwortlich ist, zu unreifen B- und T-Zellen und somit zu einer schweren Störung des murinen Immunsystems (*severe combined immunodeficiency*; SCID). *Scid* Mäuse wurden in vielfältigen Ansätzen genutzt, um humanisierte Mäuse für die HIV-Forschung herzustellen. Zur Herstellung der *scid-hu-Thy/Liv* Maus wurden kleine Stücke von fötaler humaner Leber (Liv) und Thymus (Thy) unter die Nierenkapsel der Maus transplantiert, um somit humane Organe in der Maus bereit zustellen in denen die humane Hämatopoese ablaufen kann. Diese Mäuse konnten mit HIV infiziert werden, jedoch nur durch unmittelbare Infektion in die Organoide, wodurch das HIV-Reservoir ausschließlich auf die Organoide beschränkt war. Dieses Modell wurde später weiterentwickelt und findet heutzutage als *BLT-Mausmodell* sehr breite Anwendung. Eine weitere Anwendung der *scid* Maus lag in der Übertragung von humanen hämatopoetischen Stammzellen (huHSC) oder humanen mononukleären Zellen des peripheren Blutes (huPBMCs), welche jedoch nur schlecht in dem *scid* Mausmodell überleben konnten.
Ein Durchbruch wurde mit der NOD *scid* Maus erzielt. *Scid* Mäuse wurden mit *non-obese diabetes* (NOD) Mäusen gekreuzt, was zu einer Erhöhung der Immundefizienz führte. Nicht nur T- und B-Zellen waren betroffen, sondern auch das angeborene Immunsystem, sowie die Komplementkaskarde. Durch die zusätzliche Gendeletion der γ-Kette des Interleukin-2 Rezeptors (IL2Rcγ; CD132) konnte zudem die Aktivität der murinen NK-Zellen unterbunden werden.
Neben der NOD *scid* IL2Rc$\gamma^{-/-}$ (NSG) Maus, ist die NOD Rag2$^{-/-}$IL2Rc$\gamma^{-/-}$ (NRG) eine phänotypisch ähnliche Maus, welche radioresistenter ist und statt des mutierten *scid*-Gens kein *recombination-activation*-Gen (*rag*) mehr trägt. Dieses Gen ist ebenfalls für die V(D)J Rekombination von T- und B-Zellen zuständig. NSG und NRG Mäuse werden heute vielfach für die Herstellung humanisierter Mäuse genutzt, da sie humane Zellen/Organteile sehr gut tolerieren und einen hohen Grad an Humanisierung erlauben.

Für die Impfstoffentwicklung ist es notwendig, dass das humanisierte Mausmodell über ein humanes Immunsystem verfügt, welches funktionstüchtige sowie zelluläre und humorale Immunantworten unterstützt. Um dies zu erreichen, wurden in dieser Arbeit neue immundefiziente Mausstämme (NOD Rag1$^{-/-}$ γc$^{-/-}$; NRG oder NOD scid$^{-/-}$ γc$^{-/-}$; NSG) benutzt, bei welchen das murine *major histocompatibility complex* Klasse II (MHC II) Molekül (A$\beta^{-/-}$) durch eine Gendeletion nicht mehr exprimiert wird. Stattdessen wird das humane DQ8 MHC II Molekül (huDQ8tg) in der Maus exprimiert. In diesem Mausmodell interagiert das huDQ8tg in der Maus mit dem T-Zellrezeptor von humanen Spenderzellen, um so die Funktionalität von humanen T-Helferzellen in der Maus zu unterstützen und zu verbessern.

In dieser Arbeit wurde die Humanisierung von NRG A$\beta^{-/-}$DQ8tg Mäusen mit humanen mononukleären Zellen des peripheren Blutes (huDQ8-PBMCs) und humanen hämatopoetischen Stammzellen (huDQ8-HSCs), positiv für huDQ8, untersucht.

Zu Beginn der Arbeit wurden freiwillige Blutspender genotypisiert, um HLA-DQ8 positive (DQ8^{+}) Spender zu ermitteln. 75 Blutspender wurden untersucht und 7 davon als DQ8^{+} ermittelt. Die Häufigkeit von DQ8^{+} Spendern liegt deutschlandweit bei ~17.3 %, wohingegen es nur ~9.3 % aller untersuchten Spender in dieser Arbeit waren. Die PBMCs dieser DQ8^{+} Spender wurden für die Humanisierung von NRG A$\beta^{-/-}$ DQ8tg und NRG Mäusen genutzt.

Das Übertragen von huPBMCs in immundefiziente Mäuse resultiert normalerweise in einer Abstoßungsreaktion der humanen Zellen (*graft-versus-host-disease*; GvHD), was schnell zum Tod der transplantierten Mäuse führt. In dieser Arbeit konnte hingegen gezeigt werden, dass NRG A$\beta^{-/-}$ DQ8tg Mäuse, welche mit huDQ8-PBMCs humanisiert waren, signifikant länger leben und zudem eine geringere Neigung zu Abstoßungsreaktionen aufweisen als NRG Mäuse ohne huDQ8tg. Ebenfalls untersucht wurde der intermediäre Mausstamm NRG A$\beta^{-/-}$, welcher weder das murine MHC II, noch das humane MHC II exprimiert. Die untersuchten Eigenschaften von NRG A$\beta^{-/-}$ lagen stets zwischen denen von NRG und NRG A$\beta^{-/-}$DQ8tg Mäusen.
Des Weiteren zeigten NRG A$\beta^{-/-}$ DQ8tg Mäuse eine höhere Repopulation von humanen Zellen im Blut. Allerdings repopulierten, unabhängig von der Expression des huDQ8tg, ausschließlich humane T-Zellen in den Mäusen.

Nach dem Transfer von huDQ8-PBMCs expandierten die zytotoxischen huCD8 T-Zellen in NRG und NRG $A\beta^{-/-}$Mäusen sehr stark, wohingegen sie in NRG $A\beta^{-/-}$DQ8tg Mäusen nur leicht expandierten. Zusätzlich wurden in Organen wie Leber, Niere, Darm und Haut von NRG und NRG $A\beta^{-/-}$Mäusen vermehrt huCD8 T-Zellen nachgewiesen, jedoch nur sehr wenige in NRG $A\beta^{-/-}$ DQ8tg Mäusen. Dies demonstrierte fortgeschrittene Abstoßungsreaktionen in NRG und NRG $A\beta^{-/-}$ Mäusen. Die Ursache für die verzögerte Entwicklung der Abstoßungsreaktion in NRG $A\beta^{-/-}$ DQ8tg Mäusen scheint bei den xenoreaktiven huCD8 T-Zellen zu liegen, welche in NRG $A\beta^{-/-}$ DQ8tg Mäusen weniger aktiviert zu sein scheinen als in NRG oder NRG $A\beta^{-/-}$ Mäusen. Wie gezeigt werden konnte, liegt der zugrundeliegende Mechanismus jedoch nicht in unterschiedlicher Zytokinexpression der Mäuse begründet, sondern eher in $DQ8^{+}$ regulatorischen T-Zellen, welche zu Beginn die Abstoßungsreaktion unter Kontrolle halten.

Entgegen der Erwartungen, förderte die Expression des huDQ8tg nicht das Überleben von B Zellen in der Maus. Darüber hinaus wurde die Repopulation von humanen B Zellen in der Maus durch Gabe des B-Zell Überlebensfaktors huBLyS untersucht. Dies blieb jedoch erfolglos, so dass es unmöglich war humorale Immunantworten in huDQ8-PBMC repopulierten NRG $A\beta^{-/-}$ DQ8tg Mäusen zu untersuchen.

Humanisierte NRG $A\beta^{-/-}$ DQ8tg Mäuse wurden schließlich mit HIV-1 und HIV-2 infiziert, wobei sich Ähnlichkeiten zur Infektion im Menschen zeigten. Die HIV-1 Infektion in der Maus zeigte einen sehr aggressiven Anstieg des viralen Titers im Plasma, wohingegen nur ein mäßiger Anstieg des viralen Titers bei der HIV-2 Infektion nachgewiesen werden konnte. Da sich jedoch keine neuen humanen T-Zellen aus humanen Stammzellen bilden können, ging der virale Titer im Serum wie auch in Lymphknoten und der Milz zurück.

Hiermit wurde gezeigt, dass humanisierte huDQ8tg Mäuse ein einzigartiges und sehr wertvolles Modell für die HIV Forschung darstellen. Die Humanisierung mit huDQ8-PBMCs in huDQ8tg Mäusen ist einfach durchzuführen und leicht nutzbar für kurzweilige Experimente wie das Testen von antiviralen Stoffen.

Um Abstoßungsreaktionen zu verhindern, wurden ebenfalls Humanisierungen mit humanen hämatopoetischen Stammzellen (huHSCs) durchgeführt. Im Vergleich zu Mäusen repopuliert mit huDQ8-PBMC, differenzierten in NRG A$\beta^{-/-}$DQ8tg Mäusen, welche als Neugeborene mit humanen DQ8 positiven hämatopoetischen Stammzellen (huDQ8-HSCs) rekonstituiert wurden, verschiedene humane Immunzellen (T-Zellen, B-Zellen, Monozyten, NK-Zellen) aus. Humanisierte Tiere hatten eine normale Lebenserwartung und es traten keine GvHD Reaktionen auf.

In dieser Arbeit wurde die Humanisierung von Jungtieren mit huDQ8-HSCs aus dem Nabelschnurblut sowie von mit dem *granulocyte colony-stimulating factor* (G-CSF) mobilisierten adulten Spendern untersucht. Durch die heterozygote Züchtung des NRG A$\beta^{-/-}$ DQ8tg Mausstammes im Hinblick auf das DQ8tg, waren nur etwa die Hälfte aller Nachkommen transgen für huDQ8. Die mit huDQ8-HSCs rekonstituierten NRG A$\beta^{-/-}$ Tiere wurden somit als Vergleichsgruppe für die NRG A$\beta^{-/-}$ DQ8tg Tieren aus demselben Wurf herangezogen.

Bei beiden Humanisierungen waren die Rekonstitutionsraten und -kinetiken ähnlich, jedoch war es nicht möglich adulte Mäuse mit mobilisierten hDQ8-HSCs zu rekonstituieren. Im Alter von etwa 5 Wochen nach Rekonstitution konnten bereits humane Zellen im Blut der Mäuse nachgewiesen werden, wobei B1-B-Zellen, neben Monozyten und NK-Zellen, die größte Population darstellten. Humane T-Zellen entwickelten sich später und nach etwa 10 Wochen konnten diese im Blut nachgewiesen werden. Zu Beginn bestand die T-Zellpopulation ausschließlich aus huCD4-T-Zellen, jedoch bildeten sich in den nachfolgenden Wochen auch huCD8 Zellen, sodass nach etwa 14 Wochen ein gleichmäßiges Verhältnis an huCD4- und huCD8-T-Zellen vorlag. Ab etwa 20 Wochen nach Rekonstitution verringerte sich der Anteil aller humanen Zellen im Blut. Diese Entwicklungskinetik konnte bei verschiedenen Stammzellspendern beobachtet werden, auch wenn es bei einzelnen NRG A$\beta^{-/-}$ oder NRG A$\beta^{-/-}$ DQ8tg Mäusen zu Abweichungen kam.
Unterschiede in der Humanisierungsrate von NRG A$\beta^{-/-}$ oder NRG A$\beta^{-/-}$ DQ8tg Mäusen wurden nicht festgestellt. Das huDQ8tg in Mäusen stellte für die Humanisierung keinen Vorteil dar, jedoch wurde angenommen, dass das huDQ8tg die Reifung humaner T-Zellen im Mausthymus fördert und somit deren Immunantworten verbessert.

In einem *ex vivo* Ansatz wurden humanen T Zellen mit PMA/Ionomycin stimuliert und deren Interferon gamma (IFNγ) Expression untersucht. Es konnte gezeigt werden, dass huCD4 und huCD8 T-Zellen in NRG Aβ$^{-/-}$ sowohl als auch in NRG Aβ$^{-/-}$ DQ8tg Mäusen fähig waren auf diesen Stimulus IFNγ zu sekretieren, was deren Funktionalität zeigte. Ebenfalls konnte nach Impfung der humanisierten Mäuse mit einem T-Zell-abhängigem Impfstoff, basierend auf dem Tetanus Toxoid, spezifische humane IgM und IgG Antikörper im Serum nachgewiesen werden. Die Bedeutung des humanen MHC II DQ8tg für die Bildung spezifischer Immunantworten konnte in diesen Untersuchungen allerdings noch nicht hinreichend genug beantwortet werden, da die Versuchstierzahl zu gering war.

Des Weiteren wurden huDQ8-HSC-humanisierte NRG Aβ$^{-/-}$ DQ8tg Mäuse mit HIV-1 infiziert. Hier konnte gezeigt werden, dass infizierte Mäuse über einen Zeitraum von mehr als 100 Tagen einen stabilen HIV RNA Titer im Blutplasma aufwiesen.

Zusammenfassend konnte gezeigt werden, dass humanisierte huDQ8tg Mäuse ein einzigartiges und sehr wertvolles Modell für die HIV-Forschung darstellen. Die Humanisierung mit huDQ8-PBMCs in huDQ8tg Mäusen ist einfach durchzuführen und das Modell ist für kurzweilige Experimente, wie das Testen von antiviralen Stoffen, leicht nutzbar. Im Gegensatz dazu ist die Rekonstitution mit huDQ8-HSCs für Langzeitexperimente, wie das präklinische Testen von Medikamenten oder Impfstoffen, gut geeignet. Dieses neue huDQ8tg Mausmodell ist unter anderem eine wertvolle Ergänzung für die *in vivo* Untersuchungen der frühen Ereignisse einer HIV Infektion.

I. Introduction

1. The human immunodeficiency virus

1.1. Historical overview

In June 1981 a number of young gay men in the United States were diagnosed with symptoms usually not seen in individuals with a healthy immune status. These individuals showed a more aggressive form of *Kaposi's sarcoma* (Hymes et al., 1981) or a rare lung infection called *Pneumocystis carinii pneumonia* (Gottlieb et al., 2001). Soon after these first reports of the *acquired immunodeficiency syndrome* (AIDS), a number of further cases with similar symptoms, including intravenous drug users, and recipients of blood transfusions, were discovered. At that time, the leading hypothesize was that a retrovirus might be the etiological agent that causes AIDS. The only human retrovirus known at that time was the *human T-lymphotropic virus* (HTLV), causing transformation of T-cells. Researchers around Luc Montagnier and Françoise Barré-Sinoussi at the Institute Pasteur in Paris tried to culture cells from a patient's lymph node, and observed T-cell transformation. Interestingly, they did not find any activity associated with HTLV, indicating that the causing agent was a new human virus (Barré-Sinoussi et al., 2010). However, in 1983 they were the first to isolate this new human retrovirus, and named it *lymphadenopathy-associated virus* (LAV) (Barré-Sinoussi et al., 1983) even though they could not show the new human virus being responsible for AIDS. Concurrently, in 1984, the group of Robert C. Gallo confirmed the identification of the causing agent of AIDS by isolating a new virus that they called HTLV-III (Gallo, et al., 1984). A very controversial debate started but soon it became obvious that both groups had isolated the same virus. Although the group of Gallo was not the first to have isolated the virus, they are recognized to be the first demonstrating that HIV is the causing agent of AIDS (Popovic et al., 1984). Hence, in 1986 the international committee on the taxonomy of viruses decided to replace both names by the new term *human immunodeficiency virus* (HIV) (Coffin et al., 1986).

Soon after first reports in 1981 in the USA, the spread of AIDS was very rapid. Fourteen countries reported cases of AIDS in 1982, 33 countries already in 1983 and in 2012 it has been 186 countries. By the end of 2011, 34 million people worldwide

were estimated to be living with HIV (UNAIDS Global Report, 2012). According to a report from the World Health Organization in 2012 on the global AIDS epidemic, 2.5 million people were newly infected with HIV, and about 1.7 million people died of AIDS in 2011. HIV is responsible for approximately 25 million deaths, thus rendering it the most serious pandemic to date.

1.2. Origin and epidemiology

The *Human Immunodeficiency Virus* (HIV) belongs to the *Retroviridae* family in the *Lentivirus* genus. HIV was introduced into the human population by multiple cross species transmissions from nonhuman primates infected with the *Simian Immunodeficiency Virus* (SIV). To date, two types of HIV have been characterized: HIV type 1 (HIV-1) and HIV type 2 (HIV-2). HIV is the result of at least twelve distinct transmission events of different SIVs to humans, resulting in HIV-1 group M, N, O and P, and in HIV-2 group A-H (Sharp et al., 2010). HIV-1 M and N precursors are found in chimpanzees (SIVcpz) (Gao et al., 1999; Keele et al., 2006), whereas HIV-1 O derived from either SIVcpz or SIVgor (infecting the Western Lowland Gorilla, Van Heuverswyn et al., 2006). The recently detected HIV-1 group P shows high similarities to SIVgor (Plantier et al., 2009). The primate reservoir for HIV-2 is the Sooty mangabey (smm). At least eight times SIVsmm was transmitted to humans, resulting in HIV-2 A-H (Heeney et al., 2006; Van Heuverswyn et al., 2007; de Silva et al., 2008). All these zoonotic transmission events took place during the first half of the 20th century or later (Korber et al., 2000; Lemey et al., 2003 and 2004). Infections with HIV-1 group M make up the largest part of the current HIV pandemic. Probably 98 % of all HIV-positive people are infected with this subtype (Sharp et al., 2010).

Both HIV-1 and HIV-2 are very similar in terms of transmission routes, and disease symptoms (Clavel et al., 1987). HIV-1 is the virus that was initially discovered (Barré-Sinoussi et al., 1983; Gallo, et al., 1984). It is more virulent, more infective and the cause of the majority of HIV infections globally whereas HIV-2 is largely restricted to a very small region of West Africa (Horsburgh and Holmberg, 1988).

1.3. Morphologic structure

HIV virions are spherically shaped with a diameter of about 100 nm (Fig. 1). Each viral particle is surrounded by a lipid bilayer membrane envelope derived from the host cell's plasma membrane. The viral glycoproteins 41 (gp41) (with a transmembrane domain) and glycoprotein 120 (gp120) (associated with gp41) are incorporated into this membrane, being necessary for viral entry into the host cell (Hallenberger et al., 1997). The capsid, consisting of the capsid protein p24 (CA), is linked to the envelope via the matrix protein p17 (MA). Inside the capsid, the reverse transcriptase (RT) and integrase (IN) are associated with the RNA genome. HIV virions contain a single- and positive-strand RNA genome. Two copies lie within the capsid of the virion. Also the protease (PR) is present within the capsid.

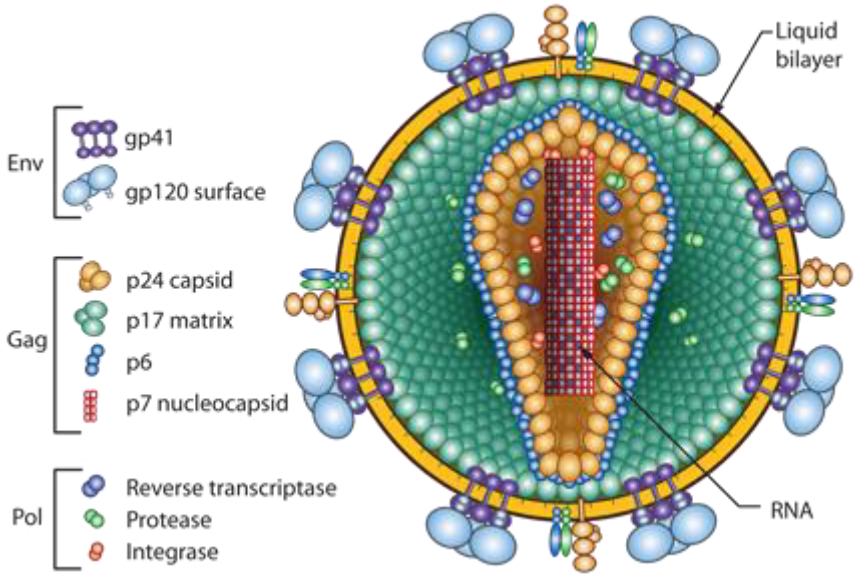

Fig. 1: Structure of an HIV virion particle
The envelope of the spherical HIV virion is derived from the host cell's plasma membrane. The envelope protein is incorporated into the envelope and binds to the viral receptor and co-receptor. A linker between the outer envelope and the inner capsid is a layer built up by the matrix protein p17. The capsid that consists of p24 encloses two RNA genomes associated with the reverse transcriptase and the integrase.
Taken from: Los Alamos National Laboratory (2014).
http://www.lanl.gov/science/1663/march2011/images/virus.png

1.4. Genomic organization

The genome has a length of about 9 kb, and is flanked by 5' and 3' long terminal repeats (LTRs), which are essential for viral replication (Fig. 2). Besides the major genes for structural proteins that can be found in all retroviruses (*gag, pol, env*), the HIV genome also encodes for several nonstructural genes (*tat, rev, nef, vpr, vif, vpu/vpx*) unique to HIV (Feinberg et al., 1992).

The *gag* gene encodes the polyprotein Gag, which can be divided into the structural proteins matrix protein (MA, p17), capsid protein (CA, p24), and nucleocapsid protein (NC, p7). The *pol* gene encodes enzymatically active proteins, named protease (PR, p11), reverse transcriptase (RT, p66), and integrase (IN, p32) (Gelderbloom et al. 1991). The polyprotein Env (gp160) can be divided into gp120 and gp41. The accessory genes *nef, vpr, vif* and *vpu/vpx,* and the regulatory genes *rev* and *tat* belong to HIV's nonstructural genes. The two viral genes *rev* and *tat* are essential regulatory genes that accumulate within the nucleus, and bind to defined regions of the viral RNA (Dayton et al., 1986; Felber et al., 1989). The accessory genes are not essential for viral replication *in vitro*, but antagonize host restriction factors or change the microenvironment within infected cells to support viral persistence, replication, dissemination and transmission (Malim et al., 2008; Kirchhoff, 2010). The genes v*if, nef* and *vpr* are present in both HIV-1 and HIV-2. Due to different evolutionary lineages of SIV's where HIV evolved from, the gene *vpu* is specific for HIV-1 and *vpx* for HIV-2.

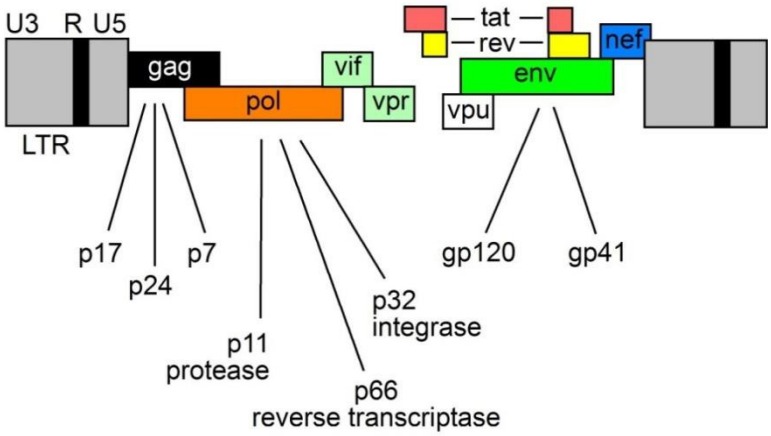

Fig. 2: Organization of the HIV-1 genome
The genome of HIV is flanked with 5' and 3' LTRs at both ends. The main genes of all retroviruses encoding for structural proteins are gag, pol and env. Unique for HIV are the accessory genes tat, rev, vif, vpr and nef. The evolutionary lineage that gave rise to HIV-2 additionally acquired the accessory gene vpx instead of vpu in HIV-1 (not shown).
Taken from: http://hivbook.files.wordpress.com/2011/11/figure-2.jpg (2014)

1.5. Replication cycle

HIV's replication can be divided into two general phases, the *early* and the *late* phase (Freed, 2001). The early phase is characterized by the steps until the viral genome is integrated into the host genome. The late phase comprises all steps producing new virus particles including the expression and assembly of viral proteins and RNA as well as the release of viral particles. An overview of the viral replication cycle is shown in Fig. 3 and described in the following.

Early phase: viral entry, reverse transcription, nuclear import and integration

At the beginning of an infection, HIV requires a host cell expressing the CD4-receptor on its cell surface. Therefore, the virus mainly targets $CD4^+$ T-lymphocytes, macrophages, microglia, and dendritic cells. The **virus attaches** to the target cell by its surface envelope glycoprotein gp120 binding to the CD4-receptor on the host cell (Dalgleish et al., 1984; Klatzmann et al., 1984a and 1984b). Through this process, conformational changes in the transmembrane unit of the gp120 protein are induced facilitating the exposure of a second binding site for a required co-receptor (Berger et al., 1999). This co-receptor (also see 1.1.6) is either the chemokine CC-receptor 5 (CCR5, mainly expressed on macrophages) or the chemokine CXC-receptor 4 (CXCR4, mainly expressed on $CD4^+$ T-cells) (Wyatt and Sodroski, 1998). Binding to such a co-receptor activates the transmembrane glycoprotein gp41 to reorient, allowing its N-terminal fusion peptide to insert into the target membrane. The viral and cellular membranes are then brought into close proximity (Esté and Telenti, 2007; Wyatt and Sodroski, 1998), so that the viral lipid bilayer and the host cell's plasma membrane are fused, and the **viral core enters** the cytoplasm of the host cell.

In a process that is not fully understood, the viral core is uncoated within the host cell. A reverse transcription complex, consisting of the viral RNA coated with nucleocapsid proteins (MA, CA, Vpr) and viral enzymes (RT, IN), is built for the **reverse transcription** of the two single stranded copies of viral RNA into double stranded DNA (dsDNA) (Mougel et al., 2009). The viral RT has no proofreading activity, and can also "jump" between templates so that this process is error-prone, and the resulting dsDNA is not an exact genetic copy of the original RNA. Consequently, a high frequency of genetic recombination, together with a high mutation rate ($3x10^{-5}$

per replication cycle) leads to an enormous heterogeneous population of virions (termed quasispecies) (Freed, 2001; Jung et al., 2002). After the viral genome is reverse transcribed, the viral dsDNA forms a preintegration complex (PIC) together with other cellular and viral proteins. This complex is then **transported to the nucleus** (Freed, 2001). In the nucleus, the IN being part of the PIC, catalyzes the insertion of the dsDNA into the host chromosome via its LTRs (Freed, 2001). The integrated dsDNA, also called the provirus, is then expressed by the host cell mimicking to be an original host cell gene. **Integration** of HIV's genome into the host cells' genome is an irreversible process marking an important point of HIV infection (Simon et al., 2006).

Late phase: gene expression, budding, maturation

In the next step, after the viral genome has integrated into the host cells genome, viral proteins, and genomic RNA are synthesized by the machinery of the host cell. Initially, gene expression of the viral genes is relatively low. However, the expression of HIV-specific genes is increased by a **positive feedback loop** due to the activity of the *viral Tat* (trans-activator of transcription) protein (Cullen, 1991; Kim and Sharp, 2001). Processing of viral RNA transcripts is regulated by the viral Rev (regulator of virion) protein at a later time. **Early** expressed viral RNAs are multiple spliced RNAs that lead to the expression of viral regulatory proteins like Tat and Rev. The expression of structural proteins encoded by unspliced or single spliced RNAs is mediated by Rev. After a sufficient amount of Rev is expressed, it protects viral transcripts from being spliced. Hence, only at a **late stage**, unspliced, singly spliced or partially spliced transcripts are generated leading to structural viral proteins. Furthermore, Rev mediates the transport of less spliced RNAs out of the nucleus into the cytoplasm. By binding of Rev to the *Rev responsive element*, a highly structured RNA region that is located within the env gene, and present in all less spliced HIV RNAs, RNAs protected from splicing are transported into the cytoplasm via the cellular nuclear export machinery (Cullen, 1991; Freed, 2001). In the cytoplasm, singly spliced transcripts are translated into Gag, Gag-Pol and Env precursors. The Env precursor is subsequently cleaved by a cellular enzyme, and gp120 as well as gp41 products are transported from the endoplasmic reticulum to the cell membrane where the Gag and Gag-Pol polyproteins, the unspliced RNA transcripts and other viral proteins are assembled into a new virion. **New virions** spiked with Env

glycoproteins start to bud from the cell membrane, and are subsequently released from the cell as immature viruses. After budding, the viral protease cleaves the viral polyproteins Gag and Pol into the final proteins (Freed, 2001; Moulard and Decroly, 2000). This process is called **maturing of the immature virus**. The mature virus is now ready to infect a new cell.

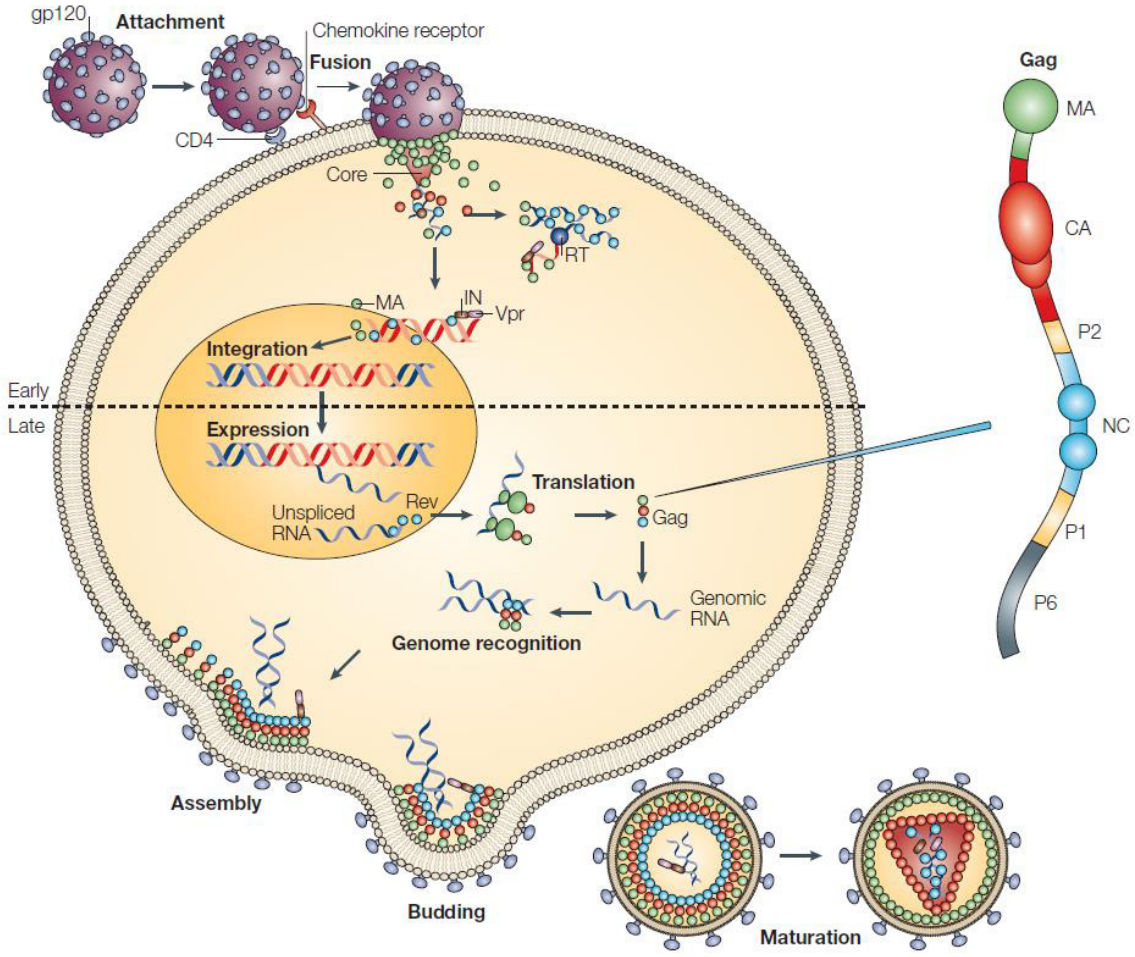

Fig. 3: The replication cycle of HIV
The replication of HIV can be divided into two phases. During the early phase (upper portion) the viral entry into the host cell, the reverse transcription of the viral RNA into double stranded RNA (dsDNA), the nuclear import and the integration of the viral dsDNA occur more or less in an ordered series of events. In the late phase of infection, viral proteins are expressed and transported to the plasma membrane where they assemble and bud from. New virions are immature and undergo a maturation step in which viral polyproteins are cleaved. Mature virions can infect new cells.
Taken from D'Souza et al., 2005

1.6. Tropism of HIV

Historically, different HIV-1 isolates originated from HIV-1 infected patients were first categorized according to their infectivity *in vitro* (Asjo et al., 1986). Fig. 4 gives an overview of the first categorization of HIV strains.

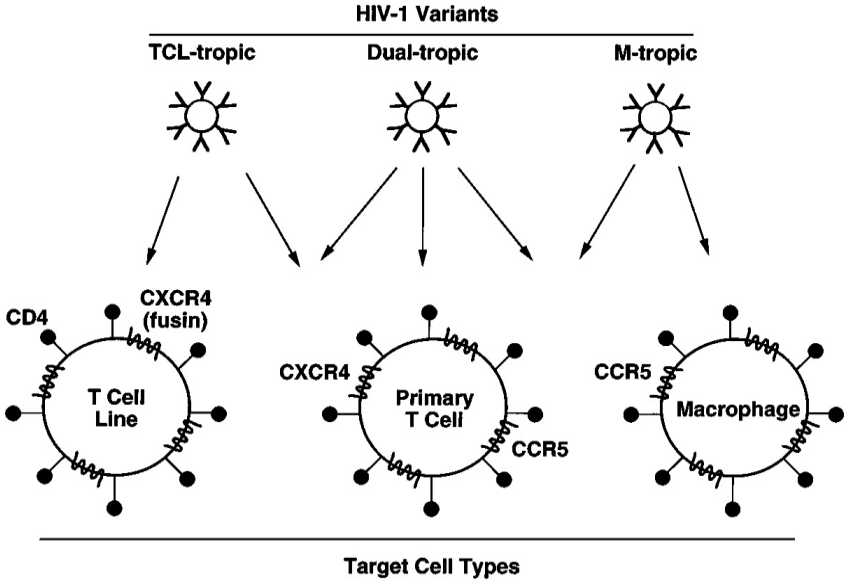

Fig. 4: Tropism of HIV
Dependent on the co-receptor usage, HIV strains can be divided into three different groups. TCL-tropic strains are specific for using CXCR4 as a co-receptor and M-tropic strains mainly use CCR5 as a co-receptor. Dual-tropic strains display an intermediate tropism and can use both co-receptors for cell entry. Taken from Berger et al., 1999

It was found that all HIV-1 strains infect and replicate in activated primary $CD4^+$ T-lymphocytes but when other target cells were examined, the tropism did not seem to be the same (Evans et al., 1987; Fenyo et al., 1989). For example, some isolates show efficient infectivity of $CD4^+$ T-cell lines, but only poor infectivity of primary macrophages. Thus, these viruses were designated **T-cell line–tropic (TCL-tropic)** and were found to **induce syncytia** in assays using a highly permissive T-cell line (Berger et al., 1998). In addition, other HIV-1 strains showed the opposite preference, so that the infection of primary macrophages was much more efficient than the infection of T-cell lines. Such viruses were designated **macrophage-tropic (M-tropic)** or **nonsyncytium-inducing**. HIV isolates that were found to replicate efficiently in both target cell types were designated **dual-tropic**. These *in vitro* tropism phenotypes soon demonstrated to have profound implications for HIV-1 transmission and pathogenesis in humans (Cheng-Mayer et al., 1988).

Shortly after HIV infection and during the asymptomatic phase, patients obtain predominantly M-tropic viruses (van't Wout et al., 1994) whereas TCL-tropic viruses can be isolated from many patients as the infection progressed to AIDS (Embretson et al., 1993). Due to this tropism model of HIV it was obvious that, in addition to the $CD4^+$-receptor expressed on immune cells, HIV requires different co-receptors for entering target cells. Finally, in 1996, members of the *G protein-coupled receptor superfamily,* the chemokine receptors **CCR5** (chemokine CC-receptor 5) and **CXCR4** (chemokine CXC-receptor 4) have been identified as the principal co-receptors of HIV-1 (Feng et al., 1996). M-tropic HIV-1 strains mainly use the CCR5 co-receptor for their entry and thus, are able to replicate in $CD4^+$ macrophages. Interestingly, in humans, HIV-1 uses CCR5 as primary co-receptor for cell entry, regardless of their viral genetic subtype. Comparatively, TCL-tropic strains use the CXCR4 co-receptor for infecting cells but only at a much later stage after HIV infection. Nowadays, HIV strains that only use the CCR5 co-receptor are termed **R5-viruses**. Those that only use CXCR4 co-receptor are termed **X4-viruses**, and those that use both, **X4R5-viruses**.

Over the course of the HIV infection, the co-receptor usage of HIV changes from a preference for CCR5 to a preference for CXCR4 in about 50% of infected individuals, known as the **co-receptor switch phenomenon** (Berger et al., 1999). In Fig. 5 the time line of the co-receptor class switch during HIV infection is shown. The switch from CCR5 to CXCR4 using HIV strains is associated with accelerated $CD4^+$ T-cell decline, and progression to disease, which is the hallmark of AIDS (Connor et al., 1997; Bjorndal et al., 1997; Scarlatti et al., 1997; Bazan et al., 1998). Therefore, the co-receptor switch could be a key element of HIV pathogenesis. However, the reasons for the co-receptor switch only remain poorly understood.

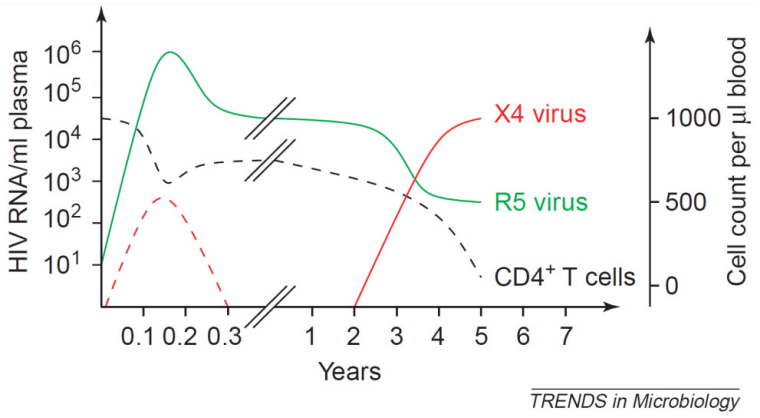

Fig. 5: HIV co-receptor switch

Over the course of HIV infection, the usage of co-receptors is changing. R5 viruses are the primary viruses, and present throughout the entire course of infection. X4 viruses develop from R5 viruses at a later stage in HIV infection. Taken from Regores et al., 2005

1.7. Transmission and immunopathogenesis of HIV

HIV is transmitted from one person to another through body fluids, mostly via sexual transmission across mucosal surfaces. Further, HIV can be transmitted via contaminated blood transfusions, contaminated needles shared among intravenous drug users and from infected mothers to their children during pregnancy, childbirth, and breast feeding (Sloan RD et al. 2013). Also, it is possible being infected with more than one HIV strain, known as superinfection (van der Kuyl et al., 2007).

Transmission of HIV-1 results in the establishment of a new infection, typically starting from a single virus particle. The clinical course of HIV generally includes different phases or stages: *primary infection*, *acute phase*, *clinical latency* and *AIDS*. Fig. 6 shows the different clinical stages of the course of HIV infection.

Soon after HIV enters the body, it is widely disseminated, predominantly to lymphoid tissues. Viral replication within the lymphatic tissues is extensive in the early stages of the disease, and even in the hematopoietic system (Pantaleo 1993, Embretson 1993, Carter 2010). During the **primary infection** with HIV, there is a burst of virus into the plasma, followed by a minor decline in viremia. During this time, a robust HIV specific immune response of cytotoxic T-cells is generated, which coincides with the early suppression of plasma viremia in most patients. Virologically, at around day 21 after infection, the viral load is often higher than $1x10^7$ copies per milliliter (Graziosi et al., 1993; McMichael, 2006). This is commonly referred to as the **acute phase** of HIV infection. Immunologically, this is accompanied by a rapid depletion of about half of the $CD4^+$ T-cells (Mattapallil et al., 2005) resulting in flu-like symptoms (Schacker et al., 1996). The **clinical latency** of the disease is a phase in which the virus can be controlled in absence of clinical symptoms over a long time, lasting from months to several years. The viral load only slowly increases whereas $CD4^+$ T-cells slowly but continuously deplete. When the immune system is too weak and finally collapses, the third phase of the infection is reached, the **acquired immunodeficiency syndrome (AIDS)**. It is commonly diagnosed when $CD4^+$ T-cell counts fall below 200 cells per milliliter, and the immune system is no longer capable of controlling the virus and other pathogens so that the patient becomes vulnerable to opportunistic infections which in most cases lead to death.

On the contrary, the clinical course of HIV-2 infections is generally characterized by a longer asymptomatic stage, lower plasma HIV-2 viral loads and lower mortality rates compared to HIV-1 infections (Marlink et al., 1994; Matheron et al., 2003). However, HIV-2 infections can also progress to AIDS. Due to very similar transmission routes, concomitant HIV-1 and HIV-2 infections may occur and should be considered in patients from an area with high prevalence of HIV-2 like West Africa (Horsburgh and Holmberg, 1988).

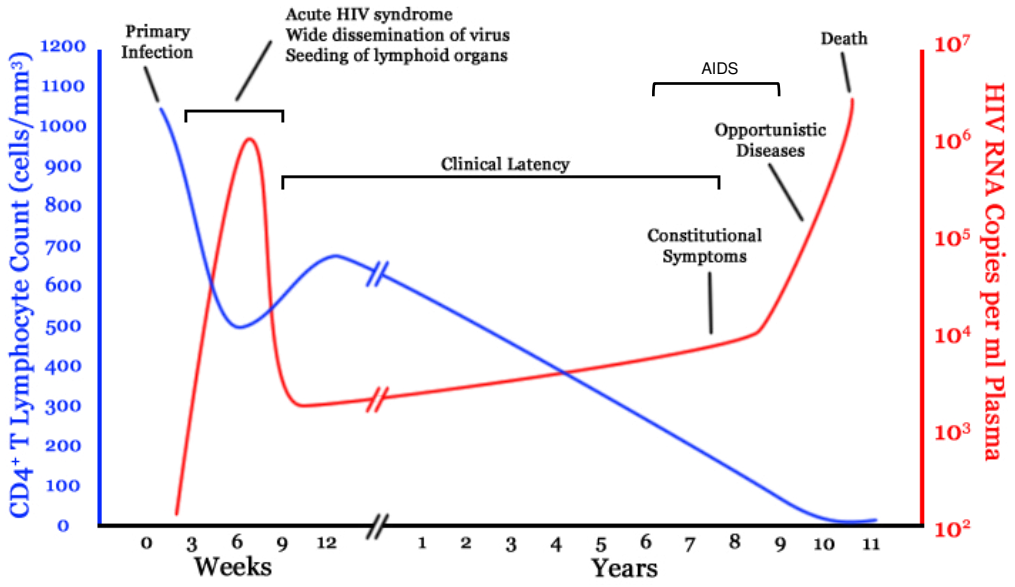

Fig. 6: The different phases of HIV infection with their progression to AIDS.
A typical course of HIV infection can be divided into distinct stages: Primary infection, clinical latency and AIDS.
Taken from the website http://www.lef.org/protocols/images/hiv_aids_01.jpg but originally published by Pantaleo et al., 1993.

2. Animal Models for HIV infection

Humans are not allowed to be intentionally infected with HIV for prospective studies. Many people are diagnosed only at a rather late point after the initial HIV infection, and those with a diagnosis may not wish to be "treated" as experimental subjects. Animal models represent a key component of many fields in biomedical research. One of the major limitations in searching for cures and vaccines for HIV has been the lack of an appropriate animal model that recapitulates all features of HIV infection in humans. Since the virus exclusively infects and causes disease in humans, finding an animal model for HIV has proven to be very difficult. As a matter of course, when considering species other than humans as models for HIV infection, it is compulsory that the cells and proteins of these species must support viral replication. This, at least partially accounts for the inability of HIV to replicate or cause disease in most species other than humans (Hatziioannou et al., 2012). A **hypothetical perfect animal model** would hold different features: **(1)** it would be permissive for infection by replication-competent HIV-1 and -2 strains **(2)** and manifest identical clinical symptoms known from HIV patients. The model **(3)** should be susceptible to natural transmission modes of HIV including vaginal and rectal routes. Of course **(4)** acute infections could be staged, and the development of AIDS can be monitored over time. Following this, **(5)** the animals would exhibit cells and proteins that promote the replication of HIV including $CD4^+$ T-cells, co-receptors CXCR4 and/or CCR5, factors for transcription and restriction as well as nuclear export factors and other host cell factors for HIV assembly and budding. **(6)** Immunologic as well as virological parameters of disease could be first observed and then manipulated. At best, the animal model could be used to learn more about the disease process and **(7)** to demonstrate the efficacy of experimental antiviral compounds or vaccines, prior to their use in human clinical trials. Furthermore, **(8)** the animal model should comprise low housing costs, **(9)** is easily available, **(10)** fast utilizable and **(11)** gives reliable and reproducible results that **(12)** can be applied perfectly to humans. In the following, currently used animal models for HIV infection and AIDS are described.

2.1. Non-human primate models

HIV-1 was found to be a direct descendant of the *simian immunodeficiency virus* (SIV) that infects Central Africa chimpanzees (Gao et al., 1999; Keele et al., 2006). But then, infection of chimpanzees (and all other non-human primates) with HIV-1 rarely results in the development of disease, demonstrating the incapability for being an animal model for HIV infections (Alter et al., 1984; O'Neil et al., 2000). In contrast, many species of African monkeys and apes are **natural hosts for SIV**, but generally do not develop disease as a consequence of SIV infection. Consequently, African monkeys and apes are not useful as pathogenic model. Interestingly, SIV infection of Asian macaques, which are **non-natural SIV hosts**, results in high viral loads, progressive $CD4^+$ T-cell depletion, and opportunistic infections (Hatziioannou et al., 2012). Therefore, SIV infected Asian macaques almost resemble HIV-1 infection in humans. Thus, numerous advances in our understanding of viral transmission, pathogenesis and latency can be attributed to the use of the macaque model. Comparisons of non-pathogenic SIV infections in African monkeys with pathogenic SIV infection in Asian monkeys have led to a number of important insights into AIDS pathogenesis (Chahroudi et al., 2012). Using SIV infected Asian macaques as animal models for resembling HIV infection in humans has been a milestone in HIV research, but nevertheless SIV and HIV are different viruses that only share some features. Macaques are outbred and thus, a study group of animals exhibits high genetic diversity leading to manifold variations in the course of SIV infection within the group. Also, macaque genes controlling the immune response to SIV are not directly orthologous to the human genes controlling immune responses to HIV (Ling et al., 2002; Stremlau et al., 2004; Liao et al., 2007). Taken together, these features of SIV infected non-human primate models complicate adequate interpretation of studies as well as the transfer, and practical applicability for HIV infected humans.

2.2. Small animal models

Compared to non-human primate models which are closely related to humans but have high maintenance costs, and possess other difficulties, a small animal model is in favor being an animal model for HIV infection and AIDS.

Cats

Although cats are also not susceptible to HIV-1, feline immunodeficiency virus (FIV) infection in domestic cats can serve as a surrogate model for HIV-1 infection in humans. Pathogen-free cats have been inoculated with FIV, and develop immunodeficiency similar to HIV-1 infection in humans or SIV infection in rhesus monkeys (Pedersen et al., 1989). FIV infection of cats results in an acute phase with mild symptoms, a variable latent phase, and progressive $CD4^+$ T-cell depletion (Pedersen et al., 1987; Torten et al., 1991). The genome of FIV shares 30-50% homology with HIV-1, and encodes a reverse transcriptase enzyme that is inhibited by the same antiviral drugs as HIV-1. However, FIV lacks certain accessory genes that are present in HIV-1, and contains other basal retroviral proteins that are absent from primate lentiviruses. Furthermore, FIV uses CD134 rather than CD4 as a primary receptor although the co-receptor usage is similar (Shimojima, et al., 2004). So, unlike HIV-1, which infects only $CD4^+$ T-cells and macrophages, FIV can also infect B cells and $CD8^+$ T-cells (Dean et a., 1996). The chronic phase of FIV infection is also unpredictable, and can be as long as a decade (Ackley et al., 1990) making certain applications of this model impractical. Thus, this model is currently not widely used.

Rabbits

Experimentally, rabbits can be infected with HIV-1, even though a very high inoculum of HIV-1 is required to establish viremia (Filice et al., 1988). However, to date no AIDS-like pathology has been reported in HIV-1 infected rabbits (Kulaga et al., 1989; (Filice et al., 1990). Also, rabbits transgenic for the human $CD4^+$-receptor did not significantly improve to support the infection of rabbits with HIV-1 (Dunn et al, 1995). Now, it is evident that rabbit cells do not provide essential cofactors for HIV-1 replication and also express proteins that inhibit HIV-1 infection (Tervo et al., 2010). Therefore, HIV-1 infection of rabbits is considered experimentally only, and is generally not applicable as an animal model for HIV infections and AIDS.

Rats and Mice

Initial attempts to infect rats and mice with HIV-1 regarding HIV replication *in vivo,* and also development of disease, were unsuccessful (Morrow et al., 1987). Consequently, generating rats and mice transgenic for proteins that are necessary for

HIV-1 replication have been constructed. A **rat model** transgenic for the human $CD4^+$ receptor and human CCR5 co-receptor was established. This transgenic rat model demonstrated susceptibility to HIV-1 *in vivo*, although during the early infection only low plasma viremia and thus, no disease has been observed (Keppler et al., 2002; Goffinet et al., 2007a and b). Even during the early times after HIV discovery, a variety of transgenic **mouse models** have been established for HIV research. Leonard et al., (1988) created transgenic mice which contain the complete HIV-1 provirus. HIV-1 expression or signs of disease were not detected in any founder animals, even though integrated pro-virus could be demonstrated. Unfortunately, all transgenic mice perished in a laboratory accident shortly after the publication of this model (Ezzell, 1988). Mice transgenic for the human $CD4^+$-receptor and human CCR5 co-receptor (Browning et al., 1997) as well as transgenic mice harboring subgenomic fragments (Dickie et al., 1991; Vogel et al., 1988; Khillan et al., 1988) or reporter genes linked to the HIV-1 LTR (Khillan et al., 1988; Leonard et al., 1989; Prakash et al., 1990; Skowronski et al., 1991) or HIV encoded gene products (Hanna et al., 1998; Poudrier et al., 2001; Weng et al., 2004; Priceputu et al., 2005) have been created. However, these studies provided insights into the pathogenic potential of HIV gene products, but none of these models support robust viral replication or the development of disease. A reason might be a block to HIV-1 infection (Lores et al., 1992; Bieniasz et al., 2000; Zhang et al., 2008) most likely at a post-receptor level (Adachi et al., 1986; Chesebro et al., 1990). Hence, none of these described transgenic mice are presently used in HIV research to large extends. Currently, several different **"humanized mouse" models** being supremely promising for HIV/AIDS research have been developed, and are described in the following.

3. Humanized mice for HIV research

Humanized mice are defined as genetically immunodeficient mice that have been engrafted with human cells and/or human tissues and/or transgenically express human genes. Humanized mice provide a powerful tool for the investigation and manipulation of the human hematopoietic and immune system *in vivo* especially during infection with human pathogens. Although several different humanized mouse models have been developed for different purposes, here only those are described that are used most frequently in HIV research.

3.1. Historical foundations

Scid mice

Scid mice were the first used for humanization approaches. They are derived from the CB17 strain, and obtain a spontaneous autosomal recessive mutation in the gene that encodes for the *catalytic subunit of a DNA-dependent protein kinase* (Prkdc) that is needed for V(D)J recombination in developing T- and B-lymphocytes (Bosma et al., 1983; Schuler et al., 1986; Malynn et al., 1988). Hence, functional murine B- and T-cells are absent and thus causing *severe combined immunodeficiency* (SCID) (Custer et al., 1985; Bosma et al., 1987). The *scid* mutation is responsible for defective DNA repair and thus, *scid* mice are very radiosensitive (Fulop et al., 1990). Many humanized mice described in the following, have been developed using *scid* genetic backgrounds.

Scid-hu-Thy/Liv mice

The *scid*-hu-Thy/Liv mice are generated by surgical transplantation of aborted human fetal thymus and liver cells/tissues under the kidney capsule of CB17-*scid* mice (McCune et al., 1988). At 4-6 months post-implantation, human fetal thymus/liver tissues form a conjoint organoid that resembles the human thymus. The generation and maintenance of human T-cells is mostly limited to the implanted organoid. Multilineage human hematopoiesis as well as robust peripheral human leukocytes are absent, so that no human immune responses could be generated (Greiner et al., 1998). These mice are highly susceptible to HIV infections but require direct inoculation of HIV into the human organoid (Namikawa et al., 1988; Aldrovandi et al., 1993). Depletion of human $CD4^+$ T-cells as well as high viral loads exclusively in the human tissue could be detected (Kaneshima et al., 1991). Since HIV-1 infection in *scid*-hu-Thy/Liv mice is restricted to the implanted organ, the use of this model is limited. Moreover, this model still exhibits innate immunity, including NK-cells which decrease the success of engraftment (Dorshkind et al., 1985). Also, a substantial degree of “leakiness” leading to the development of murine T- and B-cells in older animals is a limitation (McCune et al., 1996). Applications of this model include studies of the mechanisms of $CD4^+$ T-cell loss and the efficacy of antiretroviral drugs in suppressing acute HIV-1 infection (Shih et al., 1991; Jamieson and Zack et al.,

1999). The improved continuation of this humanized mouse model is the *BLT mouse* described in section 3.2.

HuPBL-scid mice

For the generation of huPBL-*scid* mice, human peripheral blood mononuclear cells (PBMCs/PBL) are transferred into the peritoneal cavity of CB17-*scid* mice (Mosier et al., 1988). Human T- and B- cells, as well as macrophages recirculate in the blood stream of recipient mice and mainly disseminate to the lymphoid tissues including lymph nodes, spleen and bone marrow (Mosier et al., 1988, Hatziioannou et al., 2012). Moreover, human cells are maintained for many weeks, and also display to a certain extent weak immune effector functions. For example, transferred human B-cells were documented to produce specific antibodies from prior antigen exposure (Mosier et al., 1988), which is an advantage over *scid*-hu-Thy/Liv mice. However, there are no notable primary immune responses detectable due to the lack of *de novo* multilineage human hematopoiesis. Unfortunately, a significant drawback of this humanized mouse model is the development of g*raft-versus-host-disease* (GvHD) (Hoffmann-Fezer et al., 1993). Within days after the transfer, human cells react against the murine environment with an acute activation. The activation marker HLA-DR is upregulated, and human cells, predominantly human T-cells, increase their proliferation rates, resulting in xenoreactive T-cells. Mice with a significant high level of human T-lymphocytes suffer from severe GvHD, and show higher mortality rates than mice with no or only transient T-cell level. Interestingly, huPBL-*scid* mice can be infected with HIV-1 by intraperitoneal injection with cell-free viruses or engraftment with HIV-1 infected human cells (Mosier et al., 1991). Depletion of human $CD4^+$ T-cells in the mouse is seen in both infection routes (Mosier et al., 1993a). Additionally, HIV can be detected in tissues that have been infiltrated by human cells. In HIV research the huPBL-*scid* mouse model has been used to demonstrate the efficacy of potential vaccine candidates for example based on monoclonal antibodies (Safrit et al., 1993; Parren et al. 1995; Gauduin et al., 1997) or the HIV Env glycoprotein (Mosier et al., 1993b; Delhem et al., 1998). Like the *scid*-hu-Thy/Liv mice, this model cannot be used for studying mucosal transmission.

HuSRC-scid mice

HuSRC-*scid* mice emerged from *scid* mice repopulated with human hematopoietic stem cells. The ability of intravenously injected human bone marrow cell suspensions to engraft into sublethally irradiated *scid* mice was first documented in 1992 by Lapidot et al. (Lapidot et al., 1992). The term *SRC-scid repopulating cells* refers to the ability of human stem cells to engraft in irradiated *scid* mice following intravenous injection (Larochelle et al., 1996; Bhatia et al., 1997). Human cell engraftment levels in huSRC-*scid* mice after transfer of human bone marrow suspensions were low (0.5%-5%). and the differentiation of human stem cells required administration of various exogenous human cytokines (Lapidot et al., 1992). In contrast, human umbilical cord blood engrafts in irradiated *scid* mice without the need for exogenous cytokines. However, due to murine NK-cell activity which is one of the main impediments for poor engraftment (Christianson et al., 1996), only low engraftment levels are reached (Vormoore et al., 1994). Hence, the huSRC-*scid* mouse model is very limited for the use in infection research.

Taken together, variations of humanized *scid* mice built the foundation for all subsequently developed humanized mouse models that are described in the following.

3.2. The big breakthroughs

NOD scid mice

The first big breakthrough was the development of immunodeficient *non-obese diabetic* (NOD)-*scid* mice (Shultz et al., 1995). *Scid* mice were crossed with NOD mice to generate *NOD scid mice*. This mouse strain obtains multiple genetic deficiencies that result additional defects in innate immunity like an impaired complement system cascade and most notably in a low activity of murine NK-cells. These characteristics substantially improved the efficiency of human cell and tissue engraftment (Shultz et al., 1995; Hesselton et al., 1995; Lowry et al., 1996; Pflumio et al., 1996). However, NOD *scid* mice suffer from a high incidence of thymic lymphomas, which greatly limits their lifespan (Prochazka et al., 1992). Also, residual activity of NK-cells and other components of innate immunity remain in humanized NOD *scid* mice so that they are limited as a model for human immunity.

NSG mice (NOD or NOG scid IL2Rcγ$^{-/-}$ mice)

The second breakthrough was the development of immunodeficient NOD *scid* mice with a deficient common γ-chain of the interleukin- 2-receptor (IL2Rcγ; CD132). The IL-2-receptor consists of one α, one β and one γ chain. The α and β chain are necessary for ligand binding, whereas the γ chain with its cytoplasmic domain is highly required for signal transduction (Nakamura et al., 1994; Nelson et al., 1994) following cytokine interactions (Leonard, 2001; Rochman et al., 2009) towards immune cell growth and development (Siegel et al., 1987; Wang et al., 1987). Two different versions of NOD *scid* mice with defective IL2Rcγ have been generated: **NOG** *scid* mice and **NSG** mice. NOG mice were established in the Central Institute for Experimental Animals (Kawasaki, Kanagawa, Japan) and harbor a mutation (deletion of exon 7) that truncates IL2Rcγ in the intracellular-signaling domain (Ito et al., 2002). In comparison, NSG mice established in the Jackson Laboratory (Bar Harbor, USA), harbor a mutation that completely deletes the intracytoplasmic domain of IL2Rγ (Shultz et al., 2005). Interestingly, mice of both strains completely lack mature B-cells and T-cells and have extremely low or no NK-cell activity (Leonard et al., 2001). The addition of Il2Rcγ$^{-/-}$ prevents the development of lymphomas, improving the lifespan of NOG *scid* and NSG mice compared to that of NOD *scid* mice. Of all *scid* mice, NOG *scid* and NSG mice yield the highest level of human cell engraftment using human hematopoietic (CD34^{+}) stem cells derived from cord blood, fetal liver or adult blood (McDermott et al., 2010). Humanized immune cells disseminate to numerous organs, among which is the peripheral blood, liver, lung, lymphoid organs and mucosal tissues (Shultz et al., 2005; Ishikawa et al., 2005; Brehm et al., 2010). When infected with HIV-1, infected cells invade various tissues, develop high levels of plasma viremia, and also HIV-specific antibodies can be detected (Watanabe et al., 2007). NSG mice have been used as a model for HIV-1 induced neuropathogenesis (Gorantla et al., 2010; Dash et al., 2011) and both, NOG and NSG mice have been used to investigate the efficacy of various gene therapy approaches to inhibit HIV-1 replication (Kumar et al., 2008; Holt et al., 2010; Joseph et al., 2010; Balazs et al., 2011).

NRG mice

Another breakthrough is the NRG mouse model based on NOD Il2Rcγ$^{-/-}$ mice. NRG mice obtain a deletion in the *V(D)J recombination-activating gene 2* (Rag2) that is

essential for immunoglobulin and T-cell-receptor gene rearrangement. Therefore, NRG mice lack functional T-cells, B-cells and NK-cells. Notably, NSG mice show a similar degree of immunodeficiency as NRG mice (Goldmann et al., 1998). A major benefit of NRG mice compared to NSG mice is the tolerance of much higher levels of irradiation conditioning and hence, they support higher levels of both human cord blood stem cell engraftment following irradiation-conditioning and human peripheral blood mononuclear cells engraftment in unconditioned adult mice (Shultz et al., 2000). Also, NRG mice have been successfully used in HIV research (Baenziger et al., 2006; Berges et al., 2006; Choudhary et al., 2009).

BLT mice

As one of the upgraded humanized mouse models, BLT mice have been established recently from the earlier *scid*-hu-Thy/Liv mouse model (Melkus et al., 2006). BLT is an acronym for *bone marrow-liver-thymus*. As in the standard *scid*-hu-Thy/Liv mouse model, human fetal liver and thymus from an abortion are placed under the renal capsule of young adult immunodeficient mice (e.g. NSG or NRG). However, after three weeks, mice are sublethally irradiated and additional engraftment with autologous human stem cells creates the BLT mouse model (Wege et al., 2008). These cells home to the bone marrow and also migrate to the scaffold organoid generated by the initial transplantation of the human fetal liver and thymus tissue. One of the main advantages of BLT mice over other mouse models is the presence of a functional autologous human thymus that permits appropriate T-cell education and human HLA cell restriction mimicking T-cell development in humans. In BLT mice, human cell engraftment is highly efficient, even to the gastro-intestinal tract with multilineage generation of T-cells, B-cells, macrophages, NK-cells and dendritic cells (Lan et al., 2006). Innate and adaptive immune responses appear to be generally more complete in the BLT mice than in humanized mice generated by transplanting human stem cells alone. Notably, BLT mice are more prone to GvHD than other models (Rongvaux et al., 2013). Intraperitoneal HIV infection of BLT mice results in high levels of sustained viremia, $CD4^+$ T-cell depletion and virus-specific humoral and cellular immune responses. Notably, good mucosal human cell engraftment also permits HIV infection via natural routes of transmission (Sun et al., 2007). Thus, BLT mice provide a useful tool for HIV research (Denton et al., 2008 and 2010; Wahl et al., 2012).

A brief summary of various approaches for engraftment of a human immune system in various immunodeficient mouse strains that were described previously is given in Fig. 7. Importantly, the NRG mouse model as well as the NSG mouse model show high levels of human cell engraftment in various mouse tissues, but nevertheless, engrafted human stem cells maturate in the mouse thymus. For this reason the overall adaptive immune response is substantially weak, and hardly comparable to responses in humans. In contrast, BLT mice equipped with a human thymus under the renal capsule provide a human organ where human progenitor cells can develop and maturate. However, generating BLT mice is a challenging two step procedure that requires surgical skills, and human fetal tissue. In the following, mouse models are described that were developed to resolve the drawback of the BLT mouse model with focus on NSG or NRG mice expressing human genes.

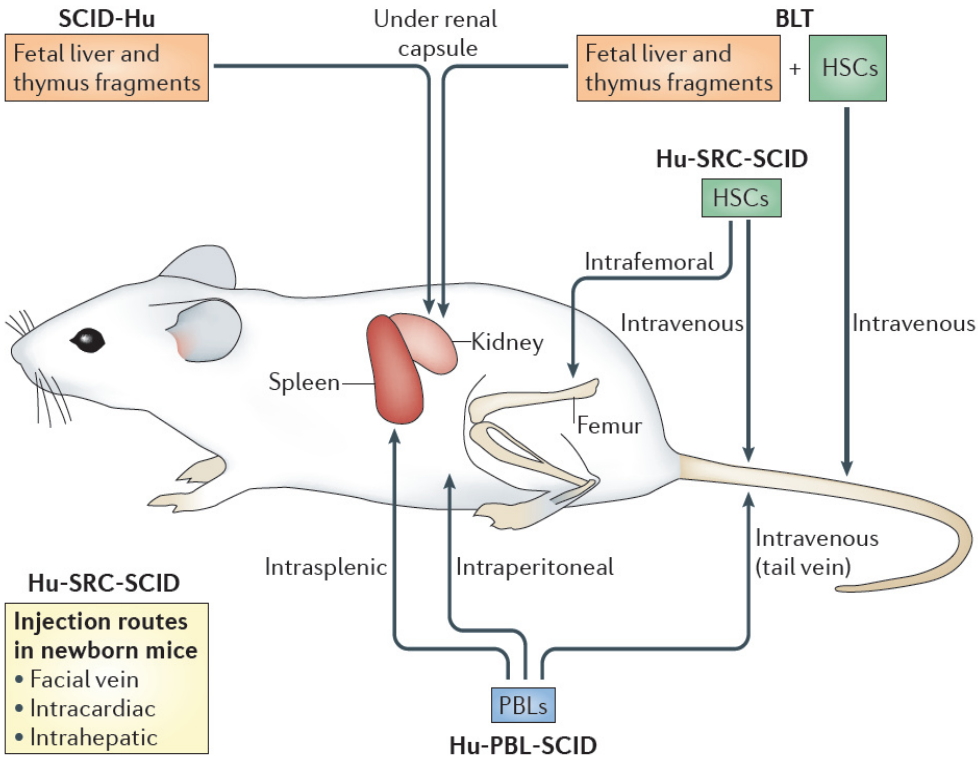

Fig. 7: Approaches for generating humanized mice.
Here, several ways are depicted how humanized mice can be generated. Hu-PBL-SCID mice are generated transferring human PBLs into adult mice. Hu-SRC-SCID mice are generated transferring human stem cell into adult or newborn mice after previous irradiation. SCID-hu mice and BLT mice require transplantation of fetal liver and thymus tissue in to adult mice, while BLT mice also are reconstituted with human stem cells. Abbreviations: Hu-human; PBL-peripheral blood; SCID-immunodeficient mice lacking the catalytic subunit of a DNA-dependent protein kinase; SRC-scid repopulated cells; BLT-bone, marrow, liver, thymus. Taken from Shultz et al., 2012.

3.3. Next generation humanized mice

The first step on the agenda of generating humanized mice for biomedical research, particularly HIV research, can be considered as successfully completed. Immunodeficient mouse strains supporting high human cell engraftment and moreover, the differentiation into various subsets of human immune cells over a long period of time, are available. Currently available humanized mouse models are capable of recapitulating key features of HIV infection with progression towards disease. Furthermore, first drug tests and vaccine studies as well as gene therapy approaches to prevent and limit HIV infection were successfully performed. However, in these available models the development, maintenance and function of many human hematopoietic cell types are suboptimal, and lead to incomplete responses of the innate and adaptive immune system. These conditions are mainly due to the reduced or absent cross reactivity of certain molecules (e.g. cytokines, growth factors) produced by the mouse host on the human cells that are required for hematopoietic and immune system development. Therefore, much effort has been made to improve these models to overcome these disadvantages.

Improvement of humanized mice by genetic expression of human genes

Different protocols have been used to overcome limitations such as poor mouse-to human cross-reactivity, insufficient education, maintenance and activation of human cells as well as limited migration factors for human immune cells in the xenogeneic environment. Exogenously delivery of diverse human cytokines or growth factors to humanized mice enhanced engraftment and response of the targeted cell type (Shultz et al., 2005; Chen et al., 2009; van Lent et al., 2009; O'Connell et al., 2010; Huntington et al., 2011; Hu et al., 2011; Pek et al., 2011). However, continuous application of human cytokines or growth factors is hardly feasible for studies requiring large groups of mice. Thus, humanized mice genetically expressing human cytokines in the genome of recipient mice were developed (Billerbeck et al., 2011; Rathinam et al., 2011; Willinger et al., 2011; Rongvaux et al., 2011; Brehm et al., 2012; Takagi et al., 2012). Different techniques are available to generate genetic modified mice. In general, the technique of *overexpression* of cytokines under the control of an ubiquitously active promoter has to be used with caution. Abnormal expression of a cytokine can induce nonphysiological or adverse effects on the development and function of the human immune system in mice (Nicolini et al.,

2004). In contrast, using the *knock in technology*, where the human gene directly replaces the mouse gene and is driven by the mouse promoter, resulted in more physiological expression of the encoded protein enhancing the development of the human cell lineage targeted by that specific factor. However, adverse effects were also observed (Strowig et al., 2011; Willinger et al., 2011; Rathinam et al., 2011; Rongvaux et al., 2011). Although some murine cytokines do not exert their functions on human cells, many of the genetically expressed human factors cross-react with mouse cells that could cause unexpected phenotypical changes in the mouse (Manz et al., 2007).

Additionally, immunodeficient mouse strains have been developed to minimize the reactivity of human immune cells against host tissue. Such strains include NSG mice lacking *major histocompatibility* (MHC) class I (Strowig et al., 2009; Jaiswal et al. 2009; King et al., 2009; Shultz et al., 2010; Covassin et al. 2011) or class II molecules (Danner et al., 2011; Suzuki et al., 2012). These mice were specifically designed to reduce xenogeneic GvHD, and to improve the education of human cells in the mouse thymus as well as the communication of human cells towards better adaptive immune responses.

4. The human immune system

4.1. Origin and development of the immune system

All cells of the immune system are components of the blood referred to as white blood cells or leukocytes. All blood cells derive from a pluripotent *hematopoietic stem cell* (HSC) in a process during embryonic and adult stages called *hematopoiesis*. In mammals, HSCs originate from mesodermal precursors and are among the first cell types to emerge during embryogenesis (McGrath et al., 2005). *Embryonic hematopoiesis* involves multiple anatomical sites (extraembryonic yolk sac, intraembryonic aorta–gonad–mesonephros region, placenta), most of which are not involved in *adult hematopoiesis*. HSCs arise and migrate between these multiple sites and seed the fetal liver being the predominant site of embryonic hematopoiesis. In the fetal liver, HSCs undergo dramatic expansion and differentiation before

migrating into the bone marrow (BM) after birth (Johnson et al., 2005). The BM contains a specialized environment that regulates the balance of HSC and comprises the stem cell niche mediating life-long *adult hematopoiesis*. By definition, HSCs are a type of adult stem cells capable both of unlimited self-renewal and differentiation into all mature peripheral blood cell types (Lemischka, 1991; Spangrude et al., 1991). Hematopoiesis occurs in a hierarchical fashion in the red marrow of the BM. HSCs give rise first to multipotential progenitors and then to precursors with varying commitments to multiple or single pathways in the lymphoid or myeloid compartment. Fig. 8 gives an overview of the lineages generated during hematopoiesis. HCSs develop either into common myeloid progenitors giving rise to dendritic cells, granulocytes, erythrocytes and thrombocytes or into common lymphoid progenitors that give rise to the lymphoid lineage including natural killer (NK-) cells, T-cells and B-cells. Immune cells from the *myeloid progenitors* develop and mature in the BM and subsequently migrate into the bloodstream where they circulate throughout the body. Mast cells, dendritic cells and monocytes (then called macrophages) migrate into tissues where they perform their functions. Immune cells of the *lymphoid lineage* originate in the BM from common lymphoid progenitor cells. B-cells continue their maturation in the BM, while T-cells migrate to the thymus to mature. NK-cells are capable of maturing in the thymus or other lymphoid organs but primarily, they mature in the BM (Sun et al., 2011). After completion of maturation, lymphoid cells enter the blood stream and circulate through peripheral lymphoid tissues such as lymph nodes or spleen where they function to initiate adaptive immune responses.

The human hematopoiesis is a very complex and highly regulated process. Various human cytokines, growth factors and nuclear (transcription) regulatory factors account for the meticulous regulation and are required for human HSC development (Orkins, 2000). As noted previously, murine factors do not entirely fulfill these requirements hampering the reconstitution of immunodeficient mice with human HSC (Rongvaux et al., 2013). As a matter of course, this representation simplifies hematopoietic development but should be sufficient in understanding the key features of human hematopoiesis. Still, the overall model of hematopoiesis is not fully available. This description followed the simplified “classical model” but also there is evidence for a “myeloid-based model” in which there are different precursors identified (Kawamoto et al., 2009).

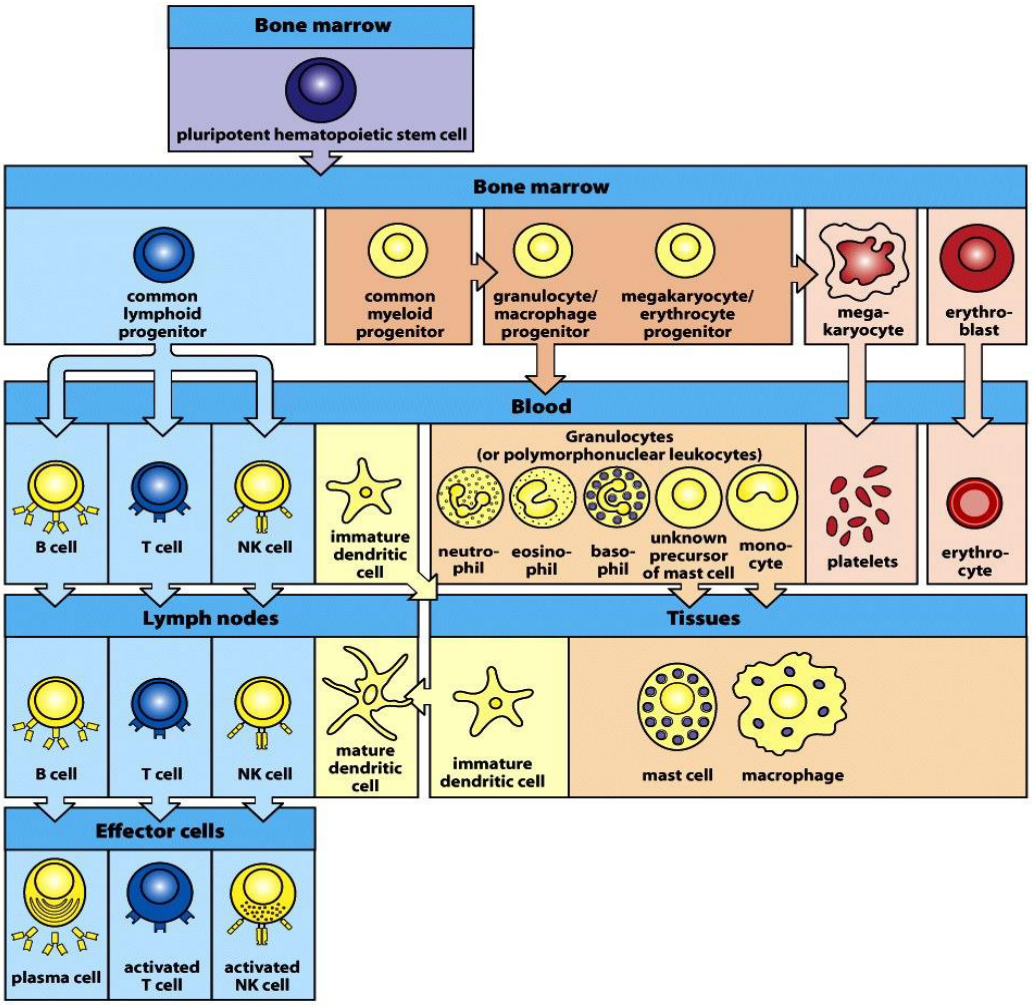

Fig. 8: Overview of the human hematopoiesis.
Starting with a pluripotent hematopoietic stem cell (HSC), all common progenitors of the lymphoid or myeloid lineage develop in the bone marrow (BM). Lymphoid progenitors give rise to T-, B- and NK-cells while myeloid progenitors develop into dendritic cells, granulocytes, thrombocytes, erythrocytes and monocytes. Taken from Murphy et al., 2008

4.2. The innate and adaptive immune system

The term *immunity* is defined as resistance to various infectious diseases such as HIV infection. The collection of cells, tissues and molecules mediating resistance to infections is summarizes as *immune system*. The orchestrated reaction of all components of the immune system is denoted as *immune response*. The human immune system consists of several layers that provide a protective shield against infectious agents.

The **first layer** is a *physical barrier* compiled by skin, mucosa, saliva, stomach acid as well as flushing action by urine and tears that should stop infectious agents before entering the body.

The **second layer** of host defense mechanism is the ***innate immune system*** that nonspecifically but rapidly controls and clears invading pathogens. It consists of the *complement system*, a system made of soluble plasma protein, and also unique cell subsets including phagocytes, cytolytic cells and professional antigen presenting cells. Innate immune cells are mostly derived from the *myeloid lineage* of hematopoiesis. Innate immune cells use an array of pattern recognition receptors to detect patterns associated with bacteria, viruses or parasites. These patterns relate to carbohydrate, protein or lipid structures that are unique to pathogens, but normally not produced in human cells (Murphy et al. 2008). Neutrophils, eosinophils and basophiles are termed granulocytes and are referred to as polymorphonuclear lymphocytes containing irregular shaped nuclei and cytoplasmic granules. *Neutrophils* are the most abundant granulocytes. They are recruited to inflammatory sites and are capable of phagocytosing and enzymatically digestion of microbes. *Eosinophils* are important for combating antibody coated multicellular parasites, such as helminthes. Also, they contribute to pathologic processes in allergic diseases. *Basophils* share structural and functional similarities with mast cells. They can be recruited to tissue sites and contribute to immediate hypersensitive (allergic) reactions. *Mast cells*, together with eosinophils and basophils, orchestrate allergic responses by releasing histamine and active agents (Geering et al., 2013). *Macrophages* are an important first defense in innate immunity. They differentiate within tissues from circulating *monocytes*. Activated macrophages phagocytose, engulf and kill microorganisms by releasing digesting enzymes. Also, they act as general scavenger cells in the body clearing dead cells and cell debris. They induce inflammation by the release of pro-inflammatory cytokines that recruit cells of the innate and adaptive immune response. Furthermore, *natural killer (NK-) cells* belong to the innate immune system, although they are derived from the lymphoid lineage of hematopoiesis. NK-cells belong to the group of cytotoxic lymphocytes with distinctive granular cytoplasm. They provide unspecific but rapid responses to intracellular infected or abnormal cells like tumor cells and also activate phagocytic innate immune cells (Sun et al, 2011). NK-cells secrete several chemokines and cytokines,

such as interferon-γ (IFNγ), to antagonize HIV infection via noncytolytic control. *Dendritic cells* (DCs) belong to a phagocytic cell type but are not meant for clearing microorganism, as macrophages, but function as professional antigen-presenting cells. DCs take up pathogens and display their antigens on their surface so that naïve T-cells will recognize invading pathogens and become activated. Thus, they are important for the initiation of adaptive immune responses to protein antigens and built the bridge between innate and adaptive immune system (Heuzé et al., 2013).

The **third layer** of defense is termed the ***adaptive immune system***. The adaptive immune system develops more slowly and mediates the following, even more effective defense against infections. It consists of T- and B-lymphocytes (known as cell-mediated immunity) derived from lymphoid lineage and their products such as antibodies (known as humoral immunity). This third layer of defense provides protection against extracellular and intracellular infections that had been successful in crossing the first and second layers of defense. Fig. 9 shows an overview of the components of the innate and adaptive immune system. T- and B-lymphocytes are the most important cells of the adaptive immune system with very distinct functions.

B-lymphocytes develop and mature in the BM from progenitor B-cells. The early phase of development is characterized by immunoglobulin (Ig) rearrangements and dependent on interactions with BM stromal cells but not antigens. It ends in an immature B-cell carrying a cell surface IgM antigen receptor. Immature B-cells undergo negative selection processes by which those immature B-cells are removed that highly bind to self-cell surface antigens derived from the body's own proteins. Subsequently, surviving immature B-cells emerge into the periphery maturating to express IgD and IgM. Mature B-cells are activated in secondary lymphoid organs, such as the spleen, by encounter with their specific foreign antigen. Activated B-cells proliferate and differentiate into either plasma cells producing antibodies specific for the foreign antigen or into memory B-cells (ten Boekel et al., 1995; Ghia et al, 1998).

T-lymphocyte progenitors develop in the BM but mature in the thymus. The maturation of T-cells is similar to the orderly and stepwise development of B-cells but also contains unique phases. These phases are marked by changes in the expression of surface proteins, such as the T-cell co-receptor complex CD3 and the

co-receptors CD4 or CD8 which reflect the state of functional maturation (Borowski et al., 2002). When immature T-cells enter the thymus they lack these characteristic surface proteins for mature T-cells and their receptor genes are unrearranged ("double-negative T-cells"). Subsequent interactions with thymic stroma cells trigger the initial phase of differentiation along the T-cell lineage pathway. Immature T-cells start to rearrange the α and β chain genes of the T-cell receptor genes leading to immature T-cells expressing CD4 and CD8. These double-positive T-cells undergo selection processes in the thymus that is highly dependent on major histocompatibility complex class I and II (MHC). Thymic stromal cells express MHC I and II molecules carrying self-peptides (Benz et al., 2004). The T-cell receptor of $CD4^+CD8^+$ T-cells recognizes MHC I or II molecules that present self-antigens. Those that are compatible with self-MHC receive survival signals (positive selection), whereas those that interact too strongly with self-antigens are removed by negative selection, similar to the B-cell development (Zerrahn et al., 1997). This process is tremendously important to educate maturating T-cells to eliminate infected cells that only present foreign peptides on MHCs to protect against self-destruction (Anderson et al., 1996). After positive selection, surviving T-cells mature into single positive $CD4^+$ T-helper-cells (when encountered MHC II) or cytotoxic $CD8^+$ T-cells (when encountered MHC I) that leave the thymus to circulate in the periphery. Once mature, T-cells encounter specific foreign antigens in lymphoid organs and are activated to proliferate and migrate to the site of infection to eliminate infected cells.

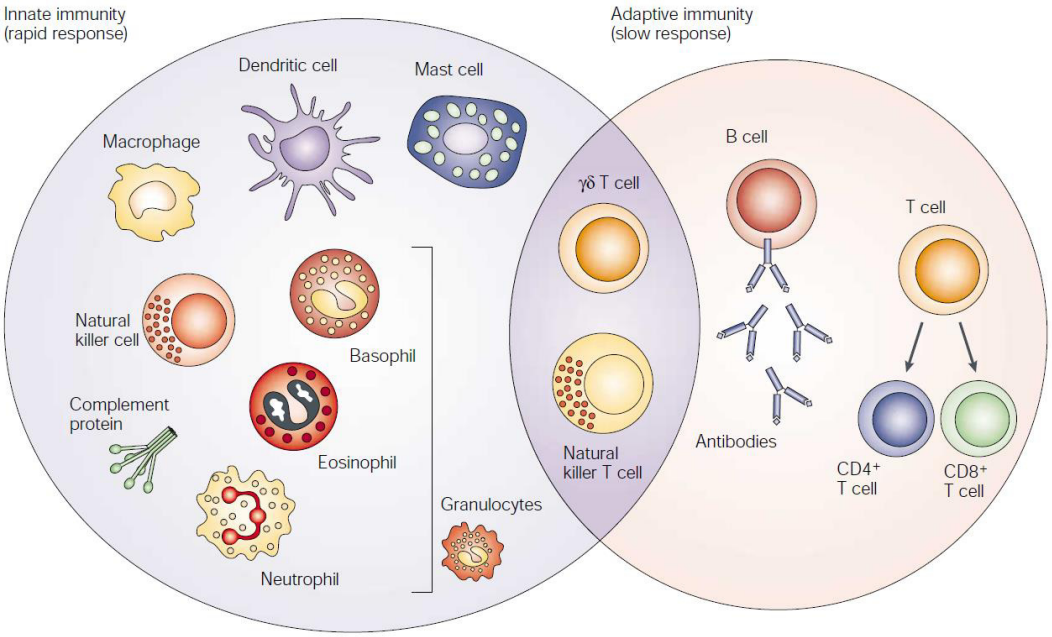

Fig. 9: Components of the innate and adaptive immune system
Distinct cell types belong to the innate immune system and are separated from the adaptive immune system. Natural killer T-cells as well as $\gamma\delta$ T-cells are believed to bridge both types of immune system. The complement system at the innate site and antibodies at the adaptive site summarize the humoral immune system. Taken from Dranoff et al., 2004

4.3. Adaptive immune responses

Adaptive immune responses play a crucial role in immunity and consist of cell mediated immune responses against intracellular infectious agents and humoral immune responses against extracellular infectious agents. After initial response to specific pathogens, adaptive immune responses create immunological memory, leading to an enhanced response to subsequent encounters with that same pathogen. This process is the basis of vaccination and cannot be comprised by innate immunity. In the following, typical adaptive immune responses are described.

Cell-mediated immune responses

Cell-mediated immunity is the arm of adaptive immune responses combating intracellular infections. This type of immunity is mediated by T-lymphocytes. Two types of intracellular infections can be distinguished. First, those pathogens that are phagocytosed and survive in vesicles of the host cell and second those, which enter the host cell via receptors on the surface and reside within the cytoplasm, like HIV.
Responses of T-cells to cell-associated antigens consist of a series of sequential steps including antigen recognition and activation resulting in increased numbers of antigen specific and effector T-cells (Dustin, 2003). After the maturation into single positive naïve T-cells, $CD4^+$ or $CD8^+$ T-cells leave the thymus and circulate in the periphery. During an infection, the migration of naïve T-cells into lymphoid organs is directed by chemokines produced by previous acting innate immune cells, such as DCs or macrophages. They capture and phagocytose pathogens and subsequently load their antigens to MHCs. When naïve T-cells encounter these antigen-presenting cells in the lymphoid organ, they are activated to perform effector functions. $CD4^+$ T-cells are activated by recognizing antigens on MHC II, whereas $CD8^+$ T-cells are activated by recognizing MHC I associated antigens. Once naïve T-cells are activated, they differentiate into effector T-cells.

Activated $CD8^+$ T-cells differentiate into cytotoxic T-lymphocytes (CTLs) and are important in the defense of intracellular pathogens (Weninger et al., 2002). They kill any infected cell by binding to a death inducing receptor, and also by releasing granzymes and perforin into the target cell. These enzymes activate caspases inducing target cell apoptosis and thereby eliminating the reservoir of infection.

In contrast, *activated CD4⁺ T-cells* differentiate into various effector cells with distinct functions (Weninger et al. 2002; Seder et al., 2003). The main subsets of effector CD4⁺ T-cells are T_H1, T_H2, T_H17 and regulatory T-cells (T_{reg}) distinguishable by the cytokines they secrete, however, the most acute response is mediate by T_H1 and T_H2 subsets (Mosmann et al., 1997). T_H1 CD4⁺ T-cells have a dual function. First, they activate macrophages that harbor intracellular infections resulting in increased microbicidal activities of phagocytes and killing of the ingested pathogen. Second, they provide co-stimulatory signals to antigen-activated B-cells enhancing antibody production and class switching. In comparison, T_H2 CD4⁺ T-cells provide similar functions to B-cells; however B-cells are stimulated to primarily secrete IgE antibodies, important for parasitic infections and allergy. Both effector cells, T_H1 CD4⁺ T-cells and CTLs, as well as NK-cells, produce and secrete high amounts of specific cytokines, such as *interferon* γ(IFNγ). Its principle functions are immunostimulatory and immunomodulatory effects to innate and adaptive immune responses (Krug et al., 2003). It mainly functions to activate macrophages to further support eradication of infection.

Humoral immune responses

Humoral immunity is the second arm of adaptive immune responses combating extracellular pathogens or toxins. This type of immunity is mediated by antibodies produced by B-lymphocytes. Antibodies have three main ways to contribute to immunity. First, antibodies bind to extracellular pathogens or toxins and thus prevent their spread and entry into the cell. This process is called *neutralization*. Second, antibodies can bind to pathogens and mark them for phagocytotic cells to destroy them. This process is called *opsonization*. Third, antibodies can coat pathogens and thus *activating proteins of the complement system*. Together, antibodies are key mediators in humoral immune responses against extracellular pathogens but also enhance the innate immune system (Zabel et al., 2013).

Mature B-cells that develop and maturate in the BM circulate throughout the body where they are activated by antigen encounter in blood or lymphoid tissues. Similar to T-cells, after antigen encounter they migrate into lymphoid organs where activation is completed. Depending on the type of antigen, B-cells need a second signal for full activation and differentiation into effector cells (Liu et al., 1991). B-cells encountering *thymus-dependent (TD) antigens* require two signals for activation. The first signal is

delivered through binding to the TD antigen and the second signal is delivered by a cognate $CD4^+$ T helper cell that was primed before with the same TD antigen and recognizes TD antigen loaded MHC II on the B-cell. This occurs after antigen encounter when activated T- and B-cells migrate to specialized zones of lymphoid tissues where they meet. In contrast, B-cells that bind *thymus-independent (TI) antigens* do not need T-cell help because the second signal can be delivered by the TI antigen itself. After activation of mature B-cells, they migrate to form germinal center where they proliferate and differentiate into plasma cells that secrete antibodies (Moser et al., 2006). Antibodies circulate in blood and lymph where they perform their functions to eradicate infections.

The innate and adaptive immune system with all its cells and components perfectly match to eliminate invading pathogens most efficient and rapidly so that no infection ever would have a change to conquer the whole body. In fact, some viruses, especially HIV, developed nice strategies to circumvent the highly complex human immune system.

4.4. Antiviral host factors

During the initial stage of HIV infection, a complex network of innate immune factors is activated. Immune cells express a number of inflammatory proteins including cytokines, chemokines and antiviral restriction factors.
Among the cytokines, *interferons* (IFNs) play the major role in virus infection and confer the first defense (Yamamoto et al., 1986). Type I IFNs (IFN-α, -β, -ε, -κ, and -ω) are the innate cytokines produced by innate immune stimuli of virus infected cells and have multiple properties including induction of immune activation, enhanced antigen presentation, and antiviral activity. Type II IFN, such as IFN-γ is secreted by T-cells under certain conditions of activation and by NK-cells. Although originally defined as an agent with direct antiviral activity, the properties of IFN-γ include regulation of several aspects of the immune response: the stimulation of bactericidal activity of phagocytes, the stimulation of antigen presentation through MHC class I and II molecules, the orchestration of leukocyte-endothelium interactions, effects on

cell proliferation and apoptosis as well as the stimulation and repression of a variety of genes whose functional significance remains obscure (Farrar et al., 1993)

Antiviral restriction factors are early, potent, and specific cellular blocks against retroviral replication. They are germ line encoded factors that mediate a cell intrinsic immune response and are part of an immune repertoire in absence of previous exposure. A series of anti-HIV restriction factors were discovered recently.

Apolipoprotein B editing catalytic polypeptide (APOBEC3) is a member of the cytidine deaminase family and mutates cytidine to uridine in negative sense single stranded DNA by deamination resulting in guanosine to adenosine hypermutation in positive sense viral cDNA. Thereby, HIV cDNA is vulnerable to nuclease degradation (Harris et al., 2003; Mangeat et al., 2003). However, HIV-1 viral infectivity factor (Vif) protein inhibits the packaging of APOBEC3G in virus producer cells (Marin et al. 2003; Yu et al., 2003). The *tripartite motif-containing 5* (TRIM5) is another restriction factor implicated in early steps of HIV replication. TRIM5 functions as E3 ubiquitin ligase and recognizes motifs within the viral capsid. Hence, the uncoating process of HIV in the cytosol is interrupted. Reverse transcription of the viral genome and its transport into the nucleus does not occur (de Silva et al., 2011; Pertel et al., 2011). The glycosylated type II transmembrane protein *tetherin* (THN) restricts HIV transmission from one cell to another and is upregulated by type I IFNs. It prevents budding of newly formed virus particles from plasma membrane of HIV-1 infected cells. Tethered virus particles are subjected to endocytosis and degraded in lysosomes. However, the viral protein unique (vpu) of HIV interacts directly or indirectly with tetherin and reduces its expression at the surface (Neil et al., 2006; Rong et al., 2009; Kuhl et al., 2010). The myeloid cell specific restriction factor, *SAM-domain HD-domain containing protein 1* (SAMHD1) restricts HIV-1 replication in noncycling, resting cells. SAMHD1 decreases the intracellular desoxyribonucleotide level resulting in an early post-entry restriction at the level of reverse transcription (Goldstone et al., 2011; Baldauf et al., 2012). Furthermore, studies have shown that HIV infection as well as innate immune response to viral infection could be controlled by 20–22 nucleotide long *noncoding host RNA molecules* (micro RNAs, miRNAs). These miRNAs control gene expression by binding to the 3’ UTR region of the target mRNAs. They can regulate the expression of both cellular and viral genes. For example, distinct differences in miRNA profiles have been reported in HIV-1 infected peripheral blood mononuclear cells compared to control. Anti-HIV-1 miRNAs exert negative effects on

the viral replication [115]. However, HIV has also evolved viral miRNA to counterattack the host machineries. Some viral miRNAs are expressed and regulate viral as well as host gene expression to facilitate virus replication and establishment of latency (Bartel et al., 2004; Triboulet et al., 2007; Huang et al., 2007; Wang et al., 2009; Nathans et al., 2009; Sun et al., 2012; Houzet et al., 2012).

5. Aim of this work

HIV vaccine preclinical testing is difficult because HIV's only relevant hosts are humans and no correlates of protection are known. Usually, monkeys infected with the simian immunodeficiency virus (SIV) are used as surrogated models whose results can only partially be adapted to the human disease. Novel humanized mice should be established capable to be utilized in preclinical testing of HIV vaccines or drugs. In this context, humanization of mice should be performed with human peripheral blood mononuclear cells (PBMCs) as well as human hematopoietic stem cells (HSC). In order to generate a robust humanized mouse model with efficient human adaptive immune responses, immune deficient mice (NOD Rag1$^{-/-}$$\gamma$c $^{-/-}$) expressing human MHC class II (HLA-DQ8) on a mouse class II deficient background (A$\beta^{-/-}$) should be used. In these animals, the human HLA-DQ8 should interact with the matching T-cell receptors of transferred human lymphocytes and therefore should support the functionality of the transferred human cells in mice. Furthermore, reconstitution with human hematopoietic progenitor cells should support the development and maturation of human immune cells in the humanized thymus, such that human cells will not recognize mouse cells as foreign. Different protocols of humanization with PBMCs and HSCs should be tested and optimized with regard to the engraftment of human cell subsets and the establishment of a functional human adaptive immune system. Consequently, humanized mice should be infected with HIV. For the evaluation of this model for its application in preclinical testing, HIV pathogenesis as well as HIV specific immune responses should be monitored.

II. Material and methods

6. Material

6.1. Laboratory Equipment

Equipment	Type	Company
Agarose gel apparatus	Mini Horizontal Submarine Unit	Hoefer (Holliston, USA)
Autoclave	Varioklav	H+P (Oberschleissheim)
Cell counter	Z1 Coulter Particle Counter	Beckman Coulter (Brea, USA)
Centrifuges	RC 26 Plus (Rotor SLA-1500) Eppendorf 5810R (Rotor A-4-62) Biofuge fresco (Rotor 3325B) Eppendorf 5415C (Rotor F-45-18-11) Galaxy MiniStar Biofuge primo R (Rotor 7590) Megafuge 1.0 R Eppendorf Concentrator 5301	Heraeus Sorvall (Hanau) Eppendorf (Hamburg) Heraeus Sorvall (Hanau) Eppendorf (Hamburg) VWR (Darmstadt) Heraeus Sorvall (Hanau) Heraeus Sorvall (Hanau) Eppendorf (Hamburg)
Clean Bench	Sterilgard III Advanced	The Baker Company (Sanford; USA)
COBAS® TaqMan® 48 Analyzer	Quantitative real time RT PCR for determination of HIV Titer	Roche (Mannheim)
Counting Chamber	Neubauer	Brand (Wertheim)
Coverplate	Shandon	Thermo Shandon Limited (Astmoor, Runcorn Cheshire, USA)
Ear puncher	DF 401	Aesculap (Tuttlingen)
Flow cytometer	BD LSR II and BD SORP	BD (Heidelberg)
Freezing container	5100 Cryo 1°C "Mr. Frosty"	Nalgene Labware
Ice machine	AF80	Scotsman (Vernon Hills, USA)
Incubator	BBD 6220	Hereaus Sorvall (Hanau)
Microplate reader	GENios Microplate Reader	(Tecan)
Microscope	Axiovert 25	Carl Zeiss AG (Göttingen)
Microwave	-	Bosch (Gerlingen-Schillerhöhe)
N_2 storage tank	Chronos/Apollo	Messer Group (Sulzbach)
Pipet Boy	pipetus®	Integra Biosciences (Fernwald)
Power Supply	Power-Pac 300 Power-Pac 3000	BioRad (München) BioRad (München)
Refrigerator Freezer	4°C/-20°C -80°C	Liebherr (Biberach) Heraeus Sorvall (Hanau)
Rotation microtome	Leica RM2255	Leica
Scales	LA1200S TE214S-OCE	Sartorius (Göttingen) Sartorius (Göttingen)
Spin tissue processor	STP-120	Thermo Fisher, Mikrom
Thermocycler	Professional Thermocycler	Biometra (Göttingen)
Thermomixer	Compact or comfort	Eppendorf (Hamburg)
Tissue block system	System 88	Medite (Burgdorf)
UV detection apparatus	Gel iX Imager	Intas (Göttingen)
Vacuum aspiration	Vacuboy	Integra Biosciences (Fernwald)
Veterinary inhalational anesthesia apparatus	Matrix	Midmark (Versailles, USA)
Vortexer	Vibrofix VF1 electronic	IKA (Staufen)
Water bath	System 1068	GFL (Burgwedel)

6.2. Consumables

Consumable	Type	Company
Blood collection tubes	EDTA (lavender) Serum (gold)	BD (Heidelberg)
Cell culture flask	T25, T75, T175	Greiner (Kremsmünster, Austria)
Cell culture plates	6-, 24-, 96-wells	Sarstedt (Nümbrecht)
Cell strainer	40 µm, 75 µm Filcon 70 µm	BD (Heidelberg) Keul (Steinfurt)
Centrifugal unit	Nylon membrane filter, 0.45 µm	VWR
Cover slip	24 x 50 mm	Menzel (Braunschweig)
Cryovials	1.8 ml	Greiner (Kremsmünster, Austria)
Dissecting set	diverse	VWR (Darmstadt)
ELISA cover plate	25 µm, PE, adhesive	Roth (Karlsruhe)
ELISA plates	96 well, high binding capacity	BD (Heidelberg)
FACS tubes	5ml Micronics 1.4 ml	BD (Heidelberg) Integra Biosciences (Fernwald)
Glass Pasteur pipettes	150 mm, #612-1701	VWR (Darmstadt)
Glass slide	Superfrost Ultra Plus	Menzel (Braunschweig)
Gloves	Latex	Braun (Sempach, Switzerland)
LeucoSep tubes	50 ml	Greiner (Kremsmünster, Austria)
MACS column	LS	Miltenyi (Bergisch Gladbach)
Microliter pipets	10 µl, 200 µl, 1000 µl	Eppendorf (Hamburg)
NanoDrop	2000c	Thermo Fisher (Schwerte)
Needle (cannula)	27G, 30G (U100 insulin)	Braun (Sempach, Switzerland)
Petri Dish	35 mm, Nunc™ Cell Culture	Thermo Fisher (Schwerte)
Pipet tips	1 ml, 200 µl, 20 µl	Eppendorf (Hamburg)
Pipets with filter	1 ml, 200 µl, 100 µl, 10 µl	Nerbe Plus (Winsen/Luhe)
Plastic pipets	50 ml, 10 ml, 5 ml	Greiner (Kremsmünster, Austria)
Reaction tubes	1.5 ml	Eppendorf (Hamburg)
Reagent tubes	15 ml and 50 ml PP tubes	Greiner (Kremsmünster, Austria)
Restrainer mice	Type A, 100mm x 32 mm	G&P Kunststofftechnik (Kassel)
Skin disinfection	Desderman	Schülke & Mayr (Norderstedt)
Surface disinfection	Terralin	Schülke & Mayr (Norderstedt)
Surgical mask	Coldex	Attends (Schwalbach)
Syringes	1 ml, 5 ml, 10 ml HIV infection: Insyte-N Autoguard; 0.7 x 14 mm	Braun (Sempach, Switzerland) BD (Heidelberg)

6.3. Chemicals

Chemicals	Type	Company
Acetic Acid	CH_3COOH	Roth (Karlsruhe)
Acetone	$(CH_3)_2CO$	Merck (Darmstadt)
Agarose	SeaKem® ME	Lonza AG (Köln)
Ammonia	liquid	Merck (Darmstadt)
Ampicillin (Sodium Salt)	-	Roth (Karlsruhe)

Citric acid	$C_6H_8O_7$	Merck (Darmstadt)
Dimethylsulfoxide	DMSO; Hybrid-Max	Sigma-Aldrich (Taufkirchen)
Eosin	-	Merck (Darmstadt)
Ethanol	CH_3CH_2OH	Materiallager (Paul-Ehrlich-Institut)
Ethylenediaminetetraacetic acid	EDTA	Merck (Darmstadt)
Formaldehyde	37%	Sigma-Aldrich (Taufkirchen)
Haematoxylin	-	Serva (Mannheim)
Hydrochloric acid	37%, HCl	Merck (Darmstadt)
Hydrogen peroxide	H_2O_2	Sigma-Aldrich (Taufkirchen)
Isoflurane	-	Baxter (Unterschleißheim)
Isopropanol	Propan-2-ol; C_3H_7OH	Materiallager (Paul-Ehrlich-Institute)
Methanol	CH_3OH	Materiallager (Paul-Ehrlich-Institute)
Paraffinum Liquid	-	Merck (Darmstadt)
Paraformaldehyde	PFA	Merck (Darmstadt)
Potassium chloride	KCl	Sigma-Aldrich (Taufkirchen)
Potassium phosphate monobasic	KH_2PO_4	Sigma-Aldrich (Taufkirchen)
Propanol	$CH_3CH_2CH_2OH$	Materiallager (Paul-Ehrlich-Institute)
Sodim chloride	NaCl	Sigma-Aldrich (Taufkirchen)
Sodium azide	NaN_2	Merck (Darmstadt)
Sodium phosphate dibasic	Na_2HPO_4	Sigma-Aldrich (Taufkirchen)
Tris-acetate	TAE	Sigma-Aldrich (Taufkirchen)
Tween 20	-	Sigma-Aldrich (Taufkirchen)
Water	H_2O	Materiallager (Paul-Ehrlich-Institute)
X-Gal	-	Roth (Karlsruhe)
Xylene	$C_6H_4(CH_3)_2$	Merck (Darmstadt)

6.4. Supplements

Supplements	**Type**	**Company**
Ampicillin (Sodium Salt)	Amp	Roth (Karlsruhe)
Bovine serum albumin	BSA	Sigma-Aldrich (Taufkirchen)
Brefeldin A (BFA)	B7651-5MG	Sigma-Aldrich (Taufkirchen)
Fetal Calf Sera	FCS; 10% in cell culture media	Biowest (Renningen)
Heparin5000 U/ml	#L6510	Biochrom (Berlin)
Human Flt-3L	#W1400950010	Biochrom (Berlin)
Human Interleukin-6	#RIL6I	Sigma-Aldrich (Taufkirchen)
Human SCF	#W1885950010	Biochrom (Berlin)
Human TPO	#W1975950010	Biochrom (Berlin)
Interleucin-2	IL-2; #I2644-10UG	Sigma-Aldrich (Taufkirchen)
Ionomycin	10634-1MG	Sigma-Aldrich (Taufkirchen)
L-Glutamin, 200 mM	1% in cell culture media	Lonza AG (Cologne)
Mounting medium	ImmunohistoMount Entellan Roti-Histokitt	Sigma-Aldrich (Taufkirchen) Merck (Darmstadt) Roth (Karlsruhe)
Penicillin/Streptomycin	P/S	Invitrogen (Carlsbad, USA)

Phorbol myristoyl acetate	PMA; P81391MG	Sigma-Aldrich (Taufkirchen)
Phytohemagglutinin	PHA	Sigma-Aldrich (Taufkirchen)
Stem Reginin 1 (SR-1)	Hydrochloride, #ab142174	Abcam (Burlingame,USA)
T4 DNA Ligase	400000 U/ml	NEB (Frankfurt)
Taq polymerase	5 U/µl	Qiagen (Hildesheim)
Tetanus toxoid	for ELISA	Section 3/2, Paul-Ehrlich-Institute

6.5. Enzymes and Reagents

Enzyme/Reagent	**Type/Ingredients**	**Company**
DNA ladder	GeneRuler™ 1 kb Plus DNA Ladder 50 bp Ladder 2 log Ladder	Fermentas (Schwerte) NEB (Frankfurt Main) NEB (Frankfurt Main)
Gel Red	Nucleic acid stain, #41003	Biotium (Hayward, USA)
Peroxidase Substrate	True Blue for Immunohistochemistry	KPL (Maryland, USA)
Peroxidase Substrate	TMB Substrate for ELISA	Interchim (Montlucon, France)
Red Blood Cell Lysis	BD FACS lysing solution	BD (Heidelberg)
Restriction enzymes	BamHI (100000 U/ml) NdeI (100000 U/ml)	NEB (Frankfurt)
T4 DNA Ligase	400000 U/ml	NEB (Frankfurt)
Taq polymerase	5 U/µl	Qiagen (Hildesheim)
Tetanus toxoid	for ELISA	Section 3/2, Paul-Ehrlich-Institut
Trypan Blue	0.4 %; use 1:1 dilution	Sigma-Aldrich (Taufkirchen)
Vaccine TetanolPur®	Tetanus Toxoid, PZN: 2038952	Novartis Behring (Marburg)

6.6. Buffer and Media

Buffer/Media	**Type/Ingredients**	**Company**
Cell Culture Media	DMEM	Lonza AG (Cologne)
Citrate-EDTA buffer for target retrieval	10mM Citric Acid 2mM EDTA 0.05% Tween 20 pH 6.2	-
Density gradient medium	Lymphoprep™ Density: 1.077 g/mL Isolation of PBMCs	Stem Cell Technology (Köln)
DNA loading buffer	6x, #R0611	Fermentas (Schwerte)
Eosin solution	300 ml eosin stock solution 300 ml 96% ethanol 1 ml acetic acid 300 ml H_2O	-
Eosin stock solution	10 g eosin 500ml 96% ethanol 500 ml H_2O	-
FACS Buffer	10g BSA (2 %), 20 ml 0.5 M EDTA pH 8.0 (20 mM), 0.15 g NaN_3 in 500 ml PBS, sterile filtration	-

Fixation medium for TZM-bl assay	1x PBS 1 % Formaldehyde (37%) 0.2 % Glutaraldehyde (25%), sterile	-
HCL-Ethanol	576 ml 96%0 ethanol 524 ml H_2O 2,8 ml 37% HCL	-
KardasewitschSolution	200 ml 25% ammonia liquid 800 ml 70% ethanol	-
KCM solution	Transformation of bacteria 500 mM KCl 150 mM $CaCl_2$ 250 mM $MgCl_2$	-
LB agar	5 g/l yeast extract 10 g/l pepton 10 g/ l Sodium chloride 12 g/l agar-agar in H_2O + 1 ml/l Ampicillin stock solution (100 mg/ml in H_2O)	Medienlabor (Paul-Ehrlich-Institute)
PBS	138 mM NaCl 2.7 mM KCl 1.5 mM KH_2PO_4 8.2 mM Na_2HPO_4 pH 7.1 with HCl, in H_2O, sterile	Medienlabor (Paul-Ehrlich-Institute)
PBS-T for immunohistochemistry	1 x PBS 0.05% Tween 20	-
Peroxidase Blocking Solution	for immunohistochemistry 3% H_2O_2 in PBS	-
Restriction enzyme buffer	NEB3	NEB (Frankfurt)
Staining medium for TZM-bl assay	1x PBS 0,2 M Potassium Ferrocyanide 0,2 M Potassium Ferricyanide 2 M MgCl2 0.4 mg/ ml X-Gal (dilution in DMSO) sterile	-
T4 DNA Ligase reaction buffer	10x	NEB (Frankfurt)
TAE	Running buffer agarose gel 40 mM Tris-acetate 1 mM EDTA pH 8.3	Medienlabor (Paul-Ehrlich-Institut)
TBS-T	Washing buffer for ELISA assays 50 mM Tris 150 mM NaCl 0.05% Tween 20 pH 7.6 with HCl, in H_2O, sterile	Medienlabor (Paul-Ehrlich-Institute)

6.7. Plasmids

Plasmid	Specification	Reference
pET15b	Expression plasmid with T7 promoter, T7 transcription start, His-Tag, MCS, T7 Terminator, lacI, Amp resistence	Novagen Plasmid card in the appendix
pET15b-huBLyS	Sequence of huBLyS cloned into pET15b between BamHI and NdeHI restriction sites	This work Plasmid card in the appendix

6.8. Human cells and cell lines

Human material	Specification	Company
Buffy Coat	~80 ml	German Red Cross Blood donor Service Baden-Wuertemberg-Hessen, Frankfurt; Prof. Dr. Halvard Bönig
Cord blood	~10-50 ml	Hospital Langen, Hessen
Mobilized human $CD34^+$ cells	$DQ8^+$ donors	German Red Cross Blood Donor Service Baden-Württemberg Hessen, Frankfurt; Dr. Eliza Wiercinszka
TZM-bl cells	#8129	NIH AIDS Reagent Program (Germantown, USA)

6.9. Bacteria and viruses

Bacteria/virus	Specification	Company
E.coli Top 10	Genotype: F- mcrA Δ(mrr-hsdRMS-mcrBC) φ80lacZΔM15 ΔlacX74 recA1 araD139 Δ(araleu)7697 galU galK rpsL (StrR) endA1 nupG	Invitrogen, Karlsruhe
HIV-1_{NL4-3}	Plasmid KS211 Paul-Ehrlich-Institut	Adachi et al., 1986
HIV-1_{SF162} (R5-tropic)	#276	NIH AIDS Reagent Program (Germantown, USA)
HIV-1_{SF2} (X4-topic)	#2525	NIH AIDS Reagent Program (Germantown, USA)
HIV-$2_{ROD/B148}$	Plasmid KS220, Paul-Ehrlich-Institut	Clapham et al., 1992

6.10. Antibodies

6.10.1. Flow cytometry

Antibody specificity	Fluorochrom	Source	Isotype	Clone	Company	Catalogue Number
CD14 human	Pacific Blue	mouse	Ig2a, κ	M5E2	BD Bioscience	#558121
CD16/CD32 mouse	Fc Block	rat	IgG2b, κ	2.4G2	BD Bioscience	#553142
CD19 human	PE Cy5	mouse	IgG1, κ	HIB19	BD Bioscience	#555414
CD3 human	APC	mouse	IgG1, κ	UCHT1	BD Bioscience	#555335
CD3 human	AmCyan	mouse	IgG1, κ	SK7	BD Bioscience	#339186
CD34 human	PE	mouse	IgG1, κ	563	BD Bioscience	#555761
CD4 human	APC Cy7	mouse	IgG1, κ	RPA-T4	BD Bioscience	#557871
CD45 human	PE	mouse	IgG1, κ	HI30	BD Bioscience	#555483
CD45 mouse	FITC	rat	IgG2b, κ	30-F11	BD Bioscience	#553079
CD5 human	APC	mouse	IgG1, κ	UCHT2	BD Bioscience	#555355
CD56 human	PE Cy5	mouse	IgG1, κ	B159	BD Bioscience	#555517
CD8 human	PE Cy7	mouse	IgG1, κ	RPA-T8	BD Bioscience	#557746
IFNγ human	APC	mouse	IgG1, κ	B27	BD Bioscience	#554702

6.10.2. Isotype controls

Isotype Control	Fluorochrom	Source	Clone	Company	Catalogue Number
Ig2a, κ human	Pacific Blue	mouse	G155-178	BD Bioscience	#558118
IgG1, κ human	PE Cy5	mouse	MOPC-21	BD Bioscience	#555750
IgG1, κ human	PE Cy7	mouse	MOPC-21	BD Bioscience	#557872
IgG1, κ human	APC Cy7	mouse	MOPC-21	BD Bioscience	#557873
IgG1, κ human	PE	mouse	MOPC-21	BD Bioscience	#554680
IgG1, κ human	APC	mouse	MOPC-21	BD Bioscience	#555751
IgG1, κ human	AmCyan	mouse	X40	BD Bioscience	#339185
IgG2b, κ mouse	FITC	mouse	27-35	BD Bioscience	#555742

6.10.3. ELISA

Antibody specificity	Dye	Source	Company	Catalogue Number
Human IgG, whole molecule	Peroxidase	Rabbit	Sigma	A8792
Human IgM/IgG	Peroxidase	Goat	Dianova	109-035-044

6.10.4. Immunohistochemistry

Antibody specificity	Source	Company	Catalogue Number
Human CD8 antibody [EP1150], C-term	Goat	Gene Tex (Irvine, USA)	GTX62092

6.11. Kits

Kit	Type and Catalogue Number	Company
Alanine Transaminase (ALT) ELISA	MaxDiscovery™ Alanine Transaminase Color Endpoint Assay #3460-08	BiooScientific (Austin, USA)
Avidin/Biotin Blocking Kit for immunohistology	#VEC-SP-2001	Burlingame (USA)
DNA Extraction	DNeasy Blood&Tissue Kit #69506	Qiagen (Hildesheim)
DNA extraction from agarose gel	NucleoSpin® Extract II Kit	Macherey-Nagel (Düren)
HIV Titer determination	COBAS® AmpliPrep/COBAS® TaqMan® HIV-1 Test, v2.0 #05212294190	Roche (Mannheim)
HLA DQ8 genotyping	HLA-DQB1*03 #101.214-24	Olerup SSP GmbH (Stockholm, Sweden)
IFNγ ELISA	VeriKine™ #41500-1	PBL Assay Science (Piscataway, USA)
Intracellular FACS staining	Cytofix&Cytoperm #554714	BD Bioscience (Heidelberg)
Plasmid DNA Maxi Preparation	NucleoBond® Xtra Maxi Plus	Macherey-Nagel (Düren)
Plasmid DNA Mini Preparation	GeneJET™ Plasmid Miniprep Kit	Fermentas (St. Leon-Rot)
Vario MACS Kits	huCD34$^+$ #130046702 huCD19$^+$ #130050301 huCD133$^+$huCD34$^+$ #130092882	Miltenyi (Bergisch-Gladbach)
Vectastain® ABC Kit (Peroxidase Rabbit IgG1)	#VEC-PK-4001	Burlingame (USA)

6.12. Software

Software	Purpose
BD FACSDiva™ Software Version 6.1.3	Flow Cytometric Data Analysis
FCS Express V4.0	Flow Cytometric Data Analysis
GraphPad Prism Version 5.04	Data Analysis
Microsoft Office Professional Plus 2010	Calculations, Data Analysis
VectorNTI Suite 9	Sequencing, Plasmid Cards

7. Methods

7.1. Microbiological methods

Microbiological work was done to multiply and clone plasmids. The nonpathogenic *E.coli* strain K12 was used and cultivated at 37°C.

7.1.1. Bacterial Growth

The growth of *E.coli* Top10 was done in 500 ml LB media in Erlenmeyer flask at 37°C on a shaking platform (220 rmp/min). The antibiotic ampicillin (100 µg/ml) was used for selection purposes. To yield single colonies, the bacteria suspension was plated on an agar plate containing ampicillin. The plates were incubated for at least 16h at 37°C. For analytical approaches, single colonies were picked with a sterile tip, and resuspended in 5 ml LB media containing ampicillin, and grown at 37°C/220 rpm/min.

7.2. Molecular methods

Molecular methods were used to clone the sequence of the human BLyS into an expression plasmid optimized for *E.coli*.

The *E.coli* codon-optimized sequence of huBLyS was purchased by GeneArt (Regensburg) in a carrying plasmid. This sequence (see appendix) was cloned into the plasmid pET15b. Due to a His-tag sequence in the pET15b vector, the protein huBLyS could be purified using Ni-columns. Expression, isolation and purification are described in the Bachelor's thesis by Dana Püschl (Uni Gießen, 2013).

7.2.1. Transformation of E.coli

Bacteria were transformed using the **KCM-method** or **heat shock**.

For the transformation using the **KCM-method**, 20 µl of the KCM-solution, 1 µl DNA (<100ng) and 79 µl H_2O were mixed and carefully mingled with 100µl of competent bacteria (Top10) thawed on ice. After 20 min incubation on ice, the mixture was incubated for 10 min at RT. Subsequently, the suspension was plated on agar plates containing ampicillin and incubated for 16h at 37°C. Single colonies were picked and grown in LB media for further analyses.

For the transformation using the **heat shock method**, 100 µl of competent bacteria were thawed on ice. 1.7 µl of 1.44 M β-mercaptoethanol were added, carefully mingled and incubated for 10 min. Every two min, the suspension was shaken carefully. 10 µl of the ligation mix was added and incubated for 30 min on ice. The uptake of DNA by the bacteria was forced by heat shock at 90°C for exactly 45 sec in a water bath followed by an incubation of two min on ice. Subsequently, the suspension was plated on agar plates containing ampicillin and incubated for 16h at 37°C. Single colonies were picked and grown in LB media for further analyses.

7.2.2. Preparation of Plasmid DNA from bacteria

The isolation and purification of plasmids from E.coli for analytical purposes (<10 µg DNA) was done with the GeneJET™ Plasmid Miniprep Kit (Fermentas) and for preparative purposes (<500 µg) with the NucleoBond® Xtra Maxi Plus Kit (Macherey-Nagel) according to the manufacturer's protocol.

7.2.3. Digestion of DNA with restriction enzymes

The restriction of DNA was done with restrictions enzymes (NEB) using the manufacturers protocol.

7.2.4. Isolation of DNA from agarose gels

DNA fragments separated by agarose gel electrophorese were cut with a scalpel under UV-light. The extraction was done with the NucleoSpin ® Extract II Kit (Macherey-Nagel) according to the manufacturer's protocol.

7.2.5. Determination of DNA concentration

The concentration of extracted DNA was determined with the NanoDrop2000 (Thermo Scientific). 1 µl of the DNA solution was applied. Elution buffer was used as the blank value before measurement.

7.2.6. Ligation

For the ligation of DNA fragment, varying ratios of insert and vector were used. The ligation was done in a 20 µl volume using T4-DNA-ligase (NEB) and the T4-DNA-

ligase reaction buffer (NEB). 100 ng of the vector were used for ligation. The insert was added at a molar ratio of 1:1; 1:3; 1:5 and 1:10. The incubation was done at 16°C o/N. As a control of ligation, the vector without insert was ligated.

7.2.7. Sequencing of DNA

Sequencing was carried out by Eurofins MWG (Ebersberg). 1 to 3 µg of DNA was lyophilized in the vacuum centrifuged. T7 and T7term primer (Eurofins MWG) were used for forward and reverse sequencing. Analyses were done with the software Vector NTI.

7.3. Genotyping of DQ8$^+$ donors

DQ8 genotyping of human cells (PBMCs, CD34$^+$ cells from cord blood) was done using the Olerrup SSP Kit (II.1.7.) according to the manufacturers' protocol. DNA was isolated with the Qiagen DNeasy Blood&Tissue Kit (II.1.7.) and the concentration was determined with the NanoDrop. A concentration of 20-30 ng/µl was used for the PCR.

7.4. Cell culture methods

7.4.1. Isolation of huPBMCs from buffy coat and cord blood

Isolation of human peripheral blood mononuclear cells (huPBMCs) from peripheral blood (buffy coat) or human cord blood was done by density gradient centrifugation with Lymphoprep^{TM} in LeucoSep^{TM} tubes according to the manufacturers' protocol. 80 ml of the Buffy Coat was filled up to 200 ml with PBS. Cord blood was diluted 1:2 with PBS. 24 ml of the dilution was used for one LeucoSep^{TM} tube filled with 15 ml Lymphoprep^{TM}.

Residual buffy coats from whole blood donations of were obtained from the German Red Cross Blood donor Service Baden-Wuertemberg-Hessen (Frankfurt) with informed written consent by healthy volunteers. Cord blood was obtained from newborns after delivery.

7.4.2. Hematopoietic stem cell isolation by MACS

The Magnetic cell sorting (MACS) procedure is based on magnetic beads which are extremely small, superparamagnetic particles and in columns containing an

optimized matrix to generate a strong magnetic field when placed in a permanent magnet. Human lymphocytes isolated from cord blood were incubated with magnetically labeled huCD133$^+$ or huCD34$^+$ MicroBeads and loaded onto a MACS® LS-Column which was placed into the magnetic field of a MACS Vario Separator. The magnetically labeled huCD133$^+$ and huCD34$^+$ cells are retained within the column while unlabeled cells run through. After removing the column from the magnetic field, the magnetically retained huCD133$^+$ and huCD34$^+$ cells can be eluted as the positively selected stem cell fraction. The MACS procedure was done according to the manufacturers' protocol. Mobilized huCD34$^+$ cells from GCS-F treated adult donors were obtained from the German Red Cross Blood Donor Service Baden-Württemberg Hessen, Frankfurt (Dr. Eliza Wiercinszka) and purified using the same protocol. The purity of isolated huCD133$^+$ and huCD34$^+$ cells was assessed as percentage of huCD34$^+$huCD45$^+$ cells by FACS analyses, which was usually 95-99%.

7.4.3. Cell counting

The viability of cultured cells was determined by trypan blue exclusion. Trypan blue is a vital dye whose reactivity is based on the negatively charged chromopore binding proteins. This is not taken up by cells unless the membrane is damaged. Therefore, all the cells which exclude the dye are viable. The cell suspension was diluted with trypan blue solution (10 µL cells + 10µl trypan blue; dilution factor 2) and set up in a Neubauer chamber (10 µl each side). Viable cells were then counted under a light microscope. The concentration of cells per ml is calculated using the mean for each square: cell density [cells/ml] = counted cells x dilution factor x 10^4. The total cell number = cell density x volume [ml].

7.4.4. Cell cultivation

All human cells were maintained at 37ºC in an incubator with 5 % CO_2 and 90 % humidity. Human cells were grown in DMEM complemented with 10% heat inactivated fetal calf serum (FCS) and 1 % L-Glutamine (Gln). For huPBMC cultures, the medium was supplemented with antibiotics (100 U/ml penicillin and 100 mg/L streptomycin). Cells were grown in tissue culture flask (T25, T75 or T175) with a cell density between 1x10^5 and 1x10^6 cells/ ml.

7.4.5. Cryopreservation and thawing of CD34$^+$ cells

At least 1x10^6 huCD34$^+$ cells were re-suspended with at least 900 µl of freezing medium (90 % heat-inactivated FBS, 10 % DMSO). For more than 1x10^6 cells, more freezing medium was used accordingly. The cell suspension was transferred into a cryogenic vial and placed at -80ºC overnight in a "Mr. Frosty". Finally, the cells were transferred to liquid nitrogen for long-term conservation.

To thaw cells a fast management is recommended. The cells were quickly placed at 37ºC until almost all were thawed. Immediately, medium was added to a Cryovials and all cells were transferred to a 50 ml conical. To wash the cells, the 50 ml conical was filled up with medium. The cells were spin down at 300 g for 10 min and the supernatant was aspirated. This washing step was repeated to remove DMSO completely. Lastly, the cells were re-suspended in medium according to the number of cells (II. 2.2.3.) and transferred to an appropriate culture flask or re-suspended in PBS for the repopulation of mice (II. 2.3.).

7.4.6. IFNγ production after ex vivo stimulation

Approximately 100 µl blood was drawn from the retro orbital sinus of mice and collected into EDTA-blood collection tubes (BD Biosciences). Human capillary blood was taken as positive control. Blood was diluted 1:1 with PBS. 2 ml of Lymphoprep^{TM} were filled into a sterile 5 ml FACS tube and the diluted blood was carefully overlaid. After a centrifugation step (20 min, 900g, without break), the interphase was collected and cells were washed twice with PBS (centrifugation: 10 min, 300 g). Cells were re-suspended in 200 µl of complemented DMEM and seeded into a 96 well plate. For the stimulation of cells to produce of IFNγ, 100ng/ml phorbol 12-myristate 13-acetate (PMA) and 500ng/ml Ionomycin were added to the cells. After 2h incubation, 1 µg/ml Brefeldin A (BFA) was added and the incubation was continued for another 4 h. BFA inhibits the protein transport from the endoplasmic reticulum to the Golgi apparatus and thus, IFNγ could be detected by intracellular flow cytometry (2.4.1.). Stimulated cells as well as non-stimulated cells or stimulated cells without BFA incubation were taken as controls for flow cytometric analysis.

7.4.7. Ex Vivo HIV infection of human cells isolated from humanized mice

After euthanization of mice, blood and spleens were collected. PBMCs from blood were isolated as previously described (2.2.6.) and single cell suspensions from spleens were prepared (2.4.1.2.). $3x10^6$/ml cells were seeded per well of a 24 well plate. To activate T-cells, 3 µg/ml phytohemagglutinin (PHA) and 50 U/ ml interleukin-2 (IL-2) was added. After 48 h incubation, PHA was removed by washing. Cells were transferred into a 50 ml conical tube, washed three times with medium (centrifugation: 300g, 5 min) and finally, the cell pellet was re-suspended with medium containing 20 U/ml IL-2. Subsequently, cells were infected with $3x10^3$ $TCID_{50}$ of HIV-1_{SF2} (X4-topic virus) and HIV-1_{SF162} (R5-tropic virus). Following an incubation period of 2-3 h in the incubator, the viral inoculum was removed by two washing steps with medium containing 20 U/ml IL-2 (centrifugation: 300g, 5 min). Finally, the infected cells were incubated for six days in a 24 well plate before the production of new infectious vial particles was analyzed by using TZM-bl indicator cells (2.2.8.).

7.4.8. TZM-bl assay

TZM-bl is a HeLa cell line stably expressing human CD4, CCR5 and endogenous CXCR4-receptor. It was generated by introducing separate integrated copies of the ß-galactosidase genes (β-gal) under the control of the HIV-1 promoter and the Tat response element. Beta-gal expression is induced through the presence of HIV-1 Tat protein following infection. The TZM-bl indicator cell line enables simple and quantitative analysis of HIV-1 and -2 using β-gal as a reporter (NIH AIDS reagent program, 2013).

TZM-bl cells were required to be seeded subconfluently in a 24 well plate. Therefore, ~$6x10^4$ TZM-bl cells/ml were seeded per well of a 24-well plate one day before the assay. The next day, the supernatants of infected cell cultures were filtered through a 0.45 µm nylon membrane filter (VWR) and 500 µl were added to the TZM-bl cells. If necessary and possible, repetitions were included as well as dilutions of the supernatants. Following an incubation period of 48 h, the medium was aspirated and 500 µl of the fixation medium was carefully added to the cells. After 5 min of incubation at RT, the fixation medium was aspirated and the cells were washed twice with 1 ml PBS. 1 ml of staining solution was added and the cells were incubated for 50 min at 37^0C. Subsequently, the staining solution was aspirated and cells were

washed twice with PBS. 1 ml of PBS was added and infected cells visible by a blue staining were analyzed under the microscope.

7.5. Animal experiment techniques

All mice used in the experiments were bred in the animal center of the Paul-Ehrlich-Institute (Langen, Hessen, Germany). NRG mice (NOD.Cg-Rag1tm1Mom Il2rgtm1Wjl/SzJ) were purchased by the Jackson Laboratory (#007799; Bar Harbor, Maine, USA). The health status of the animal center was monitored based on the guidelines of the Federation of European Laboratory Animal Science Associations (FELASA). Mice were bred and held in individual ventilated sterile cages (max. 5 mice/ cage) and fed with standard rodent diets and water *ad libitum*. All experiments were performed according to the FELASA animal law techniques and statutory orders.

7.5.1. Retro-orbital sinus blood collection

The retro-orbital sinus blood collection is intended for blood collection. Not more than 10% of the blood volume was removed at one sampling. Isoflurane gas was used for anesthesia during the blood collection. Mice were placed into the chamber of the precision vaporizer. Induction of anesthesia was done with up to 5% isoflurane. Mice sedated within 1-2 min. After induction, anesthesia was maintained by 1-3% of isoflurane. Blood collection tubes and glass Pasteur pipets were prepared. The mouse was taken out of the chamber and restrained by the scruff method to prevent severe injury to the eye or surrounding tissues. The back of the neck and the loose skin of the head were tightened with the thumb and middle finger.

The retro-orbital sinus is the site located behind the eye at the medial or lateral canthus. The tip of the glass Pasteur pipet was placed at the medial canthus of the eye under the nictitating membrane. A short thrust past the eyeball entered the membrane of the sinus. The eyeball itself remained uninjured. As soon as the sinus was punctured, blood entered the tubing by capillary action. When the allowable amount of blood was collected, the tube was withdrawn and slight pressure with a piece of gauze on the eyeball was used to prevent further bleeding. After one min, mice recovered from anesthesia.

7.5.2. Intravenous injection

Human lymphocytes were delivered intravenously for humanization without anesthesia. To induce vascular dilatation, mice were carefully warmed under a heating lamp for several minutes. The animal was placed in a restraint device and the tail was wiped with 70% ethanol. The tail was then stabilized between the thumb and forefinger of the hand. The injection was attempted starting at the middle or slightly distal part of the tail. With the tail under tension, the sterile needle (27G needle, 1 ml syringe) was inserted, beveled up and inserted approximately parallel and at least 3 mm into the vein. When the material was injected in a slow, fluid motion and blanching of the vein occurred when the needle was positioned properly. When the required amount was injected, the needle was withdrawn and slight pressure with a piece of gauze on the injection site was used to prevent further bleeding.

7.5.3. Intraperitoneal injection

Human lymphocytes as well as the anesthetic drugs prior to HIV infection was delivered intravenously. The mouse was restrained by the scruff method and the ventral side of the animal was exposed. The head was tilted down at a slight angle and the injection site was wiped with 70% ethanol. The sterile needle (27G needle, 1 ml syringe) was placed beveled up in the lower right or left quadrant of the animal's abdomen and inserted at a 30° angle. The material was injected in a fluid motion.

7.5.4. Irradiation and intrahepatic injection

For humanization of newborn mice, human stem cells were injected into the liver. Before humanization with stem cells, mice required to be irradiated to establish a nice in the bone marrow for the human stem cells. Shortly after birth, newborns received a dosage of 4Gy irradiation. Following irradiation, usually after 16 h (overnight), newborns were reconstituted with human stem cells. Hypothermia was used for anesthesia. Pups were placed into a petri dish and packed in crushed ice. After 10 min hypothermia was induced. Upon sufficient anesthesia each pup was inoculated, immediately with human cells in a 50 µl volume. The mouse body was softly fixed and restrained between the thumb and forefinger exposing the liver. With a 30G needle and a 100U insulin syringe, a maximum of 50 µl of cells in PBS were injected

into both, the right and left lobe of the liver. After the procedure, pups were kept at RT until recovery and later placed back to their mother.

7.5.5. HIV infection

The infection of humanized mice with HIV was done under anesthesia warranting very high safety conditions for the personnel. Mice were anesthetized by intraperitoneal injection (27G needle, 1 ml syringe) of 0.1ml ketamine/xylazine cocktail at a dosage of 100 mg/kg ketamine and 20 mg/kg xylazine. During anesthesia, sterile petrolatum ophthalmic ointment was smeared onto the eyes to prevent drying during anesthesia. After 10-15 min anesthesia was induced. Mice were infected with HIV using the Insyte-N Autoguard (0.7 x 14 mm). The needle was injected i.p. and withdrawn from the tube so that the tube remained inside the mouse. Then, the mouse was infected with HIV using a 1 ml syringe. HIV was injected in a fluid motion and the syringe and the tube were withdrawn from the mouse. Until recovery from anesthesia, mice were placed under a heating lamp and monitored.

7.5.6. Euthanasia

Euthanasia refers to the practice of intentionally ending the life of laboratory animals. In this work, mice were sacrificed by using cervical dislocation following anesthesia with isoflurane. HIV infected animals were sacrificed by inhalation of CO_2 and subsequent cervical dislocation.

7.6. Immunological methods

7.6.1. Fluorescence Activated Cell Sorting

Fluorescence activated cell sorting (FACS) is a technique to characterize the phenotype of different cell types by analysis of cell surface membrane proteins or intracellular proteins.

7.6.1.1. Extracellular staining of human lymphocytes in murine blood

For the analysis of human immune cells, blood drawn from the retro orbital sinus (20 µl) was collected into EDTA-coated tubes. To block non-specific Fc receptor-

mediated antibody binding, 25 µl of the Fc block (diluted 1:25) were added to the blood samples, mixed and incubated for 20 min at RT. Subsequently, 1 µl of the required antibodies were added, mixed and incubated for 15 min at 4°C in the dark. Erythrocytes were lysed and cells were fixed at the same time by adding 900 µl of FACS lysing solution (BD Biosciences) and incubated 30 min at RT in the dark. Subsequently, cells were spin down (300g, 5 min), the supernatant was aspirated and the cell pellet was loosened by vortexing. Cells were washed twice or three times by adding 1 ml of FACS buffer followed by a centrifugation step (300g, 5 min). Cells were kept in ~100 µl FACS buffer at 4°C in the dark until analysis.

The appropriate dilution of the used antibodies was determined by previous titration. Human peripheral blood was used as positive staining control.

Control stainings with appropriate isotype-matched control antibodies were included to establish thresholds for positive staining and background linear scaled mean fluorescence intensity (MFI) values.

7.6.1.2. Isolation of human lymphocytes from mouse organs

For the analysis of human immune cells in mouse organs via extracellular staining, single cell suspensions were prepared.

The **spleen** and **lymph nodes** were placed into ice cold PBS into a 35 mm petri dish on ice. The organs were mashed with the puncher of a 5 ml syringe through a 40 µm mesh filter (BD Biosciences). The filter was rinsed with ice cold PBS and the suspensions was transferred into a 15 ml conical via a 70 µm Filcon (Keul).

Bone marrow cells were isolated from femur and tibia. One leg was collected and dissected from the pad. Fur, skin and muscles were removed. The bones were placed into ice cold PBS into a 35 mm petri dish on ice. With a cooled mortar and pestle, bones were crushed gently until the red bone marrow was suspended in PBS. Subsequently, the crushed suspension was filtered through a 40 µm mesh filter and extensively rinsed with ice cold PBS into a 50 ml conical. After a centrifugation step (300g, 10 min, 4°C), the supernatant was aspirated and the cell pellet was loosened. 15 ml of FACS buffer was added and the suspension was transferred into a 15 ml conical via a 70 µm Filcon (Keul).

PBS was exchanged for FACS buffer in every single cell suspension of all organs. After a centrifugation step (300g, 10 min, 4°C), the supernatant was aspirated and the cell pellet was loosened. The 15 ml conical was filled up with FACS buffer and

centrifuged. The cell pellet was resuspended in 1 ml FACS buffer and counted. $1x10^6$ cells of the single cell suspension in 100 µl FACS buffer were used for staining with antibodies following the previously described protocol (2.5.1.1.).

7.6.1.3. Intracellular IFNγ staining

Staining of intracellular molecules such as IFNγ requires the permeability for antibodies into the cell as well as a preserved cell morphology and intracellular antigenicity.

For the intracellular staining of IFNγ, up to 1 x 10^6 cells in 100 µl FACS buffer were used (see 2.2.6.). First, the extracellular staining was performed as described previously (2.4.1.1.). After the incubation with the extracellular antibodies the intracellular staining followed. For the intracellular staining the Cytofix&Cytoperm Kit (BD Heidelberg) was used according to the manufacturer instructions. 1 µl of the anti-human IFNγ antibody for 1 x 10^6 cells in 100 µL FACS buffer was used.

7.6.1.4. Settings of the flow cytometer and gating strategy

At least 10 000 events were acquired with an LSR II or LSR SORP instrument (BD Biosciences) using the FACS Diva Software. For the analysis of the data the software FCS Express Version 4 was used.

An important principle of flow cytometry data analysis is to selectively visualize the cells of interest while eliminating results from unwanted particles e.g. dead cells and debris. This procedure is called gating. The gating strategy used in this work is depicted in Figure 10. First, cells have been gated according to physical characteristics. For instance, subcellular debris and clumps can be distinguished from single cells by size, estimated by forward scatter (FSC). Also, dead cells have lower forward scatter and higher side scatter (SSC) than living cells. Lysed whole blood cell analysis show typical graphs for SSC versus FSC. The different physical properties of granulocytes, monocytes and lymphocytes in blood allow them to be distinguished from each other and from cellular contaminants. In this work, only lymphocytes and monocytes were of special interest. Hence, only these populations were included in the first gate (Fig. 10 A). Second, only single cells were included to the analyses. In addition to the human CD45 marker, for all analyses anti-mouse CD45 staining was included to allow for the exclusion of all murine hematopoietic

cells. Based on the huCD45 marker, all other human markers were analyzed (Fig. 10 A). Figure 10 B shows the hierarchy of the gates in the gating strategy.

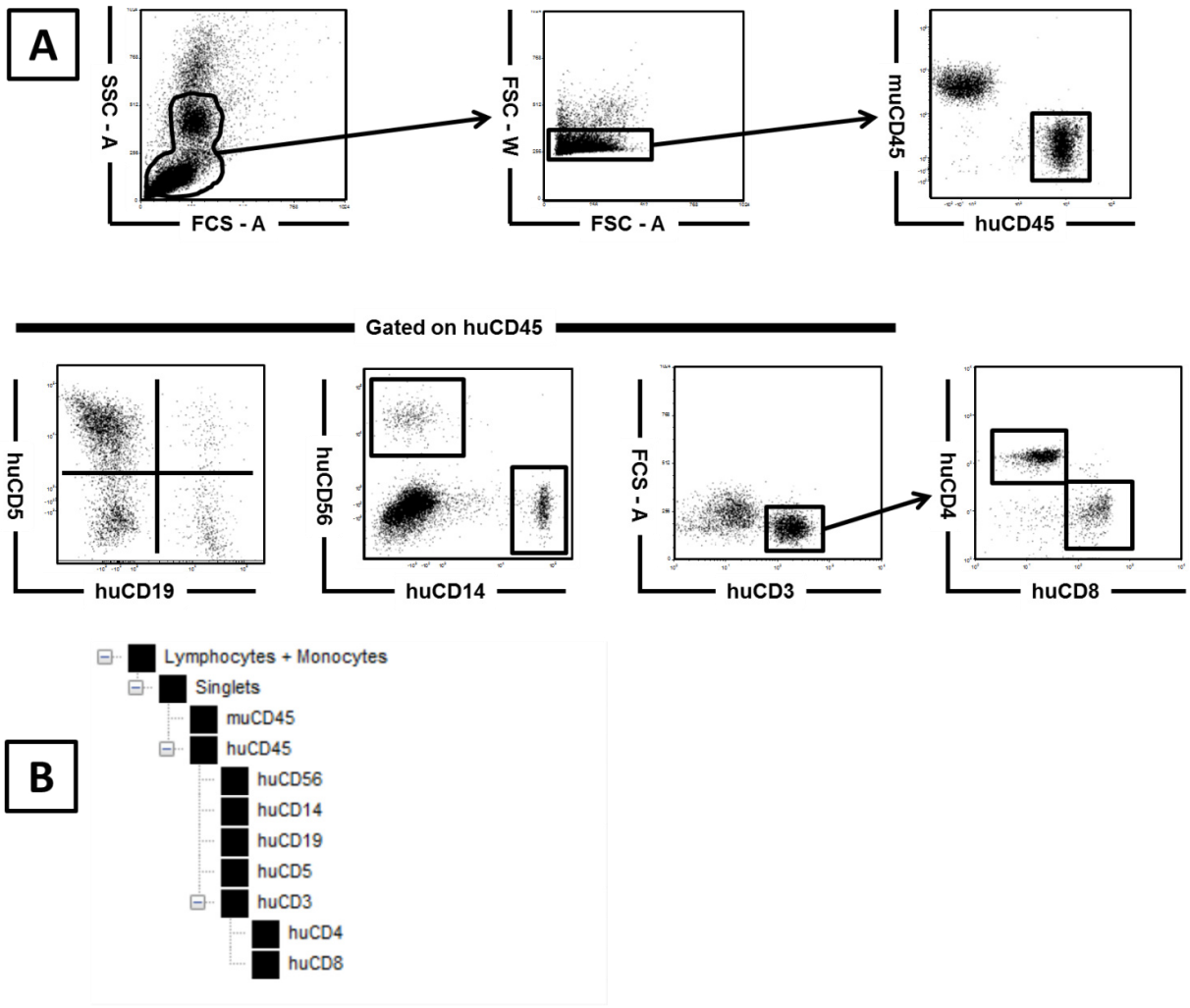

Fig. 10: Gating strategy in the flow cytometric analysis
Human and murine peripheral blood was mixed and stained with specific extracellular antibodies. In A, the used gating strategy is depicted. In B, the hierarchy of the gated used in the gating strategy is shown. Dot plot and hierarchy were taken from the software FCS Express.

7.6.2. Enzyme-linked immunosorbent assays (ELISA)

The enzyme-linked immunosorbent assay (ELISA) is a tool to identify the presence of a substance (antigen) based on antibody binding and enzymatic reaction of the substrate detectable with a photometer.

ELISAs for the analysis of **human IFNγ** and **ALT in serum** of mice were used according to the manufacturers' instructions of each kit.

7.6.2.1. Detection of tetanus toxoid specific human antibodies

The amount of tetanus toxoid specific human IgM and IgG antibodies after vaccination with the human vaccine TetanolPur® was analyzed. A 96 well plate was coated with the antigen. 100 µl of tetanus toxoid (1:1460 in 0.1 M $NaHCO_3$ (pH 8.2)) was applied to the wells and incubated o/n at 4°C. After the incubation period, the 96 well plate was washed twice with PBS/0.05 % Tween 20. To prevent unspecific binding, the plate was blocked 1h at RT with 150 µl PBS/1 % BSA per well. During the incubation time, the murine serum samples (1:2; 1:5; 1:10) were diluted in duplicates in PBS/1 % BSA. The blocking buffer was removed and 100 µl of the sample dilutions as well as the standard (duplicates) (section 3/2, Paul-Ehrlich-Institute) were applied to the wells. After an incubation period of 1.5-2h at RT on a rocking platform, the plate was washed twice with PBS/0.05 % Tween 20. 100 µl of the diluted antibodies (α-human IgG 1:5000 in PBS/1 % BSA ; α-human IgM/IgG 1:10000 in PBS/1 % BSA) were added to the wells and incubated for 1h at RT on a rocking platform. The antibody solution was removed and the plate was washed four times with PBS/0.05 % Tween 20. 100 µl of the TMB substrate were added and incubated for 5-10 min at RT in the dark. To stop the enzymatic reaction, 100 µl 2N H_2SO_4 were added. The optical density was determined at 450 nm wave length (reference 630 nm). Due to the known concentration of the dilutions of the standard curve, the amount of analyzed IgM and IgG antibodies was calculated.

7.7. Histology of mouse organs

Organs were removed from mice after death. After the fixation in 4% Formaldehyde in PBS o/n, organs were dehydrated in an infiltration automat using the following sequence: 30% ethanol for 30 min, 50% ethanol for 30 min, 70% ethanol for 60 min, 70% ethanol for 60 min, 90% ethanol for 60 min, 96% ethanol for 60 min, propanol for 120 min, xylol for 180 min, paraffin for 150 min. Subsequently, the paraffined organs were cut with a rotation microtome into 4 µm sections. The section were collected onto a glass slide and dried at 45°C. To deparaffinize the sections, the temperature was increased to 60°C for 30 min. The following sequence was used for deparaffinization: 2x 5 min xylol, 2x 5 min propanol, 5 min 96% ethanol, 4 min 96% ethanol, 2x 5 min 70% ethanol, 4 min Kardasewitsch, 1 sec. sop water, 5 min H_2O, 30 sec H_2O. In the following, the sections were stained with haematoxylin and eosin (2.5.1.) or immunohistochemically with antibodies (2.5.2.).

7.7.1. Haematoxylin and eosin staining (HE staining)

The haematoxylin and eosin (HE) staining is a general staining to distinguish nuclei (blue) and cytoplasm (pink to red).

The following sequence was used: 4 min haematoxylin, 1 sec. HCL-ethanol, 5 min running water, 90 sec. eosin, 3x 2 min 96% ethanol, 2x 2 min propanol, 4x 2 min xylol. Finally, the sections were covered with a cover slide and mounting medium (Entellan).

7.7.2. Immunohistochemical staining

Following deparaffinization, endogenous peroxidase activity was blocked using 3% H_2O_2 in PBS for 10 min. Afterwards the sections were washed 5 min with water. To retrieve the target for the antibody, the sections were incubated 30 min in citrate buffer (95°C) in a water bath. After the incubation, the citrate buffer was cooled until it became clear again (~15 min at RT). The sections were applied to the Shandon coverplate system and washed twice with PBS-T (filled up with buffer). The antibody staining (e.g. for huCD8) was done using the avidin/biotin blocking kit and the Vectastain® ABC kit according to the manufactures' instructions. Briefly, 200 µl anti-goat serum was applied to the coverplates and incubated for 20 min at RT. Next, 200 µl of the avidin blocking solution was applied and incubated for 15 min at RT. The coverplates were washed twice with PBS-T. 200µl of the biotin blocking solution were applied to the coverplates and incubated for 15 min at RT. 200µl of the primary antibody (e.g. αhuCD8; diluted 1:3000 in PBS) were incubated at 4°C o/n. Next, the sections were washed three times with PBS-T. The secondary antibody was incubated for 20-30 min at RT and subsequently washed twice with PBS-T. The before prepared Vectastain ABC reagent was incubating 30 min followed by two washing steps with PBS-T. The sections were incubated for 10 min in TrueBlue staining solution and rinsed with water. The sections were covered with a cover slide and Roti® HistoKitt and analyzed by light microscopy.

7.8. Determination of HIV Titer

Humanized mice that were infected with HIV-1 and -2, were determined for their viral load by measuring the HIV titer in serum (2.6.1.) In addition the presence of proviral HIV DNA was determined in the genome of human cells found in organs of mice

(2.6.2.). Both approaches were done with the *High Pure System Viral Nucleic Acid Kit* and the *COBAS® TaqMan® HIV-1 Test, version 2.0 (v2.0)* by Roche. This kit is an *in vitro* nucleic acid amplification test for the quantitation of Human Immunodeficiency Virus Type 1 (HIV-1) RNA in human plasma, using the for manual specimen preparation and the COBAS® TaqMan® 48 Analyzer for automated amplification and detection. The test can quantitate HIV-1 RNA over the range of 34 to $1x10^7$ copies/ ml. According to the manufacturer, this kit was especially designed for the analysis of HIV-1. However, it was found that the analysis of HIV-2 was also possible. The primers used for the analysis of HIV-1 contain highly conserved regions that can be found in HIV-2 as well. Hence, this kit was also used for the determination of HIV-2 titers and proviruses. In all runs, human plasma of HIV-negative donors as well as non-humanized HIV infected mice were used as controls.

7.8.1. Determination of HIV RNA copies in blood plasma

Murine plasma (at least 10 µl) was filled up to 550 µl with human negative tested plasma. 500 µl of this dilution was used for the assay. The determination of the HIV titer was done according to the manufacturers' instruction. Finally, the dilution factor was taken into account when the concentration was measured in HIV copies/ ml plasma.

7.8.2. Determination of the amount of integrated HIV DNA in human cells

Organs of HIV infected mice were collected and DNA was prepared using the DNA extraction kit *DNeasy Blood&Tissue*. Extracted DNA was eluted in 50 µl elution buffer. Afterwards, the amount of DNA was determined with the NanoDrop. 1µl of the eluted DNA was used for the determination of provirus. Instead of isolated HIV RNA, 1 µl of DNA from the organs was added to the master mix provided in the kit. As for HIV RNA Titer determination, the same program was used for the determination of proviral virus. Finally, the result of "HIV copies/ ml plasma" given by the Cobas TaqMan were converted into "proviral DNA per 1 ng DNA from organs" taking into account the used amount of DNA from the organs.

III. Results

8. Mouse strains used for humanization

Different immunodeficient mouse strains were used for their humanization with human peripheral blood mononuclear cells (huPBMCs) or human hematopoietic stem cells (huHSCs): **NRG Aβ$^{-/-}$ DQ8tg** as well as the crossing intermediates without the human DQ8 transgene, **NRG Aβ$^{-/-}$**. **NSG** and **NRG** mice were used as Aß$^{+}$ controls and were considered equivalent. The strain NRG Aβ$^{-/-}$ DQ8tg has no mouse MHC class II presented at the cell surface. In addition, both mouse strains carry the *human leucocyte antigen* (HLA)-DQ8 transgene (DQ8tg), as a substitute for the murine MHC II. Human alleles of both chains are present in the mice, DQA*0301 for the α-chain and DQB*0302 for the β-chain. Possessing this human MHC II transgene, these mouse strains can be categorized as the "next generation" mice for the generation of humanized mouse models (see section I.3.3).

9. Genotypes of DQ8tg mice

For the experiments animals with the distinct genotype NRG Aβ$^{-/-}$ DQ8tg were required. PCR-Genotyping (see 7.3) only detected the abundance of the DQ8tg but not if both of the alleles carry DQ8. Thus, back crossing of heterozygote animals was required (DQ8tg/? X wt/wt; DQ8tg=transgene, wt=normal, wildtype), until homozygote mice (DQ8tg/DQ8tg) could be obtained. However, Rag and Aβ deficiencies could be maintained by heterozygote breeding.

10. Phenotypes of DQ8tg mice

NRG Aβ$^{-/-}$ DQ8tg mice and the intermediate strains without DQ8tg, have a phenotype similar to NSG or NRG mice. They are albino mice with red eyes. Under sterile conditions they can have a life expectancy up to ~1.5 years. According to their genotype, these mice have a high degree of immunodeficiency. Due to their immunodeficiency, these strains do not respond to xenogeneic transplants which make them superior for humanization with human cells. Mice of the NSG background are very sensitive to irradiation while mice of the NRG background are radioresistant.

For the transfer of human stem cells mice need to be irradiated to clear the murine bone marrow to create a niche for human stem cells. Hence, only NRG A$\beta^{-/-}$ and NRG A$\beta^{-/-}$DQ8tg mice were used for reconstitution with human stem cells (see 13), while mice of NSG as well as NRG background were used both for the transfer of human PBMCs.

11. Identification of HLA-DQ8-positive blood donors

To identify donors for human DQ8-PBMCs, a cohort of voluntary blood donors was genotyped for their expression of HLA-DQ8. DNA was extracted from each donor's PBMCs after written consent and used in a *sequence specific primer polymerase chain reaction* (SSP-PCR) to genotype HLA-DQB1*03 in high resolution (see 7.3). In this test, 24 different primer mixes were used for DQB1*03 SSP subtyping. A donor expressing HLA-DQ8 (DQB1*03:02:01-05), requires the presence of specific PCR products of primer mixes 3 (135 bp), 4 (220 bp), 15 (135 bp) and 18 (175 bp), as well as correct internal controls in all primer mixes (Fig. 11). A donor who is not DQ8 positive has specific PCR products with primer mixes than those described (Fig. 12). The exact HLA genotype for HLA DQB1*03 can be identified with this PCR reaction, however solely HLA-DQ8 has been of fundamental interest. The HLA-DQB1*03 locus of 75 voluntary blood donors was genotyped in high resolution by SSP-PCR. In total, 75 voluntary blood donors were screened and seven (~9.3 %) were HLA-DQ8 positive. Interestingly, the frequency of humans positive for HLA-DQ8 (HLA DQB1*03:02) in Germany is ~17.3 %, in France 16.3 %, in Argentina 38 % and in Congo 1.1 % (http://www.allelefrequencies.net).

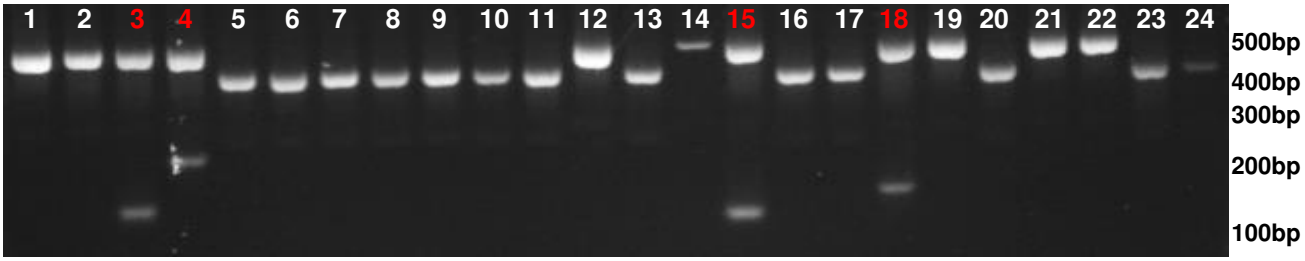

Fig. 11: SSP DQB1*03 PCR reaction of a DQ8 positive donor
To genotype donors carrying HLA-DQ8, a high resolution PCR of the HLA DQB1*03 locus was done. Internal control bands at 430 bp or 515 bp were present in every tested primer mix. The combination of specific PCR products in the primer mixes 3 (135 bp), 4 (220 bp), 15 (135 bp) and 18 (175 bp) proofed the HLA-DQ8 (HLA DQB1*03:02:01-05) genotype. PBMCs of donors with such SSP PCR pattern were used for humanization of DQ8tg mice.

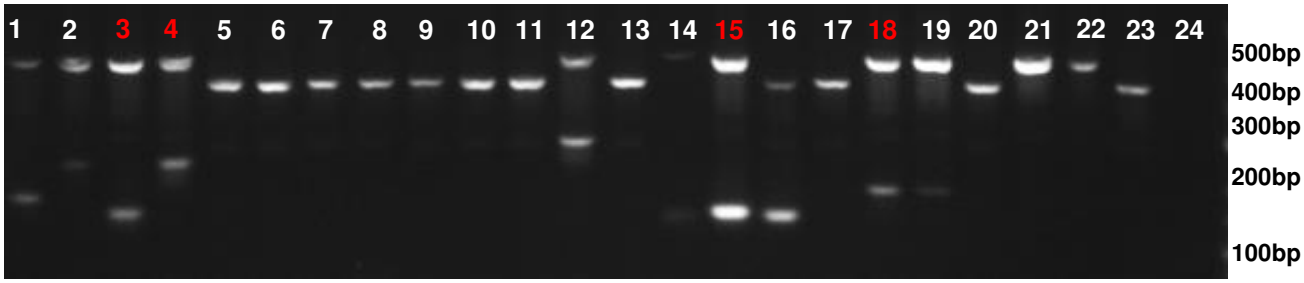

Fig. 12: SSP DQB1*03 PCR reaction of a donor negative for HLA-DQ8
The high resolution PCR of the HLA DQB1*03 locus showed the SSP PCR pattern of a donor who had other specific PCR products than required for the HLA DQ8 genotype. This donor did not carry HLA-DQ8 molecules and hence, its PBMCs were not used for humanization of DQ8tg mice.

12. Humanization with huPBMCs

12.1. The optimal amount and route to adoptively transfer huPBMCs

In order to establish an optimal protocol for the humanization with human PBMCs, different cell numbers and different routes of application were tested according to their repopulation kinetics and efficacies. In addition, transfer of mature human T cells causes graft versus host disease (GvHD) and limits the lifespan of the animals. Therefore time of survival was included into the considerations to establish the optimal engraftment conditions.

NSG mice were repopulated either intraperitoneally (i.p.) or intravenously (i.v.) with $1x10^7$ or $1x10^8$ huPBMCs, respectively. Every second day, starting at day five after human cell transfer, blood was collected for a period of fourteen following days. The percentage of all murine and human hematopoietic cells in peripheral blood, characterized by the expression of human CD45 (huCD45), was determined by FACS analysis (Fig. 13A-D). Murine CD45 cells (muCD45) in immunodeficient NSG mice are only progenitors of hematopoietic cells that fail to maturate due to their deficiency, whereas huCD45 cells cover all differentiated and mature human hematopoietic cells. After repopulation with human cells, the percentage of muCD45 cells decreased while huCD45 cells were increasing. This correlation could be found in all cases of repopulation (Fig. 13A, C-D). However, muCD45 cells did not decline when mice had only 0.1-0.5% huCD45 cells (Fig. 13B).
Repopulation kinetics and efficacies of huCD45 differed depending on the number of cells as well as route of transfer. Transferring huPBMCs i.v. (Fig. 13A and C) was

more efficient compared to i.p. (Fig. 13B and D). Fourteen days after repopulation, the frequency of huCD45 cells in NSG mice transferred i.v. with $1x10^7$ huPBMCs was ~20% (Fig. 13A) and ~70% after transfer of $1x10^8$ huPBMCs, respectively. In contrast, NSG mice transferred i.p. with $1x10^7$ huPBMCs (Fig. 13B) did not show any repopulation with huCD45 cell in the blood. Mice transferred with $1x10^8$ huPBMCs (Fig. 13D) did not reach a repopulation higher than 10%. In addition, mice were monitored for signs of disease following cell transfer. Upon ~50% engraftment with huCD45, mice started to develop disease symptoms of *graft-versus-Host-Disease* (GvHD) (see II.3.3.). The higher the number of huPBMCs transferred and the more rapid mice reached engraftment levels higher than 50%, the more prompted GvHD development in mice (see II.3.3.). Hence, i.v. transfer of $5x10^7$ huPBMCs was used for humanization of immunodeficient mice in further experiments.

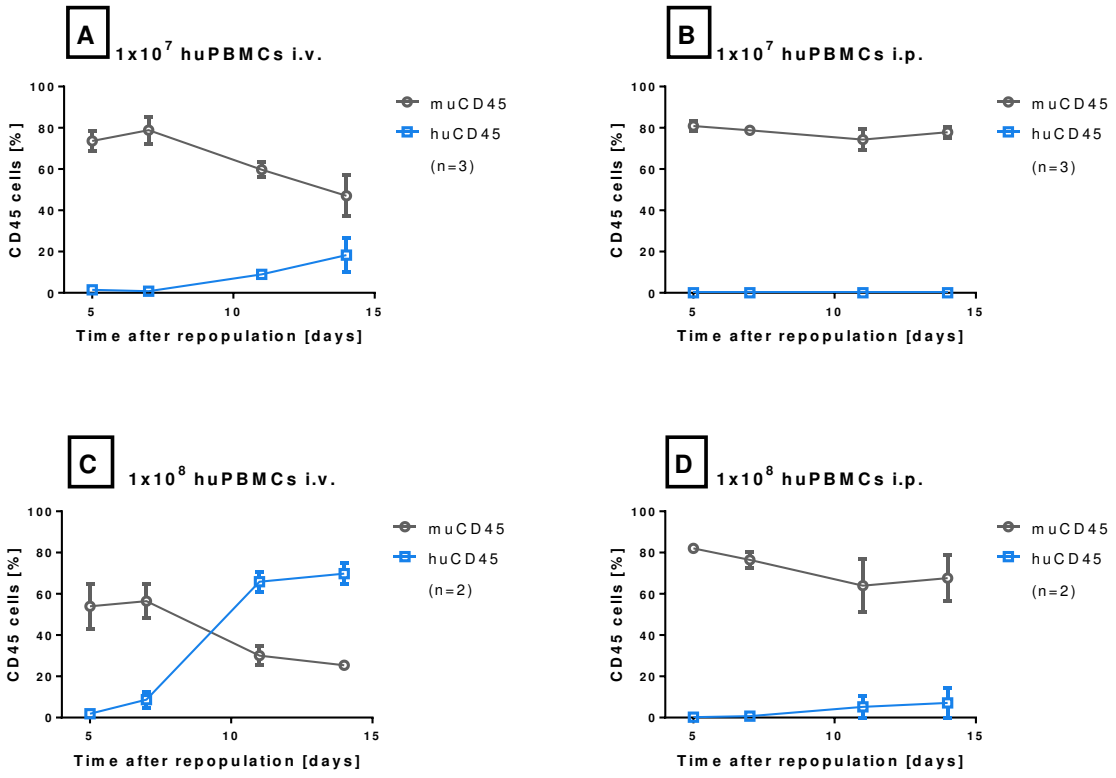

Fig. 13: Comparison of different approaches to repopulate NSG mice
Human PBMCs were transferred intravenously (i.v.) with $1x10^7$ (A) or $1x10^8$ (C) or intraperitoneally (i.p.) with $1x10^7$ (B) or $1x10^8$ (D) into NSG mice. The frequency of murine (blue) and human $CD45^+$ cells (grey) was determined at indicated points after repopulation for 14 days.

12.2. Kinetics and efficacy of matching human DQ8$^+$ cells in huDQ8tg mice

Immunodeficient mice carrying a human MHCII transgene might be superior for humanization because they might show less GvHD might enhance human cell engraftment. In order to study this topic, NRG A$\beta^{-/-}$ DQ8tg and littermates without the huDQ8tg, NRG A$\beta^{-/-}$ mice, as well as control mice NSG and NRG were repopulated with 5x10^7 huDQ8-PBMCs i.v. and analyzed for their repopulation efficacy with huCD45 cells. NRG and NSG mouse strains were used interchangeably due to the same phenotype of immunodeficiency. Figure 14 shows the repopulation kinetics of mice following the transfer of huDQ8-PBMCs from two different DQ8$^+$ blood donors (Fig. 14A and B). Figure 14A shows the analysis of huCD45 cells in NRG A$\beta^{-/-}$ DQ8tg, NRG A$\beta^{-/-}$, and NSG mice repopulated with huDQ8-PBMCs of donor 1. Fig. 14B shows the same analysis with mice repopulated with PBMCs from a different DQ8$^+$ donor. In all mice, the percentage of huCD45 cells increased quickly within the first 9–12 days following huDQ8-PBMC transfer. Interestingly, the repopulation kinetic of huCD45 cells in the mice was similar comparing the two different DQ8$^+$ donors. NRG A$\beta^{-/-}$ DQ8tg and NRG A$\beta^{-/-}$ mice possessed similar engraftment rates of up to 70% (Fig. 14A) while NSG mice always showed slightly less engraftment. However, this divergence was significant (P=0.0279) until d33, when all NSG mice left the experiment. In comparison, NRG A$\beta^{-/-}$ DQ8tg and NRG mice repopulated with huDQ8-PBMC of a different donor (Fig. 14B) showed significant differences in their engraftment rates until d21 (P=0.0125) and also throughout the entire time of the experiment (P=0.0040). NRG A$\beta^{-/-}$ DQ8tg possessed engraftment rates of up to 80% huCD45 cells while NRG mice only reached 55% of huCD45 cells. It appears that NRG A$\beta^{-/-}$ DQ8tg mice tolerated huDQ8-PBMCs better than NRG mice but also variations due to alternating DQ8$^+$ donors could account for variability in repopulation efficiencies of distinct mouse strains.

Taken together, huDQ8tg mice of NSG or NRG background, their littermates lacking huDQ8tg and NSG/NRG control mice showed similar kinetics and efficiencies of human cell engraftment following adaptive transfer of huDQ8-PBMCs. However, huDQ8tg mice showed a slightly enhanced engraftment of human cells.

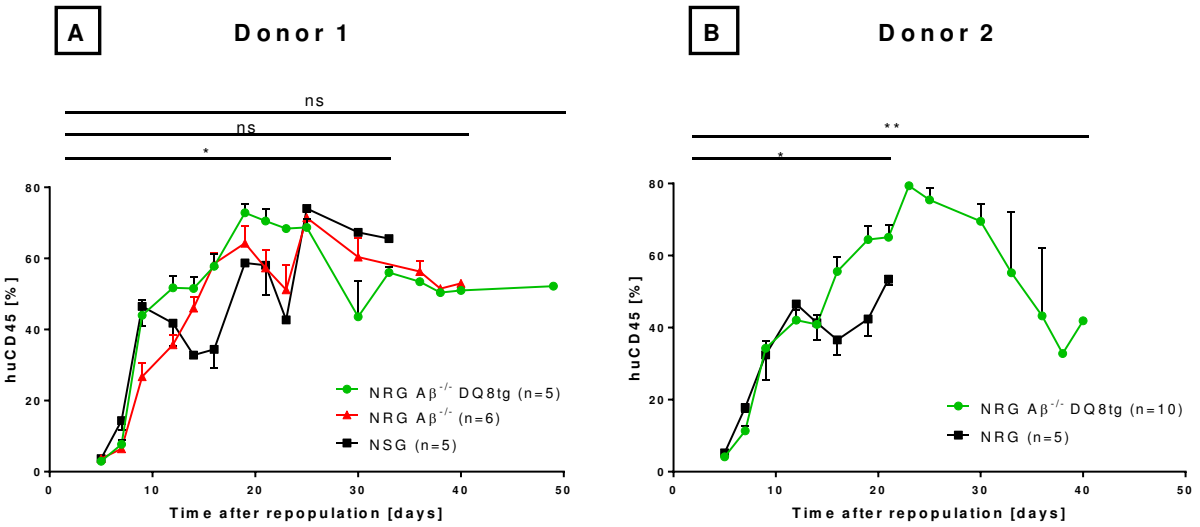

Fig. 14: Kinetics of huCD45 cells in different mouse strains

NRG Aβ$^{-/-}$ DQ8tg, NRG Aβ$^{-/-}$ as well as NSG mice (A) and NRG Aβ$^{-/-}$ DQ8tg and NRG mice (B), were transferred with 5x10^{7} huDQ8-PBMCs from two different DQ8^{+} donors. The percentage of human CD45^{+} cells was determined at the indicated points after repopulation. Repopulation kinetics in mice following transfer of huDQ8-PBMCs from donor 1 (A) were significant only until d33 after transplantation (one way ANOVA for area under curve; P=0.0279) but not until late points (one way ANOVA for area under curve; P=0.0771 and 0.1217). In case of donor 2 (B), repopulation kinetics showed significant differences (Mann-Whitney Test for area under the curve, normed to time in experiment) between the groups until d21 (P=0.0125) and throughout the entire time of the experiment (P=0.0040).

Furthermore, huDQ8tg mice might support the engraftment of different human hematopoietic cell subtypes. Hence, it has been of special interest to analyze and compare the distribution of human hematopoietic cell subtypes in the repopulated mice to that in the DQ8^{+} donor inoculum (Fig. 15). NRG Aβ$^{-/-}$ DQ8tg and NRG mice were repopulated i.v. with 5x10^{7} huDQ8-PBMCs, containing 40% CD3^{+} T-cells, 9% CD19^{+} B-cells, 5% CD56^{+} NK-cells and 6% CD14^{+} monocytes. Five days after repopulation, no difference was detectable between NRG and NRG Aβ$^{-/-}$ DQ8tg recipient mice. In both strains, more murine CD45^{+} cells (muCD45 $>$ 90%) than huCD45^{+}cells were present in the blood. Detailed FACS analysis demonstrated that huCD45^{+} cells in NRG as well as NRG Aβ$^{-/-}$ DQ8tg mice consist mainly of CD3^{+} T-cells (>98%). Other human immune cells present among the donor huDQ8-PBMCs such as NK-cells (CD56^{+}), monocytes (CD14^{+}) or B-cell types (CD5^{-}CD19^{+}, CD5^{+}CD19^{+}) could not be detected in the mice even at the earliest time (day three) (data not shown). Thus, human T-cells repopulate both strains selectively. These findings are also true when higher numbers of huDQ8-PBMCs are adoptively transferred as well as for PBMCs of different DQ8^{+} donors (data not shown).

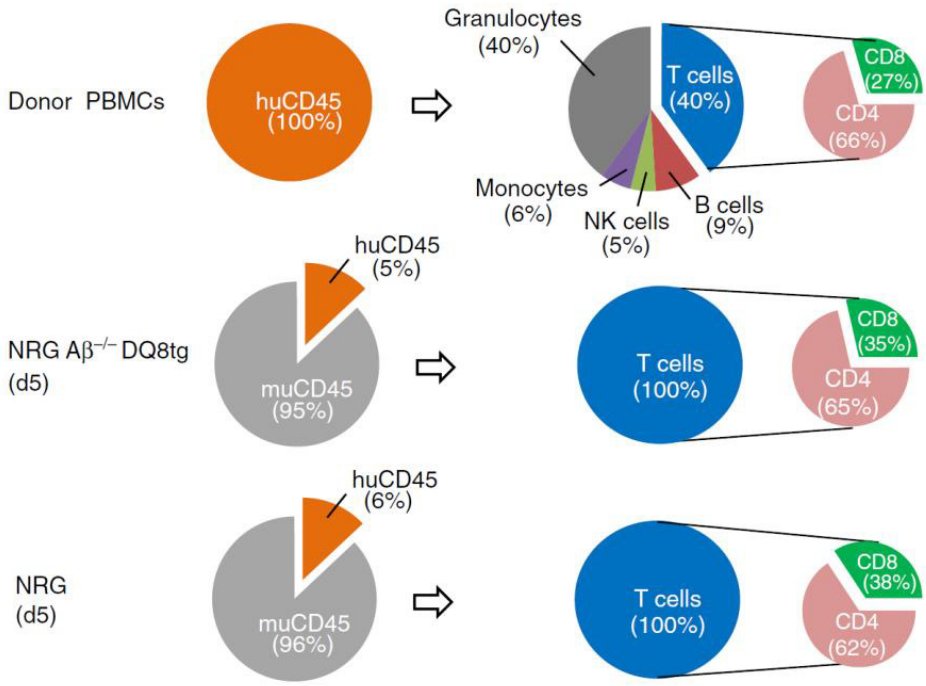

Fig. 15: Human immune cell subsets in donor PBMCs and recipient mice
Donor blood cells were analyzed by flow cytometry before the isolation of mononuclear cells (top row) or following adoptive transfer as peripheral blood cells on day 5 after repopulation. Data from one individual animal, representative of the indicated groups, are shown.

12.3. Delayed *graft-versus-Host Disease* in huDQ8tg mice

Transferring huPBMCs into immunodeficient mice results in the development of *graft-versus-Host-Disease* (GvHD) soon after transplantation (van Rijn et al., 2003). Hence, humanized mice from the experiment above were monitored for signs of disease following cell transfer. According to severity, disease symptoms such as hunched posture, ruffled hair and reduced mobility were ranked (Cooke et al., 1998) and disease scores were determined for each individual mouse (Fig. 16). Interestingly, NSG mice showed first signs of disease (clinical score >1) already seven days after repopulation while NRG Aβ$^{-/-}$ DQ8tg mice demonstrated such only from day 15 and onwards (Fig. 16A). The same could be seen for NRG control mice repopulated with huDQ8-PBMCs from a different donor (Fig. 16B). Furthermore, NSG (Fig. 16A) and NRG mice (Fig. 16B) progressed rapidly from initial symptoms to severe GvHD disease (score > 3) within 12–15 days after transfer, whereas NRG Aβ$^{-/-}$ DQ8tg mice never reached a clinical score of >3 before day 23 after transfer (Fig. 16A) or day 33 in case of donor 2 (Fig. 16B). Littermates lacking the huDQ8tg, NRG Aβ$^{-/-}$ mice, possessed an intermediate progression towards severe GvHD (Fig. 16A). First symptoms could be observed from day 13 onwards and a clinical score >3

occurred not before day 15 after cell transfer. These differences in progression towards severe GvHD, comparing DQ8tg mice with NSG or NRG mice, could be seen also after transfer of lower human cells numbers (data not shown) although the overall progression towards severe GvHD was much slower according to the lower human cell number. Still, huDQ8tg mice showed a delayed progression towards GvHD while NRG or NSG mice progressed very fast and littermates demonstrated intermediate progression towards disease.

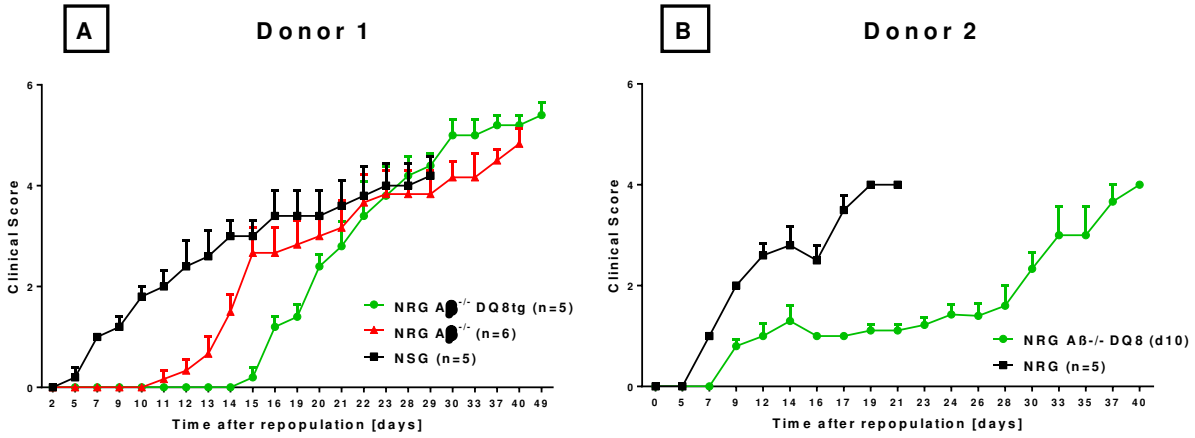

Fig. 16: Graft-versus-host disease (GvHD) in mice humanized with huDQ8-PBMCs
NRG Aβ$^{-/-}$ DQ8 (green), NRG Aβ$^{-/-}$ (red), and NSG/NRG mice (black) were repopulated with 5x10^{7} huDQ8-PBMCs from two different donors (A and B). A clinical scoring system was used to follow the course of GvHD. Animals were graded at the time-points indicated.

Furthermore, the progress of disease also correlated with weight loss of individual mice. Figure 17 presents a parameter for each mouse in the group that indicates the weight loss linked to the time in the experiment. Weight loss was significantly different between NRG Aβ$^{-/-}$ DQ8tg and NRG mice (donor 2; P=0.0150) but not NSG mice were just not statistically significant (donor 1; P=0.0518). However, the mean weight loss comparing both groups was similar. NSG mice (mean parameter 4.9) as well as NRG mice (mean parameter: 4.8) lost more weight compared to NRG Aβ$^{-/-}$ DQ8tg (mean parameter 3.1 donor 1; mean parameter 3.0 donor 2). Again, littermates lacking the huDQ8tg possessed an intermediate phenotype (mean parameter 3.6). Here, mild weight loss of DQ8tg mice also contributed to the delayed onset of GvHD.

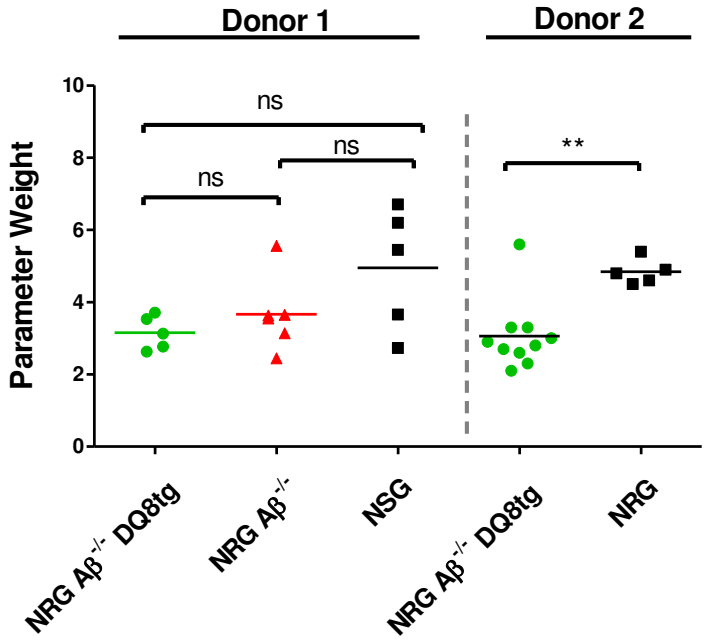

Fig. 17: Weight loss of mice humanized with huDQ8-PBMCs
NRG Aβ$^{-/-}$ DQ8 (green), NRG Aβ$^{-/-}$ (red), and NSG/NRG mice (black) were repopulated with 5x10^{7} huDQ8-PBMCs from two different donors. For each individual mouse a 'parameter weight' was calculated where the difference of the initial weight and the weight at the last day of the experiment was divided by the time in the experiment (in days). The difference between the groups of donor 2 was significant (P = 0.018).

Besides symptoms of disease including weight loss, the pathology caused by systemic GvHD usually becomes evident in organs such as liver, intestine, kidney and skin. To verify and link external symptoms for GvHD with internal processes, sera of mice were analyzed for alanine transferase (ALT) activity (Fig. 18). Determining the level of ALT in blood serum is a very convenient diagnostic parameter to monitor the progress and severity of liver destruction and thereby GvHD development. ALT is an enzyme only present in the liver but following liver damage, as it occurs in case of GvHD, ALT is leaking into the blood stream. Comparing ALT levels in mice repopulated with PBMCs, significant discrepancies were discernible but still led to one general conclusion. In case of repopulation with PBMCs from donor 1 (Fig. 18, left), there was only a mild increase of ALT in NRG Aβ$^{-/-}$ DQ8tg recipients (mean: 62 U/l), while NSG recipients showed a much higher concentration of ALT (mean: 104 U/l) compared to non-humanized mice (non-Hu; mean: 25 U/l). Surprisingly, littermates lacking the huDQ8tg also showed a mild increase of ALT (mean: 56 U/l), similar to DQ8tg mice instead of higher ALT levels specifying the

intermediate mouse strain in-between. In case of repopulation with PBMCs from donor 2 (Fig. 18, right), levels of ALT were higher in both, NRG Aβ$^{-/-}$ DQ8tg and NRG mice. However NRG mice (mean: 1300 U/l) had significantly higher (P=0.0150) ALT levels compared to NRG Aβ$^{-/-}$ DQ8tg (mean: 129 U/l).

These data demonstrated a survival advantage of HLA class II-matched mice over those expressing xenogeneic murine MHC class II.

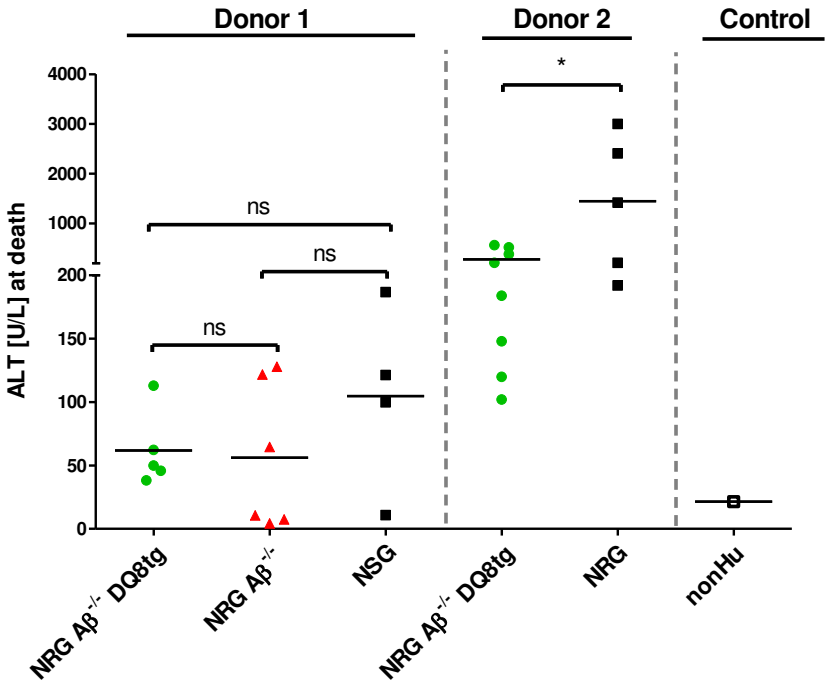

Fig. 18: Increased ALT levels in mice repopulated with huDQ8-PBMC

NRG Aβ$^{-/-}$ DQ8 (green), NRG Aβ$^{-/-}$ (red), and NSG/NRG mice (black) were repopulated with 5x10^{7} huDQ8-PBMCs from two different donors. Alanine transaminase (ALT) levels of each individual mouse in U/l at the end of the experiment were determined. The differences were also significant (P-value: 0.0150) for donor 2.

Statutory orders required euthanization of mice with a weight loss of more than 20% from the initial weight. This point in time was also taken as the end of survival. Comparing survival of NRG Aβ$^{-/-}$ DQ8tg mice with their littermates NRG Aβ$^{-/-}$ and NSG mice, there are significant differences (Fig. 19A). Indeed, the overall survival of NRG Aβ$^{-/-}$ DQ8tg mice (mean survival 30 days) was significantly longer (P=0.0257) compared to NSG mice (mean survival 16 days). Littermates NRG Aβ$^{-/-}$ mice (mean survival 22 days) possessed an intermediate group. Also, comparing survival of NRG

Aβ$^{-/-}$ DQ8tg and NRG mice repopulated with huDQ8-PBMCs (Fig. 19B) of a different donor, significant differences could be observed. NRG Aβ$^{-/-}$ DQ8tg (mean survival 29 days) lived significantly longer (P=0.0012) than NRG mice (mean survival 17 days). Taken together, although huDQ8tg mice repopulated to the same or even slightly higher levels, the onset of disease symptoms and development of fatal GvHD disease was delayed.

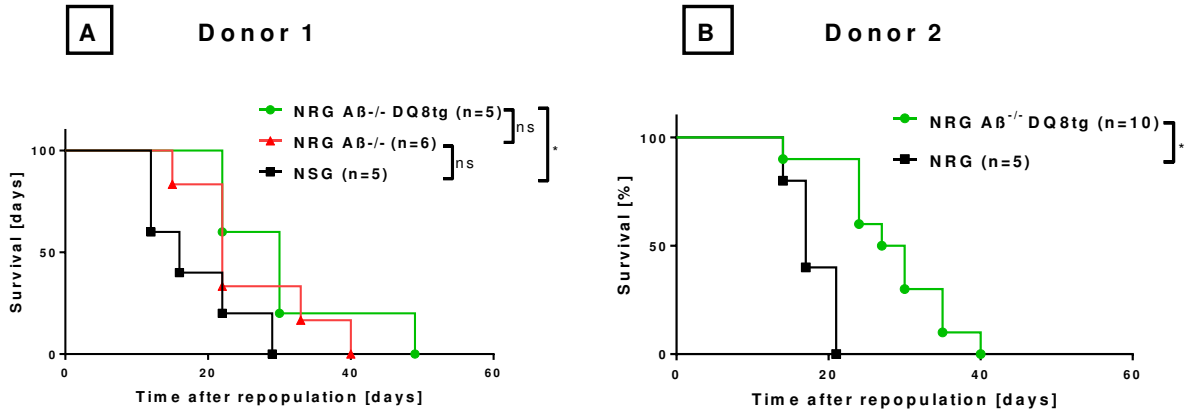

Fig. 19: Survival Curves of mice repopulated with huDQ8-PBMCs
NRG Aβ$^{-/-}$ DQ8 (green), NRG Aβ$^{-/-}$ (red), and NSG/NRG mice (black) were repopulated with 5x10^{7} huDQ8-PBMCs from different donors (A and B). NRG Aβ$^{-/-}$ DQ8 mice showed significantly higher survival rates compared to NSG mice (donor 1; P=0.0257) or NRG mice (donor 2; P=0.0012).

12.4. Contribution of human T-cells to GvHD development

Both human CD4^{+} and CD8^{+} T-cells have been shown to contribute to GvHD development in murine recipients (King et al., 2009). As describes earlier (cp. Fig. 15), exclusively huCD3^{+} T-cells expanded in mice regardless of the huDQ8tg. Hence, it was interesting to determine whether GvHD, commencing more slowly in NRG Aβ$^{-/-}$ DQ8tg recipients, could be correlated with differences in donor T-cell subsets following repopulation. The adoptive transfer of NRG Aβ$^{-/-}$ DQ8tg mice with DQ8-matched donor PBMCs represents an HLA-class II-matched transplantation while donor CD8^{+} T-cells still face xenogeneic MHC class I in all mouse strains. Therefore, it was hypothesized that the presence of huDQ8 as HLA class II molecule supports CD4^{+} T-cells to alleviate GvHD mediated by CD4^{+} T-cells. In contrast, it was also assumed that CD8^{+} T-cell-mediated GvHD either will increase due to the still

mismatching HLA class I or decrease due to missing CD4$^+$ T-cell help because of matching HLA class II molecules. The huDQ8-PBMC repopulated mice were therefore further analyzed for the frequency of huCD4$^+$ and huCD8$^+$ T-cells at day seven, nine and fourteen (Fig. 20). At day seven after repopulation no differences between the mouse strains could be seen (Fig. 20; d7). About 55% huCD4$^+$ and 35% huCD8$^+$ T-cells in all mice were observed. However, from day nine after repopulation, only in NSG (Fig. 20, d9, black squares) mice the contribution of huCD8$^+$ T-cells among huCD3$^+$ T-cells started to increase by ~5% while that of huCD4$^+$ T-cells started to decrease by ~14%. By day twelve (Fig. 20; d12) CD8$^+$ T-cells increased almost twice as much compared to day seven (~32% versus ~63%, respectively). Such a dramatic shift towards CD8$^+$ T-cells did not occur in NRG A$\beta^{-/-}$ DQ8tg mice (green circles) receiving the same number of the same donor huDQ8-PBMCs. Notably, after twelve days of repopulation (Fig. 20; d12), the frequencies of huCD4$^+$

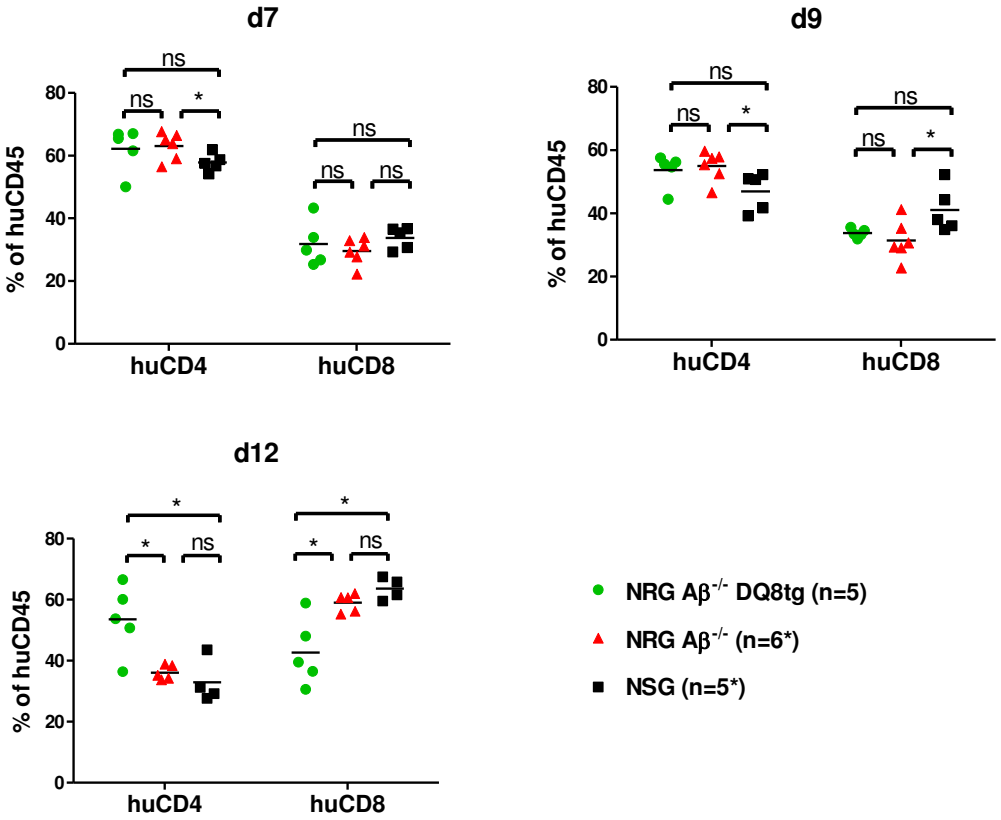

Fig. 20: Repopulation by CD4$^+$ and CD8$^+$ T-cells following adoptive huPBMC-DQ8 transfer
Repopulated mice monitored with respect to human CD4$^+$ and CD8$^+$ T-cells by flow cytometry on the indicated points in time following transfer. Each symbol represents an individual mouse. Statistically significant differences are noted in the figure.
*indicated groups comprised less animals at d12 due to low survival rates

and huCD8$^+$ T-cells in NRG A$\beta^{-/-}$ littermates (red triangles) were also shifting, such as in NSG mice proofing the intermediate manner of the NRG A$\beta^{-/-}$ mice lacking huDQ8tg. Also, after twelve days the differences between huCD4 and huCD8 T-cells of NRG A$\beta^{-/-}$ DQ8tg mice compared with NRG (P=0.0337 and P= 0.0217, respectively) as well as compared to NRG A$\beta^{-/-}$ mice (P=0.0213 and 0.0303, respectively) became significantly. In contrast, there is no significant difference comparing NSG with NRG A$\beta^{-/-}$ mice (P= 0.382 and 0.599, respectively) at days twelve after repopulation. These finding also could be found in mice repopulated with DQ8$^+$ PBMC from different donors (data not shown).

Next, it was examined whether huCD8$^+$ T-cells, expanding at an early point when GvHD developed in mice, are responsible for the clinical symptoms such as hair loss and liver damage detected as increased ALT levels in serum (cp. Fig. 18). Therefore, repopulated NRG A$\beta^{-/-}$ DQ8tg as well as NRG control mice were histologically analyzed. When the mice lost 20% of their starting weight, mice were dissected and sections of different organs including liver, skin, kidney and intestine were made and analyzed by immunohistochemical staining (IHC) for huCD8$^+$ T-cells (Fig. 21). In NRG recipients (Fig. 21, middle panels) a massive, high-grade infiltration by mononuclear cells was seen (arrows), many being huCD8$^+$ that spread into the peripheral liver parenchyma. In some sections, single hepatocytes were found to be necrotic, a hallmark for ongoing liver injury. In contrast, NRG A$\beta^{-/-}$ DQ8tg mice (bottom panels) infiltrates were less pronounced and also less CD8$^+$ T-cells could be found. In comparison, non-humanized mice (non-Hu) showed no infiltrates (Fig. 21, top panels). The skin is another organ typically affected by GvHD. In both mouse strains we observed macroscopically alterations of skin texture such as hyperkeratosis, scleroderma and desquamation, as used for clinical score grading. As expected, histological examination confirmed these observations. The skin surface appeared undulated and signs of fibrosis, folliculitis and steatitis were evident within the hypodermis [see arrows in Fig. 21, haematoxylin and eosin (H&E) staining]. Notably, these observations tended to be more severe in NRG control mice compared to NRG A$\beta^{-/-}$ DQ8tg mice. As GvHD is a systemic disease, huCD8$^+$ T-cells could be detected in other organs, such as kidney and intestine as well. Again, infiltrates were less pronounced in NRG A$\beta^{-/-}$ DQ8tg mice compared to NRG mice (Fig. 21).

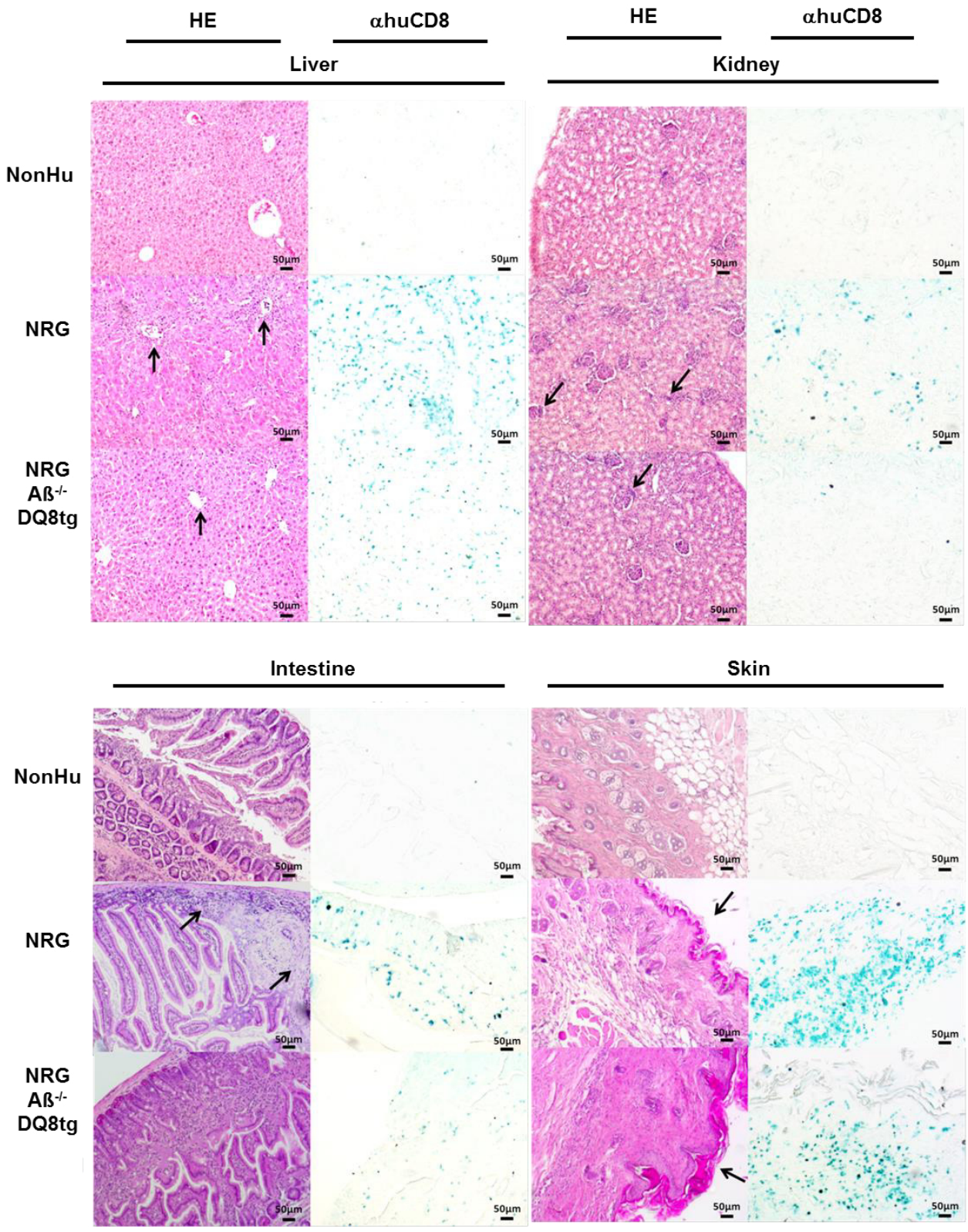

Fig. 21: Human CD8$^+$ T-cell infiltration into organs

NRG Aβ$^{-/-}$ DQ8tg and NRG mice repopulated with 5x10^7 huDQ8-PBMCs and at the end of the experiment. Sections from liver, kidney, intestine and skin were examined by haematoxylin and eosin staining (H&E, left panels) as well as immunohistochemistry (IHC) for human CD8 (in blue, right panels). Cell infiltrates are indicated by an arrow. Genotypes of the recipient mice are indicated. As reference, one non-humanized mouse was included (non-Hu).

Next, according to a published score (Covassin et al., 2011) infiltrates of huCD8$^+$ T-cell in organs were quantified (Fig. 22). Livers of NRG mice exhibited a significantly higher (P= 0.0099), infiltration by human CD8$^+$ T-cells (mean score: 2.15) compared to those of NRG A$\beta^{-/-}$ DQ8tg mice (mean score: 1.36). In addition, kidneys (mean score: 1.05) and intestines (mean score: 1.00) of NRG mice were also infiltrated more severely (P= 0.0112 and 0.0467, respectively) by huCD8$^+$ T-cells compared to NRG A$\beta^{-/-}$ DQ8tg mice (mean score: 0.58 and 0.42, respectively). This tendency of a more pronounced infiltration in NRG mice (mean score: 1.45) was also seen for the skin, although the difference was not statistically significant compared to NRG A$\beta^{-/-}$ DQ8tg mice (mean score: 1.33). Taken together, the delayed onset and mild progression of GvHD in NRG A$\beta^{-/-}$ DQ8tg mice could be due to a delay in the activation and expansion of xenoreactive CD8$^+$ T-cells.

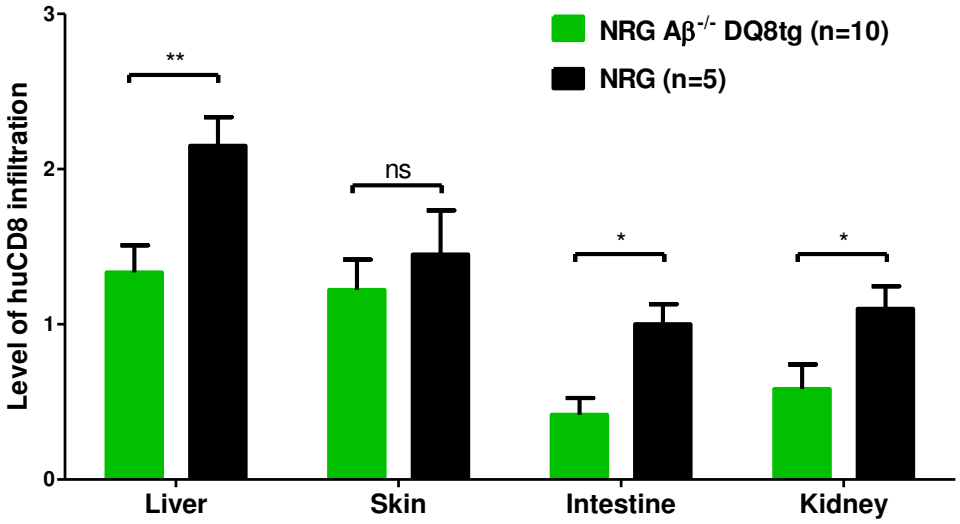

Fig. 22: Quantification of huCD8$^+$ T-cells in organs of humanized mice
Infiltrates of huCD8$^+$ T-cells in the liver, kidney, intestine and skin were scored, as identified by IHC (Fig. 18) from no infiltration (level 0) to >50% infiltration (level 3). These data are summarized graphically. Bars representing the mean level of infiltration per organ and recipient mouse per group and the corresponding standard deviation are shown. Differences were significant for liver (P = 0·0099), intestine (P = 0·0112) and kidney (P = 0·0467), but not for skin (P = 0·7431).

12.5. Alleviated GvHD in DQ8tg mice is not caused by IFNγ secretion

As shown above, repopulation with matching PBMCs in huDQ8tg mice alleviated GvHD development in the animals (see 12.2). The expansion of human CD8$^+$ T-cells was shown to be an early sign of xenogeneic GvHD; however HLA class II matching

could not prevent the onset of GvHD (see 12.3). Next, the underlying mechanism of DQ8 molecule matching and the delay in GvHD was examined. Activated T-cells produce high amounts of cytokines, such as human interferon γ (huIFNγ) that provides immunostimulatory and immunomodulatory effects to innate and adaptive immune responses (see 4.3). It was hypothesized that matching T-cells in humanized DQ8tg mice secrete less huIFNγ compared to control mice. Therefore, NRG Aβ$^{-/-}$ DQ8tg mice, their littermates and NSG mice were repopulated with 5x10^{7} huDQ8-PBMCs from different donors (Fig. 23). huIFNγ levels in serum of humanized mice were determined at day seven after repopulation (open bars) and at the end of the

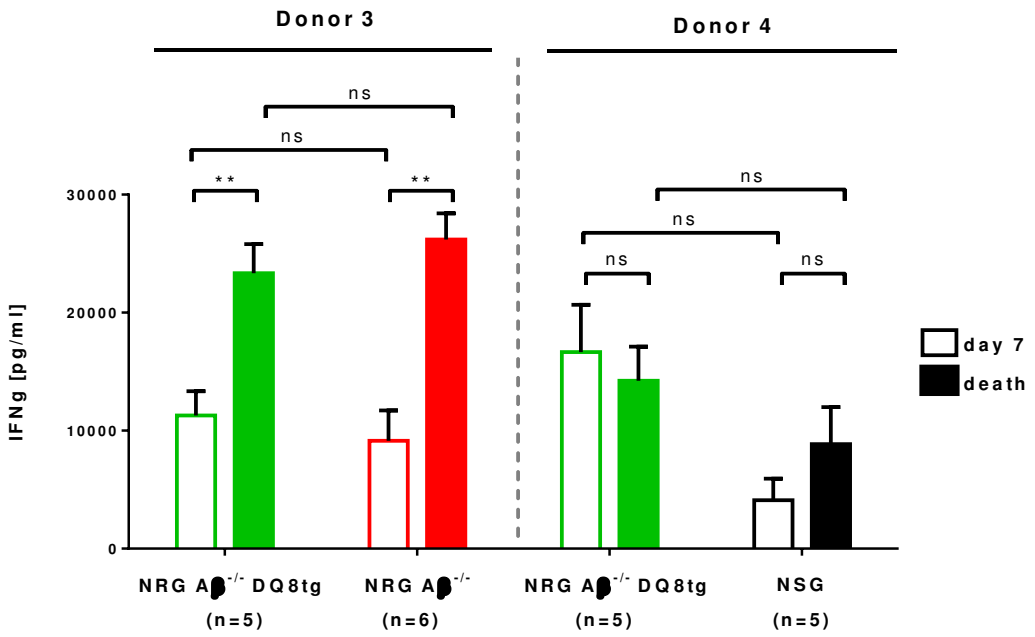

Fig. 23: Levels of IFNγ in huDQ8-PBMCs humanized mice
NRG Aβ$^{-/-}$ DQ8 (green), NRG Aβ$^{-/-}$ mice (red), and NSG mice (black) were repopulated with 5x10^{7} huDQ8-PBMCs from two different donors. Levels of IFNγ in serum were determined at day seven (open bars) after repopulation and on the last day (filled bars) in experiment when mice lost 20% of their starting weight. Standard error deviations are depicted. Statistical significances were calculated with t-test.

experiment (filled bars) when mice lost 20% of their starting weight. In case of donor 3 (Fig. 23, left), a significant increase in huIFNγ levels from day seven (~10000 pg/ml) to death (~25000 pg/ml) could be seen in NRG Aβ$^{-/-}$ DQ8tg as well as NRG Aβ$^{-/-}$ to the same extent. However, already at days seven the level of huIFNγ was abnormally high in both groups but still increasing throughout the experiment. In case of donor 4 (Fig. 23, right), levels of huIFNγ were even higher at days seven compared to donor 3

although NSG mice showed slightly less secretion of huIFNγ. In contrast, huIFNγ levels did not increase as drastically as in case of donor 3. This effect is also true for mice humanized with lower numbers of human PBMCs (data not shown). In conclusion, matching DQ8 molecules in mice did not decrease IFNγ secretion. All mice exhibit already high IFNγ expression after transfer of huDQ8-PBMCs and no clear correlation regarding HLA II matching could be seen.

12.6. Induction of humoral immune response in PBMC humanized mice

As presented earlier, only T-cells repopulate humanized mice whereas B-cells were not found even at very early points after human cell transfer (cp. 12.2). Mature B-cells are actively maintained *in vivo* by survival signals received through the B-cell antigen receptor (BCR) and the ligand *human B-lymphocyte stimulator*, huBLyS (Schmidt et al., 2008). HuBLyS facilitates the differentiation of short-lived immature B-cells into mature recirculating long-lived B-cells and actively maintains mature B-cells in the periphery (Rolink et al., 2002). The failure of efficient human B-cell engraftment and survival in humanized mice might be due to the murine environment that does not provide huBLyS as signaling ligand necessary for B-cell homeostasis (Schmidt et al., 2008). Therefore, recombinant huBLyS was used to support B-cell survival in mice and thus the establishment of a humoral immune system.

First, the gene construct for huBLyS including a His-tag for purification was cloned into a bacterial expression vector (see 7.2). HuBLyS was purified from *E.coli* via Ni-affinity chromatography and characterized *in vitro* for its functionality. Isolation and functionality tests of the recombinant huBLyS are described in the Bachelor Thesis of Dana Püschl (2013, Justus-Liebig Universität, Giessen). A concentration of 100 ng huBLyS/ml medium was found to be optimal for B-cell survival *in vitro* (Dana Püschl, 2013).

Cultivation of huCD19$^+$ B-cells isolated by magnetic sorting from PBMCs of a healthy human donor supplemented with 100 ng/ml huBLyS clearly demonstrated that huBLyS significantly enhances human B-cell survival relative to unstimulated cultures (Fig. 24). While 30-40 % of cultivated B-cells survived in presence of huBLyS, only 20-30 % survived without the survival factor. However, after five days of cultivation

the percentage of living B-cells was decreasing in both groups, but still B-cell cultures supplemented with huBLyS show significantly higher percentages.

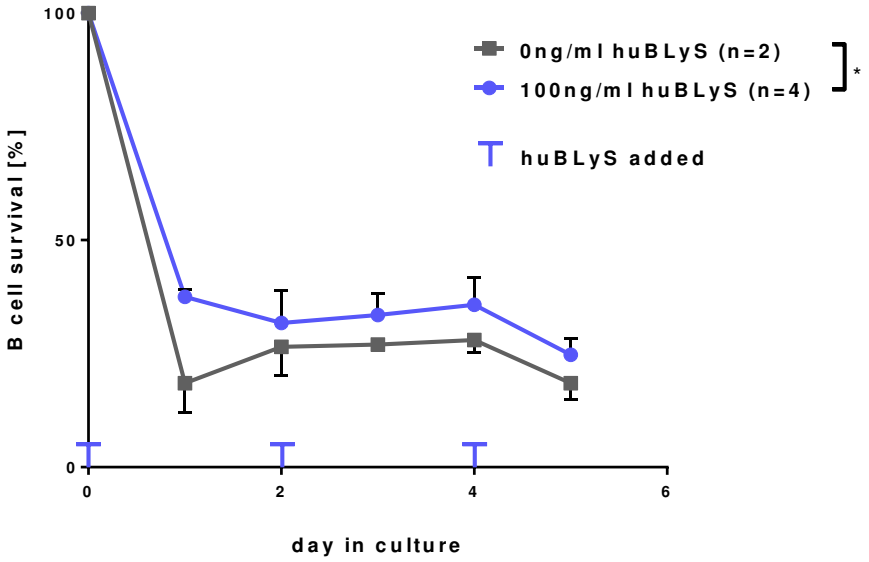

Fig. 24: *In vitro* survival of human B-cells cultivated with 100ng/ml huBLyS
Human B-cells were cultivated for five days with 100ng/ml huBLyS readded to the cultures every second day (blue line) or without huBLyS (grey lines). Viability was determined daily using cell counting with trypan blue and is represented as percentage of input cell number surviving. Statistical analysis for significance were tested by t-test for the area under curve (P=0.0340). Data were taken from Bachelor thesis of Dana Püschl, 2013.

Due to successful B-cell survival *in vitro* (cp. Fig. 24) it was expected that huBLyS also supports the establishment of a humoral immune system in humanized mice. Moreover, DQ8 matching human B-cells in DQ8tg mice were expected to produce antibodies following a stimulus and thus supporting a functional human humoral immune system. Therefore, $2x10^7$ huDQ8-PBMCs were transferred i.v. into NRG $A\beta^{-/-}$ DQ8tg mice and treated with huBLyS. This time, less human cells were transferred to expand the time window until GvHD commenced to perform immunization of humanized mice. Recipients were given recombinant huBLyS (10 µg/mouse/day) or PBS i.p. starting one day before humanization and every following day (according to Schmidt et al., 2008). The frequencies of $huCD45^+$ cells and $huCD19^+$ B-cells were determined to analyze B-cell survival in humanized mice (Fig. 25). As demonstrated earlier, huCD45 frequencies (dashed lines) slowly increased with time. Human B-cells, characterized as $CD19^+$ cells, could not be detected at any time after humanization with and without administration of huBLyS.

In summary, recombinant huBLyS purified from *E. coli* did slightly support human B-cell survival *in vitro* but not in humanized mice. The protein derived from *E.coli* might not have sufficient biological activity *in vivo* and other sources of huBLyS should be considered.

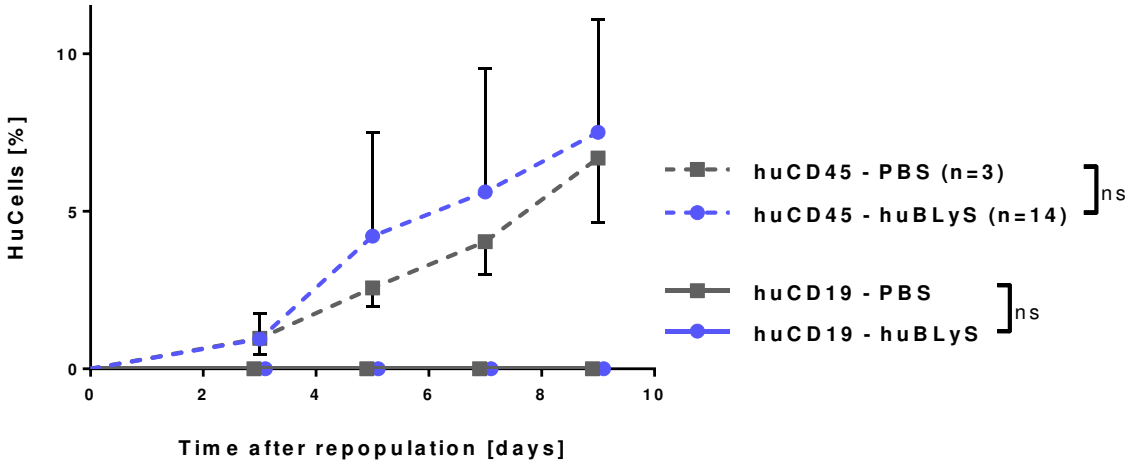

Fig. 25: Survival of human B-cells in humanized mice following administration of huBLyS
NRG Aβ$^{-/-}$ DQ8 mice (blue) were repopulated with 2x10^{7} huDQ8-PBMCs and analyzed from huCD45 cells (dashed lines) and huCD19 cells (solid lines). Statistical analysis for significance was tested by Mann-Whitney test for the area under curve (P=0.8706).

12.7. Infection of PBMC repopulated mice with HIV-1

12.7.1. Ex Vivo HIV infection of human cells isolated from humanized mice

As shown above, huCD3^{+} T-cells selectively expand in mice repopulated with huPBMCs. Particularly, CD4^{+} T-cells are of special interest because only cells carrying the CD4-receptor as well as CXCR4 (X4) or/and CCR5 (R5) co-receptor can be infected by HIV (see 1.6.). In terms of using humanized mice as models for HIV infection, a basic test of infecting human cells *ex vivo* with HIV-1 should show the feasibility using humanized mice as animal model for HIV infections.

NRG Aβ$^{-/-}$ DQ8tg (n=5) were repopulated with 1x10^{8} huDQ8-PBMCs and euthanized at day 28 post humanization. Mice were checked for huCD45 and huCD4 T-cells in peripheral blood to confirm successful humanization. The animals had between 23-

59% huCD45 cells (Table 1). Single cell suspensions from blood and spleen were prepared and cultivated. Prior HIV-1 infection, cells were activated with interleukin-2 (IL-2) and phytohemagglutinin (PHA) (see 7.4.7). Stimulated human cells were infected with $3x10^3$ $TCID_{50}$ of HIV-1_{SF2}, an X4-tropic virus or HIV-1_{SF162}, a R5-tropic virus (see 1.6). After six days of culture the supernatant was collected and analyzed in a TZM-bl cell assay (see 7.4.8) for the generation of new infectious viral particles (Tab. 1).

Tab. 1: *Ex vivo* HIV infection of human cells from humanized mice

Mouse	huCD45 [%]	huCD4 [%]	Production of infectious particles			
			Infection with HIV-1_{SF2} (X4)		Infection with HIV-1_{SF162} (R5)	
			blood	spleen	blood	spleen
K1	33.5	23.2	+	+	-	-
K2	23.5	19.9	+	+	-	-
K3	41.8	32.6	+	+	-	-
K4	43.4	46.5	-	+	-	-
K5	58.8	43.1	+	+	-	-

Five NRG $A\beta^{-/-}$ DQ8tg mice were repopulated with $1x10^8$ huDQ8-PBMCs. HuCD45 and huCD4 T-cells in blood were determined at day 28 post repopulation. Blood and splenic cells were activated and cultivated. These cells were infected with $3x10^3$ $TCID_{50}$ of HIV-1_{SF2} (X4-topic virus) and HIV-1_{SF162} (R5-tropic virus). After six days in culture, supernatants were analyzed in TZM-bl cell assay for production of viral particles. '+' production of infectious viral particles; '-' no production of infectious viral particles.

The CCR5 co-receptor expression is largely restricted to $CD4^+$ macrophages, a cell type not present in humanized mice. Contrariwise, the co-receptor CXCR4 is present on activated T-cells which predominantly could be found in humanized mice. Hence, it is not surprising that only HIV-1_{SF2} could infect human cells isolated from humanized mouse blood or spleen (Tab. 1). However, in human cells isolated from blood of mouse K4 could not be productively infected with HIV-1_{SF2} although high levels of huCD4 T-cells were detected by flow cytometry. In contrast, infection of human cells from blood and spleen of humanized mice by HIV-1_{SF162} was not successful at all. This basic *ex vivo* test is a very artificial system that does not resemble HIV-1 infections in humans but demonstrated for the first time that human cells from humanized mice are susceptible to HIV-1 infection.

12.7.2. In Vivo HIV infection of PBMC repopulated mice

In the following, the above characterized humanized DQ8tg mouse model was used for infection with both HIV-1_{NL4-3} and HIV-$2_{ROD/B148}$. HIV-1_{NL4-3} is a T-cell adapted HIV-1 strain infecting CD4 T-cells expressing the CXCR4 co-receptor (Adachi et al., 1986). Compared to HIV-1 infections, clinical courses of HIV-2 infections are characterized by mild progression and lower plasma HIV-2 viral loads. To yield detectable viral loads in humanized mice, the HIV-2 strain HIV-$2_{ROD/B148}$ was utilized to intensify viral infection in humanized mice. HIV-$2_{ROD/B148}$ can enter cells expressing the co-receptor CXCR4 independently of the CD4-receptor (Clapham et al., 1992). Hence, this strain is not restricted exclusively to human CD4 T-cells and can also enter human CD8 T-cells. Thus, the amount of infected cells is increased and could be detected easily. The murine CXCR4 might be utilized by HIV-$2_{ROD/B148}$ but only viral entry into the host cell is feasible and no reverse transcription of viral RNA and/or integration into the host genome (Tsurutani et al., 2007; Tervo et al., 2008). The infectivity of both HIV strains in humanized mice was compared. Therefore, NRG $A\beta^{-/-}$ DQ8tg mice were repopulated i.v. with $2x10^7$ $huDQ8^+$ PBMCs. Seven days post repopulation mice were infected i.p. with $2x10^6$ $TCID_{50}$ HIV-1_{NL4-3} (n=9) and HIV-$2_{ROD/B148}$ (n=6). To get an idea of the progression of disease, mice of both groups were euthanized regularly starting at day seven post infection to collect and analyze lymphoid organs (Fig. 26).

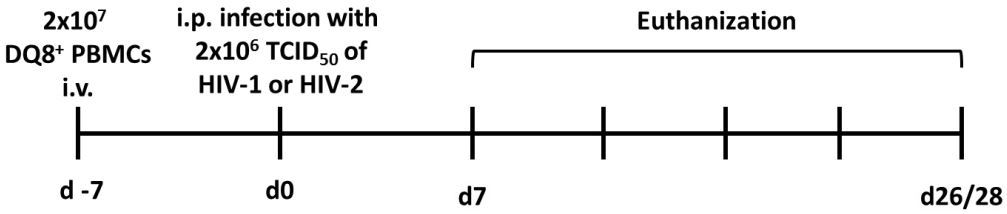

Fig. 26: Experimental set-up for HIV infection of humanized DQ8tg mice
NRG $A\beta^{-/-}$ DQ8tg mice were repopulated i.v. with $2x10^7$ $huDQ8^+$ PBMCs and infected with HIV-1_{NL4-3} and HIV-$2_{ROD/B148}$ one week later. Starting at d7 post infection mice of both groups were euthanized regularly.

Figure 27 shows the percentages of huCD45$^+$ cells, huCD3$^+$CD4$^+$ and huCD3$^+$CD8$^+$ T-cells over time in blood (upper panels), spleen (middle panels) and lymph node (bottom panels) of HIV-1_{NL4-3} (left panels) and HIV-$2_{ROD/B148}$ (right panels) infected mice. The numbers of proviral HIV DNA copies per ng genomic DNA (cps/ng DNA) of blood cells, splenic cells or lymph node cells of single mice at time of euthanization are depicted below. In fact, viral RNA copies in plasma would monitor the HIV infection over time however the integration of the HIV genome into the host cell genome was not quantified here to assure viral replication taking place. Therefore, proviral DNA in genomic DNA from blood cells and organs was determined.
NRG A$\beta^{-/-}$ DQ8tg mice were infected with HIV-1 and -2 when they exhibited ~5-10% huCD45 cells in blood (Fig. 27, upper panels, blue dashed line). Both, in HIV-1_{NL4-3} (left panels) and HIV-$2_{ROD/B148}$ infected mice, huCD45 cells in blood increased until ~d12 post infection to up to ~50%. HuCD45 cells in blood of HIV-1_{NL4-3} infected mice dramatically decreased thereafter and finally vanished (upper left panel, blue dashed line), whereas huCD45 cells in blood of HIV-$2_{ROD/B148}$ infected mice only decreased slightly from ~50% to ~40% on average (upper right panel, blue dashed line). In comparison, ~60% of huCD3$^+$CD4$^+$ T-cells in blood (upper panels, green line) as well as ~7% of huCD3$^+$CD8$^+$ T-cells were present before infection. HuCD3$^+$CD4$^+$ T cells drastically declined and huCD3$^+$CD8$^+$ T-cells increased in mice infected with HIV-1_{NL4-3} (left panel), whereas in mice infected with HIV-$2_{ROD/B148}$ huCD3$^+$CD4$^+$ T-cells only slightly declined from ~60% to ~50% (right panel) and huCD3$^+$CD8$^+$ T-cells increased from 7% to 60%.

Proviral HIV DNA in blood cells of HIV-1_{NL4-3} infected mice (upper panels, left, grey line) seemed to peak around d12 post infection correlating with the start of huCD45 decline. In contrast, proviral HIV DNA in blood cells of HIV-$2_{ROD/B148}$ infected mice remained stable, at very low levels correlating with huCD45 levels in blood. The same pattern of huCD45 cell, huCD3$^+$CD4$^+$ T-cells and huCD3$^+$CD8$^+$ T-cells correlating with the proviral HIV DNA load in cells could be found for the spleen (middle panels) and the lymph node (bottom panels). Continuously, a peak of proviral load could be found around d12 post infection indicating the beginning of huCD45 decrease in HIV-1_{NL4-3} infected mice. Also, in HIV-$2_{ROD/B148}$ infected mice the proviral load as well as the percentages of huCD45 cells remained stable or even increased in the spleen.

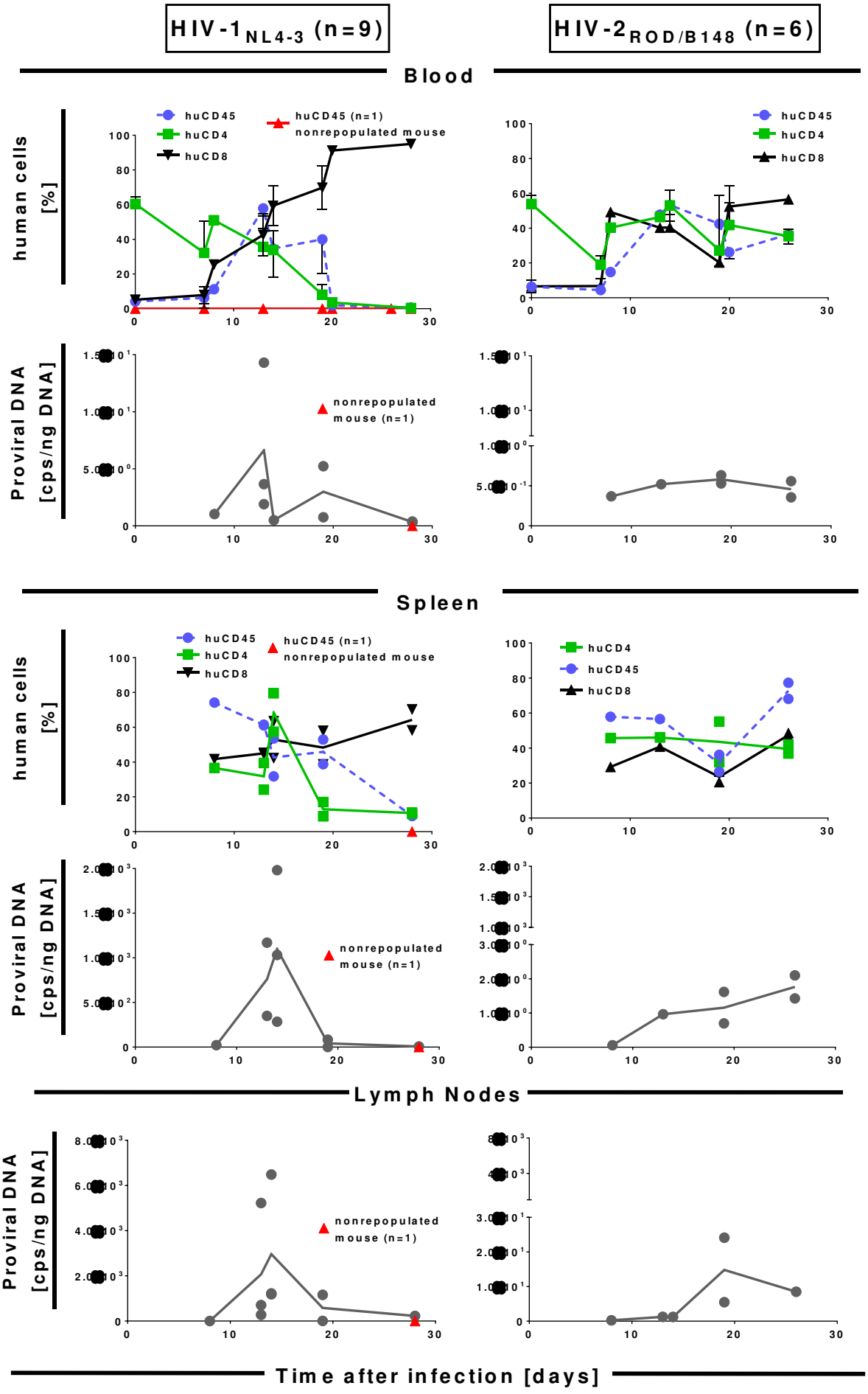
HIV-1NL4-3 (n=9)
HIV-2ROD/B148 (n=6)
Blood
Spleen
Lymph Nodes
human cells [%]
Proviral DNA [cps/ng DNA]
huCD45
huCD4
huCD8
huCD45 (n=1) nonrepopulated mouse
nonrepopulated mouse (n=1)
Time after infection [days]

Fig. 27: huDQ8-PBMC repopulated mice infected with HIV-1_{NL4-3} and HIV-$2_{ROD\ A-B}$
At d7 post repopulation mice were infected i.p. with $2x10^6$ $TCID_{50}$ HIV-1_{NL4-3} (left panels) and HIV-$2_{ROD/B148}$ (right panels). HuCD45 (blue dashed lines), huCD3$^+$CD4$^+$ T-cells (green lines) and huCD3$^+$CD8$^+$ T-cells (triangle black line) were determined over time in blood and at time of euthanization in spleen. Copies of proviral HIV DNA (grey lines) were determined by quantitative real-time PCR in 1 ng genomic DNA of blood cells, splenic cells and lymph node cells from single mice (dots) at time of euthanization. The grey line indicates the mean values. One non-repopulated mouse was infected with $2x10^6$ $TCID_{50}$ HIV-1_{NL4-3} as control.

Beside the similar pattern of human repopulation and viral inoculation dose, the absolute numbers of proviral HIV DNA copies (cps) differed enormously. In HIV-1_{NL4-3} infected mice the highest proviral copy number was found in lymph nodes (up to $3x10^3$ cps/ng DNA) and spleen (up to $1x10^3$ cps/ng DNA), whereas in blood only a low titer could be found (up to 5 cps/ng DNA). The same was true for HIV-$2_{ROD/B148}$ infected mice although the overall disparity was not as high as for HIV-1_{NL4-3} infected mice (lymph node: 10 cps/ng DNA; spleen: 1 cps/ng DNA and blood: 0.5 cps/ng DNA). Taken together, humanized mice could be productively infected with HIV-1_{NL4-3} and HIV-$2_{ROD/B148}$. The levels of huCD45 cells and huCD3$^+$CD4$^+$ and huCD3$^+$CD8$^+$ T-cells correlated with the proviral load. While the infection with HIV-1 showed a rapid progress, the infection with HIV-2 was mild and at detection level of the qPCR.

13. Reconstitution of mice with human hematopoietic stem cells

The repopulation of mice with human hematopoietic stem cells (huHSCs) is another method to generate humanized mice. Following transfer, human stem cells have the capability to reside in the murine bone marrow and built a huHSC reservoir from where the development of new human hematopoietic cells is guaranteed over a long period of time. Further, huHSCs have the ability to differentiate into various subsets of immune cells and mature in a murine environment preventing the development of GvHD. HuHSCs can be transferred into **adult mice** i.v. or i.p. and also intrahepatically (i.h.) into **newborn mice**. The latter might be the most physiological variant since, as in humans, fetal hematopoiesis takes place in the liver and after birth stem cells migrate into the bone marrow to reside (cp. 4.1). Taking advantage of this process, here, huHSCs are transferred into the liver of newborn mice.

Furthermore, huHSCs can be obtained from various sources, each with characteristic advantages and disadvantages. The easiest and safest way to obtain huHSCs is from **human cord blood**. However, the number of huHSCs largely depends on the quality of cord blood and thus is limited. Another source of huHSCs is an adult donor who had been treated with *granulocyte colony-stimulating factor* (G-CSF). **G-CSF mobilizes HSC** into the peripheral bloodstream from where they can be collected. These HSC can be obtained in relatively high numbers; however, mobilized stem cells might obtain reduced functionality. A source very rarely used in Germany is **huHSC from fetal tissue**. After abortion, fetal liver tissue is used for the isolation of huHSC. From this source high numbers of very potent huHSC can be obtained; however there are difficulties with ethical acceptance. Recently, a lot of effort was made to investigate parameters for ex vivo expansion of huHSCs from different sources (Flores-Guzman et al., 2013). Therefore, selected parameters with focus on humanization of mice were addressed in the following sections.

13.1. Breeding and genotyping of mice for humanization

Humanization with huHSC from different sources was performed using NRG A$\beta^{-/-}$ DQ8tg mice. Therefore, huHSCs were required to be DQ8^{+}. For the reconstitution of newborn mice with huDQ8-HSCs, the mouse breeding had to be highly organized. To match the day of birth with the preparation of huDQ8-HSC, *time matings* were set up. Conceptions of female mice were represented by a sperm plaque, hardly visibly in NRG A$\beta^{-/-}$ DQ8tg mice. Birth usually occurred 21 days after conception. This time was used to calculate the extract birth date to prepare huDQ8-HSCs for reconstitution. Depending on the number of littermates, the required amount of huDQ8-HSCs was prepared. After weaning, around 5-7 weeks of age, mice were genotyped. In total, ~54 % of the litters were transgenic for the huDQ8tg. The number of littermates varied from 5-12 per mother and also the number of DQ8tg mice within each litter greatly varied (~20-90 %). For this reason, the number of time matings was adjusted so that natural variations could be compensated.

13.2. Humanization of newborn mice with huDQ8-HSCs from cord blood

In order to compare different approaches for humanizing mice with human hematopoietic stem cells (huHSCs), at first humanization of newborn mice with

huHSCs isolated by magnetic sorting with an antibody directed against CD133 (see 7.4.2) from human cord blood was examined. Following birth, littermates (n=10) were sublethally irradiated (4Gy) and reconstituted intrahepatically (i.h) with $1x10^5$ fresh huDQ8-HSCs (see 7.5.4). After weaning, adult mice were genotyped for the huDQ8 transgene. In terms of developing GvHD, adult mice were monitored throughout their life span for changes in weight as early signs of disease (Fig. 28A). Mice genotyped as NRG $A\beta^{-/-}$ DQ8tg (n=6) as well as their littermates without the huDQ8tg, NRG $A\beta^{-/-}$ mice (n=4), showed a uniformly increase of weight over time. Nevertheless, individual mice of both groups lost weight but never more than 20% of their starting weight. This weight loss was not connected to other disease symptoms and mice recovered soon after. The overall health status of mice remained normal post reconstitution. Single mice within the groups also died, (Fig. 28B) however, without possessing symptoms of disease. In addition, it was observed that the expected life span of irradiated but non-reconstituted mice was a little shorter (<1 year) compared to non-irradiated non-reconstituted mice (>1 year; data not shown). Taken together, irradiated NRG $A\beta^{-/-}$ DQ8tg mice and NRG $A\beta^{-/-}$ mice did not develop GvHD following reconstitution with huDQ8-HSCs and also their life expectancies were similar but little shorter compared to non-irradiated mice of the same group.

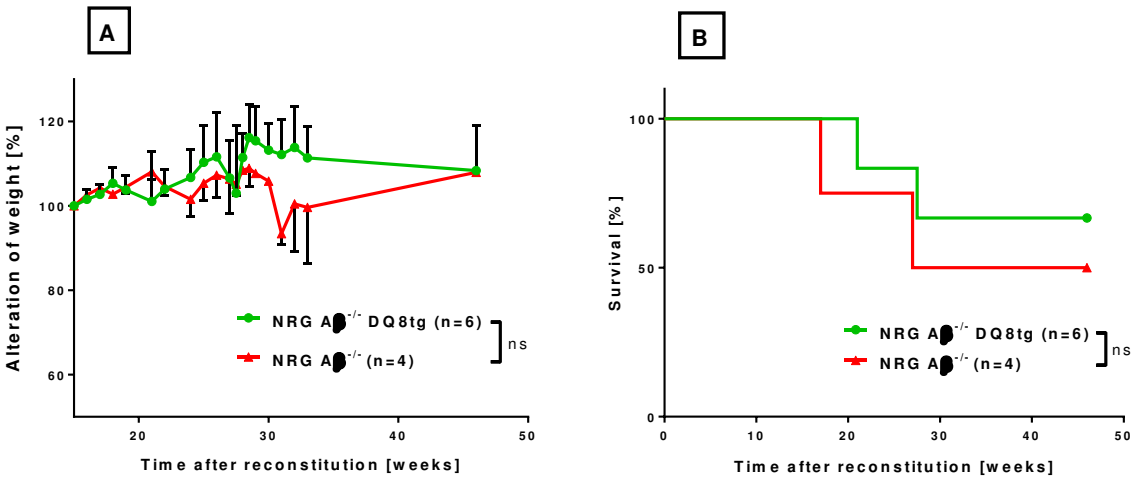

Fig. 28: Weight and survival curve of mice reconstituted as newborns with huDQ8-HSCs
NRG $A\beta^{-/-}$ DQ8 mice (green) and littermates NRG $A\beta^{-/-}$ mice (red) were irradiated with 4Gy and repopulated i.h. with $1x10^5$ huDQ8-HSC. After weaning, adult mice were monitored for alterations in weight (A) and survival (B). Statistical analysis for significance in A was tested by Mann-Whitney test for the area under curve normalized to the time in experiment (P=0.333). The difference in survival between NRG $A\beta^{-/-}$ DQ8 mice and NRG $A\beta^{-/-}$ mice was statistically not significant (P=0.5232).

Next, huDQ8-HSC reconstituted mice were monitored for their reconstitution with human cells. Starting after weaning, at five weeks post reconstitution (p.r.), percentages of huCD45 cells in peripheral blood (PBL) in NRG Aβ$^{-/-}$ DQ8tg and NRG Aβ$^{-/-}$ mice were analyzed by flow cytometry (Fig. 29). HuCD45 cells in both groups increased until week eleven post reconstitution and reached a mean peak of ~10%. However, individual mice showed even higher percentages of huCD45 cells. Earlier than week five p.r., no huCD45 in PBL could be detected. Between week eleven and 21 p.r. the percentage of huCD45 cells remained stable in both groups, however, huCD45 cells in NRG Aβ$^{-/-}$ mice started to decrease slightly after. NRG Aβ$^{-/-}$ DQ8tg and NRG Aβ$^{-/-}$ mice older than 21 weeks gradually lost their huCD45 cells. Even individual mice that had very high percentages of huCD45 showed this progress of reconstitution.

In NRG Aβ$^{-/-}$ DQ8tg mice reconstituted i.h. with 1x10^5 huDQ8-HSCs from human cord blood, huCD45 cells could be detected throughout mice's entire life span with a maximum of up to 15%. Compared to the repopulation with huDQ8-PBMCs (see 12.2), the level of reconstitution is lower, but animals are healthy and the time window is longer (~40 days versus ~40 weeks).

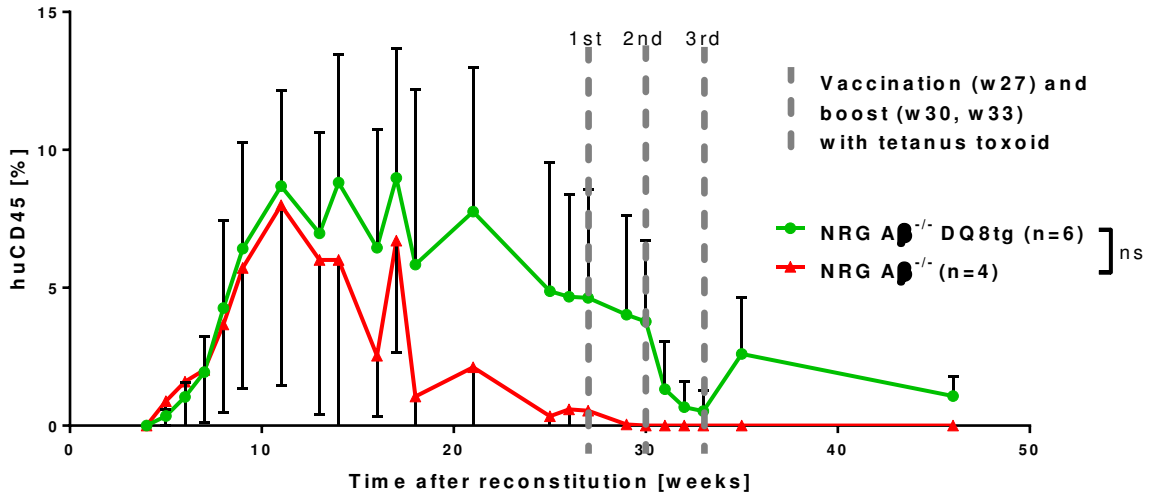

Fig. 29: HuCD45 cells in mice reconstituted as newborns with huDQ8-HSCs
NRG Aβ$^{-/-}$ DQ8 mice (green) and littermates NRG Aβ$^{-/-}$ mice (red) were analyzed by flow cytometry for huCD45 cells in blood. Statistical analysis for significance was tested by Mann-Whitney test for the area under curve normalized to the time in experiment (P=0.333).

This situation was changed when the mice were vaccinated. Starting 27 weeks post reconstitution, mice were vaccinated i.p every three weeks three times with the human vaccine Tetanol Pur® containing tetanus toxoid, a thymus dependent (TD), protein based vaccine (also see 4.3.). HuCD45 cells were expected to proliferate following this stimulus. Interestingly, huCD45 cells continuously decreased following vaccination and boost (Fig. 29).
Although huCD45 cells in NRG A$\beta^{-/-}$ mice seemed to be absent after 30 weeks p.r., this difference compared to NRG A$\beta^{-/-}$ DQ8tg mice was not significant (P=0.333).

Next, it was examined which human immune cell subsets developed in the mouse from huHSCs and differentiated into distinct lineages of human immune cells. Further, it was of interest whether the matching huDQ8tg had driven the differentiation towards a distinct human immune cell subtype. Therefore, PBLs from reconstituted NRG A$\beta^{-/-}$ DQ8tg and NRG A$\beta^{-/-}$ mice were analyzed by flow cytometry (see 7.6.1.4) for their presence of NK-cells (huCD56^{+}; Fig. 30, top row left), monocytes (huCD14^{+}; Fig. 30, top panel right), B-cells (B1: huCD5^{+}huCD19^{+} and B2: huCD5^{-}huCD19^{+}; Fig. 30 middle panels) and T-cells (huCD3^{+}huCD4^{+} or huCD3^{+}huCD8^{+}; Fig. 30 bottom panels) following reconstitution.
In addition, human cells were monitored for proliferation following vaccination with tetanus toxoid starting at week 27 post reconstitution.
Interestingly, all analyzed human immune cell subtypes could be detected in PBLs of mice but not earlier than five weeks p.r. In both groups of mice, up to 0.5% of human NK-cells were present in PBL from mice from week ten p.r. until week 20. However, later than week 20, human NK-cells seemed to disappear from the PBLs and also did not respond to vaccination. Interestingly, NRG A$\beta^{-/-}$ DQ8tg mice tended to show slightly higher levels of human NK-cells. The same development could be seen for human monocytes in PBLs of mice. From week ten to 30, monocytes in PBLs reached a level of up to 0.5% than got lost after 30 weeks p.r. Astonishingly, monocytes in PBLs of NRG A$\beta^{-/-}$ DQ8tg mice peaked around week 20 and 30 of up to 2% but declined as well after week 30 p.r. A correlation to the vaccination could not be found. A different pattern could be observed for B-cell. B1 B-cells (huCD5^{+}huCD19^{+}, middle panel, left) were already present very early in the PBLs (~w5) and peaked around week 10 to up to 10% of huCD45 cells. Until week 35, B1 B-cells could be detected in PBLs, however cells declined beginning at week 15 p.r.

Again, this pattern seemed to be unaffected by the vaccination and boost. Although B1 B-cell decline was also observed in NRG Aβ$^{-/-}$ DQ8tg mice, reduction of B1 B-cells was slightly slower compared to NRG Aβ$^{-/-}$ mice.

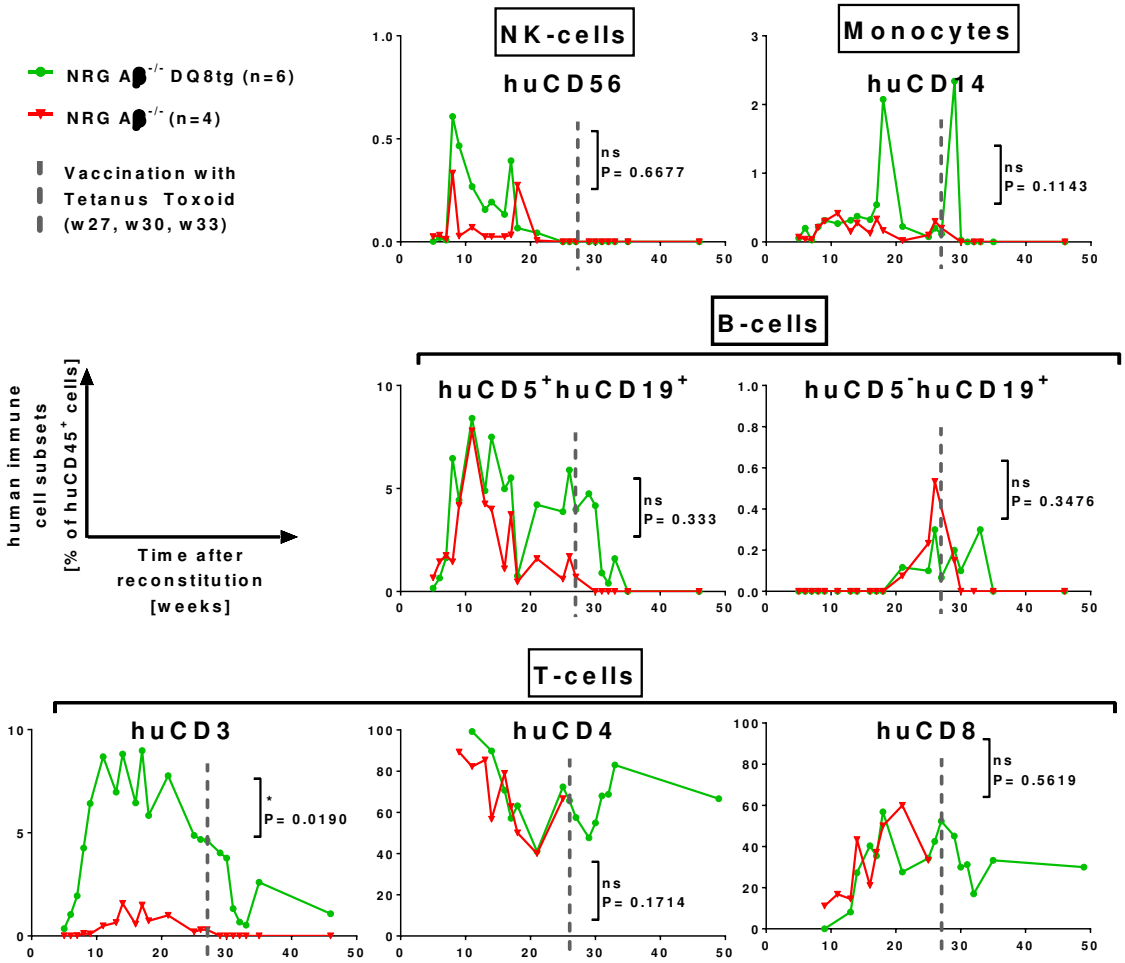

Fig. 30: Human immune cell subsets in PBL of huDQ8-HCS reconstituted mice
NRG Aβ$^{-/-}$ DQ8tg mice (green circles) and littermates NRG Aβ$^{-/-}$ mice (red triangles) were analyzed by flow cytometry for human immune cell subsets in peripheral blood (PBL) for a period of 50 weeks post reconstitution. For a better overview no standard deviations were shown. HuCD4 and huCD8 T-cells were only shown when huCD3 T-cells were present. All human cell subsets were gated on huCD45 cells shown in Fig. 28. Statistically differences were calculated with the Mann Whitney Test for the area under the curve.

In contrast, B2 B-cells (huCD5^{-} huCD19^{+}, middle panel, right) could not be detected earlier than 20 weeks p.r. Between weeks 25 and 35 p.r. B2 B-cells could be detected with up to 0.5% in PBLs but later than week 35, B2 B-cells declined as well. Since antibody producing B2 B-cells were present already before vaccination, it was not evident that vaccination was responsible for high B2 B-cell levels.

Interestingly, the reconstitution with human T-cells (lower panels) showed significant differences in PBLs. In NRG Aβ$^{-/-}$ DQ8tg mice, CD3 T-cells increased drastically from week five to ten p.r. to almost 10% and gradually declined after 20 week p.r. However huCD3 T-cells were present throughout the whole life span of the mice. In contrast, huCD3 T-cells in NRG Aβ$^{-/-}$ mice did not increase as drastically as in NRG Aβ$^{-/-}$ DQ8tg mice and also did not reach a level of more than 3% in PBLs. Around 30 weeks p.r. no huCD3 T-cells could be detected in PBLs of NRG Aβ$^{-/-}$ mice. Comparing huCD4 and huCD8 T-cells, in both groups of mice, the majority of huCD3 T-cells were huCD4 T-cells while huCD8 T-cells developed little later. Around 15 weeks p.r. the ratio of huCD4 (~60%) and huCD8 T-cells (~40%) remained relatively stable in both groups although an ample deviations due to single mice also occurred throughout the observation period. As expected, vaccination of mice did not correlate with alteration in T-cell levels.
Taken together, huDQ8-HSCs differentiated into NK-cells, monocytes, B-cells and T-cells in NRG Aβ$^{-/-}$ DQ8tg as well as NRG Aβ$^{-/-}$ mice. After the peak around week ten to 20, all human immune cell subsets started to decline. Interestingly, huCD3 T-cells in NRG Aβ$^{-/-}$ DQ8tg mice, but not in NRG Aβ$^{-/-}$ mice, were the predominant human immune cell subtype present in PBLs.

Following analyses of human cells in PBL, also organs of reconstituted mice were analyzed. Therefore, mice were euthanized 50 weeks post reconstitution and organs were collected. Spleens were analyzed for human cells as described above (Fig. 31, left). In addition, bone marrow cells were analyzed for huCD45 cells and also for huCD34 cells characterizing human hematopoietic stem cells (Fig. 31, right). Although human cells started to decline after 30 week post reconstitution and were absent in PBLs, human cells could be found in the spleen after 50 weeks post reconstitution to a very high level. However, there was no difference in the reconstitution level of NRG Aβ$^{-/-}$ DQ8tg and NRG Aβ$^{-/-}$ mice. Around 15% of huCD45 cells could be detected in spleen as well as in the bone marrow (Fig. 30). Interestingly, almost all human cells in the bone marrow were also human hematopoietic stem cells (huCD34^{+}). 20% of human CD3 T-cells could be detected in the spleen with more huCD4 T-cells (~ 40-50%) than huCD8 T-cells (~ 15-30%). The majority of B-cells were B1 B-cells (~ 10%) but B2 B-cells could be detected as well (~ 0.3%). Up to 0.5% of the human cells in the spleen were monocytes (huCD14^{+})

and no human NK-cells were found to repopulate the spleen. Notably, only the spleen as secondary lymphoid organ in reconstituted mice was highly repopulated with human cells, while others like lymph nodes were not (data not shown).

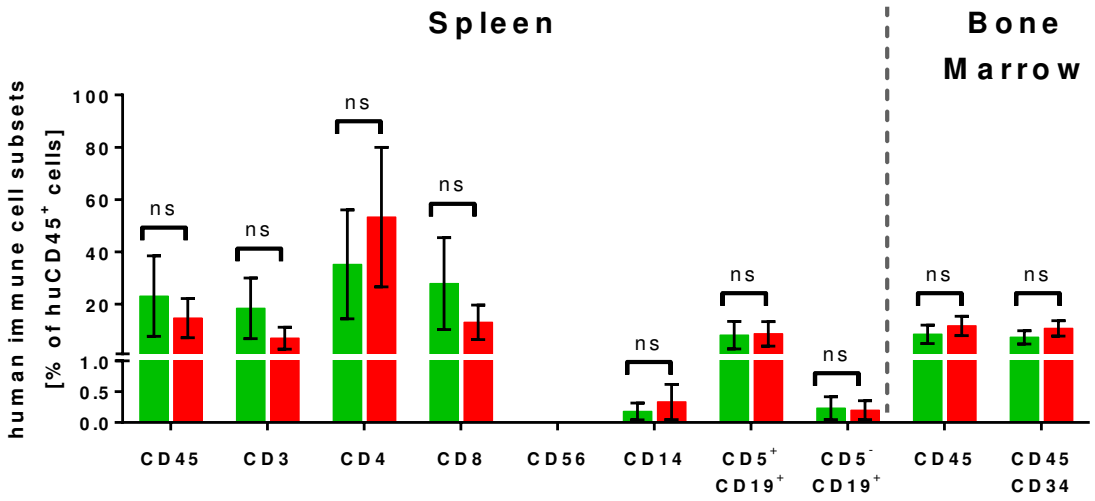

Fig. 31: Human immune cell subsets in spleen and bone marrow of huDQ8-HCS reconstituted mice

NRG A$\beta^{-/-}$ DQ8 mice (green) and littermates NRG A$\beta^{-/-}$ mice (red) were analyzed by flow cytometry for human immune cell subsets in spleen (left) and bone marrow (right). Human immune cell subsets were gated on huCD45$^+$ cells. CD4 and CD8 T-cells were gated on huCD3$^+$ cells. The standard error of the mean is depicted for every bar. Statistical differences were calculated by Mann-Whitney test (P values: CD45= 0.900; CD3= 0.500; CD4= 0.6218; CD8= 0.4578; CD56= 1; CD14= 0.6531; CD5$^+$CD19$^+$= 0.9579; CD5$^-$CD19$^+$= 0.8964).

13.3. Humanization of newborn mice with mobilized huDQ8-HSC

Besides the reconstitution of newborn mice with huDQ8-HSCs from human cord blood mobilized (m) huDQ8$^+$ hematopoietic stem cells (mhuDQ8-HSCs) were used for humanization. An advantage of mhuDQ8-HSCs was that higher cell numbers could be obtained from one donor. In order to optimize the generation of humanizing mice, mhuDQ8-HSCs were used freshly isolated, frozen/thawed as well as cultivated prior to reconstitution. In the following, these approaches are compared.

13.3.1. Humanization with freshly isolated or prior frozen/thawed mhuDQ8-HSC

In order to optimize humanization and to minimize work load, reconstitution levels of mice reconstituted with freshly isolated mhuDQ8-HSCs and frozen stored and prior

thawed mhuDQ8-HSCs were compared. First, freshly isolated and frozen mhuDQ8-HSCs from the same donor were compared. Therefore, fresh and thawed mhuDQ8-HSCs were analyzed by flow cytometry for the expression of huCD45 and huCD34 (Fig. 32). Both, fresh and thawed mhuDQ8-HSCs obtained a very pure huCD45^{+}huCD34^{+} cell population of >98%. However, freezing and thawing reduced the overall number of viable cells to about 20-40% (data not shown) and also the expression of huCD45 and huCD34 was slightly reduced (Fig. 32). In summary, it could be concluded that freezing and thawing might have an impact on the stem cell status of mhuDQ8-HSCs.

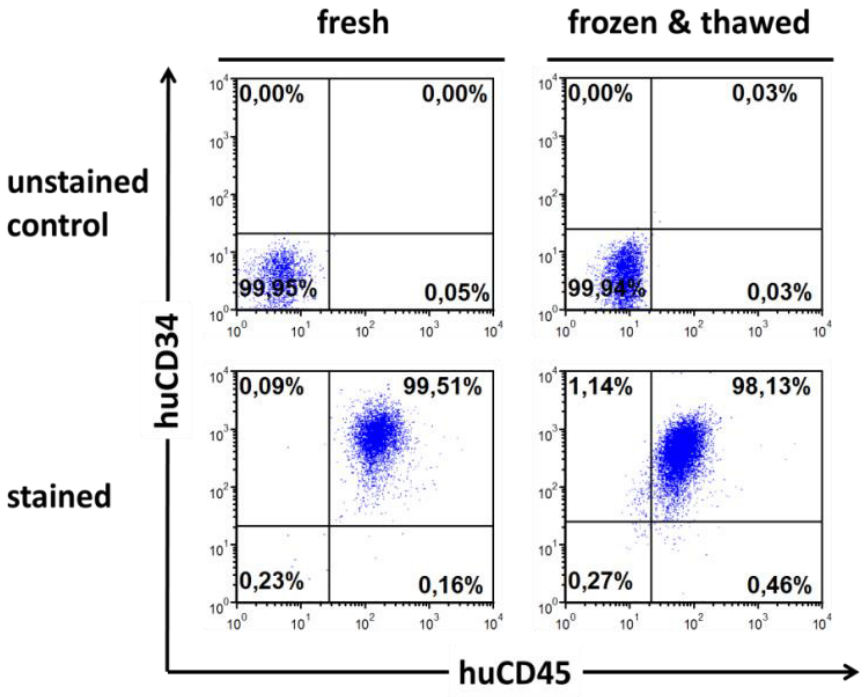

Fig. 32: Comparison of huCD34 expression of freshly isolated and thawed mhuDQ8-HSCs
Freshly isolated and thawed mhuDQ8-HSCs were analyzed by flow cytometry for their expression of huCD45 and huCD34.

Next, the reconstitution ability of the two mDQ8-HSCs was compared. Therefore, newborns were reconstituted i.h. with 1x10^{5} of either fresh mhuDQ8-HSCs or thawed mhuDQ8-HSCs. After weaning, mice were genotyped for huDQ8tg. Starting at week seven after reconstitution, mice were analyzed by flow cytometry for huCD45 cells in PBL until week 15 (Fig. 33 A) and different human cell subsets in PBL at twelve weeks after reconstitution (Fig. 33 B). NRG A$\beta^{-/-}$ DQ8tg mice (n=7) and littermates NRG A$\beta^{-/-}$ mice (n=2) reconstituted with fresh mhuDQ8-HSCs (Fig. 33 A, left) showed the same level of reconstitution with huCD45 in PBL (5-10%) that peaked around ten

weeks. In comparison, huCD45 cells in PBL of NRG Aβ$^{-/-}$ DQ8tg mice (n=3) as well as NRG Aβ$^{-/-}$ littermates (n=5) reconstituted with thawed mhuDQ8-HSCs (Fig. 33 A, right) peaked at week eleven p.r. Also, NRG Aβ$^{-/-}$ DQ8tg mice showed slightly higher reconstitution rates (10-30%) compared to NRG Aβ$^{-/}$ mice as well as mice reconstituted with fresh mhuDQ8-HSCs.

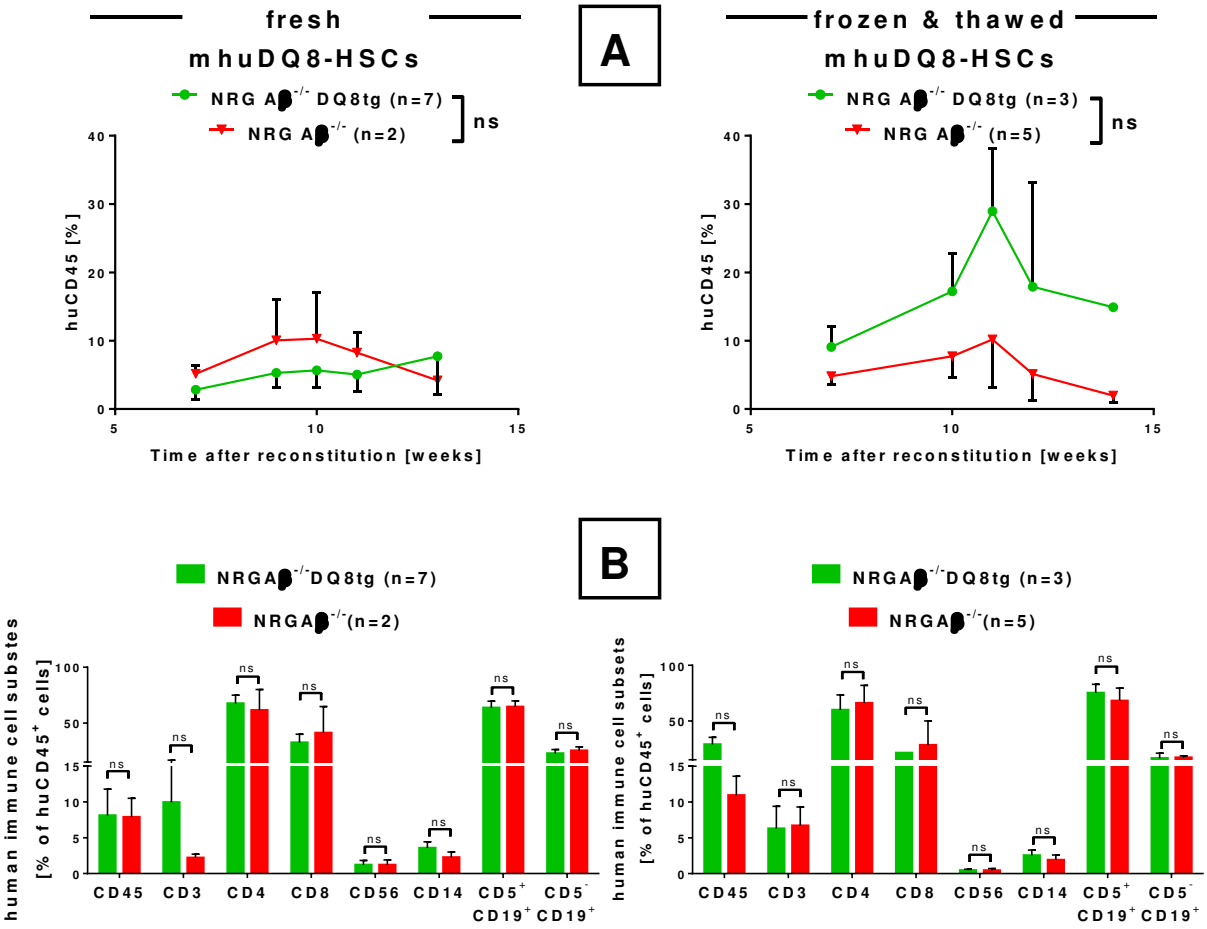

Fig. 33: Comparison of humanization with fresh and thawed mhuDQ8-HSCs
NRG Aβ$^{-/-}$ DQ8 mice (green/circles) and littermates NRG Aβ$^{-/-}$ mice (red/triangles) were analyzed by flow cytometry for huCD45 in PBL (A) and at week twelve post reconstitution in PBL (B). Human immune cell subsets were gated on huCD45^{+} cells. CD4 and CD8 T-cells were gated on huCD3^{+} cells. The standard error of the mean is depicted for every graph. Statistical differences were calculated by Mann-Whitney test for the area under the curve in A.

In Figure 33 B, the percentages of human immune cell subsets in PBL at week twelve are shown for either mice reconstituted with fresh mhuDQ8-HSCs (left) or thawed mhuDQ8-HSCs (right). Interestingly, various subsets of human immune cells could be detected in PBL of both groups. HuCD45^{+}CD3^{+} T-cells could be found to up

to 10%. T-cell subsets with slightly more huCD3$^+$CD4$^+$ (~60%) than huCD3$^+$CD8$^+$ (~40%) T-cells demonstrated a physiological ration (~1.5). The majority of human immune cells were huCD45$^+$CD5$^+$CD19$^+$ B1-cells (> 50%). B2 B-cells (huCD45$^+$CD5$^-$ CD19$^+$), NK-cells (huCD45$^+$huCD56$^+$) as well as monocytes (huCD45$^+$huCD14$^+$) were also present (< 5%). Notably, there was no significant difference in mice reconstituted with fresh or thawed mhuDQ8-HSCs. Besides the loos of cells after thawing, reconstitution with prior frozen mhuDQ8-HSCs was not detrimental for humanization. Thus, humanization of mice for the following experiments was done using stored, frozen mhuDQ8-HSCs when fresh cells were not available.

In the following, it was examined whether mhuDQ8-HSCs could be maintained in culture without hindrances until reconstitution and also whether reconstitution of human cells in mice could be enhanced with prior cultivation of mhuDQ8-HSCs. First, frozen mhuDQ8-HSCs were thawed and cultivated in the presence of supplements important for HSC growth including the human stem cell factor (huSCF), human interleukin 6 (IL-6), human thrombopoietin (huTPO) and human FMS-like tyrosine kinase ligand (huFlt3L; 100ng/ml each). Cultivated mhuDQ8-HSCs were analyzed by flow cytometry for the expression of huCD45 and huCD34 (Fig. 34 A right). As control, mhuDQ8-HSCs cultivated without supplements were analyzed (Fig. 34 A left). After two days in culture, only ~ 41% of the mhuDQ8-HSCs were found to be double positive for huCD45$^+$huCD34$^+$ while ~ 64% of the mhuDQ8-HSCs cultivated with supplements were found to be double positive. Also, mhuDQ8-HSCs cultivated with supplements exhibited a two distinct population of cells. One major huCD45$^+$huCD34$^+$ cell population and a minor huCD45$^+$ population exhibiting a lower expression of huCD34. In comparison, mhuDQ8-HSCs cultivated without supplements exhibited a more diffuse, no more well defined huCD45$^+$huCD34$^+$ population. In addition, two days cultivated mhuDQ8-HSCs proliferated up to three fold (Fig. 34B), however the presence of supplements enhanced cell proliferation (filled blue bars) compared to no supplements (filled grey bars). Hence, cultivated mhuDQ8-HSCs were able to proliferate in culture even better with supplements but the expression of huCD45 and huCD34 was reduced after two days in culture.

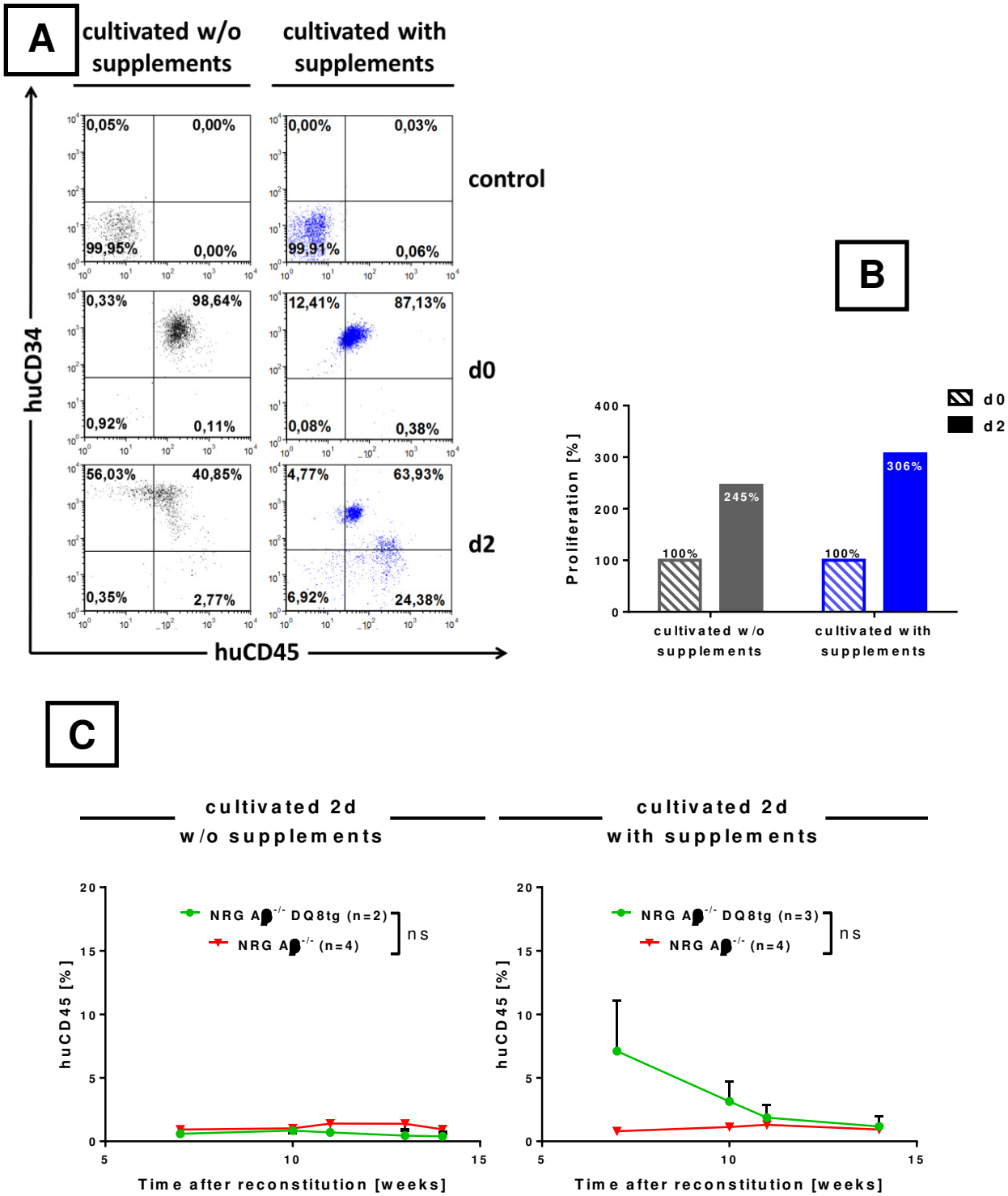

Fig. 34: Effects of *in vitro* cultivation of mhuDQ8-HSCs on engraftment into mice

Frozen mhuDQ8-HSCs were cultivated for two days in the presence of growth factors. By flow cytometry, huCD45 and huCD34 expression was analyzed (A). Absolute cell numbers were determined and proliferation of cultivated mhuDQ8-HSCs calculated (B). NRG Aβ$^{-/-}$ DQ8 mice (green/circles) as well as NRG Aβ$^{-/-}$ mice (red/triangles) were reconstituted with 1x10^5 mhuDQ8-HSCs cultivated in the absence (C, left) presence (C, right) and huCD45 cells were determined by flow cytometry starting seven weeks post reconstitution. The standard error of the mean is depicted for each curve. Statistical differences were calculated by Mann-Whitney test for the area under the curve (P=0.9958 and P=0.6286, respectively.)

To test, whether cultivated mhuDQ8-HSCs are still capable of reconstituting mice and even could enhance human cell engraftment, NRG A$\beta^{-/-}$ DQ8tg mice were reconstituted i.h. with 1x10^5 of 2d cultivated mhuDQ8-HSCs with or without supplements. After weaning, mice were genotyped for huDQ8tg. Starting at week seven after reconstitution, mice were analyzed by flow cytometry for huCD45 cells in PBL until week 14 (Fig. 34 C). NRG A$\beta^{-/-}$ DQ8tg mice (n=2) and littermates NRG A$\beta^{-/-}$ mice (n=4) reconstituted with mhuDQ8-HSCs cultivated without supplements (left) reached a level of < 2% huCD45 cells whereas NRG A$\beta^{-/-}$ DQ8tg mice (n=3) and littermates NRG A$\beta^{-/-}$ mice (n=4) reconstituted with mhuDQ8-HSCs cultivated two days in presence of supplements (right) reached slightly higher level. However this difference is not significant for the mouse groups.
Taken together, cultivating mhuDQ8-HSCs in the presence of growth factors for more than 24 hours drastically increased the absolute number of mhuDQ8-HSCs, but not their capability to reconstitute mice.

A variety of different protocols were published describing how to maintain or induce proliferation of huCD34 cells *in vitro* without any loss of their stem cell capacity. As shown above, cultivating mhuDQ8-HSCs with conventional supplements did not significantly improve their maintenance or enhancement of humanization. One of the newest factors described is stem regenin-1 (SR-1; Boitano et al., 2010). SR-1 is a chemical compound, an aryl hydrocarbon receptor antagonist that promotes the expansion of huHSCs *in vitro* (Boitano et al., 2010). Following these ideas, this compound was used to improve short-term cultivation of mhuDQ8-HSCs for more flexibility in the process of humanization. Referring to the previous protocol, frozen mhuDQ8-HSCs were thawed and cultivated including all previous introduced supplements (huSCF, huFlt3L, huTPO, huIL-6) in the absence (Fig. 35, grey) or presence of 0.75µM SR-1 (Fig. 35, blue). The proportion of huCD45$^+$huCD34$^+$ cells was analyzed by flow cytometry (Fig. 35, left panels) and proliferation was determined from absolute cell numbers (Fig. 35, right bar charts).

Starting with ~ 90% double positive mhuDQ8-HSCs, this number was reduced at day three of ~59% and at day six of ~ 30% for mhuDQ8-HSCs cultivated without SR-1. In contrast, mhuDQ8-HSCs cultivated in the presence of 0.75 µM SR-1 also showed a decline in double positive cells but to a less extent. At day three ~ 88% and at day six

~ 60% of mhuDQ8-HSCs are huCD45^{+}huCD34^{+}. Also, the overall number of viable mhuDQ8-HSCs increased *in vitro* with more mhuDQ8-HSCs cultivated in the presence of SR-1. Taken together, short-term cultivation of thawed mhuDQ8-HSCs in the presence of SR-1 yielded in drastic proliferation of mhuDQ8-HSCs with only minimal loss of their stem cell capacity. Maintaining mhuDQ8-HSCs *in vitro* with SR-1 should provide more flexibility in the humanization procedure and was used for the following humanization experiments when short-term cultivation was inevitable prior to reconstituting.

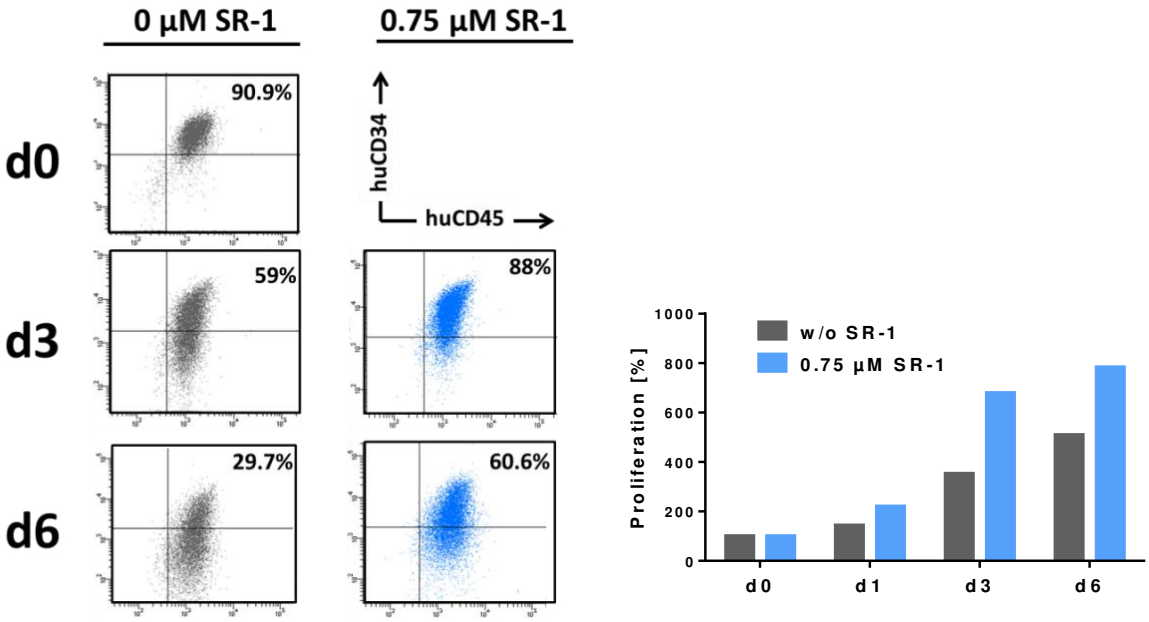

Fig. 35: Cultivation of mhuDQ8-HSCs in the presence of stem regenin-1
Frozen mhuDQ8-HSCs were thawed and cultivated for six days in the absence (grey) or presence (blue) of 0.75µM stem reginin - 1 (SR-1). By flow cytometry, huCD45 and huCD34 expression was analyzed (left panels). Absolute cell numbers were determined and proliferation of cultivated mhuDQ8-HSCs calculated (bar chart, right).

13.3.2. Humanization of adult mice with mobilized huDQ8-HSC

Humanization of newborn NRG A$\beta^{-/-}$ DQ8tg mice resulted in long-term reconstitution with human cells. However, the presence of the human transgene could not be detected directly after birth so that mice without the huDQ8tg also were reconstituted with huDQ8-HSCs, expanding the number of animals in experiments. Reconstitution of adult mice with mhuDQ8-HSCs therefore would be helpful. Hence, six weeks old adult NRG A$\beta^{-/-}$ DQ8tg mice (n=4) and NRG A$\beta^{-/-}$ mice (n=2) were sublethally

irradiated (1.5 Gy) and reconstituted i.v. with $1x10^5$ mhuDQ8-HSCs. After 14 weeks of reconstitution, mice were analyzed by flow cytometry for huCD45 cells in PBL, spleen and in addition for huCD34 cell in bone marrow (Tab. 2). Human cell engraftment in PBL, spleen and bone marrow was very low (< 0.5%) and did not increase at later points in time (data not shown). Interestingly, human hematopoietic $huCD34^+$ stem cells could be detected in the bone marrow. Due to the low level of reconstitution and the obsolete age of mice at time of analyses, humanization of adult mice with huHSCs was not continued.

Tab. 2: Humanization of adult NRG $A\beta^{-/-}$ DQ8 mice with huDQ8-HSCs

		NRG $A\beta^{-/-}$ DQ8tg (n=4)	NRG $A\beta^{-/-}$ (n=2)
huCD45	PBL	[0.01 - 0.04]	[0.02 - 0.60]
	Spleen	[0.04 - 0.12]	[0.03 - 0.07]
	Bone Marrow	[0.03 - 0.44]	[0.01 - 0.05]
huCD34	Bone Marrow	[0.04 - 0.18]	[0.01 - 0.02]

Adult six weeks old NRG $A\beta^{-/-}$ DQ8 and NRG $A\beta^{-/-}$ mice were sublethally irradiated (1.5 Gy) and reconstituted i.v. with $1x10^5$ huDQ8-HSCs. At week 14 after reconstitution, mice were analyzed for huCD45 in PBL, spleen and bone marrow as well as for huCD34 in bone marrow. Statistical analyzes were not performed due to the low reconstitution levels with human cells.

13.4. Initiation of adaptive immune responses in humanized mice

It could be shown that huDQ8-HSCs in mice could differentiate into various subsets of human immune cells (see 13.2 and 13.3). For the induction of an adaptive response, human immune cells have to communicate with each other to perform their appropriate function in mice. In the following, activation and functionality of human T and B cell subsets were investigated.

13.4.1. Ex vivo stimulation of human T-cell subsets in mice

First, human T-cells were analyzed for their activation status. Therefore, in a new experiment, NRG $A\beta^{-/-}$ DQ8tg (n=4) and NRG $A\beta^{-/-}$ mice (n=3) were reconstituted with

$1x10^5$ mhuDQ8-HSCs and analyzed at week 20 post reconstitution. Blood from each mouse was collected and PBMCs were purified by Ficoll gradient. The percentages of huCD45 (mean ~ 55%) (Fig. 36 A) as well as $huCD3^+CD4^+$ T-cells (mean ~ 35%) and $huCD3^+CD8^+$ T-cells (mean ~15%) of all human lymphocytes in PBMCs of mice (Fig. 36 B) were determined by flow cytometry. To avoid deceptive results in flow cytometry analyses, mice that had a reconstitution level below 10% huCD45 cells were excluded from further analyses. Subsequently, PBMCs were cultivated for six hours with *phorbol 12-myristate 13-acetate* (PMA) and *ionomycin* stimulating T-cells to produce interferon γ (IFNγ) (see 7.4.6). IFNγ has immunostimulatory and

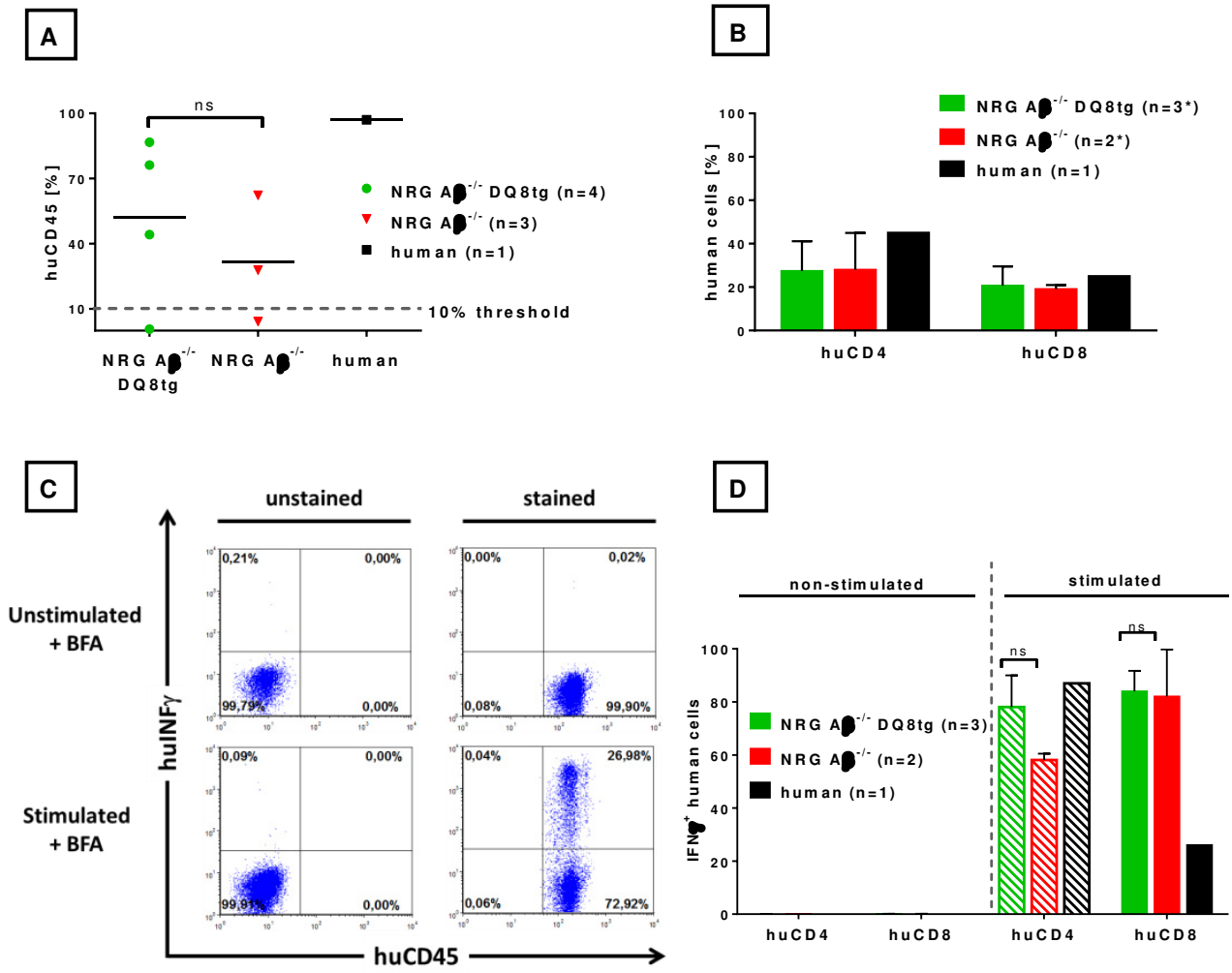

Fig. 36: *Ex Vivo* activation and stimulation of human T-cells in mice to secrete IFNγ

NRG $A\beta^{-/-}$ DQ8 mice (green) and littermates NRG $A\beta^{-/-}$ mice (red) were repopulated with mhuDQ8-HSCs. After 20 weeks post reconstitution, blood was collected. PBMCs were purified and stimulated with PMA and ionomycin. Percentages of huCD45 (A) as well as huCD4 and huCD8 T-cells (B) in PBMCs were analyzed by flow cytometry. Mice with less than 10% huCD45 were excluded from further analyses (*). Human PBMCs (black) as positive control were stimulated and the percentages of human cell producing IFNγ in presence of brefeldin A (BFA) were determined by flow cytometry (C). $IFN\gamma^+$ huCD4 (n=0.1017) or huCD8 T-cells (n= 0.9951) in PBMCs of mice were determined (D). Statistical analyses were performed by Mann-Whitney test.

immunomodulatory effects to innate and adaptive immune responses and is secreted by activated T-cells in high amounts (see 4.3). To detect produced IFNγ inside T-cells by flow cytometry, *brefeldin A* (BFA) was added to the cultures for four hours before the final analysis (see 7.4.6). In Figure 36 C, human PBMCs as positive control were stimulated and analyzed for huCD45 and IFNγ expression by flow cytometry. About 27% of stimulated human PBMCs produced IFNγ (Fig. 36 C, lower panel, right) whereas no IFNγ was detected without stimulation (Fig. 36 C, upper panels). Figure 36 D, shows the analysis for stimulated huCD4 T-cells (striped bars) and huCD8 T-cells (filled bars) in PBMCs of mice. Non-stimulated human cells did not produce IFNγ (Fig-36 D, left) whereas ~ 80% of stimulated huCD4 and huCD8 T cells produce IFNγ (right). Notably, only 30% of huCD8 T-cells in the human control (filled black bar) were found to produce IFNγ. Taken together, human T-cells were capable of *ex vivo* activation and stimulation to secrete IFNγ. In contrast to human T-cells in huDQ8-PBMC repopulated mice (see 12.4), human T-cells in mice reconstituted with mhuDQ8-HSCs were not activated without external stimulus.

13.4.2. Vaccination of humanized mice to induce humoral immune responses

Next, the functionality of human B-cells in humanized mice was examined. As described before (see 16.1 and 16.2), human B1 B-cells ($huCD5^+huCD19^+$) were found to be the predominant subset of B-cells whereas B2 B-cells ($huCD5^-huCD19^+$) could be detected as minor population, mainly at later points post reconstitution. Human B2 B-cells are known as conventional antibody producing cells that develop following stimulation by an antigen (see 4.3). Humanized mice were held in a sterile environment to control their exposure towards antigens that could elicit immune responses. To analyze whether human B-cells were capable of stimulation by an antigen and thus eliciting humoral immune responses, humanize mice were vaccinated. Therefore, NRG $A\beta^{-/-}$ DQ8tg mice reconstituted with $1x10^5$ mhuDQ8-HCSs were analyzed for huCD45 in PBL. Only mice exhibiting more than 10% huCD45 cell in blood, were vaccinated (NRG $A\beta^{-/-}$ DQ8tg: n=2; NRG $A\beta^{-/-}$: n=2). Starting 24 weeks post reconstitution, mice were vaccinated every three weeks three times with the vaccine *Tetanol Pur®* containing *tetanus toxoid,* a thymus dependent (TD), protein based vaccine. Following the last vaccine boost, mice were euthanized

(Fig. 37 A). During the vaccination, mice were monitored for signs of disease represented by alterations in weight (Fig. 37 B). Weight of mice in both groups increased throughout the challenge experiment. No further signs of disease could be observed. Figure 37 C gives an overview of human immune cell subsets in PBL. Weekly, PBL of the vaccinated mice was analyzed for huCD45, huCD3 T-cells and their subsets huCD4 and huCD8, monocytes (huCD14), NK-cells (huCD56) and B1 B-cells ($huCD5^+huCD19^+$) and B2 B-cells ($huCD5^-huCD19^+$). Interestingly, the percentage of huCD45 cells did not alter but remained stable throughout the vaccination in NRG $A\beta^{-/-}$ DQ8tg mice (green) and NRG $A\beta^{-/-}$ mice (red). Surprisingly, NRG $A\beta^{-/-}$ mouse K3#M2 lost almost all huCD45 cells. $HuCD45^+CD3^+$ T-cells slightly increased of up to 40% while the ratio of huCD4 (~ 50%) and huCD8 (~ 50%) cell was almost constant throughout the experiment. Monocytes and NK-cells showed distinct populations but the percentages decreased by time to <5%. At the beginning, human B1 B-cells represented the predominant human immune cell type (~ 60%) in PBL of humanized mice however this population slightly decreased during the challenge and after the third boost at week seven, only ~10% of B1 B-cells could be detected. In contrast, human B2 B-cells steadily increased in percentage from ~ 10% at day 0 to ~ 40% after seven weeks of challenge with the vaccine. Taken together, challenging humanized mice with the TD antigen stimulated B2-cells to proliferate and expand. Whether B2 B-cells were functional upon antigen stimulation was tested by analysis of secreted antibodies. Weekly during immunization, sera of mice were tested by ELISA (see 7.6.2.1) for the presence of tetanus toxoid specific human immunoglobulins M and G (huIgM and huIgG; Fig. 37 D left and right, respectively). Increasing levels of huIgM could be detected as early as one week after the first vaccine challenge. The maximum of 0.1 IU IgM/ml serum was reached two weeks after the first immunization and decreased already one week later. The second and third boost did not further increase IgM levels in serum.

In contrast, huIgG levels could be detected first after two weeks of immunization. The maximum of 0.3 IU IgG/ml serum (mouse K1#M2) was reached after the second boost at week four. Notably, a third immunization did not further increase huIgG levels in humanized mice. In vaccinated humans, 0.11 – 0.5 IU tetanus antitoxin specific IgGs/ml are considered to provide immunity (Robert-Koch-Institute, 2013). In summary, upon stimulation with a TD antigen, human B-cells in humanized mice

were capable to secrete huIgM and huIgG antibodies demonstrating their functionality.

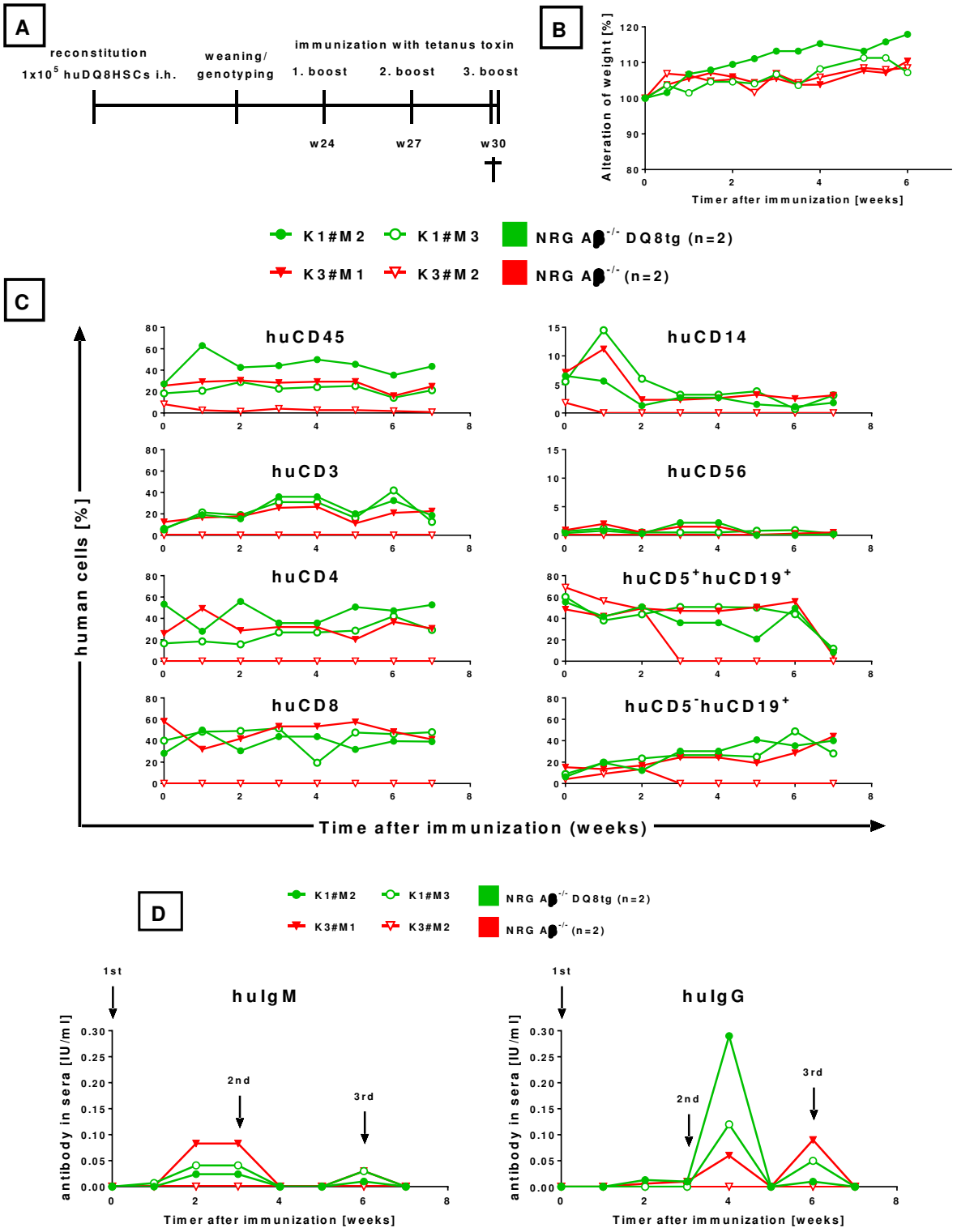

Fig. 37: Immunization of humanized mice with the TD antigen tetanus toxoid

NRG Aβ$^{-/-}$ DQ8 mice (green, circles) and NRG Aβ$^{-/-}$ mice (red, triangles) reconstituted with 1x10^5 mhuDQ8-HSCs were vaccinated with *tetanus toxoid* with three following booster injections, starting 24 weeks post reconstitution (A). Health status of mice during immunization was represented by changes in weight (B). By flow cytometry, human immune cells were weekly analyzed in PBL including huCD45 cell, huCD3 T-cells (huCD4 and huCD8), monocytes (huCD14), NK-cells (hu8CD56) and B-cells (huCD5$^+$huCD19$^+$ and huCD5$^-$huCD19$^+$) (C). In sera of mice, human immunoglobulins M and G (huIgM and huIgG) were tested weekly by ELISA (D).

13.5. Infection of humanized mice with HIV

Various human immune cell subsets were present in humanized mice and human T cells as well as B-cells were capable of inducing adaptive immune responses. Now, humanized mice were infected with HIV-1_{NL4-3} and monitored for the pathogenesis. To evaluate the minimal level of human cells in humanized mice required for productive HIV infection, mice containing low levels of huCD45 cell (0.1- 0.5%) were used. A cohort of reconstituted NRG $A\beta^{-/-}$ DQ8tg mice were infected i.p. with either $1x10^6$ *tissue culture infectious dose 50* ($TCID_{50}$) (n=5) or $2x10^6$ $TCID_{50}$ (n=2). HuCD45 cells in PBL of infected mice were determined by flow cytometry (Fig. 38 left) and HIV RNA copies/ml serum were determined by quantitative real-time PCR for a period of 100 days post infection (Fig. 38 right). Percentages of huCD45 cells remained unaltered low (0.1 - 0.5%), however there was a peak of ~ 18% in a single mouse at day 38 post infection. Due to the low levels of human cells, the frequencies of huCD4 or huCD8 T-cells were not determined. Copies of HIV RNA in sera of mice were detectable throughout the entire observation period. The maximum was reached at day eleven post infection ($2x10^5$ copies/ml) while at a later date the titer decreased and remained detectable between $0.5x10^3$ and $2x10^3$ copies/ml. Although the percentages of huCD45 cell prior HIV infection were quite low, a long-term HIV infection in humanized mice could be maintained.

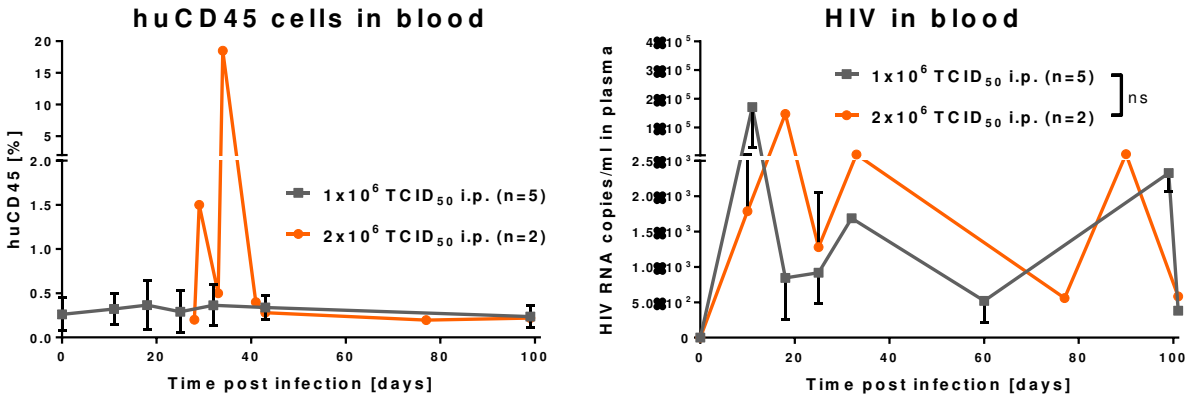

Fig. 38: Infection of low level reconstituted humanized mice with HIV
NRG $A\beta^{-/-}$ DQ8tg mice reconstituted with 0.1 - 0.5% huCD45 were infected i.p. with $1x10^6$ or $2x10^6$ $TCID_{50}$ HIV-1_{NL4-3}. Over a period of 100 days post infection, huCD45 cells (left) and copies of HIV RNA in sera of mice were determined. Standard deviations were depicted and statistical analyses were calculated by Mann-Whitney test for the area under the curve.

14. Outlook

Although NRG Aβ$^{-/-}$ DQ8tg mice humanized with huDQ8-PBMCs were superior compared to NRG Aβ$^{-/-}$ mice lacking the DQ8tg, this could not be shown clearly for NRG Aβ$^{-/-}$ DQ8tg mice reconstituted with huDQ8-HSCs. Therefore, prospective studies have to focus on the importance of the MHC class II matching in more detail.

So far, *ex vivo* TCR-independent T-cell stimulation isolated from huHSC reconstituted mice, resulted in activated and functional T-cells independent of the DQ8tg. However, *ex vivo* TCR-dependent stimulation was not performed. Hence, prospective studies should focus on studying *ex vivo* and *in vivo* T-cell stimulation as well as specific T-cell responses to further determine the importance of the DQ8tg for the induction of human T-cell responses in humanized mice.

In addition, it could be shown that human B-cells were able to secrete human IgG antibodies *in vivo* upon vaccination with a T-cell dependent tetanus vaccine. However, due to small mouse numbers the relevance of the DQ8tg could not be demonstrated here. Therefore, future studies should focus on the importance of the DQ8tg for specific B-cell responses upon activation with T-cell dependent and independent stimuli *in vivo.*

Furthermore, it was shown that huDQ8-HSC reconstituted DQ8tg mice with low human cell engraftment were able to maintain an HIV infection for a long period of time. Prospective studies should focus on the investigation of α-HIV specific immune responses such as neutralizing antibodies and cytotoxic T-cell responses. Because of the low number of human cells it was not possible to monitor the huCD4 T-cell decline following HIV infection and therefore it will be necessary to investigate mice with high number of human cells. This will be also of importance concerning HIV-2 infections.

Moreover, it might be interesting to generate BLT mice with DQ8tg mice, since they possess a more robust reconstitution and specific immune responses might be enhanced compared to non-transgenic BLT mice. Also it will be interesting to examine different routes of HIV infection such as the more natural route via mucosal tissues.

IV. Discussion

The major challenge in HIV vaccine development is preclinical testing. HIV's only relevant hosts are humans and no correlates of protection are known. Here, novel humanized mice have been established for preclinical testing of HIV vaccines or drugs. Humanization of mice was performed with human peripheral blood mononuclear cells (huPBMCs) as well as human hematopoietic stem cells (huHSCs). In order to generate a robust model with efficient human adaptive immune responses, immune deficient mice (NOD Rag1$^{-/-}\gamma c^{-/-}$) expressing human MHC class II (HLA-DQ8) on a mouse class II deficient background (A$\beta^{-/-}$) were used. In these animals, the human HLA-DQ8 (huDQ8) molecule supported the functionality of the transferred huDQ8-PBMCs in mice as well as the development and maturation of human immune cells in the humanized thymus following reconstitution with huDQ8-HSCs. Different protocols of humanization with huDQ8-PBMCs and huDQ8-HSCs were tested and optimized with regard to the engraftment of human cell subsets and the establishment of a functional human adaptive immune system. Consequently, the humanized mice were analyzed for their ability to induce adaptive immune responses, support HIV infections which allow evaluating this model for its application in preclinical testing.

15. Humanization of immunodeficient mice with huPBMCs

15.1. Amount of human cells and route of application

In order to establish an optimal protocol for the humanization with huPBMCs, different cell numbers (1x10^7 or 1x10^8 huPBMCs) and different routes of application (i.p. or i.v.) were tested according to their repopulation kinetics and overall efficacies. In addition, mice were monitored for signs of disease following cell transfer because due to their priming in human thymus, mature human T-cells cause GvHD (Hoffmann-Fezer et al., 1993).

In this work, the transfer of 1x10^8 huPBMCs i.v. into NSG mice led to a very rapid onset of GvHD, while it took longer after the transfer of 1x10^7 huPBMCs. An almost linear dependency of the onset of GvHD and number of transferred human cells was

found. The higher the number of transferred cell, the faster the onset of GvHD appeared. These finding are in agreement with those from van Rijin and colleagues. They repopulated NRG mice i.v. with $3x10^6$ huPBMCs and found high engraftment rates (mean: ~ 60% huCD45 cells) two to four weeks post repopulation which also was associated with an acute GvHD syndrome. Lower doses of huPBMCs correlated with a higher variability in engraftment and a later increase in human cells (van Rijn et al., 2003). King and colleagues (2003) made a similar finding using NSG mice. They determined the effect of huPBMC cell dose on GvHD disease development and injected $5x10^6$, $1x10^7$ and $2x10^7$ huPBMCs i.v. into NSG mice. They found a strong correlation between the median survival time (22 days, 17 days and 12 days respectively) and the transferred cell dose. All cohorts of mice given even low doses ($5x10^6$) of PBMCs developed xenogeneic GvHD (King et al., 2009). Even though very low doses of transferred huPBMCs were reported to result in the development of GvHD, in this work the transfer of $5x10^7$ huPBMCs was found to be sufficient for consistent engraftment with an acceptable increase in huCD45 cells before severe GvHD developed.

Transferring huPBMCs i.v. was more efficient than i.p. application. Even the transfer of high numbers of huPBMCs ($1x10^8$) i.p. led to only low humanization rates. Pearson and colleagues (2008) reported that the engraftment of NSG mice was independent on the route of transfer. They described that the transfer of $2x10^7$ huPBMCs typically results in 15% to 45% huCD45 cells in the PBL within 4 weeks transferred by both routes. Here, only the engraftment rates following i.v. transfer were comparable with the observations by Pearson. So far it is not clear why different observation were made using the same mouse strain. On the one hand, differences in engraftment regarding both routes might be due to variations amongst PBMC donors. However, Pearson reported that NSG mice overcome donor-to-donor variability compared to NOD *scid* mice. On the other hand, human cells transferred i.p. need to migrate in a more active way to get access into the blood stream or lymph in order to be broadly distributed throughout the entire body. Apparently, the majority of human cells died shortly after repopulation because they were hardly detectable in PBL even at a later point in time. Possibly, human cells did not get sufficient survival or migration signals in the peritoneum to enter the blood stream or lymph. For this reason, different

mechanisms for human cells to engraft in mice might be imaginable following the i.v. or i.p. routes of huPBMC transfer.

In this work, it was not tested to what extent huCD45 cells could be observed in secondary lymphoid organs at very early time after i.p. cell transfer. It remains elusive whether human cells are capable of migrating into organs shortly after repopulation. However, at a later date no or only low levels of huCD45 cells (<0.5%) were detectable. Possibly, human cells rapidly migrated into secondary lymphoid organs (e.g. spleen) were they did not survive or they did not migrate at all from the site of transfer and promptly died. Whether human cells are capable of surviving and migrating due to essential signals provided by the murine microenvironment or by human cells themselves, needs to be further investigated.

15.2. Effects of matching human DQ8$^+$ cells in huDQ8tg mice

A robust humanized mouse model for testing vaccines requires a functional human immune system with efficient innate and adaptive immune responses. In addition, these animals should not develop GvHD so they can be used for long-term experiments in preclinical trials.

Here, the development of GvHD upon adoptive transfer of human DQ8$^+$ PBMCs (huDQ8-PBMCs) into immunodeficient recipient mice (NRG A$\beta^{-/-}$DQ8tg, NRG A$\beta^{-/-}$ or conventional NRG mice) were studied. The presence of the human HLA-DQ8 in NRG A$\beta^{-/-}$DQ8tg recipient mice significantly enhanced the overall repopulation rate by huDQ8-PBMCs compared to conventional NRG mice with only murine MHC. NRG A$\beta^{-/-}$ mice possessed an intermediate phenotype. However, exclusively human CD3$^+$ T-cells were engrafted in all mouse strains. Beside this, the noticeable difference between the strains was the time frame until GvHD became fatal. While xenogeneic repopulation of NRG and NRG A$\beta^{-/-}$ mice with huDQ8-PBMCs resulted in a rapid induction of GvHD and poor survival, allogeneic transfer of HLA-class II-matched huDQ8-PBMCs into NRG A$\beta^{-/-}$ DQ8tg recipients, resulted in a milder form of GvHD such that the mice survived significantly longer. Clearly, liver destruction, as measured by serum ALT level, was less pronounced in NRG A$\beta^{-/-}$DQ8tg and NRG A$\beta^{-/-}$ recipients compared to that seen in NRG mice. As expected for a systemic

disease, this also correlated with infiltration of cytotoxic huCD8$^+$ T-cells into the liver and other organs like kidney, intestine and skin. The delayed onset and mild progression of GvHD in the DQ8 haplotype matched recipients corresponded with the delay in the expansion of huCD8$^+$ T-cells. HuCD8$^+$ T-cells reacted towards xenogeneic murine MHC class I molecules and not towards allogeneic class II MHC molecules in NRG and NRG A$\beta^{-/-}$ recipients. The development of GvHD was most aggressive in NRG/NSG mice because human T-cells recognized both murine MHC class I and II molecules as foreign while MHC class II molecules in NRG A$\beta^{-/-}$ mice were absent and thus not recognizable by human T-cells but still murine MHC I molecules causing GvHD. It could be concluded that the expansion of human CD8$^+$ T-cells was an early sign of xenogeneic GvHD, however, HLA class II matching in NRG A$\beta^{-/-}$ DQ8tg mice could not prevent the onset of GvHD.

Mechanistically, two scenarios could be envisioned for why NRG A$\beta^{-/-}$DQ8tg mice developed an attenuated form of GvHD. Doubtlessly, these scenarios must account for the fact that xenoreactive huCD8$^+$ T-cells apparently were activated less efficiently in DQ8tg mice. One explanation might be that the introduction of huDQ8tg and removal of murine MHC class II reduced the frequency and thus the helper-activity of xenoreactive CD4$^+$ T-cells. This would be expected since the frequency of HLA class II matched huCD4$^+$ T-cells being activated was much smaller compared to the proportion of huCD4$^+$ T-cells encountering xenogeneic murine class II. HuCD4$^+$ T-cells in NRG A$\beta^{-/-}$ DQ8tg recipients thus would recognize murine peptides presented by huDQ8 and this situation would mimic an allogeneic class II matched scenario where huCD4$^+$ T-cells might solely react towards murine minor histocompatibility antigens. The lower frequency of activated huCD4$^+$ T-cells may then not suffice to allow for an efficient mounting of the xenoreactive response of huCD8$^+$ T-cells. Alternatively, the second explanation might be that, huDQ8 matching regulatory huCD4$^+$ T-cells (Tregs) in donor PBMCs may be induced, due to their ability to interact with their restricting HLA class II, huDQ8. In this way they initially could keep the GvHD-mediating T-cells under control. However, it is unclear whether reactivity towards xenogeneic class II or allogeneic matched class II minor antigens, respectively, would favor either conventional huCD4$^+$ T helper or regulatory T-cells in this setting.

Human interferon gamma (IFNγ) levels in the serum of recipient mice were elevated shortly after the transfer of huDQ8-PBMCs and remained unaltered throughout the experiment which was equally true for all examined mouse strains. These data favor a scenario in which the xenoreactive huCD8$^+$ T-cell activation was responsible for the fatal GvHD induction but due to class II haplotype matching, changing the quality or quantity of the huCD4$^+$ T-cell response, the xenoreactive CD8$^+$ T-cells took longer mounting their response in DQ8 matched recipient mice. A clear mechanistic solution will require further analyses with respect to huCD4$^+$ T-cell subsets, their cytokine profiles, and analyses with respect to the regulatory capability of transferred huCD4$^+$ Treg cells. Finally, NRG Aβ$^{-/-}$DQ8tg mice are a useful model to experimentally test for modalities reducing GvHD in partially-allogeneic or minor-histocompatibility disparate settings.

A further refinement would be to cross NRG Aβ$^{-/-}$ DQ8tg with MHC class I knockout mice. In these, the CD8$^+$ mediated component of GvHD would be eliminated and this may make the mice even suitable for long term studies. Overall, this newly generated mouse strain shows prolonged survival and delayed onset of GvHD after transplantation with haplotype matched human PBMCs. Thus, it is a superior model to study GvHD and it could be valuable to investigate CD4$^+$ T-cell responses or activities of antiviral substances for certain human pathogens like the human immunodeficiency virus (HIV).

15.3. Attempts to the induction for humoral immune responses

A crucial limitation of the huPBMC-DQ8tg mouse model for vaccine testing is that MHC class II expression did not enable human B-cells to engraft and survive in DQ8tg mice.

Only the transfer of very high numbers of human cells (>1x10^8) enabled human B-cells to repopulate the spleen (<1%), however they only persist until seven days following repopulation (personal communication Zoé Waibler, Paul-Ehrlich-Institute). Unfortunately, survival of human B-cells was not supported by matching DQ8 molecules, which indicates that the survival and maintenance of human B-cells was not mediated by matching HLAs but other factors. Most likely, these factors are absent in the donor inoculum or the mouse itself. Indeed, mature B-cells *in vivo* are

actively maintained not only by survival signals received through the B-cell antigen receptor but also the cytokine human B-lymphocyte stimulator (huBLyS) plays a pivotal role in B-cell survival, maintenance and proliferation in humans (Schiemann et al., 2001; Mackay et al., 2002). HuBLyS facilitates the differentiation of short-lived immature B cells into mature recirculating long-lived B-cells and maintains mature B-cells in the periphery by facilitating their survival through non-canonical NF-kB mediated signals (Rolink et al., 2002; Sasaki et al., 2004 and 2006). Mainly, huBLyS is produced by stromal cells, macrophages, dendritic cells and neutrophils (Claudio et al., 2002). Given the critical role of huBLyS in normal B-cell homeostasis, the failure of efficient human B-cell engraftment and survival in mice humanized with huPBMC may be due to a deficiency of huBLyS. On the one hand, this failure could be due to species differences between human and murine BLyS so that insufficient survival signals were present. On the other hand, it might be possible that huBLyS producing cells themselves did not survive following transfer or that these cells were not transferred at all into mice so that they could not provide human B-cells with a survival and maintenance signal. In 2008, Schmidt and colleagues evidenced these hypotheses and found that recombinant huBLyS improved human peripheral blood B-cell survival *in vitro*, while murine BLyS was ineffective. In addition they reported a markedly enhanced engraftment of human B-cells in humanized mice supplemented with recombinant huBLyS (Schmidt et al., 2008).

In this work, *in vitro* cultivation of human B-cells in the presence of recombinant huBLyS showed a slightly better survival of human B-cells. However, *in vivo* B-cell engraftment was not supported by administration of huBLyS. Possibly due to the overall low number of human cells transferred or the route of application. Hence, human B-cell engraftment in humanized mice might require a defined number of transferred human cells that guarantees sufficient numbers of human B-cells in mice. Notably, other application routes of transferring human cells into mice might be more successful for B-cell survival. Conceivably, injecting human cells directly into the spleen, as described by Schmidt et al. might be more effective than i.v. transfer done here. Prospectively, the administration of recombinant huBLyS purified from a mammalian cell line rather than purified from *E.coli* might be more promising supporting human B-cells survival since proper protein folding is supported, which should enhance its biological activity. The half-life of huBLyS is very low and huge

amounts of the protein need to be administered daily. Circumventing this problem, huBLyS could be stabilized by various means e.g. PEGylation or linkage to stabilizing proteins like the Fc part of immunoglobulins.

Optimization of huBLyS activity in NRG $A\beta^{-/-}$ DQ8tg mice humanized with huDQ8-PBMC might develop into a fast and easy method for studying human humoral immune responses in mice, including the collaboration of human T-cells with human B-cells. Potentially, the transfer of PBMCs of vaccinated persons followed by a challenge infection with a human pathogen in the mouse might give indications on the effectiveness of vaccines. Nevertheless, this approach might not be applicable for long-term studies, since the development of GvHD restricts the life of the animals.

15.4. Infection of huPBMC-humanized mice with HIV

The huPBMC-DQ8tg mouse model described here might be of considerable value for human immunodeficiency virus (HIV) antiviral compound testing, since HIV has a very limited host tropism and replicates only in human $CD4^+$ T-cells.

The very basic test of infecting human cells taken from humanized mice with different HIV strains demonstrated for the first time that human cells from huPBMC-DQ8tg humanized mice are susceptible to HIV infection. However, it is a very artificial system that did not resemble HIV infections in humans. During natural HIV infection, CCR5 is the primary co-receptor used and its expression is largely restricted to $huCD4^+$ macrophages (Feng et al., 1996; Wyatt and Sodroski, 1998), a cell type not present in the huPBMC-DQ8tg mouse model. Activated T-cells, predominantly found in these mice, mainly express the co-receptor CXCR4 (Bleul et al., 1997; Maier et al., 2000). Therefore, only X4 HIV isolates were able to infect human cells from huPBMC-huDQ8tg mice *ex vivo*. Notably, HIV-2 isolates were not tested for *ex vivo* infectivity of human cells. HIV-2 is generally considered capable of using a broad range of co-receptors. The use of CXCR4 co-receptor was observed only for HIV-2 variants from viremic individuals indicating a more promiscuous nature of HIV-2 (Sol et al., 1997; Guillon et al., 1998; McKnight et al., 1998; Owen et al, 1998; Mörner et al, 1999). Hence, human cells from huPBMC-huDQ8tg mice might be capable of being infected with HIV-2 as well.

To this end, infectivity of HIV-1 and -2 was also tested *in vivo*. Causing a systemic and acute infection, HIV was administered via the intraperitoneal route with a very high viral load ($2x10^6$ $TCID_{50}$). In this regard, it is questionable whether this HIV infection resembles infection in humans. However, infection by a more natural route of infection, like mucosal tissues, might not be successful in huPBMC repopulated mice since they did not exhibit dendritic cells or macrophages. HuPBMC humanized NRG $A\beta^{-/-}$DQ8tg mice were infected with HIV-1_{NL4-3}, a T-cell adopted HIV strain infecting CD4 T-cells expressing CXCR4 (Adachi et al., 1986) and HIV-$2_{ROD/B14}$, a strain infecting cells exclusively via the co-receptor CXCR4, however independently of CD4 expression (Clapham et al., 1992).

In humans, initial viremia expands exponentially with a doubling time of approximately 0.3 days during the first 2–3 weeks of infection (Fiebig et al., 2003). The estimated average peak of HIV-1 RNA load in blood plasma was calculated by Pilcher and colleagues being around day 20 after infection (6 days after onset of symptoms, for patients with an acute retroviral syndrome) (Pilcher et al., 2004). Experimental primate models of mucosal HIV infection have demonstrated that maximal levels of viral expression occurred in different tissue compartments sequentially over short periods of time (Zhang et al., 1999; Spira et al. 1996; Bogers et al., 1998). However, there are still missing data for the detection of viral loads in blood or organs a few hours following primary infection. To this end, humanized DQ8tg mice provide a powerful tool to investigate early activities following HIV infection.

The determination of viral RNA copies in plasma and organs is an excellent diagnostic tool to track HIV infection although the detection of viral RNA copies in plasma might not demonstrate productive infection of cells with HIV. In HIV infected huPBMC repopulated mice false-positive results, due to remaining input virus, have to be considered. However, in the plasma of some infected humanized DQ8tg mice infectious virus was found 15 and 25 days respectively, after inoculation in a cell based assay (data not shown).

A successful infection with HIV results in the integration of HIV's genome into the host genome and is not determined by measurement of viral RNA copies in plasma.

Therefore, proviral DNA in genomic DNA from blood cells and organs was determined in this work. Around d12 after infection, HIV-1_{NL4-3} infected mice reached a peak of their proviral load in blood as well as spleen and lymph nodes, indicating the high infectivity of HIV-1_{NL4-3} as seen in the *ex vivo* experiment. Remarkably, the highest proviral load was found in lymph nodes (up to 6000 cps/ng DNA for HIV-1_{NL4-3} and 30 cps/ng DNA for HIV-$2_{ROD/B14}$) and the lowest in peripheral blood (up to 15 cps/ng DNA for HIV-1_{NL4-3} and 0.5 cps/ng DNA for HIV-$2_{ROD/B14}$). These findings were in agreement with observations made in patients by Jobe and colleagues in 1999. They found that the proviral load in lymph nodes is higher than in peripheral blood in HIV-2 as well as in HIV-1 infections (Jobe et al., 1999). These results indicate a tropism for the lymph nodes resulting in higher viral load in this compartment in both infections. The underlying mechanism probably involves trapping of HIV by follicular dendritic cells and increased viral replication but could also be the result of sequestration of infected huCD4 T-cells (Pantaleo et al., 1993; Meylan et al., 1996). Additionally, they described that the mean percentage of huCD4 T-cells was higher in lymph nodes as in blood of patients. The mechanisms underlying the relative increase of huCD4 T-cells in the lymph node compartment are not known, but could involve migration of huCD4 T-cells into these tissues (Meeusen et al., 1996; Westermann et al., 1997; Rosenberg et al., 1998) or alternatively, huCD4 T-cells within lymph nodes may be less susceptible to HIV-induced depletion. However, these observations might not be applicable to HIV infected DQ8tg mice humanized with huPBMC due to absent human dendritic cells.

Following acute viremia in humans, immune responses develop and the viral load decreases and becomes stable during clinical latency (see I.1.7.). In infected humanized mice, the proviral load also decreased but this might have other reasons. Since PBMC repopulated mice did not obtain a complete human immune system, it cannot be assumed that immune cells combated the virus, as it is the case in humans (Chang et al., 2010). Two mechanisms explaining a declining proviral load could be favored here. First, huCD8 T-cells might kill infected CD4 T-cells. This might account for their decline and increasing CD8 levels. Second, the virus itself induces apoptosis of huCD4 T-cells. Conceivable might be both mechanisms in infected humanize mice. However, in huPBMC humanized mice, the infected huCD4 T-cells

were eradicated since no new human T-cells developed from human hematopoietic stem cells and thus, the proviral was not maintained.

In HIV-1_{NL4-3} infected mice, decreased viral load paralleled decreasing huCD45 levels. HuPBMCs do not contain hematopoietic stem cells which could support the development of new huCD4 T-cells in the thymus. Hence, in correlation to dying huCD4 T-cells also less provirus was detected in the DNA of blood cells, splenic cells or lymphoid cell. Also, no clear correlation between the relative amount of human cells and the proviral load could be observed. Mice with more human cells did not exhibit the higher viral load and vice versa. The higher proviral load in spleen or lymph nodes compared to blood cells might be explained by higher absolute numbers of huCD4 T-cells in these compartments.

In contrast, the pathogenesis of HIV-2 infected patients differs from HIV-1 infected patients (see I.1.7.). The clinical courses of HIV-2 infections in humans are characterized by a longer asymptomatic stage and lower plasma HIV-2 viral loads compared to HIV-1 infections (Marlink et al., 1994; Matheron et al., 2003). To yield detectable viral loads, an HIV-2 strain was chosen that might amplify viral infection in humanized mice. HIV-$2_{ROD/B14}$ can enter cells via the co-receptor CXCR4 independently of the CD4-receptor (Clapham et al., 1992). Hence, this strain is not restricted exclusively to human CD4 T-cells and thus can also enter human CD8 T cells. The murine form of CXCR4 could be utilized by HIV-$2_{ROD/B14}$ since the human and murine CXCR4 share ~91% sequence homology (Heesen et al., 1996). However, only the entry of HIV-$2_{ROD/B14}$ into murine cells would be feasible (Tachibana et al., 1997; Bieniasz et al., 1997) but no reverse transcription of viral RNA (Garber et al., 1998) and/or integration into the host genome or later events in the virus' life cycle occur (Mariani et al., 2000; Baumann et al., 2004; Hatziioannou et al., 2004; Tsurutani et al., 2007; Tervo et al., 2008). As in humans, also humanized mice infected with HIV-$2_{ROD/B14}$ showed a different replicative kinetics compared to mice infected with HIV-1_{NL4-3}. In all observed organs huCD45 and huCD4 T-cell levels declined only slightly. Also, the proviral load remained stable or increased slightly demonstrating the mild progression of HIV-2 infections similar to humans. However, the absolute values were close to the background values and a robust interpretation of the data is difficult. Even though the PCR data obtained for HIV-

$2_{ROD/B14}$ gave good indications that the results obtained with HIV-1_{NL4-3} were not generated by residual input virus.

In summary, infection of huPBMC humanized mice with HIV-1_{NL4-3} and HIV-$2_{ROD/B14}$ showed similarities to the replication of the virus in humans and might be used for studies requiring short-term replication and would be suitable to study entry inhibitors. However, some features such as the route of infection, the use of primary HIV strains remains artificial or the induction of immune responses need to be optimized in the future.

16. Reconstitution of immunodeficient mice with huHSCs

Hematopoietic stem cells (HSCs) have the capability to reside in the murine bone marrow and built a reservoir from where the development of new human hematopoietic cells is guaranteed for life time. Transfer of huHSCs into immunodeficient mice allows for their differentiation into various subsets of immune cells and their maturation in a murine environment and avoids the development of GvHD. HuHSCs can be obtained from various sources. Here, huHSC mainly from G-CSF treated adult donors but also from human umbilical cord blood were used for humanization due to their easy accessibility.

16.1. Humanization with huDQ8-HSCs from cord blood

Humanization with huHSC from cord blood still is considered to be one of the standard methods to generate humanized mice (Hiramatsu et al., 2003; Ito et al., 2002; Watanabe et al., 2007). Here, huHSC from cord blood were isolated by magnetic sorting with an antibody directed against CD133 and injected i.h. into irradiated newborn mice. CD133 is frequently found on multipotent progenitor cells, including early immature hematopoietic progenitor and stem cells. In the hematopoietic system, CD133 is restricted to a subset of $CD34^{bright}$ progenitor and stem cells (Bühring et al., 1999). $CD133^{+}CD34^{+}$ cells were shown before to repopulate in NOD *Scid* mice (de Wynter et al., 1998) and thus, this population was used for studying the humanization of NRG $A\beta^{-/-}$ DQ8tg mice.

In this work, the transfer of $1x10^5$ huHSC from fresh cord blood into a NRG $A\beta^{-/-}$ DQ8tg or NRG $A\beta^{-/-}$ DQ8tg mouse respectively, led to engraftment rates of up to ~15% huCD45 cells in blood. Between w11 and w21 post reconstitution the percentage of huCD45 cells remained stable in both groups. Although NRG $A\beta^{-/-}$ DQ8tg mice obtained slightly higher levels of huCD45 in blood, this was not significantly different compared to NRG $A\beta^{-/-}$ mice.

It is reported that sex-associated factors play a pivotal role in the survival, proliferation, and self-renewal of huHSCs in humanized mice (Notta et al., 2010; Martin-Padura et al., 2010). The initial phase of engraftment characterized by homing of transplanted huHSCs into the bone marrow was described to be similar between male and female mice, indicating that sex-specific factors influence long-term, but not initial phases of huHSC engraftment (Notta et al., 2010; Martin-Padura et al., 2010). The role of sex hormones in immune function is well documented and the expression of cognate receptors on huHSCs implies the potential to respond to ligand binding to positively or negatively regulate human HSCs. However, the expression of receptors, such as estrogen and progesterone receptors, vary during ontogeny (Igarashi et al., 2001). Here, male and female recipients were used simultaneously because no huge discrepancy in huHSC engraftment was observed. However, it could be possible that enormous standard deviations could be explained by differences in male and female engraftment.

Different protocols were published for the generation of humanized mice and all differ regarding the choice of the appropriate immunodeficient mouse strain, the investigation of human lymphohaematopoietic cell types a well as the source and engraftment methodology. These scientific and logistical challenges have been highlighted in reviews (Legrand et al., 2006; Shultz et al., 2007; Bernard et al., 2008) but no outstanding protocol for the generation of humanized mice has been favored in detail and is used by most researchers.

Lepus and colleagues generated humanized NSG mice by i.h. injection of $1x10^5$ cryopreserved, positively selected huCD34$^+$HSCs from cord blood into newborns and reached up to 60% huCD45 cell engraftment in blood (Lepus et al., 2009).

McDermott and colleagues reported human cell engraftment of up to 45% in blood of NSG mice humanized with 0.25-2x10^4 cryopreserved and negatively selected huCD34$^+$ HSCs injected into the right femur of adult mice (McDermott et al., 2010). Pearson and colleagues reported that NRG mice, humanized as adults with 3x10^4 T cell-depleted huHSC from cord blood, reached huCD45 levels of up to 45% in blood (Pearson et al., 2008). It is questionable, whether these findings can be directly compared due to the differing protocols in different laboratories.

Also, donor dependent inequalities, technical differences in injecting huHSCs as well as different gating strategies in flow cytometric analyses might contribute to the varying humanization rates. For instance, in this work, cells first had been gated according to physical characteristics (forward/side scatter) and only lymphocytes and monocytes were taken for further analyses with murine CD45 cells excluded. Others working with humanized mice used a different strategy. For instance, Lepus and colleagues gated on all leukocytes (Lepus et al., 2009) and McDermott gated only on huCD45$^+$ cells, while Pearson gated on huCD45 with excluding muCD45 (Pearson et al., 2008). Again, it is questionable to what extend these data can be compared since no consistent gating strategy was applied.

Concordantly, humanization was shown to be dependent on the number of huHSCs transferred into mice independent of their age (Ito et al., 2002; Liu et al., 2010). In this work, 1x10^5 huHSCs from cord blood were transferred per mouse, a number that is higher than the recommended minimum of 2-5x10^4 huHSCs/ mouse (Ito et al., 2002). Furthermore, Liu and colleagues reported that both the level and pace of hematopoietic engraftment and immune recovery were dependent upon the dose of purified progenitors that were administered in the transplant (Liu et al. 2010). They humanized adult NSG mice by transplanting aldehyde dehydrogenase bright CD34^{bright} progenitor cells, a subset representing the entire spectrum of transplantable progenitor cells by simultaneously enriching short and long term progenitor cells (Storms et al., 1999 and 2005; Hess et al. 2004 and 2006). They found that high doses of progenitor cells (>1x10^4) were associated with a robust human hematopoietic chimerism resulting in long term engraftment (>19w) whereas at lower progenitor cell doses (<3x10^3), the chimerism was weak and the human hematopoietic lineage development was frequently incomplete, resulting in short-

term-engraftment (<10w). In contrast, the report by Lang and colleagues indicated that the dose of infected huCD34^{+}HSCs (5x10^{4} - 1x10^{6}) did not affect the level of human cell engraftment (Lang et al., 2011).

In this work, varying amounts of huHSCs were not tested due to the limited access to cord blood. However, huDQ8-HSCs differentiated into NK-cells, monocytes, B-cells and T-cells in NRG A$\beta^{-/-}$ DQ8tg as well as NRG A$\beta^{-/-}$ mice and were present in mice longer than >19w post reconstitution. Thus, the transfer of 1x10^{5} huCD34^{+}HSCs i.h. into newborns resulted in a long term engraftment in NRG A$\beta^{-/-}$ DQ8tg as well as NRG A$\beta^{-/-}$ mice, so that vaccination studies are possible.

As also found by others, human T- and B-cell engraftment is a dynamic and predictable process being mutually dependent on each other (Lang et al., 2013). Here, the very first human cells in blood were found to be human B1 B-cells (<w5), whereas human T-cells developed later (~w10).
It is reported that immature B-cells dominate the human population early after engraftment, and that T-cells appear weeks later, coincident with B-cell maturation, and Ig production, although B-cell production was not sustained over time. Also, the generation of mature, naive B-cells in humanized mice was found to be dependent on the presence of human T-cells (Lang et al., 2013).
Human T-cells in NRG A$\beta^{-/-}$ DQ8tg and NRG A$\beta^{-/-}$ mice developed not before w10 post reconstitution. Interestingly, NRG A$\beta^{-/-}$ DQ8tg mice exhibited significantly higher numbers of human CD3 T-cells over time (~10%) compared to mice without the human DQ8 transgene (~2%). However, this observation did not lead to significant differences in all of the performed humanization experiments (data not shown), but a general trend could be seen. This finding is supported by a report by Danner and colleagues, demonstrating a critical role for the engraftment and the development and function of T- and B-cells in NRG mice expressing DR4, another MHC II molecule (Danner et al,. 2011). They reported that human CD4 and CD8 T-cell subsets as well as B-cells were highly functional indicated by their expression of human cytokines and antibodies of different classes, respectively.
The humanization of NRG A$\beta^{-/-}$ DQ8tg or NRG A$\beta^{-/-}$ mice with huDQ8-HSCs from cord blood did not lead to conclusive results as evidenced by Danner and colleagues

but a trend of the importance of matching DQ8 HLA class II molecules for human T-cell engraftment could be observed.

The development of mice with an adaptive human immune system including all cells of the lymphocytes lineage such as NK-cells, T-cells and B-cells as well as monocytes has been the focus of investigation in this work. However, human immune cells of other lineages such as the myeloid lineage or granulocytes were not examined here. Indeed, there are some reports describing the differentiation of huHSCs from cord blood into human granulocytes and human myeloid cells (Ishikawa et al., 2007; Tanaka et al., 2012) or into human erythroid cells existing as an immature phenotype in the bone marrow of NSG mice (Hu et al., 2011) or human platelets (Hu et al, 2012). It might be well possible that these cells also could develop from huHSCs in NRG A$\beta^{-/-}$ DQ8tg and thus contribute to the human innate immune system in the humanized DQ8tg mouse model.

NRG A$\beta^{-/-}$ DQ8tg and NRG A$\beta^{-/-}$ mice reconstituted with 1x10^5 huHSCs gradually lost their huCD45 cells starting at w21 of age. However, some human immune cell subsets such as macrophages or NK-cells extinguished earlier.
The presence of matching HLA II, DQ8, did not prevent declining human cells. This effect is also known by others and probably due to the inability of mouse cytokines to react with human receptors, leading to survival signal and trophic factor deficiencies in transplanted human cells (Watanabe et al., 2007; André et al., 2010).
A strategy to overcome this is drawback and to create a more favorable immunologic environment for human cells within the mouse host is to supplement humanized mice with human cytokines. Similar approaches to transiently increase hematopoietic cell lineages in humanized were already done by continuously injecting proteins including human IL-15 (Huntington et al., 2011), huBLyS (Schmidt et al. 2008) or by hydrodynamic injection of a plasmid DNA mixture including IL-15 and Flt-3L or Flt-3L and granulocyte monocyte-CSF(GM-CSF) and IL-4 (Chen et al., 2009). The expression of human IL-7 in BRG mice by *in vivo* lentiviral gene delivery led to stable but supraphysiological levels resulting in increased abundance of T-cells (O'Conell et al., 2010) and humanized mice transgenic for human cytokines exhibit robust human hematopoietic reconstitution (Nicolini et al., 2004; Rongvaux et al., 2011; Billerbeck et al., 2011).

However, due to the complexity of the immune system no approach to supplement mice with human cytokines was found enhancing the development of the entire human immune system in mice including functional cells.

Although NRG Aβ$^{-/-}$ DQ8tg and NRG Aβ$^{-/-}$ mice gradually lost their huCD45 cells in blood starting at w21, huCD45 cells were detected in spleen and bone marrow 50 weeks following reconstitution.
In spleen human T-cells, B-cells and monocytes but no NK-cells were present. Almost all huCD45 cells in bone marrow were huCD34^{+}, indicating, that long term cell engraftment was successful and the decline of huCD45 cells in blood might be due to the inappropriate immunologic environment as described above.
Besides obvious enlarged spleens of reconstituted NRG Aβ$^{-/-}$ DQ8tg and NRG Aβ$^{-/-}$ mice, the architecture of the spleens was not observed in this work. However, it was shown before that the spleen of reconstituted mice developed white pulp regions, consisting of T- and B-cell areas, although the B-cell areas in non-immunized mice was smaller (Traggiai et al. 2004; Lepus et al., 2010). Also, the livers of NRG Aβ$^{-/-}$ DQ8tg and NRG Aβ$^{-/-}$ mice did not show macroscopic abnormalities (data not shown) indicating that humanized NRG Aβ$^{-/-}$ DQ8tg and NRG Aβ$^{-/-}$ mice did not develop GvHD as it was the case following transfer of huPBMCs.

In stem cell repopulated mice (and humans) there is a remaining risk of development of GvHD. In contrast to acute GvHD mediated by mature T-cells from the PBMC donor (see III.1.2.), chronic GvHD (cGvHD) is thought to be caused by donor cells that develop *de novo* within the host from the transplanted huHSCs (Chu et al., 2008).
The relative contributions of the implicated cell types in cGvHD including T-cells, B-cells and macrophages remain poorly understood. Pathology resembling cGvHD in huHSC reconstituted mice is explained by different ways. First, cGvHD could arise through an MHC class II mismatch and/or second, through a minor histocompatibility mismatch and/or third, through a protocol that interferes with the negative selection of T-cells by MHC class II (Lockridge et al., 2013).
In each of these scenarios, donor T-cells play a central role in disease pathogenesis. In NRG Aβ$^{-/-}$ DQ8tg mice the possibility of developing cGvHD is dramatically reduced since mice do not express murine MHC II. In addition, the expression of the human

MHC II DQ8 leads to matching MHC II TCR interactions and no interference with the negative selection process of T-cells in the thymus during maturation. Therefore, the overall health status of reconstituted mice remained normal and comparable to irradiated but non-reconstituted mice. However, individual mice died without showing any symptoms or macroscopically abnormalities of the organs. This might be due to the mentioned mismatching minor MHCs that are not matched in NRG A$\beta^{-/-}$ DQ8tg and the induction of cGvHD, but most likely it is a question of normal survival following irradiation.

HuHSC reconstituted NRG A$\beta^{-/-}$ DQ8tg and NRG A$\beta^{-/-}$ developed T-cells and B-cells that should be able to mediate an adaptive immune responses and also no GvHD occurred, which is the requirement for long term studies such as vaccination studies.
Vaccination of NRG A$\beta^{-/-}$ DQ8tg and NRG A$\beta^{-/-}$ mice with TetanolPur®, a protein based antigen, starting at w27 following reconstitution was performed. In one mouse tetanus toxoid specific IgG antibody production could be detected although the value was only slightly higher than background levels (data not shown) indicating that vaccination might be possible. This finding is supported by the report of Danner and colleagues who demonstrated a critical role of MHCII molecules for the development of functional helper T-cells to support class switching of B-cells upon vaccination with tetanus toxoid (Danner et al., 2011). HuCD45 cells started to decline at w21 and thus, vaccination was expected to give a proliferation stimulus to the human cells. However, this was not the case here. Possibly, the protein based vaccine as a stimulus was not sufficient enough as stimulation signal and due to missing human cytokines human cells did not react as they would in a normal human environment. Otherwise, it might be possible that vaccination was successful, but huIgG antibodies could not be detected by ELISA due to the low total number of human B-cells present in mice.
These experiments looked promising but need to be repeated to examine the contribution of the DQ8 transgene.

16.2. Humanization with mobilized huDQ8-HSCs

Besides humanization of with huHSCs from human cord blood, also mobilized huDQ8^{+} hematopoietic stem cells (mhuHSCs) were used. They are easy accessible in high numbers from G-CSF treated adult donors.

Here, huHSCs from a G-CSF treated adult donor were isolated by magnetic sorting with an antibody directed against CD34 and injected i.h. into irradiated newborn mice. HuCD34 is a well-established marker of huHSCs and progenitor cells and thus, the huCD34^{+} population was used for studying humanization of NRG A$\beta^{-/-}$ DQ8tg mice. Newborn NRG A$\beta^{-/-}$ DQ8tg or NRG A$\beta^{-/-}$ mice were reconstituted with mhuDQ8-HSCs under differing conditions to optimize human cell engraftment in mice.

16.3. Humanization with freshly or prior frozen/thawed mhuDQ8-HSCs

Freshly isolated and frozen mhuDQ8-HSCs from the same donor were compared for their expression of huCD45 and huCD34 and their viability.

Both, fresh and thawed mhuDQ8-HSCs obtained a very pure huCD45^{+}huCD34^{+} cell population of >98%. However, freezing and thawing reduced the overall number of viable cells to about 20-40% and the expression of huCD45 and huCD34 was slightly reduced.

Similar observations were made by Scholbach and colleagues by comparing huHSCs from cryoconserved and fresh cord blood. Following purification with magnetic beads, they found that the huCD34^{+} population was lower in cryoconserved cord blood (72.9%) compared to fresh cord blood (95.5%) and that the amount of huCD34^{+} HSCs in cryoconserved cord blood was lower ($6.5x10^{4}$) compared to fresh cord blood ($1.4x10^{5}$). Although this group used frozen human whole cord blood samples and in this work only purified mhuDQ8-HSC were frozen, similar observations were made. One obvious reason for this might be the proportion of DMSO as freezing protection used in whole cord blood as well as in purified mhuDQ8-HSC samples. As already known, this commonly results in an increased number of destroyed cells.

Here, it was also found that thawed mhuDQ8-HSCs exhibit slightly reduced expression of huCD34 and huCD45. Therefore, newborn NRG A$\beta^{-/-}$ DQ8tg and NRG A$\beta^{-/-}$ mice were reconstituted i.h. with $1x10^{5}$ of either fresh mhuDQ8-HSCs or thawed

mhuDQ8-HSCs and the reconstitution ability was compared. Interestingly, humanized NRG A$\beta^{-/-}$ DQ8tg and NRG A$\beta^{-/-}$ mice possessed similar engraftment rates of huCD45 cells (10-15%) and also humanized mice did exhibit similar human immune subsets in blood and organs as detected in mice, humanized with huHSCs from cord blood. Hence, frozen mhuDQ8-HSCs are a reasonable alternative to freshly isolated mhuDQ8-HSCs and allowing scientists to be independent of daily changing birth rate of mice.

In a study comparing the engraftment potential of huHSC from cord blood and from a mobilized adult donor, it was found that transplantation of cord blood stem cells provided the greatest number and breadth of developing cells and also higher human immunological competence could be demonstrated (Lepus et al., 2009). Here, a direct comparison between engraftment rates of mice reconstituted with cord blood huHSC or mobilized stem cells could not be arranged. However, we observed that it is essential to transfer much higher numbers of mobilized huHSC (>1x10^5) to achieve similar engraftment rates in mice reconstituted with cord blood huHSCs.

To what extend huCD45 cells extinguished at later dates cannot be answered because humanized mice were euthanized in w12. In some individual mice long-term engraftment was observed until w35 post reconstitution (data not shown). However, in a few cases of individual mice human cells extinguished already before w12 (data not shown) equally in mice transferred with fresh or frozen mhuHSCs. A reasonable explanation for this progression remains elusive.

Here again, the critical time period of ~12 weeks for T-cell development was observed, as it also was the case in mice humanized with huHSCs from cord blood. NRG A$\beta^{-/-}$ DQ8tg mice reconstituted with mhuDQ8-HSCs possessed slightly higher T-cells (~10%) at w12 compared to humanized mice lacking the huDQ8tg.
However, Shultz and colleagues reconstituted NSG mice with 7x10^5 mhuHSCs and made similar findings. They also observed early B-cell engraftment but a late onset of T-cell development (10w, 12%). However they could promote the development of human T-cells (w10, 81%) following *in vivo* treatment with an Fc-IL-7 fusion protein (Shultz et al., 2012).

On the one hand, this report, as well as our findings, indicates that the reconstitution of humanized mice with human T-cells is independent of MHC II molecules, but dependent on human cytokines such as IL-7. On the other hand, it was shown by Danner and colleagues that MHC II has a critical role for the development of human T-cells in mice, although only at later dates following reconstitution (w25) the difference between MHCII transgenic mice (~27% huCD3 T-cells in blood) and control mice (~5% huCD3 T-cells in blood) became significant (Danner et al., 2011).

The ability of stem cells to engraft in mice was unpredictable in all approaches tried here. When freshly isolated mhuHSCs were tested in a colony-forming unit (CFU) assay in the blood donation center in Frankfurt, the detection of hematopoietic progenitors in mobilized peripheral blood directly correlated with the power of isolated huCD34 mhuHSCs to engraft in humanized mice (personal communication Dr. Eliza Wiercinszka). Yet, CFU assays were only performed with fresh but not for frozen mhuDQ8-HSCs. This method provides a possibility to test the potential of fresh or frozen mhuHSCs to engraftment in mice and could be performed prior transfer to select only mhuHSCs with a very high capability of engraftment. However, this test does not entirely guarantee successful engraftment of mhuHSCs and timing might be difficult.

16.4. Improvement of humanization with cultivated mhuDQ8-HSCs

Humanization of newborn NRG A$\beta^{-/-}$ DQ8tg mice with fresh mhuHSCs needs to be highly organized. To optimize the humanization process, short term cultivation of fresh and frozen mhuHSCs prior cell transfer was used to bridge the time until newborn mice were ready for transfer.

Selected cytokines and growth factors including human Flt3 ligand (Yonemura et al., 1997), human SCF (Hoffman et al., 1993; Yagi et al., 1999; Nakauchi et al., 2001) human TPO (Yagi et al., 1999; Piacibello et al., 1998) and human IL-6 (Varnum-Finney et al., 2003; Bordeaux-Rego et al., 2010) have been used to maintain and expand HSCs in culture, either alone or in combination (Takizawa et al., 2011).

Here, these supplements promoted proliferation of mhuHSCs and also the expression of huCD34 and huCD45 remained higher, but the capability to engraft in NRG A$\beta^{-/-}$ DQ8tg mice did not appear to be enhanced.

The report by Lang and colleagues supports these finding. They found that short term cultivation (1-8d) of huHSCs from G-CSF treated adult donors, led to a reduced rate and degree of human chimerism in BRG mice compared to fresh isolated huHSCs. In contrast, huHSC from cord blood led to improved human chimerism (Lang et al., 2011).
One explanation for this could be the high sensitivity of huHSCs to their microenvironment. HuHSCs from cord blood are untouched while those from adult donors were affected by the G-CSF treatment. Unfortunately, the CFU assay was not performed so that it remains elusive whether cultivation of mhuHSCs in presence of cytokines and growth factors maintained their engraftment capability and pluripotency in culture.

In 2010 a purine derivative compound named stem regenin-1 (SR-1) was described by Boitano and colleagues to induce proliferation of HSCs via direct binding to an antagonism of the aryl hydrocarbon receptor (Boitano et al. 2010). They reported that SR-1 promoted *in vitro* expansion of mhuHSCs by 17-fold in media containing huSCF, TPO, huIL-6 and Flt3 ligand. Also, improved early and long-term *in vivo* repopulation capacity in immunocompromised mice was observed. In addition, the proliferative effect of SR-1 on mhuHSCs was reversible and did not occur in the absence of cytokines. Interestingly, there were species-specific differences on SR-1 bioactivity, as the compound did not expand murine HSCs, but potently affected huHSCs (Boitano et al. 2010). Therefore, SR-1 was examined in this work for short-term cultivation of mhuHSCs before reconstituting NRG $A\beta^{-/-}$ DQ8tg or NRG $A\beta^{-/-}$ mice.
Here as well, cultivation of mhuHSCs with SR-1 was found to enhance proliferation (by 50% at d3), but in the same way the expression of huCD34 and huCD45 was reduced about 20%.
It was not tested whether SR-1 as a supplement in culture also enhances human cell engraftment. Nevertheless, SR-1 and above mentioned cytokines were used for short-term cultivation prior humanization to provide more flexibility in the humanization procedure. Importantly, the proliferation of mhuHSCs was ignored in such regard that only the starting number of seeded mhuHSCs was taken into account for cell transfer and not the cell number following one or two days in culture.

Thus, short-term cultivation (<d3) was intended for maintaining mhuHSCs *in vitro* without loss of their stem cell capacity.

Long-term *in vitro* cultivation as well as *ex vivo* expansion of huHSC is difficult because huHSCs are very sensitive to their microenvironment and it requires highly defined conditions to support the net self-renewal of long-term HSCs *in vitro*. Cultivation of huHSCs with defined cytokines typically led to growth of progenitors and mature cells while losing or at best maintaining the long-term HSCs (Sauvageau et al., 2004). Furthermore, it is clear that hematopoiesis is a dynamic and regulated process through nonlinear feedback control mechanisms (Broxmeyer et al., 1995). Hematopoietic culture systems generate large numbers of endogenously produced soluble factors that also were reported to have inhibitory effects on huHSC and progenitor cell expansion (Madlambayan et al., 2005; Kirouac et al., 2010).

In 2012, Csaszar and colleagues successfully developed a complex fed-batch media dilution system, enabling reduction of inhibitory signals in HSC culture media, demonstrating the highly regulated self-renewing and multilineage repopulating ability of HSC (Csaszar et al., 2012).

Besides reconstitution of newborn NRG A$\beta^{-/-}$ DQ8tg mice, also irradiated adult mice were used for humanization with mhuDQ8-HSCs in this work. Contrary to expectation, adult mice engrafted only poorly with huCD45 cells, although the same amount of mhuDQ8-HSCs cells was used. This was in concordance with findings by Brehm and colleagues (Brehm et al., 2010), but in contrast, other researchers prefer the humanization with mhuHSCs in adult mice than in newborns (personal communication Paula Cannon, University of Southern California, 2013).

Speculating, these differences might be due to variations in the donor mhuDQ8-HSCs or to insufficient numbers of transferred mhuDQ8-HSCs. Possibly, adult mice need to be reconstituted with higher cell number than newborn mice to achieve the same engraftment rate of human cells. Furthermore, reconstitution of adult NRG A$\beta^{-/-}$ DQ8tg mice has some advantages including well definable groups of male/female mice, DQ8tg or non-tg mice before reconstitution. Also, the transfer of mhuDQ8-HSCs into adult mice might be more manageable for the experimenter.

Nevertheless, reconstitution of adult mice for long-term studies might be impractical due to high required numbers of huHSCs and the advanced age of mice (>17w) at the starting point of the study.

Here, the reconstitution of NRG Aβ$^{-/-}$ DQ8tg and NRG Aβ$^{-/-}$ mice as newborns with huDQ8-HSC from cord blood and mobilized donors was successful. Due to the limited access to huDQ8^{+} cord blood only the reconstitution of newborns with mhuDQ8-HSCs was continued. However, the reconstitution of mice with huHSCs from cord blood and the induction of adaptive immune responses looked promising so that it should be investigated again in future.

16.5. Initiation of adaptive immune responses in humanized mice

A functional adaptive human immune system in humanized DQ8tg mice is important for the use of this mouse model as a vaccination model.

In reconstituted NRG Aβ$^{-/-}$ DQ8tg and NRG Aβ$^{-/-}$ mice, huDQ8-HSCs were able to differentiate into various subsets of human immune cells including T-cells and B-cells as well as monocytes and NK-cells. Whether these human cells were functional and mediated appropriate immune responses was investigated by *ex vivo* as well as *in vivo* approaches.

16.5.1. Ex vivo stimulation of human T-cell subsets in mice

The generating an adaptive immune response is facilitated by educating the human T-cells in an autologous thymic microenvironment, as it is the case in huDQ8tg mice reconstituted with huDQ8-HSCs, where the HLA II provides the autologous environment. It was expected that human T-cells in huDQ8tg mice possessed a higher functionality than non-transgenic mice due to their maturation with human MHC II and thus a better education in the murine thymus. Therefore, human T-cells were analyzed for their activation status.

In NRG Aβ$^{-/-}$ DQ8tg and NRG Aβ$^{-/-}$ mice reconstituted as newborn with mhuDQ8-HSCs, human T-cells in blood were not activated as no secretion of IFNγ was detected. In contrast, mice repopulated with huPBMCs possessed highly activated human T-cells resulting in the onset of GvHD. Furthermore, huCD3 T-cells in mhuDQ8-HSC reconstituted mice could be activated by PMA/ionomycin *ex vivo* and secreted IFNγ, indicating their capability of mediating immune responses; however, no differences could be observed between NRG Aβ$^{-/-}$ DQ8tg or NRG Aβ$^{-/-}$ mice.

Particularly in T-cells, PMA/ionomycin treatment induces calcium influx, thereby bypassing T-cell receptor signaling pathways leading to unspecific stimulation (Miller et al., 1997). Since the treatment with PMA/ionomycin is sufficient to induce activation of various cell types to produce cytokines *in vitro*, it does not necessarily account for the same activation profile of human T-cells *in vivo* (Chang et al., 2005). Notably, human T-cells were not tested for their activation potential *in vivo* so that it is unclear whether human CD4 and/or huCD8 T-cells in huDQ8tg mice are superior in their functionality. However, it was reported by Watanabe and colleagues that human T-cells in reconstituted NOG mice were functionally impaired, as their response to *in vitro* polyclonal T-cell stimulation with PMA/ionomycin was very poor (Watanabe et al., 2009). The same was found by other groups (Matsumara et al. 2003) and those using NSG mice (Ishikawa et al., 2005) or BRG mice (Traggiai et al., 2004; Baenziger et al. 2006). This indicates that either the matching DQ8tg plays a pivotal role in NRG A$\beta^{-/-}$ DQ8tg mice or only the absent murine MHCII in NRG A$\beta^{-/-}$ mice. Unfortunately, normal NRG mice were not included in the study groups, so that this direct comparison is missing.

Danner and colleagues reported that human DR4^{+} T-cells developed in their DR4 MHC II transgenic mice were functional upon stimulation with PMA/ionomycin detected by secretion of cytokines, while control mice lacking the DR4 transgene failed to do so (Danner et al., 2011). However, the DR4tg mouse still expressed the murine MHCII and hence, control mice being littermates lacked the DR4tg while expressing murine MHCII. Regarding this finding, the role of the matching DQ8tg remains elusive and it is not clear to what extend it is important for the functionality of human T-cells to mount immune responses, especially, because the additional control with NRG mice was not included. However, it could be shown that human T-cells from NRG A$\beta^{-/-}$ DQ8tg as well as NRG A$\beta^{-/-}$ mice were functional upon stimulation *ex vivo*.

16.6. Vaccination of humanized mice to induce humoral immune responses

To obtain information about huCD4 helper T-cell communication with B-cells and their functionality to promote B-cell proliferation and antibody production, humanized NRG A$\beta^{-/-}$ DQ8tg and NRG A$\beta^{-/-}$ mice were vaccinated with a tetanus toxoid based vaccine belonging to the group of thymus-depend (TD-) antigens. TD-antigens recruit

CD4 T helper T-cells to provide stimulatory effects on B-cells to promote proliferation and antibody production.

As in mice reconstituted with huDQ8-HSCs from cord blood, also NRG Aβ$^{-/-}$ DQ8tg and NRG Aβ$^{-/-}$ mice reconstituted with mobilized huDQ8-HSCs mainly possessed B1 B-cells. However, antibody producing human B2 B-cell numbers increased following vaccination of NRG Aβ$^{-/-}$ DQ8tg and NRG Aβ$^{-/-}$ mice.
In both mouse strains, tetanus-specific huIgM levels peaked around w2 and w3 following vaccination and declined thereafter, whereas specific huIgG levels where higher and reached a peak first at w4 following vaccination. No correlation between the relative amount of huCD45 cells or B2 B-cells and the amount of specific antibodies was found. Due to the number of only two mice per group it was not discriminable whether DQ8tg mice were superior to class switching and secretion of specific antibodies. However, human B-cells in NRG Aβ$^{-/-}$ DQ8tg and NRG Aβ$^{-/-}$ mice were capable of secreting anti-tetanus toxoid specific huIgM antibodies that were able to undergo immunoglobulin class switching into specific huIgG antibodies.

In contrast, previous studies in IL2cγ$^{-/-}$ genetic stocks of humanized mice lacking human MHC II molecules, showed that the antigen-specific huIgM response was enhanced while the huIgG response was impaired when vaccinated with tetanus toxoid (Traggiai et al., 2004), immunized with DNP-KLH, a T-dependent antigen (Matsumura et al., 2003), and infected with HIV (Baenziger et al., 2006). In addition, mice from the same IL2cγ$^{-/-}$ genetic stocks but transgenic for human MHC I did show the same results when infected with dengue virus (Jaiswal et al., 2009) and Epstein-Barr virus (Strowig et al., 2009).

Interestingly, converse results were reported by other groups, who investigated the humoral immune response in NRG mice transgenic for DR4, a human MHC II molecule (Danner et al., 2011), and NOG mice also transgenic for DR4 but lacking the murine MHC II (Suzuki et al., 2012). The latter is similar to the DQ8tg mouse model used in this work. Both groups showed that the introduction of human MHC II DR4 did not significantly improve the reconstitution with human B-cells, as it also was observed in this work. In addition, DR4tg mice developed a robust specific huIgG antibody response following vaccination with tetanus toxoid (Danner et al., 2011) and

also following immunization with ovalbumin (Suzuki et al., 2012), while all control mice did not.

Here, NRG Aβ$^{-/-}$ DQ8tg as well as NRG Aβ$^{-/-}$ mice were capable of secreting tetanus toxoid specific huIgM and huIgG antibodies, although the critical role of the matching DQ8 molecules for secretion of specific antibodies and class switching needs to be further examined. These data indicate that MHC II transgenic mouse models are a significant advance in humanized mouse technology, as it was demonstrated as a reliable model in which proper adaptive immune responses occur (Danner et al., 2011; Suzuki et al., 2012).

In contrast, BLT mice were found to be a very robust humanized animal model for vaccination purposes. They are generated by implanting human fetal liver and thymus from an abortion into NSR or NRG mice with subsequent engraftment of autologous human stem cells resulting in high levels of multilineage human cell engraftment in all tissues (Melkus et al., 2006; Wege et al., 2008). The presence of a functional autologous human thymus in BLT mice permits appropriate T-cell education and human HLA T-cell restriction mimicking T-cell development in humans. Nevertheless, the need for xenotransplantation of human tissues was thought to be eliminated by DR4 (Danner et al., 2011; Suzuki et al., 2012) or DQ8 (this work) transgenic mice, where human T-cells are educated in the murine thymus in the presence of human MHC II molecules. However, MHC class I and minor MHC II classes are still mismatching in these models.

BLT mice feature more complete and robust innate and adaptive immune responses, with both specific T-cell responses to Epstein-Barr virus infection (Melkus et al., 2006) and specific huIgM and huIgG responses following immunization with DNP-KLH (Tonomura et al., 2008) and HIV infection (Brainard et al., 2009).

Although, studies have shown both huIgM and huIgG antigen specific responses, the majority showed responses with varying robustness, especially only weak huIgG antibody production following immunization with HIV-1/West Nile virus envelop proteins (Biswas et al., 2011) or vaccination with tetanus toxoid (Rajesh et al., 2010). Also in matching human MHC class I BLT mice, only robust specific T-cell and IgM responses following dengue virus infection was observed, while dengue specific huIgG responses were still low.

To date, there are no reports available comparing immune responses of BLT mice with matching human MHC class II molecules. Speculating, as it was demonstrated before in this work and by others (Danner et al. 2011, Suzuki et al., 2012), using huHSCs reconstituted mice, matching human MHC II molecules in BLT mice might enhance robust huIgG responses. However, this might not directly enhance class switching at gene level during V(D)J recombination of B-cells. Hence, appropriate human cytokines or other factors still might be necessary.

16.7. Infection of mhuDQ8-HSC reconstituted mice with HIV-1

NRG A$\beta^{-/-}$ DQ8tg mice reconstituted with mhuDQ8-HSC engrafted a functionally active human immune system and due to the lack of GvHD these humanized mice are capable of long-term, HIV infection studies.

As in huDQ8-PBMC repopulated mice, HIV-1_{NL4-3} was administered via the intraperitoneal route causing a systemic and acute infection. Infection by a more natural route of infection, like mucosal tissues, was not tested in this work; however this might be successful since they also exhibit dendritic cells and macrophages. Interestingly, the reconstitution of mucosal tissues with human cells in other huHSC-reconstituted mice was found to appear sporadic and inconsistent (Mitchell et al., 2009; Choudhary et al. 2009; Holt et al., 2010) but some reports describe successful HIV infection of humanized mice via the rectal (Sun et al., 2007: Berges et al., 2008) or vaginal routes (Berges et al., 2008; Neff et al., 2011). In contrast, reproducible multilineage generation of human reconstitution including mucosal tissues such as the gastrointestinal tract and the female reproductive tract (Lan et al., 2006; Melkus et al., 2006; Sun et al., 2007; Denton et al., 2008) is one advantage of BLT mice making this model superior especially for studying HIV infections.

HIV-1_{NL4-3} used here is a T-cell adapted HIV-1 strain infecting huCD4 T-cells expressing the CXCR4 co-receptor. Infection of humanized mice with HIV strains using other co-receptors, such as CCR5 or a dual tropic viruses, was not performed in this work but according to several reports it is expected to be effective (reviewed in Berges and Rowan, 2011; Denton and Garcia, 2011).

NRG A$\beta^{-/-}$ DQ8tg mice especially with very low levels of huCD45 were infected to determine the threshold of human cell engraftment required for a sustainable HIV-1_{NL4-3} infection in mice. So far there are no reports available that describe the examination of the minimum level of human cell engraftment or minimal dose of virus required to achieve consistent HIV-1 infection in humanized mice. However, it has been reported that mice with as low as 5% cells in peripheral blood could be infected by i.p. injection (Berges et al., 2006) and that infection with low doses of HIV-1 (100-500 $TCID_{50}$) by direct injection routes were unsuccessful (Gorantla et al., 2007; An et al., 2007). Since engraftment levels vary amongst humanized mice and infection routes differ by study, a uniform minimal dose applicable to all engraftment models cannot be envisioned at the moment.

Notably, detected HIV titers in this work of $1x10^3$ - $2x10^5$ copies HIV RNA/ml plasma following infection with HIV-1_{NL4-3} were comparable to HIV-1_{NL4-3} infection of NRG mice in other studies ($1x10^3$-$1x10^6$), although the relative number of human cells was higher (mean: 29.4 ± 18.2%; Baenziger et al., 2006).

Interestingly, NRG A$\beta^{-/-}$ DQ8tg humanized mice infected with $1x10^6$ $TCID_{50}$ seemed to exhibit equal viral RNA copies in their plasma over a 100 day time period than NRG A$\beta^{-/-}$ DQ8tg humanized mice infected with $2x10^6$ $TCID_{50}$. This is explainable because the infection of mice with higher viral doses might not result in higher viral loads due to the limited amount of human T-cells that can be infected. Speculating, all of the human CD4 T-cells in mice of both groups were infected with HIV due to the small number of total huCD45 cells and the high infectious dose of HIV.

The characteristic decline of huCD4 T-cells could not be observed by flow cytometric analyses in this work, due to the low level of huCD45 cells (<0.5%). However, HIV RNA titers were detectable over the entire examination period so that decreasing huCD4 T-cells can be assumed. Due to low engraftment levels of NRG A$\beta^{-/-}$ DQ8tg mice infected with HIV-1_{NL4-3}, it would be nice to investigate how HIV RNA titers could be maintained. First, it might be possible that huCD4 T-cells continuously differentiate from human progenitor cells in the bone marrow so that in turn those could be infected by HIV-1. Notably, this was not observed in mice humanized with huPBMCs, where no new CD4 T-cells developed in the mouse. Second, it was shown by several

reports that some intermediate hematopoietic progenitor cells expressed HIV-1 entry receptors and were susceptible to direct infection by HIV (Deichmann et al., 1997; Sasaki et al., 2009; Carter et al., 2010 and 2011; Nixon et al., 2013). Also, blood progenitors from HIV infected BLT mice showed impaired hematopoietic potential and gave rise to progeny that harbor provirus (Nixon et al., 2013; Akkina, 2013). Human intermediate progenitor cells only exhibit a relatively short lifespan (Benveniste et al., 2010) and thus might not represent a stable but dynamic reservoir maintained by low-level viremia. This explanation would be in line with the observed low HIV RNA titers in low engrafted NRG A$\beta^{-/-}$ DQ8tg mice.

Low engraftment levels in DQ8tg mice humanized with huDQ8-HCs demonstrated a reproducible HIV infection. However, specific anti-HIV responses of human T- and B-cells following HIV infection need to be further investigated in low as well as high engrafted DQ8tg mice. In summary, the DQ8tg mouse model presents a valuable *in vivo* model for HIV infection studies and perhaps also an alternative to the laborious BLT mouse model.

V. Summary

Human immunodeficiency virus (HIV) vaccine preclinical testing is difficult because HIV's only relevant hosts are humans and no correlates of protection are known. In order to generate a robust animal model able to mount human immune responses, immune deficient mice (NOD Rag1$^{-/-}$ $\gamma c^{-/-}$; NRG or NOD *scid*$^{-/-}$ $\gamma c^{-/-}$; NSG) expressing human MHC class II HLA-DQ8 (huDQ8tg) on a mouse class II deficient background (A$\beta^{-/-}$) were used to generate humanized mice. In this animal model, the human HLA-DQ8 transgene interacts with the matching T-cell receptors of transferred human peripheral blood mononuclear cells positive for DQ8 (huDQ8-PBMCs) or human hematopoietic stem cells positive for DQ8 (huDQ8-HSCs). Therefore the functionality of the transferred human cells in mice should be supported and improved to mice without transgene.

The transfer of huPBMCs into immunodeficient mice results in fatal graft-versus-host-disease (GvHD). HuDQ8tg mice that were adoptively transferred with huDQ8-PBMCs showed a significantly prolonged overall survival compared to mice expressing mouse MHC class II molecules. This correlated with an increased time span until onset of GvHD. DQ8tg mice showed significantly enhanced repopulation rates but surprisingly, only human CD3^{+} T-cells engrafted. The presence of HLA class II did not advance B-cell engraftment and humoral immune responses were undetectable. Also, human B-cell engraftment could not be enhanced by adding exogenously the B-cell survival factor huBLyS during huDQ8-PBMC transfer. Furthermore, these mice were infected with HIV-1 or HIV-2. Comparable to humans, infection with HIV-1 showed a rapid viral replication in humanized mice, while the infection with HIV-2 was mild.

To avoid GvHD and to obtain all subtypes of hematopoietic human cells, NRG A$\beta^{-/-}$ mice were reconstituted with huDQ8-HSCs from human umbilical cord blood or adult donors treated with the granulocyte colony-stimulating factor (G-CSF).

Compared to huDQ8-PBMC repopulated mice, huDQ8-HSC reconstituted newborns mice developed nearly all subpopulation of the human immune system and had a normal life expectancy. Human T-cells as well as human B-cells and also monocytes and NK-cells could be detected to a maximum around 10 to 20 weeks after huDQ8-HSC transfer. Notably, reconstitution was equal with huDQ8-HSCs from cord blood or adult donors, although huDQ8-HSC from adult donors failed to reconstitute adult DQ8tg mice when the same number of huDQ8-HSCs was transferred.
Following *ex vitro* activation with PMA/ionomycin, human T-cells were functional and secreted IFNγ. Also, human B-cells were functional as they produced specific human IgM and IgG antibodies upon vaccination with a T-cell dependent tetanus vaccine. However, a critical role of the human MHC II DQ8tg for inducing specific immune responses was not studied here.
HIV-1 infection of DQ8tg mice reconstituted with huDQ8-HSCs showed a stable titer of HIV RNA in the plasma over a 100 day period, demonstrating a successful long-term HIV infection.

Overall, it can be concluded that humanized DQ8tg mice engrafted with huDQ8 cells are a unique and valuable model for HIV infections.
DQ8tg mice repopulated with huDQ8-PBMCs are easy to generate and utilizable for short-term HIV infection studies while DQ8tg mice reconstituted with huDQ8-HSCs provide a suitable model for long-term HIV infection studies. Thus, this novel humanized mouse model is an important resource to study early stages of HIV infection in its human host cells as well as preclinical drug or vaccine testing.

VI. References

Ackley, CD, Yamamoto, JK, Levy, N, Pedersen, NC, Cooper, MD. *Immunologic abnormalities in pathogen-free cats experimentally infected with feline immunodeficiency virus*. J. Virol. 64, 5652 5655 **(1990)**

Adachi A, Gendelman HE, Koenig S, Folks T, Willey R, Rabson A, Martin MA. *Production of acquired immunodeficiency syndrome-associated retrovirus in human and nonhuman cells transfected with an infectious molecular clone*. J Virol.;59(2):284-91 **(1986)**

Akkina R. *New insights into HIV impact on hematopoiesis.* Blood. 26;122(13):2144-6 (2013)

Aldrovandi GM, Feuer G, Gao L, Jamieson B, Kristeva M, Chen IS, Zack JA. *The SCID-hu mouse as a model for HIV-1 infection*. Nature 363:732–6 **(1993)**

Alter, HJ. Eichberg JW, Masur H, Saxinger WC, Gallo R, Macher AM, Lane HC, Fauci AS. *Transmission of HTLV-III infection from human plasma to chimpanzees: an animal model for AIDS*. Science 226, 549–552 **(1984)**

An DS, Poon B, Fang RHT, Weijer K, Blom B, Spits H, Chen ISY, Uittenbogaart CH. *The human immune system (HIS) Rag2-/-γc-/- mouse, a novel chimeric mouse model for HIV-1 infection.* Clinical Vaccine Immunology.14:391-396 **(2007)**

André MC, Erbacher A, Gille C, Schmauke V, Goecke B, Hohberger A, Mang P, Wilhelm A, Mueller I, Herr W, Lang P, Handgretinger R, Hartwig UF. *Long-term human CD34+ stem cell-engrafted nonobese diabetic/SCID/IL-2R gamma(null) mice show impaired CD8+ T cell maintenance and a functional arrest of immature NK cells.* J Immunol. 1;185(5):2710-20 **(2010)**

Asjo, B, Albert, J, Karlsson, A, Morfeld-Manson, K, Biberfeld, G, Lidman, K, Fenyo, EM. *Replicative properties of human immunodeficiency virus from patients with varying severity of HIV infection*, Lancet ii, 660 **(1986)**

Baenziger S, Tussiwand R, Schlaepfer E, Mazzucchelli L, Heikenwalder M, Kurrer MO, Behnke S, Frey J, Oxenius A, Joller H. *Disseminated and sustained HIV infection in CD34+ cord blood cell-transplanted Rag2-/- {gamma}c-/- mice.* Proc Natl Acad Sci USA 103:15951-15956 **(2006)**

Balazs AB, Chen J, Hong CM, Rao DS, Yang L, Baltimore D. *Antibody-based protection against HIV infection by vectored immunoprophylaxis.* Nature 481, 81–84 **(2011)**

Baldauf HM, Pan X, Erikson E, Schmidt S, Daddacha W, Burggraf M, Schenkova K, Ambiel I, Wabnitz G, Gramberg T. *SAMHD1 restricts HIV-1 infection in resting CD4(+) T cells*. Nat Med, 18(11):1682–1689 **(2012)**

Barré-Sinoussi, F, Chermann, JC, Rey, F, Nugeyre, MT, Chamaret, S, Gruest, J, Dauguet, C, Axler-Blin, C, Vézinet-Brun, F, Rouzioux, C, Rozenbaum, W, Montagnier, L. *Isolation of a T-lymphotropic retrovirus from a patient at risk for acquired immune deficiency syndrome (AIDS)*. Science, 220(4599):868–871 **(1983)**

Barré-Sinoussi, F, *HIV: A discovery opening the road to novel scientific knowledge and global health improvement.* Virology 20;397(2):255-9 **(2010)**

Bartel DP. *MicroRNAs: genomics, biogenesis, mechanism, and function.* Cell. 2004 Jan 23;116(2):281-97 **(2004)**

Baumann JG, Unutmaz D, Miller MD, Breun SK, Grill SM, Mirro J, Littman DR, Rein A, Kewal, Ramani VN. *Murine T cells potently restrict human immunodeficiency virus infection*. J Virol 78(22):12537-12547 **(2004)**

Bazan HA, Alkhatib G, Broder CC, Berger EA. *Patterns of CCR5, CXCR4 and CCR3 usage by envelope glycoproteins from human immunodeficiency virus type 1 primary isolates.* J. Virol. 72:4485–91 **(1998)**

Benveniste P, Frelin C, Janmohamed S. *Intermediate-term hematopoietic stem cells with extended but time-limited reconstitution potential*. Cell Stem Cell 6(1):48-58 **(2010)**

Berger EA, Doms RW, Feny¨o EM, Korber BTM, Littman DR, Moore JP, Sattentau QJ, Schuitemaker H, Sodroski J, Weiss RA. *A new classification for HIV-1*. Nature 391:240 **(1998)**

Berger, EA, Murphy, PM, Farber, JM. *Chemokine receptors as HIV-1 coreceptors: roles in viral entry, tropism, and disease*. Annu Rev Immunol, 17:657–700 **(1999)**

Berges BK, Akkina SR, Folkvord JM, Connick E, Akkina R. *Mucosal transmission of R5 and X4 tropic HIV-1 via vaginal and rectal routes in humanized Rag2-/-gc-/- (RAG-hu) mice.* Virology 373:342-351 **(2008)**

Berges BK, Rowan MR. *The utility of the new generation of humanized mice to study HIV-1 infection: transmission, prevention, pathogenesis, and treatment.* Retrovirology 11;8:65 **(2011)**

Berges BK, Wheat WH, Palmer BE, Connick E, Akkina R. *HIV-1 infection and CD4 T cell depletion in the humanized Rag2-/-gc-/- (RAG-hu) mouse model*. Retrovirology. 1;3:76 **(2006)**

Bhatia M, Wang JCY, Kapp U. *Purification of primitive human hematopoietic cells capable of repopulating immunedeficient mice*. Proc Natl Acad Sci USA 94:5320-5325 **(1997)**

Bieniasz PD, Cullen BR. *Multiple blocks to human immunodeficiency virus type 1 replication in rodent cells*. J Virol. 74(21):9868–77 **(2000)**

Bieniasz PD, Fridell RA, Anthony K, Cullen BR**.** *Murine CXCR-4 is a functional coreceptor for T-cell-tropic and dual-tropic strains of human immunodeficiency virus type 1*. J. Virol. 71:7097-7100 **(1997)**

Billerbeck E, Barry WT, Mu K, Dorner M, Rice CM, Ploss A. *Development of human CD4$^+$FoxP3$^+$ regulatory T cells in human stem cell factor-, granulocyte-macrophage colony-stimulating factor-, and interleukin-3-expressing NOD-SCID IL2Rγ(null) humanized mice*. Blood 17;117(11):3076-86 **(2011)**

Biswas S, Chang H, Sarkis PT, Fikrig E, Zhu Q, Marasco WA. *Humoral immune responses in humanized BLT mice immunized with West Nile virus and HIV-1 envelope proteins are largely mediated via human CD5+ B cells*. Immunology. 134(4):419-33 **(2011)**

Bjorndal A, Deng H, Jansson M, Fiore JR, Colognesi C, Karlsson A, Albert J, Scarlatti G, Littman DR, Feny¨o EM. *Coreceptor usage of primary human immunodeficiency virus type 1 isolates varies according to biological phenotype*. J. Virol. 71:7478–87 **(1997)**

Bleul CC, Wu L, Hoxie JA, Springer TA, Mackay CR. *The HIV coreceptors CXCR4 and CCR5 are differentially expressed and regulated on human T lymphocytes* Proc Natl Acad Sci USA 4; 94(5): 1925–1930 **(1997)**

Bogers WM, Koornstra WH, Dubbes RH, ten Haaft PJ, Verstrepen BE, Jhagjhoorsingh SS, Haaksma AG, Niphuis H, Laman JD, Norley S, Schuitemaker H, Goudsmit J, Hunsmann G, Heeney JL, Wigzell H. *Characteristics of primary infection of a European human immunodeficiency virus type 1 clade B isolate in chimpanzees.* J. Gen. Virol. 79:2895-2903 **(1998)**

Boitano AE, Wang J, Romeo R, Bouchez LC, Parker AE, Sutton SE, Walker JR, Flaveny CA, Perdew GH, Denison MS, Schultz PG, Cooke MP. *Aryl hydrocarbon receptor antagonists promote the expansion of human hematopoietic stem cells.* Science. 10;329(5997):1345-8 **(2010)**

Bordeaux-Rego P, Luzo A, Costa FF, Olalla Saad ST, Crosara-Alberto DP. *Both Interleukin-3 and Interleukin-6 are necessary for better ex vivo expansion of CD133+ cells from umbilical cord blood.* Stem Cells Dev. 19(3):413-22 **(2010)**

Bosma, GC, Custer, R, Bosma, MJ. *A severe combined immunodeficiency mutation in the mouse*. Nature 301, 527–530 **(1983)**

Bossen C, Schneider P. *BAFF, APRIL and their receptors: structure, function and signaling*. Semin Immunol 18: 263–275 **(2006)**

Brainard DM, Seung E, Frahm N, Cariappa A, Bailey CC, Hart WK, Shin HS, Brooks SF, Knight HL, Eichbaum Q, Yang YG, Sykes M, Walker BD, Freeman GJ, Pillai S, Westmoreland SV, Brander C, Luster AD, Tager AM. *Induction of robust cellular and humoral virus-specific adaptive immune responses in human immunodeficiency virus-infected humanized BLT mice*. J Virol. 83(14):7305-21 **(2009)**

Brehm MA, Cuthbert A, Yang C, Miller DM, DiIorio P. *Parameters for establishing humanized mouse models to study human immunity: analysis of human hematopoietic stem cells engraftment in 3 immunodeficient strains of mice bearing the IL2Rgamma(null) mutation.* Clin Immunol 135: 84–98 **(2010)**

Brehm MA, Racki WJ, Leif J, Burzenski L, Hosur V. *Engraftment of human HSCs in nonirradiated newborn NOD-scid IL2rγnull mice is enhanced by transgenic expression of membrane bound human SCF*. Blood 119:2778–88 **(2012)**

Browning J, Horner JW, Pettoello-Mantovani M, Raker C, Yurasov S, DePinho RA, Goldstein H. *Mice transgenic for human CD4 and CCR5 are susceptible to HIV infection.* Proc. Natl Acad. Sci. USA 94, 14637–14641 **(1997)**

Broxmeyer HE, Cooper S, Hague N, Benninger L, Sarris A, Cornetta K, Vadhan-Raj S, Hendrie P, Mantel C. *Human chemokines: enhancement of specific activity and effects in vitro on normal and leukemic progenitors and a factor-dependent cell line and in vivo in mice.* Ann. Hematol. 71, 235–246. **(1995)**

Bühring HJ, Seiffert M, Bock TA, Scheding S, Thiel A, Scheffold A, Kanz L, Brugger W. *Expression of novel surface antigens on early hematopoietic cells.* Ann N Y Acad Sci. 30;872:25-38 **(1999)**

Carter CC, McNamara LA, Onafuwa-Nuga A. *HIV-1 utilizes the CXCR4 chemokine receptor to infect multipotent hematopoietic stem and progenitor cells.* Cell Host Microbe. 9(3):223-234 **(2011)**

Carter CC, Onafuwa-Nuga A, McNamara LA. *HIV-1 infects multipotent progenitor cells causing cell death and establishing latent cellular reservoirs.* Nat Med 16:446-51 **(2010)**

Chahroudi, A, Bosinger, SE, Vanderford, TH, Paiardini, M, Silvestri, G. *Natural SIV hosts: showing AIDS the door.* Science 335, 1188–1193 **(2012)**

Chang JJ, Altfeld M. *Innate immune activation in primary HIV-1 infection.* J Infect Dis. 15;202 Suppl 2:S297-301 **(2010)**

Chang MS, Chen BC, Yu MT, Sheu JR, Chen TF, Lin CH. *Phorbol 12-myristate 13-acetate upregulates cyclooxygenase-2 expression in human pulmonary epithelial cells via Ras, Raf-1, ERK, and NF-kappaB, but not p38 MAPK, pathways*. Cell Signal. 17(3):299-310 **(2005)**

Chen Q, Khoury M, Chen J. *Expression of human cytokines dramatically improves reconstitution of specific human-blood lineage cells in humanized mice*. Proc Natl Acad Sci USA 22;106(51):21783-8 **(2009)**

Cheng-Mayer C, Seto D, Tateno M, Levy JA. *Biologic features of HIV-1 that correlate with virulence in the host.* Science 240, 80 **(1988)**

Chesebro, B., Wehrly, K. and Maury, W. *Differential expression in human and mouse cells of human immunodeficiency virus pseudotyped by murine retroviruses*. J. Virol. 64, 45534557 **(1990)**

Choudhary, SK. Rezk NL, Ince WL, Cheema M, Zhang L, Su L, Swanstrom R, Kashuba AD, Margolis DM. *Suppression of human immunodeficiency virus type 1 (HIV-1) viremia with reverse transcriptase and integrase inhibitors, CD4$^+$ T-cell recovery, and viral rebound upon interruption of therapy in a new model for HIV treatment in the humanized Rag2$^{-/-}\gamma c^{-/-}$ mouse*. J. Virol. 83, 8254–8258 **(2009)**

Christianson, SW. Greiner DL, Schweitzer IB, Gott B, Beamer GL, Schweitzer PA, Hesselton

RM, Shultz LD. *Role of natural killer cells on engraftment of human lymphoid cells and on metastasis of human T-lymphoblastoid leukemia cells in C57BL/6J-scid mice and in C57BL/6J-scid bg mice.* Cell. Immunol. 171, 186–199 **(1996)**

Chu YW, Gress RE. *Murine models of chronic graft-versus-host disease: Insights and unresolved issues*. Biol Blood Marrow Transplant. 14: 365-378 (2008)

Clapham PR, McKnight A, Weiss RA. *Human immunodeficiency virus type 2 infection and fusion of CD4-negative human cell lines: induction and enhancement by soluble CD4.* J. Virol. 66:3531–3537 **(1992)**

Claudio E, Brown K, Park S, Wang H, Siebenlist. *U BAFF-induced NEMO-independent processing of NF-kappa B2 in maturing B cells.* NatImmunol 3: 958–965 **(2002)**

Clavel, F, Mansinho, K, Chamaret, S, Guetard, D, Favier, V, Nina, J, Santos-Ferreira, MO, Champalimaud, JL, Montagnier, L. *Human immunodeficiency virus type 2 infection associated with AIDS in West Africa.* N Engl J Med, 316(19):1180–1185 **(1987)**

Coffin, J., Haase, A., Levy, J. A., Montagnier, L., Oroszlan, S., Teich, N., Temin, H., Toyoshima, K., Varmus, H., and Vogt, P. *What to call the AIDS virus?* Nature, 321(6065):10 **(1986)**

Connor RI, Sheridan KE, Ceradini D, Choe S, Landau NR. *Change in coreceptor use correlates with disease progression in HIV-1-infected individuals*. J. Exp. Med. 185:621–28 **(1997)**

Cooke KR, Hill GR, Crawford JM et al. *Tumor necrosis factoralpha production to lipopolysaccharide stimulation by donor cells predicts the severity of experimental acute graft-versus-host disease.* J Clin Invest; 102:1882–91 **(1998)**

Covassin, L. Laning J, Abdi R, Langevin DL, Phillips NE, Shultz LD, Brehm MA. *Human peripheral blood CD4 T cell-engrafted non-obese diabetic-scid IL2rγnull H2Ab1tm1Gru Tg (human leucocyte antigen D related 4) mice: a mouse model of human allogeneic graft versus- host disease*. Clin. Exp. Immunol. 166, 269–280 **(2011)**

Cullen, B. R. Regulation of HIV-1 gene expression. FASEB J, 5(10):2361–2368 **(1991)**

Custer, RP, Bosma, GC, Bosma, MJ. *Severe combined immunodeficiency (SCID) in the mouse.* Am. J. Pathol. 120, 464-477 **(1985)**

D'Souza, V. and Summers, M. F. *How retroviruses select their genomes.* Nat Rev Microbiol. 3(8):643-55. **(2005)**

Dalgleish, AG, Beverley, PC., Clapham, PR., Crawford, DH., Greaves, MF., and Weiss, RA. *The CD4 (T4) antigen is an essential component of the receptor for the AIDS retrovirus.* Nature, 312(5996):763–767 **(1984)**

Danner, R. Chaudhari SN, Rosenberger J, Surls J, Richie TL, Brumeanu TD, Casares S. *Expression of HLA class II molecules in humanized NOD.Rag1KO.IL2RgcKO mice is critical for development and function of human T and B cells.* PLoS ONE 6, e19826 **(2011)**

Dash, PK. Gorantla S, Gendelman HE, Knibbe J, Casale GP, Makarov E, Epstein AA, Gelbard HA, Boska MD, Poluektova LY.*Loss of neuronal integrity during progressive HIV-1 infection of humanized mice.* J. Neurosci. 31, 3148–3157 **(2011)**

Dayton AI, Sodroski JG, Rosen CA, Goh WC, Haseltine WA. *The trans-activator gene of the human T cell lymphotropic virus type III is required for replication*. Cell 44 (6): 941-947 **(1986)**

De Silva S, Wu L. *TRIM5 acts as more than a retroviral restriction factor*. Viruses 3(7):1204-9 **(2011)**

De Silva TI, Cotton M, Rowland-Jones SL. *HIV-2: the forgotten AIDS virus.* Trends Microbiol, 16(12):588–595 **(2008)**

De Wynter EA, Buck D, Hart C, Heywood R, Coutinho LH, Clayton A, Rafferty JA, Burt D, Guenechea G, Bueren JA, Gagen D, Fairbairn LJ, Lord BI, Testa NG. *CD34+AC133+ cells isolated from cord blood are highly enriched in*

long-term culture-initiating cells, NOD/SCID-repopulating cells and dendritic cell progenitors. Stem Cells 16(6):387-96 **(1998)**

Dean GA, Reubel GH, Moore PF, Pedersen NC. *Proviral burden and infection kinetics of feline immunodeficiency virus in lymphocyte subsets of blood and lymph node*. J. Virol. 70, 5165–5169 **(1996)**

Deichmann M, Kronenwett R, Haas R. *Expression of the human immunodeficiency virus type-1 coreceptors CXCR-4 (fusin, LESTR) and CKR-5 in CD341 hematopoietic progenitor cells*. Blood 89(10):3522-3528 **(1997)**

Denton PW, Estes JD, Sun Z, Othieno FA, Wei BL, Wege AK, Powell DA, Payne D, Haase AT, Garcia JV. *Antiretroviral pre-exposure prophylaxis prevents vaginal transmission of HIV-1 in humanized BLT mice*. PLoS Med. 15;5(1):e16 **(2008)**

Denton PW, García JV. *Humanized mouse models of HIV infection.* AIDS Rev.;13(3):135-48 **(2011)**

Denton, P. W. Krisko JF, Powell DA, Mathias M, Kwak YT, Martinez-Torres F, Zou W, Payne DA, Estes JD, Garcia JV. *Systemic administration of antiretrovirals prior to exposure prevents rectal and intravenous HIV-1 transmission in humanized BLT mice*. PLoS ONE 5, e8829 **(2010)**

Dickie, P, Felser, J, Eckhaus, M, Bryant, J, Silver, J, Marinos, N. and Notkins, A.L. *HIV associated nephropathy in transgenic mice expressing HIV-1 genes.* Virology 185, 109-119 **(1991)**

Dorshkind K, Pollack SB, Bosma MJ, Phillips RA. *Natural killer cells are present in mice with severe combined immunodeficiency*. J Immunol. 134:3798-3801 **(1985)**

Dranoff G, *Cytokines in cancer pathogenesis and cancer therapy*. Nature Reviews Cancer 4, 11-22 **(2004)**

D'Souza V, Summers MF. *How retroviruses select their genomes.* Nat Rev Microbiol.3(8):643-55 **(2005)**

Dunn CS, Mehtali M, Houdebine LM, Gut JP, Kirn A, Aubertin AM. *Human immunodeficiency virus type 1 infection of human CD4-transgenic rabbits*. J. Gen. Virol. 76, 1327–1336 **(1995)**

Egberink H. Borst M, Niphuis H, Balzarini J, Neu H, Schellekens H, De Clercq E, Horzinek M, Koolen M. *Suppression of feline immunodeficiency virus infection in vivo by 9-(2-phosphonomethoxyethyl)adenine*. Proc. Natl Acad. Sci. USA 87, 3087–3091 **(1990)**

Ema H, Nakauchi H. *Expansion of hematopoietic stem cells in the developing liver of a mouse embryo*. Blood 95: 2284–2288 (2000)

Embretson J, Zupancic M, Ribas JL. *Massive covert infection of helper T lymphocytes and macrophages by HIV during the incubation period of AIDS*. Nature, 362: 359-62 **(1993)**

Esté JA, Telenti A. *HIV entry inhibitors.* Lancet, 370(9581):81–88 **(2007)**

Evans LA, McHugh TM, Stites DP, Levy JA. *Differential ability of HIV isolates to productively infect human cells*. Immunol. 138, 3415 **(1987)**

Ezzell C, *Laboratory accident kills AIDS mice*. Nature Dec 15;336(6200):613 **(1988)**

Fais S, Lapenta C, Santini SM, Spada M, Parlato S, Logozzi M, Rizza P, Belardelli F. *Human immunodeficiency virus type 1 strains R5 and X4 induce different pathogenic effects in hu-PBL-SCID mice, depending on the state of activation/differentiation of human target cells at the time of primary infection.* J Virol. 73(8):6453-9 **(1999)**

Farrar MA, Schreiber RD. *The molecular cell biology of interferon-g and its receptor*. Annu Rev Immunol.11:571-611 **(1993)**

Feinberg, MB, Greene, WC. Molecular Insights into human immunodeficiency virus type1 pathogenesis. Current Opinion in Immunology. 4:466-474 **(1992)**

Felber BK, Hadzopoulou-Cladaras M, Cladaras C, Copeland T, Pavlakis GN. *rev*

protein of human immunodeficiency virus type 1 affects the stability and transport of the viral mRNA. Proc. Natl. Acad. Sci. U S A 86 (5): 1495-1499 **(1989)**

Feng Y, Broder CC, Kennedy PE, Berger EA. *HIV-1 entry cofactor: functional cDNA cloning of a seven transmembrane, G protein-coupled receptor*. Science 272:872–77 **(1996)**

Fenyö EM, Albert J, Asjö B. *Replicative capacity, cytopathic effect and cell tropism of HIV.* AIDS. 1989;3 Suppl 1:S5-12 **(1989)**

Fiebig EW, Wright DJ, Rawal BD, Garrett PE, Schumacher RT, Peddada L, Heldebrant C, Smith R, Conrad A, Kleinman SH, Busch MP. *Dynamics of HIV viremia and antibody seroconversion in plasma donors: implications for diagnosis and staging of primary HIV infection*. AIDS. 17:1871-1879 **(2003)**

Filice G, Cereda PM, Orsolini P, Soldini L, Romeno E, Rondanelli EG. *Kinetics of p24-antigenemia, IgM, IgG antibodies to p24 and p41 and virus isolation in rabbits experimentally infected with HIV-1*. Microbiologica 3, 215-224 **(1990)**

Filice G, Cereda PM, Varnier OE. *Infection of rabbits with human immunodeficicency virus*. Nature 335, 366-369 **(1988)**

Flores-Guzmán P, Fernández-Sánchez V, Mayani H. *Concise review: ex vivo expansion of cord blood-derived hematopoietic stem and progenitor cells: basic principles, experimental approaches, and impact in regenerative medicine.* Stem Cells Transl Med.;2(11):830-8 **(2013)**

Freed, E. O. *HIV-1 replication*. Somat Cell Mol Genet, 26(1-6):13–33 **(2001)**

Fulop GM. Phillips RA. *The scid mutation in mice causes a general defect in DNA repair*. Nature 347, 479–482 **(1990)**

Gallo RC, *Frequent detection and isolation of cytopathic retroviruses (HTLV-III) from patients with AIDS and at risk for AIDS*. Science 224, 500–503 **(1984)**

Gao F, Bailes E, Robertson DL, Chen Y, Rodenburg CM, Michael SF, Cummins LB, Arthur LO, Peeters M, Shaw GM, Sharp PM, Hahn BH. *Origin of HIV-1 in the chimpanzee Pan, troglodytes troglodytes*. Nature 397, 36–441 **(1999)**

Garber ME, Wei P, Kewal, Ramani VN, Mayall TP, Herrmann CH, Rice AP, Littman DR, Jones KA. *The interaction between HIV-1 Tat and human cyclin T1 requires zinc and a critical cysteine residue that is not conserved in the murine CycT1 protein*. Genes Dev. 12:3512-3527 **(1998)**

Garcia S, Freitas AA. *Humanized mice: current states and perspectives*. Immunol. Lett. 146, 1–7 **(2012)**

Gelderblom HR. *Assembly and morphology of HIV: potential effect of structure on viral function*. AIDS, 5(6):617–637 **(1991)**

Glimm H, Eisterer W, Lee K, Cashman J, Holyoake TL, Nicolini F, Shultz LD, von Kalle C, Eaves CJ. *Previously undetected human hematopoietic cell populations with short-term repopulating activity selectively engraft NOD/SCID-beta2 microglobulin-null mice*. J. Clin. Invest. 107, 199–206 **(2001)**

Goffinet C, Allespach I, Keppler OT. *HIV-susceptible transgenic rats allow rapid preclinical testing of antiviral compounds targeting virus entry or reverse transcription*. Proc Natl Acad Sci USA. a;104(3):1015–20 **(2007a)**

Goffinet C, Michel N, Allespach I, Tervo HM, Hermann V, Krausslich HG, et al. *Primary T-cells from human CD4/CCR5-transgenic rats support all early steps of HIV-1 replication including integration, but display impaired viral gene expression*. Retrovirology;4:53 **(2007b)**

Goldman JP. Blundell MP, Lopes L, Kinnon C, Di Santo JP, Thrasher AJ. *Enhanced human cell engraftment in mice deficient in RAG2 and the common cytokine receptor γ chain*. Br. J. Haematol. 103, 335–342 **(1998)**

Goldstone DC, Ennis-Adeniran V, Hedden JJ, Groom HC, Rice GI, Christodoulou E, Walker PA, Kelly G, Haire LF, Yap MW. *HIV-1 restriction factor SAMHD1 is a deoxynucleoside triphosphate*

triphosphohydrolase. Nature, 480(7377):379–382 **(2011)**

Gorantla S, Sneller H, Walters L, Sharp JG, Pirruccello SJ, West JT, Wood C, Dewhurst S, Gendelman HE, Poluektova L. *Human Immunodeficiency Virus Type 1 pathobiology studied in humanized Balb/c-Rag2-/- {gamma}c-/- mice.* J Virol 81:2700-2712 **(2007)**

Gorantla, S. Makarov E, Finke-Dwyer J, Castanedo A, Holguin A, Gebhart CL, Gendelman HE, Poluektova L.. *Links between progressive HIV-1 infection of humanized mice and viral neuropathogenesis*. Am. J. Pathol. 177, 2938–2949 **(2010)**

Gottlieb MS, Schroff R, Schanker HM, Weisman JD, Fan PT, Wolf RA, Saxon A. *Pneumocystis carinii pneumonia and mucosal candidiasis in previously healthy homosexual men: evidence of a new acquired cellular immunodeficiency*. N. Engl. J. Med. 305, 1425–1431 **(1981)**

Graziosi C, Pantaleo G, Butini L, Demarest JF, Saag MS, Shaw GM, Fauci AS. *Kinetics of human immunodeficiency virus type 1 (HIV-1) DNA and RNA synthesis during primary HIV-1 infection*. Proc Natl Acad Sci USA,90:6405-6409 **(1993)**

Greiner DL, Hesselton RA, Shultz LD. *SCID mouse models of human stem cell engraftment*. Stem Cells 16, 166–177 **(1998)**

Guillon C, van der Ende ME, Boers PH, Gruters RA, Schutten M, Osterhaus AD. *Coreceptor usage of human immunodeficiency virus type 2 primary isolates and biological clones is broad and does not correlate with their syncytium-inducing capacities*. J Virol.;72(7):6260-3 **(1998)**

Hallenberger S, Moulard M, Sordel M, Klenk HD, Garten W. *The role of eukaryotic subtilisin-like endoproteases for the activation of human immunodeficiency virus glycoproteins in natural host cells*. J. Virol. 71 (2): 1036-1045 **(1997)**

Hanna Z, Kay DG, Rebai N, Guimond A, Jothy S, Jolicoeur P. *Nef harbors a major determinant of pathogenicity for an AIDS-like disease induced by HIV-1 in transgenic mice*. Cell 95(2):163–75 **(1998)**

Harris RS, Bishop KN, Sheehy AM, Craig HM, Petersen-Mahrt SK, Watt IN, Neuberger MS, Malim MH. *DNA deamination mediates innate immunity to retroviral infection*. Cell. 13;113(6):803-9 **(2003)**

Hartmann, K. Donath A, Beer B, Egberink HF, Horzinek MC, Lutz H, Hoffmann-Fezer G, Thum I, Thefeld S. *Use of two virustatica (AZT, PMEA) in the treatment of FIV and of FeLV seropositive cats with clinical symptoms*. Vet. Immunol. Immunopathol. 35, 167–175 **(1992)**

Hatziioannou T, Cowan S, Bieniasz PD. *Capsid-dependent and -independent postentry restriction of primate lentivirus tropism in rodent cells.* J Virol 78(2):1006-1011 **(2004)**

Hatziioannou T, Evans DT. *Animal models for HIV/AIDS research*. Nat Rev Microbiol. Dec;10(12):852-67 **(2012)**

Heeney JL, Dalgleish AG, Weiss RA. *Origins of HIV and the evolution of resistance to AIDS*. Science, 313(5786):462–6 **(2006)**

Heesen M, Berman MA, Benson JD, Gerard C, Dorf ME**.** *Cloning of the mouse fusin gene, homologue to a human HIV-1 co-factor.* J. Immunol. 157:5455-5460 **(1996)**

Hess DA, Meyerrose TE, Wirthlin L, Craft TP, Herrbrich PE, Creer MH, Nolta JA. *Functional characterization of highly purified human hematopoietic repopulating cells isolated according to aldehyde dehydrogenase activity*. Blood 104(6):1648–1655 **(2004)**

Hess DA, Wirthlin L, Craft TP, Herrbrich PE, Hohm SA, Lahey R, Eades WC, Creer MH, Nolta JA. *Selection based on CD133 and high aldehyde dehydrogenase activity isolates long-term reconstituting human hematopoietic stem cells*. Blood 107(5):2162–2169 **(2006)**

Hesselton RM, Greiner DL, Mordes JP, Rajan TV, Sullivan JL, Shultz LD. *High levels of human peripheral blood mononuclear cell engraftment and enhanced susceptibility to HIV-1 infection in NOD/LtSz-scid/scid mice.* J. Infect. Dis. 172, 774–782 **(1995)**

Hiramatsu H, Nishikomori R, Heike T, Ito M, Kobayashi K, Katamura K, Nakahata T. *Complete reconstitution of human lymphocytes from cord blood CD34+ cells using the NOD/SCID/γcnull mice model*. Blood 102:873-880 **(2003)**

Hoffman R, Tong J, Brandt J, Traycoff C, Bruno E, McGuire BW, Gordon MS, McNiece I, Srour EF. *The in vitro and in vivo effects of stem cell factor on human hematopoiesis.* Stem Cells 11 Suppl 2:76-82 **(1993)**

Hoffmann-Fezer G, Gall C, Zengerle U, Kranz B, Thierfelder S. *Immunohistology and immunocytology of human T-cell chimerism and graft-versus-host disease in SCID mice.* Blood. 15;81(12):3440-8 **(1993)**

Holt, N, Wang J, Kim K, Friedman G, Wang X, Taupin V, Crooks GM, Kohn DB, Gregory PD, Holmes MC, Cannon PM. *Human hematopoietic stem/progenitor cells modified by zinc-finger nucleases targeted to CCR5 control HIV-1 in vivo*. Nature Biotech. 28, 839–847 **(2010)**

Horsburgh CR, Holmberg SD. *The global distribution of human immunodeficiency virus type 2 (HIV-2) infection*. Transfusion, 28(2):192–195 **(1988)**

Houzet L, Klase Z, Yeung ML, Wu A, Le SY, Quinones M, Jeang KT. *The extent of sequence complementarity correlates with the potency of cellular miRNA-mediated restriction of HIV-1*. Nucleic Acids Res 40(22):11684–11696 **(2012)**

Hu Z, Van Rooijen N, Yang YG. *Macrophages prevent human red blood cell reconstitution in immunodeficient mice*. Blood 118:5938–46 **(2011)**

Huang J, Wang F, Argyris E, Chen K, Liang Z, Tian H, Huang W, Squires K, Verlinghieri G, Zhang H. *Cellular microRNAs contribute to HIV-1 latency in resting primary CD4+ T lymphocytes*. Nat Med, 13(10):1241–1247 **(2007)**

Huang X, Cho S, Spangrude GJ. *Hematopoietic stem cells: generation and self-renewal*, Cell Death Differ. Nov;14(11):1851-9. (2007)

Huntington ND, Alves NL, Legrand N, Lim A, Strick-Marchand H, Mention JJ, Plet A, Weijer K, Jacques Y, Becker PD, Guzman C, Soussan P, Kremsdorf D, Spits H, Di Santo JP. *IL-15 transpresentation promotes both human T-cell reconstitution and T-cell-dependent antibody responses in vivo.* Proc Natl Acad Sci USA 12;108(15):6217-22 **(2011)**

Hymes KB, Cheung T, Greene, JB, Prose NS, Marcus A, Ballard H, William DC, Laubenstein LJ. *Kaposi's sarcoma in homosexual men-a report of eight cases.* Lancet, 2(8247):598–600 **(1981)**

Igarashi H, Kouro T, Yokota T, Comp PC, Kincade PW. *Age and stage dependency of estrogen receptor expression by lymphocyte precursors.* Proc Natl Acad Sci U S A 98(26):15131-15136 **(2001)**

Ishikawa F, Niiro H, Iino T, Yoshida S, Saito N, Onohara S, Miyamoto T, Minagawa H, Fujii S, Shultz LD, Harada M, Akashi K. *The developmental program of human dendritic cells is operated independently of conventional myeloid and lymphoid pathways.* Blood 15;110(10):3591-660 **(2007)**

Ishikawa F, Yasukawa M, Lyons B, Yoshida S, Miyamoto T, Yoshimoto G, Watanabe T, Akashi K, Shultz LD, Harada M. *Development of functional human blood and immune systems in NOD/SCID/IL2 receptor γ chainnull mice*. Blood 106, 1565–1573 **(2005)**

Ito M, Hiramatsu H, Kobayashi K, Suzue K, Kawahata M, Hioki K, Ueyama Y, Koyanagi Y, Sugamura K, Tsuji K, Heike T, Nakahata T. *NOD/SCIDγcnull mouse: an excellent recipient mouse model for engraftment of human cells*. Blood 100:3175-3182 **(2002)**

Jaiswal S, Pearson T, Friberg H, Shultz LD, Greiner DL. *Dengue Virus Infection and Virus-Specific HLA-A2 Restricted Immune Responses in Humanized NOD-scid IL2rcnull Mice*. PLoS One 4: e7251 **(2009)**

Jamieson BD, Zack JA. *Murine models for HIV disease*. AIDS 13(SupplA) S5–11 **(1999)**

Johnson GR, Moore MAS. *Role of stem cell migration in initiation of mouse fetal liver haematopoiesis*. Nature. 25;258(5537):726-8 **(1975)**

Joseph A, Zheng JH, Chen K, Dutta M, Chen C, Stiegler G, Kunert R, Follenzi A, Goldstein H.*Inhibition of in vivo HIV infection in humanized mice by gene therapy of human hematopoietic stem cells with a lentiviral vector encoding a broadly neutralizing anti-HIV antibody*. J. Virol. 84, 6645–6653 **(2010)**

Jung A, Maier R, Vartanian JP, Bocharov G, Jung V, Fischer U, Meese E, Wain-Hobson S, Meyerhans A. *Recombination: Multiply infected spleen cells in HIV patients.* Nature, 418(6894):144 **(2002)**

Kaneshima H, Shih CC, Namikawa R, Rabin L, Outzen H, Machado SG, McCune JM. *Human immunodeficiency virus infection of human lymph nodes in the SCID-hu mouse*. Proc. Natl. Acad. Sci. USA 15, 45234-527 **(1991)**

Kawamoto H, Wada H, Katsura Y. *A revised scheme for developmental pathways of hematopoietic cells: the myeloid-based model*. Int Immunol. 22(2):65-70 **(2010)**

Keele BF, Van Heuverswyn F, Li Y, Bailes E, Takehisa J, Santiago ML, Bibollet-Ruche F, Chen Y, Wain LV, Liegeois F, Loul S, Ngole EM, Bienvenue Y, Delaporte E, Brookfield JF, Sharp PM, Shaw GM, Peeters M, Hahn BH. *Chimpanzee reservoirs of pandemic and nonpandemic HIV-1*. Science 313, 523–526 **(2006)**

Keppler OT, Welte FJ, Ngo TA, Chin PS, Patton KS, Tsou CL, Abbey NW, Sharkey ME, Grant RM, You Y, Scarborough JD, Ellmeier W, Littman DR, Stevenson M, Charo IF, Herndier BG, Speck RF, Goldsmith MA. *Progress toward a human CD4/CCR5 transgenic rat model for de novo infection by human immunodeficiency virus type 1*. J. Exp. Med. 195, 719–736 **(2002)**

Khillan JS, Deen KC, Yu SH, Sweet RW, Rosenberg M, Westphal H. *Gene transactivation by the TAT gene of human immunodeficiency virus in transgenic mice*. Nucleic Acids Res. 16, 1423 1430 **(1988)**

Kim JB, Sharp PA. *Positive transcription elongation factor B phosphorylates hSPT5 and RNA polymerase II carboxyl-terminal domain independently of cyclin-dependent kinase-activating kinase.* J Biol Chem, 276(15):12317–12323 **(2001)**

King MA, Covassin L, Brehm MA, Racki W, Pearson T, Leif J, Laning J, Fodor W, Foreman O, Burzenski L, Chase TH, Gott B, Rossini AA, Bortell R, Shultz LD, Greiner DL. *Human peripheral blood leucocyte non-obese diabetic-severe combined immunodeficiency interleukin-2 receptor gamma chain gene mouse model of xenogeneic graft-versus-host-like disease and the role of host major histocompatibility complex.* Clin Exp Immunol. 157(1):104-18 **(2009)**

Kirchhoff F. *Immune evasion and counteraction of restriction factors by HIV-1 and other primate Lentiviruses*. Cell Host Microbe 8 (1): 55-67 **(2010)**

Kirouac DC, Ito C, Csaszar E, Roch A, Yu M, Sykes EA, Bader GD, Zandstra PW. *Dynamic interaction networks in a hierarchically organized tissue.* Mol. Syst. Biol. 6, 417 **(2010)**

Klatzmann D, Barré-Sinoussi F, Nugeyre MT, Danquet C, Vilmer E, Griscelli C, Brun-Veziret F, Rouzioux C, Gluckman JC, Chermann JC. *Selective tropism of lymphadenopathy associated virus (LAV) for helper-inducer T lymphocytes.* Science 225, 59–63 **(1984b)**

Klatzmann D, Champagne E, Chamaret S, Gruest J, Guetard D, Hercend T, Gluckman JC, Montagnier L. *T-lymphocyte T4 molecule behaves as the receptor for human retrovirus LAV*. Nature 312, 767–768 **(1984a)**

Korber B, Muldoon M, Theiler J, Gao F, Gupta R, Lapedes A, Hahn BH, Wolinsky S, Bhattacharya T. *Timing the ancestor of the HIV-1 pandemic strains*. Science 288 (5472): 1789-1796 **(2000)**

Kuhl BD, Sloan RD, Donahue DA, Bar-Magen T, Liang C, Wainberg MA. *Tetherin restricts*

direct cell-to cell infection of HIV-1 Retrovirology 24;7:115 **(2010)**

Kulaga H, Folks T, Rutledge R, Truckenmiller ME, Gugel E, Kindt TJ. *Infection of rabbits with human immunodeficiency virus 1*. Journal of Experimental Medicine 169, 321 326 **(1984)**

Kumar P, Ban HS, Kim SS, Wu H, Pearson T, Greiner DL, Laouar A, Yao J, Haridas V, Habiro K, Yang YG, Jeong JH, Lee KY, Kim YH, Kim SW, Peipp M, Fey GH, Manjunath N, Shultz LD, Lee SK, Shankar P**.** *T cell-specific siRNA delivery suppresses HIV-1 infection in humanized mice*. Cell 134, 577–586 **(2008)**

Kwant-Mitchell A, Ashkar AA, Rosenthal KL. *Mucosal innate and adaptive immune responses against herpes simplex virus type 2 in a humanized mouse model*. J Virol. 2009 Oct;83(20):10664-76 **(2009)**

Lan P, Tonomura N, Shimizu A, Wang S, Yang YG. *Reconstitution of a functional human immune system in immunodeficient mice through combined human fetal thymus/liver and CD34+ cell transplantation*. Blood, 108:487-492 **(2006)**

Lang J, Kelly M, Freed BM, McCarter MD, Kedl RM, Torres RM, Pelanda R. *Studies of lymphocyte reconstitution in a humanized mouse model reveal a requirement of T cells for human B cell maturation.* J Immunol. 1;190(5):2090-101 **(2013)**

Lang J, Weiss N, Freed BM, Torres RM, Pelanda R. *Generation of hematopoietic humanized mice in the newborn BALB/c-Rag2null Il2rγnull mouse model: a multivariable optimization approach*. Clin Immunol. 140(1):102-16 **(2011)**

Lapenta C, Parlato S, Spada M, Santini SM, Rizza P, Logozzi M, Proietti E, Belardelli F, Fais S. *Human lymphoblastoid CD41 T cells become permissive to macrophage-tropic strains of human immunodeficiency virus type 1 after passage into severe combined immunodeficient mice through in vivo upregulation of CCR5: in vivo dynamics of CD41 T-cell differentiation in pathogenesis of AIDS.* J Virol.;72(12):10323-7 **(1998)**

Lapidot T, Pflumio F, Doedens M, Murdoch B, Williams DE, Dick JE. *Cytokine stimulation of multilineage hematopoiesis from immature human cells engrafted in SCID mice*. Science. 255(5048):1137-41 **(1992)**

Larochelle A, Vormoor J, Hanenberg H. *Identification of primitive human hematopoietic cells capable of repopulating NOD/SCID mouse bone marrow: implications for gene therapy*. Nat Med 2:1329-1337 **(1996)**

Lemey P, Pybus OG, Rambaut A, Drummond AJ, Robertson DL, Roques P, Worobey M, Vandamme AM. *The molecular population genetics of HIV-1 group O*. Genetics 167 (3): 1059-1068 **(2004)**

Lemey P, Pybus OG, Wang B, Saksena NK, Salemi M, Vandamme AM. *Tracing the origin and history of the HIV-2 epidemic*. Proc. Natl. Acad. Sci. USA 100 (11): 6588-6592 **(2003)**

Lemischka IR. *Clonal, in vivo behavior of the totipotent hematopoietic stem cell.* Semin Immunol, 3, 349–355 (1991)

Leonard J, Khillan JS, Gendelman HE, Adachi A, Lorenzo S, Westphal H, Martin MA, Meltzer MS. *The human immunodeficiency virus long terminal repeat is preferentially expressed in Langerhans cells in transgenic mice.* AIDS Res. and Human Retroviruses 5, 421-430 **(1989)**

Leonard JM, Abramczuk JW, Pezen DS, Rutledge R, Belcher JH, Hakim F, Shearer G, Lamperth L, Travis W, Fredrickson T. *Development of disease and virus recovery in transgenic mice containing HIV proviral DNA*. Science 242, 1665–1670 **(1988)**

Leonard W.J. *Cytokines and immunodeficiency diseases*. Nat. Rev. Immunol. 1, 200–208.3 **(2001)**

Lepus CM, Gibson TF, Gerber SA, Kawikova I, Szczepanik M, Hossain J, Ablamunits V, Kirkiles-Smith N, Herold KC, Donis RO, Bothwell AL, Pober JS, Harding MJ. *Comparison of Human Fetal Liver, Umbilical Cord Blood, and Adult Blood Hematopoietic Stem Cell Engraftment in NOD-scid/γc−/−, Balb/c-Rag1−/−γc−/−, and C.B-17-scid/bg*

Immunodeficient Mice. Hum Immunol.;70(10):790-802 **(2009)**

Liao CH, Kuang YQ, Liu HL, Zheng YT, Su B. *A novel fusion gene, TRIM5-cyclophilin A in the pig-tailed macaque determines its susceptibility to HIV-1 infection*. AIDS. 2007 Dec;21 Suppl 8:S19-26 **(2007)**

Ling B, Veazey RS, Luckay A, Penedo C, Xu K, Lifson JD, Marx PA. *SIVmac pathogenesis in rhesus macaques of Chinese and Indian orgin compared with primary HIV infections in humans*. AIDS. 2002 Jul 26;16(11):1489-96 **(2002)**

Liu C, Chen BJ, Deoliveira D, Sempowski GD, Chao NJ, Storms RW. *Progenitor cell dose determines the pace and completeness of engraftment in a xenograft model for cord blood transplantation*. Blood. Dec 16;116(25):5518-27. (2010)

Lockridge JL, Zhou Y, Becker YA, Ma S, Kenney SC, Hematti P, Capitini CM, Burlingham WJ, Gendron-Fitzpatrick A, Gumperz JE. *Mice engrafted with human fetal thymic tissue and hematopoietic stem cells develop pathology resembling chronic graft-versus-host disease.* Biol Blood Marrow Transplant.;19(9):1310-22 **(2013)**

Lores P, Boucher V, Mackay C, Pla M, Von Boehmer H, Jami J. *Expression of human CD4 in transgenic mice does not confer sensitivity to human immunodeficiency virus infection*. AIDS Res Hum Retroviruses 8(12):2063–71**(1992)**

Lowry PA, Shultz LD, Greiner DL, Hesselton RM, Kittler EL, Tiarks CY, Rao SS, Reilly J, Leif JH, Ramshaw H, Stewart FM, Quesenberry PJ. *Improved engraftment of human cord blood stem cells in NOD/LtSz-scid/scid mice after irradiation or multiple-day injections into unirradiated recipients.* Biol Blood Marrow Transplant. 2(1):15-23. **(1996)**

Mackay F, Browning JL BAFF: a fundamental survival factor for B cells. Nat Rev Immunol 2: 465–475. (2002)

Madlambayan GJ, Rogers I, Kirouac DC, Yamanaka N, Mazurier F, Doedens M, Casper RF, Dick JE, Zandstra PW. *Dynamic changes in cellular and microenvironmental composition can be controlled to elicit in vitro human hematopoietic stem cell expansion*. Exp. Hematol. 33, 1229–1239 **(2005)**

Maier R, Bartolomé-Rodríguez MM, Moulon C, Weltzien HU, Meyerhans A. *Kinetics of CXCR4 and CCR5 up-regulation and human immunodeficiency virus expansion after antigenic stimulation of primary CD4(+) T lymphocytes*. Blood 1;96(5):1853-6 **(2000)**

Malim M.H. and Emerman M. *HIV-1 accessory proteins--ensuring viral survival in a hostile environment*. Cell Host Microbe 3 (6): 388-398 **(2008)**

Malynn BA, Blackwell TK, Fulop GM, Rathbun GA, Furley AJ, Ferrier P, Heinke LB, Phillips RA, Yancopoulos GD, Alt FW. *The scid defect affects the final step of the immunoglobulin VDJ recombinase mechanism*. Cell 54, 453-460 **(1988)**

Mangeat B, Turelli P, Caron G, Friedli M, Perrin L, Trono D. *Broad antiretroviral defence by human APOBEC3G through lethal editing of nascent reverse transcripts*. Nature 3;424(6944):99-103 **(2003)**

Manz MG. *Human-hemato-lymphoid-system mice: opportunities and challenges.* Immunity 26, 537–541 **(2007)**

Mariani R, Rutter G, Harris ME, Hope TJ, Kräusslich HG, Landau NR. *A block to human immunodeficiency virus type 1 assembly in murine cells*. J Virol.;74(8):3859-70 **(2000)**

Marin M, Rose KM, Kozak SL, Kabat D. *HIV-1 Vif protein binds the editing enzyme APOBEC3G and induces its degradation*. Nat Med. 9(11):1398-403 **(2003)**

Marlink R, Kanki P, Thior I. *Reduced rate of disease development after HIV-2 infection as compared to HIV*-1. Science 265(5178):1587-1590 **(1994)**

Martin-Padura I, Agliano A, Marighetti P, Porretti L, Bertolini F. *Sex-related efficiency in NSG mouse engraftment.* Blood. 7;116(14):2616-7 **(2010)**

Matheron S, Pueyo S, Damond F. *Factors associated with clinical progression in HIV-2 infected-patients: the French ANRS cohort.* AIDS 17(18):2593-2601 **(2003)**

Matsumura T, Kametani Y, Ando K, Hirano Y, Katano I, Ito R, Shiina M, Tsukamoto H, Saito Y, Tokuda Y, Kato S, Ito M, Motoyoshi K, Habu S. *Functional CD5+ B cells develop predominantly in the spleen of NOD/SCID/gammac(null) (NOG) mice transplanted either with human umbilical cord blood, bone marrow, or mobilized peripheral blood CD34+ cells.*Exp Hematol. 31(9):789-97 **(2003)**

Mattapallil JJ, Douek DC, Hill B, Nishimura Y, Martin M, Roederer M. *Massive infection and loss of memory CD4+ T cells in multiple tissues during acute SIV infection.* Nature, 434(7037):1093–1097 **(2005)**

McCune JM, *Development and applications of the SCID-hu mouse model*. Sem. Immunol.8(4),187–196 **(1996)**

McCune JM, Namikawa R, Kaneshima H, Shultz LD, Lieberman M, Weissman IL. *The SCID-hu mouse: murine model for the analysis of human hematolymphoid differentiation and function*. Science. 1988 Sep 23;241(4873):1632-9. **(1988)**

McDermott SP, Eppert K, Lechman ER, Doedens M, Dick JE. *Comparison of human cord blood engraftment between immunocompromised mouse strains*. Blood 15;116(2):193-200. **(2010)**

McGrath KE, Palis J. *Hematopoiesis in the yolk sac: more than meets the eye*. Exp Hematol 33: 1021–1028 **(2005)**

McKnight A, Dittmar MT, Moniz-Periera J, Ariyoshi K, Reeves JD, Hibbitts S, Whitby D, Aarons E, Proudfoot AE, Whittle H, Clapham PR. *A broad range of chemokine receptors are used by primary isolates of human immunodeficiency virus type 2 as coreceptors with CD4*. J. Virol. 72:4065-4071 **(1998)**

McMichael AJ. HIV vaccines. Annu Rev Immunol, 24:227–255 **(2006)**

Meeusen NTE, Premier RR, Brandon RM. *Tissue-specific migration of lymphocytes: a key role for TH1 and TH2 cells?* Immunol Today 17:421–4 **(1996)**

Melkus MW, Estes JD, Padgett-Thomas A, Gatlin J, Denton PW, Othieno FA, Wege AK, Haase AT, Garcia JV. *Humanized mice mount specific adaptive and innate immune responses to EBV and TSST-1*. Nature Med. 12, 1316–1322 **(2006)**

Meylan ARP, Burgisser P, Werich-Suter C, Spertini F. *Viral load and immunophenotype of cells obtained from lymph nodes by fine needle aspiration as compared with peripheral blood cells in HIV-infected patients*. J AIDS Hum Retrovir 13:39–47 **(1996)**

Miller RA, Garcia G, Kirk CJ, Witkowski JM. *Early activation defects in T lymphocytes from aged mice*. Immunol Rev 160: 79–90 **(1997)**

Mörner A, Björndal A, Albert J, Kewalramani VN, Littman DR, Inoue R, Thorstensson R, Fenyö EM, Björling E. *Primary human immunodeficiency virus type 2 (HIV-2) isolates, like HIV-1 isolates, frequently use CCR5 but show promiscuity in coreceptor usage*. J. Virol. 73:2343-2349 **(1999)**

Morrow WJ, Wharton M, Lau D, Levy JA. *Small animals are not susceptible to human immunodeficiency virus infection.* J. Gen. Virol. 68, 2253–2257 **(1987)**

Mosier DE, Gulizia RJ, Baird SM, Wilson DB. *Transfer of a functional human immune system to mice with severe combined immunodeficiency*. Nature 15;335(6187):256-9. **(1988)**

Mougel M, Houzet L, Darlix JL. *When is it time for reverse transcription to start and go?* Retrovirology. 2009 Mar 4;6:24 **(2009)**

Moulard M, Decroly E. *Maturation of HIV envelope glycoprotein precursors by cellular endoproteases*. Biochim Biophys Acta, 1469(3):121–132 **(2000)**

Murphy K, Travers P, Walport M. *Janeway's immunobiolo*gy, 7th ed. Garland Science, New York **(2008)**

Nakamura, Y, Russell SM, Mess SA, Friedmann M, Erdos M, Francois C, Jacques Y, Adelstein S, Leonard WJ. *Heterodimerization of the IL-2 receptor beta- and gamma-chain cytoplasmic domains is required for signalling*. Nature 369, 330–333 **(1994)**

Nakauchi H, Sudo K, Ema H. *Quantitative assessment of the stem cell self-renewal capacity* Ann N Y Acad Sci. 938:18-24 **(2001)**

Namikawa R, Kaneshima H, Lieberman M, Weissman IL, McCune JM. *Infection of the SCID-hu mouse by HIV-1*. Science 242(4886):1684–6 **(1988)**

Nathans R, Chu CY, Serquina AK, Lu CC, Cao H, Rana TM. *Cellular microRNA and P bodies modulate host-HIV-1 interactions*. Mol Cell. 26;34(6):696-709 **(2009)**

Neff CP, Kurisu T, Ndolo T, Fox K, Akkina R. *A Topical Microbicide Gel Formulation of CCR5 Antagonist Maraviroc Prevents HIV-1 Vaginal Transmission in Humanized RAG-hu Mice*. PLos One, 6:e20209 **(2011)**

Neil SJ, Eastman SW, Jouvenet N, Bieniasz PD. *HIV-1 Vpu promotes release and prevents endocytosis of nascent retrovirus particles from the plasma membrane*. PLoS Pathog. 2(5):e39 **(2006)**

Nelson BH, Lord JD, Greenberg PD. *Cytoplasmic domains of the interleukin-2 receptor beta and gamma chains mediate the signal for T-cell proliferation*. Nature. 26;369(6478):333-6 **(1994)**

Nicolini FE, Cashman JD, Hogge DE, Humphries RK, Eaves CJ. *NOD/SCID mice engineered to express human IL-3, GM-CSF and Steel factor constitutively mobilize engrafted human progenitors and compromise human stem cell regeneration*. Leukemia 18:341–47 **(2004)**

Nicolini FE, Cashman JD, Hogge DE, Humphries RK, Eaves CJ. *NOD/SCID mice engineered to express human IL-3, GM-CSF and steel factor constitutively mobilize engrafted human progenitors and compromise human stemcell regeneration*. Leukemia, vol. 18, no. 2, pp. 341–347 *(2004)*

Nixon CC, Vatakis DN, Reichelderfer SN, Dixit D, Kim SG, Uittenbogaart CH, Zack JA. *HIV-1 infection of hematopoietic progenitor cells in vivo in humanized mice.* Blood 26;122(13):2195-204 **(2013)**

Notta F, Doulatov S, Dick JE. *Engraftment of human hematopoietic stem cells is more efficient in female NOD/SCID/IL-2Rgc-null recipients*. Blood 115(18):3704–3707 **(2010)**

Notta F, Doulatov S, Laurenti E, Poeppl A, Jurisica I, Dick JE. *Isolation of single human hematopoietic stem cells capable of longterm multilineage engraftment.* Science. 8;333(6039):218-21 **(2011)**

O'Connell RM, Balazs AB, Rao DS, Kivork C, Yang L, Baltimore DRM. *Lentiviral vector delivery of human interleukin- 7 (hiL-7) to human immune system (HIS) mice expands T lymphocyte populations.* PLoS One 6;5(8):e12009 **(2010)**

O'Neil SP, Novembre FJ, Hill AB, Suwyn C, Hart CE, Evans-Strickfaden T, Anderson DC, de Rosayro J, Herndon JG, Saucier M, McClure HM. *Progressive infection in a subset of HIV-1-positive chimpanzees*. J. Infect. Dis. 182, 1051–1062 **(2000)**

Owen SM *Genetically divergent strains of human immunodeficiency virus type 2 use multiple coreceptors for viral entry*. J. Virol. 72:5425-5432 **(1998)**

Pantaleo G, Graziosi C, Demarest JF, Butini L, Montroni M, Fox CH, Orenstein JM, Kotler DP, Fauci AS. *HIV infection is active and progressive in lymphoid tissue during the clinically latent stage of disease.* Nature 25;362(6418):355-8 **(1993)**

Pearson T, Greiner DL, Shultz LD. *Creation of "humanized" mice to study human immunity.* Curr Protoc Immunol. Chapter 15:Unit 15.21 **(2008)**

Pearson T, Shultz LD, Miller D, King M, Laning J, Fodor W, Cuthbert A, Burzenski L, Gott B, Lyons B, Foreman O, Rossini AA, Greiner DL.

Non-obese diabetic–recombination activating gene-1 (NOD–Rag 1 null) interleukin (IL)-2 receptor common gamma chain (IL 2 rγnull) null mice: a radioresistant model for human lymphohaematopoietic engraftment Clin Exp Immunol. 154(2): 270–284 **(2008)**

Pedersen NC, Yamamoto JK, Ishida T, Hansen H. *Feline immunodeficiency virus infection*. Vet. Immunol. Immunopathol. 21, 111-129 **(1989)**

Pedersen, N. C., Ho, E. W., Brown, M. L. & Yamamoto, J. K. *Isolation of a T-lymphotropic virus from domestic cats with an immunodeficiency-like syndrome*. Science 13;235(4790):790-3 **(1987)**

Pek EA, Chan T, Reid S, Ashkar AA. *Characterization and IL-15 dependence of NK cells in humanized mice*. Immunobiology 216:218–24 **(2011)**

Pertel T, Hausmann S, Morger D. *TRIM5 is an innate immune sensor for the retrovirus capsid lattice*. Nature, vol. 472, no. 7343, pp. 361–365 **(2011)**

Pflumio F, Izac B, Katz A, Shultz LD, Vainchenker W, Coulombel L**.** *Phenotype and function of human hematopoietic cells engrafting immune-deficient CB17-severe combined immunodeficiency mice and nonobese diabetic-severe combined immunodeficiency mice after transplantation of human cord blood mononuclear cells*. Blood. 15;88(10):3731-40 **(1996)**

Piacibello W, Sanavio F, Garetto L, Severino A, Danè A, Gammaitoni L, Aglietta M. *The role of c-Mpl ligands in the expansion of cord blood hematopoietic progenitors*. Stem Cells 16 Suppl 2:243-8 **(1998)**

Pilcher CD, Tien HC, Eron JJ Jr, Vernazza PL, Leu SY, Stewart PW, Goh LE, Cohen MS; Quest Study; Duke-UNC-Emory Acute HIV Consortium. Acute HIV Consortium. *Brief but efficient: acute HIV infection and the sexual transmission of HIV*. J Infect Dis. 15;189(10):1785-92 **(2004)**

Plantier JC, Leoz M, Dickerson JE, De Oliveira F, Cordonnier F, Lemée V, Damond F, Robertson DL, Simon F. *A new human immunodeficiency virus derived from gorillas*. Nat. Med. 15 (8): 871-872 **(2009)**

Popovic M, Sarngadharan MG, Read E, Gallo RC. *Detection, isolation, and continuous production of cytopathic retroviruses (HTLV-III) from patients with AIDS and pre-AIDS*. Science, 224(4648):497–500 **(1984)**

Poudrier J, Weng X, Kay DG, Pare G, Calvo EL, Hanna Z. *The AIDS disease of CD4C/HIV transgenic mice shows impaired germinal centers and autoantibodies and develops in the absence of IFN-gamma and IL-6*. Immunity. 15(2):173–85 **(2001)**

Prakash O, Mukherjee PK, Wang TY, Mondal D, Coleman R. *Tissue-specific activation of the HIV-1 long terminal repeat (LTR) by morphine in transgenic mice*. V Intl. Conf. on AIDS 2, 340 **(1990)**

Priceputu E, Rodrigue I, Chrobak P, Poudrier J, Mak TW, Hanna Z. *The Nef-mediated AIDS-like disease of CD4C/human immunodeficiency virus transgenic mice is associated with increased Fas/FasL expression on T cells and T-cell death but is not prevented in Fas- , FasL tumor necrosis factor receptor 1-, or interleukin-1beta-converting enzyme-deficient or Bcl2-expressing transgenic mice*. J Virol. 79(10):6377–91 **(2005)**

Prochazka M, Gaskins HR, Shultz LD, Leiter EH. *The nonobese diabetic scid mouse: model for spontaneous thymomagenesis associated with immunodeficiency*. Proc Natl Acad Sci USA 15;89(8):3290-4 **(1992)**

Rathinam C, Poueymirou WT, Rojas J, Murphy AJ, Valenzuela DM. *Efficient differentiation and function of human macrophages in humanized CSF-1 mice*. Blood 118:3119–28 **(2011)**

Rizza P, Santini SM, Logozzi MA, Lapenta C, Sestili P, Gherardi G, Lande R, Spada M, Parlato S, Belardelli F, Fais S. *T-cell dysfunctions in hu-PBL-SCID mice infected with human immunodeficiency virus (HIV) shortly after reconstitution: in vivo effects of*

HIV on highly activated human immune cells. J. Virol. 70:7958.–7964 **(1996)**

Rochman Y, Spolski R, Leonard WJ. *New insights into the regulation of T cells by gamma(c) family cytokines*. Nat Rev Immunol. 9(7):480-90 **(2009)**

Rochman Y, Spolski R, Leonard WJ**.** *The HIV coreceptor switch: a population dynamical perspective*. Trends Microbiol.13(6):269-77 **(2005)**

Rolink AG, Tschopp J, Schneider P, Melchers F. *BAFF is a survival and maturation factor for mouse B cells*. Eur J Immunol 32: 2004–2010 **(2002)**

Rong L, Zhang J, Lu J, Pan Q, Lorgeoux RP, Aloysius C, Guo F, Liu SL, Wainberg MA, Liang C. *The transmembrane domain of BST-2 determines its sensitivity to down-modulation by human immunodeficiency virus type 1Vpu.* J Virol.83(15):7536-46 **(2009)**

Rongvaux A, Willinger T, Takizawa H, Rathinam C, Auerbach W. *Human thrombopoietin knockin mice efficiently support human hematopoiesis in vivo*. Proc. Natl. Acad. Sci. USA 108:2378–83 **(2011)**

Rosenberg JY, Anderson OA, Pabst R. *HIV-induced decline in blood CD4/CD8 ratios: viral killing or altered lymphocyte trafficking?* Immunol Today; 19:10–17 **(1998)**

Rudd CE, Janssen O, Cai YC, da Silva AJ, Prasad KV. *Two-step TCRzeta/CD3–CD4 and CD28 signaling in T cells: SH2/SH3 domains, protein-tyrosine and lipid kinases.* Immunol Today 15: 225–234 **(1994)**

Sasaki Y, Casola S, Kutok JL, Rajewsky K, Schmidt-Supprian M. *TNF family member B cell-activating factor (BAFF) receptor-dependent and -independent roles for BAFF in B cell physiology*. J Immunol 173: 2245–2252 **(2004)**

Sasaki Y, Derudder E, Hobeika E, Pelanda R, Reth M. *Canonical NF-kappaB activity, dispensable for B cell development, replaces BAFF-receptor signals and promotes B cell proliferation upon activation*. Immunity 24: 729–739 **(2006)**

Sasaki Y, Matsuoka Y, Hase M, *Marginal expression of CXCR4 on c-kit(1)Sca-1 (1) Lineage (-) hematopoietic stem/progenitor cells*. Int J Hematol. 90(5):553-560 **(2009)**

Sauvageau G, Iscove NN, Humphries RK. *In vitro and in vivo expansion of hematopoietic stem cells.* Oncogene 23: 7223–32 **(2004)**

Scarlatti G, Tresoldi E, Bjorndal A, Fredriksson R, Colognesi C, Deng HK, Malnati MS, Plebani A, Siccardi AG, Littman DR, Fenyo EM, Lusso P. *In vivo evolution of HIV-1 coreceptor usage and sensitivity to chemokine-mediated suppression.* Nature Med. 3:1259–65 **(1997)**

Schacker T, Collier AC, Hughes J, Shea T, Corey L. *Clinical and epidemiologic features of primary HIV infection*. Ann Intern Med 125:257-264 **(1996)**

Schiemann B, Gommerman JL, Vora K, Cachero TG, Shulga-Morskaya S, Dobles M, Frew E, Scott ML. *An essential role for BAFF in the normal development of B cells through a BCMA-independent pathway.* Science. 14;293(5537):2111-4 (2001)

Schmidt MR, Appel MC, Giassi LJ, Greiner DL, Shultz LD, Woodland RT. *Human BLyS Facilitates Engraftment of Human PBL Derived B Cells in Immunodeficient Mice*; PLoS ONE. 3(9): e3192 **(2008)**

Scholbach J, Schulz A, Westphal F, Egger D, Wege AK, Patties I, Köberle M, Sack U, Lange F. *Comparison of hematopoietic stem cells derived from fresh and cryopreserved whole cord blood in the generation of humanized mice*.PLoS One 7(10):e46772 **(2012)**

Schuler W, Weiler IJ, Schuler A, Philips RA, Rosenberg N, Mak TW, Kearney I.F, Perry RP, Bosma MJ. *Rearrangement of antigen receptor genes is defective in mice with severe combined immune deficiency*. Cell 46, 963-972 **(1986)**

Sharp PM, Hahn BH. *The evolution of HIV-1 and the origin of AIDS*. Philos. Trans. R. Soc.

Lond. B. Biol. Sci. 365 (1552): 2487-2494 **(2010)**

Shih CC., Kaneshima H, Rabin L, Namikawa R, Sager P, McGowan J, McCune JM. *Postexposure prophylaxis with zidovudine suppresses human immunodeficiency virus type 1 infection in SCID-hu mice in a time-dependent manner*. J. Inf. Dis. 163, 625-627 **(1991)**

Shimojima M, Miyazawa T, Ikeda Y, McMonagle EL, Haining H, Akashi H, Takeuchi Y, Hosie MJ, Willett BJ. *Use of CD134 as a primary receptor by the feline immunodeficiency virus.* Science. 20;303(5661):1192-5 **(2004)**

Shultz LD, Lang PA, Christianson SW, Gott B, Lyons B, Umeda S, Leiter E, Hesselton R, Wagar EJ, Leif JH, Kollet O, Lapidot T, Greiner DL. *NOD/LtSz-Rag1null mice: an immunodeficient and radioresistant model for engraftment of human hematolymphoid cells, HIV infection, and adoptive transfer of NOD mouse diabetogenic T cells.* J. Immunol. 164, 2496–2507 **(2000)**

Shultz LD, Lyons BL, Burzenski LM, Gott B, Chen X. *Human lymphoid and myeloid cell development in NOD/LtSz-scid IL2Rγnull mice engrafted with mobilized human hemopoietic stem cells*. J. Immunol. 174:6477–89 **(2005)**

Shultz LD, Saito Y, Najima Y, Tanaka S, Ochi T. *Generation of functional human T-cell subsets with HLA-restricted immune responses in HLA class I expressing NOD/SCID/IL2rcnull humanized mice*. Proc Natl Acad Sci USA 107: 13022–13027 **(2010)**

Shultz LD, Schweitzer PA, Christianson SW, Gott B, Schweitzer IB, Tennent B, McKenna S, Mobraaten L, Rajan TV, Greiner DL. *Multiple defects in innate and adaptive immunologic function in NOD/LtSz scid mice*. J. Immunol. 154, 180–191 **(1995)**

Siegel JP, Sharon M, Smith PL, Leonard WJ. *The IL-2 receptor beta chain (p70): role in mediating signals for LAK, NK, and proliferative activities.* Science. 1987 Oct 2;238(4823):75-8 **(1987)**

Simon V, Ho DD, Abdool Karim Q. *HIV/AIDS epidemiology, pathogenesis, prevention, and treatment.* Lancet, 368(9534):489–504 **(2006)**

Skowronski J. *Expression of a human immunodeficiency virus type 1 long terminal repeat/Simian Virus 40 early region fusion gene in transgenic mice*. J Virol. 65(2):754-62. **(1991)**

Sloan RD, Kuhl BD, Mesplède T, Münch J, Donahue DA, Wainberg MA. *Productive entry of HIV-1 during Cell-to-Cell Transmission via Dynamin-Dependent Endocytosis*. J Virol. 87(14):8110-23 **(2013)**

Sol N, Ferchal F, Braun J, Pleskoff O, Tréboute C, Ansart I, Alizon M. *Usage of the coreceptors CCR-5, CCR-3, and CXCR-4 by primary and cell line-adapted human immunodeficiency virus type 2*. J. Virol. 71:8237-8244 **(1997)**

Spangrude GJ, Smith L, Uchida N, Ikuta K, Heimfeld S, Friedman J, Weissman IL. *Mouse hematopoietic stem cells*. Blood, 78, 1395–1402 **(1991)**

Spira AI, Marx PA, Patterson BK, Mahoney J, Koup RA, Wolinsky SM, Ho DD. *Cellular targets of infection and route of viral dissemination after an intravaginal inoculation of simian immunodeficiency virus into rhesus macaques*. J. Exp. Med183:215-225 **(1996)**

Storms RW, Green PD, Safford KM, et al. *Distinct hematopoietic progenitor compartments are delineated by the expression of aldehyde dehydrogenase and CD34*. Blood.106(1):95–102 **(2005)**

Storms RW, Trujillo AP, Springer JB. *Isolation of primitive human hematopoietic progenitors on the basis of aldehyde dehydrogenase activity*. Proc Natl Acad Sci USA. 96(16):9118–9123 **(1999)**

Stremlau M, Owens CM, Perron MJ, Kiessling M, Autissier P, Sodroski J. *The cytoplasmic body component TRIM5α restricts HIV-1 infection in Old World monkeys*. Nature 427(6977):848-53 **(2004)**

Strowig T, Gurer C, Ploss A, Liu YF, Arrey F. *Priming of protective T cell responses against virus-induced tumors in mice with human immune system components*. J Exp Med 206: 1423–1434 **(2009)**

Strowig T, Rongvaux A, Rathinam C, Takizawa H, Borsotti C. *Transgenic expression of human signal regulatory protein αin Rag2$^{-/-}$γc$^{-/-}$ mice improves engraftment of human hematopoietic cells in humanized mice*. Proc. Natl. Acad. Sci. USA 108:13218–23 **(2011)**

Stuart H. Orkin *Diversification of haematopoietic stem cells to specific lineages*, Nature Reviews Genetics 1, 57-64 **(2000)**

Sun G, Li H, Wu X, Covarrubias M, Scherer L, Meinking K, Luk B, Chomchan P, Alluin J, Gombart AF, Rossi JJ. *Interplay between HIV-1 infection and host microRNAs.* Nucleic Acids Res 40(5):2181–2196 **(2012)**

Sun JC, Lanier LL. *NK cell development, homeostasis and function: parallels with CD8+ T cells.* Nat Rev Immunol. 26;11(10):645-57 **(2011)**

Sun Z, Denton PW, Estes JD, Othieno FA, Wei BL, Wege AK, Melkus MW, Padgett-Thomas A, Zupancic M, Haase AT, Garcia JV. *Intrarectal transmission, systemic infection, and CD4+ T cell depletion in humanized mice infected with HIV-1*. J. Exp. Med. 204, 705–714 **(2007)**

Suzuki M, Takahashi T, Katano I, Ito R, Ito M, Harigae H, Ishii N, Sugamura K. *Induction of human humoral immune responses in a novel HLA-DR-expressing transgenic NOD/Shi-scid/γcnull mouse*. Int. Immunol. 24, 243–252 **(2012)**

Tachibana K, Nakajima T, Sato A, Igarashi K, Shida H, Iizasa H, Yoshida N, Yoshie O, Kishimoto T, Nagasawa T**.** *CXCR4/fusin is not a species-specific barrier in murine cells for HIV-1 entry*. J. Exp. Med. 185:1865-1870 **(1997)**

Takagi S, Saito Y, Hijikata A, Tanaka S, Watanabe T. *Membrane-bound human SCF/KL promotes in vivo human hematopoietic engraftment and myeloid differentiation*. Blood 119:2768–77 **(2012)**

Takizawa H, Schanz U, Manz MG. *Ex vivo expansion of hematopoietic stem cells: mission accomplished?* Swiss MedicalWeekly, vol. 141, w13316 **(2011)**

Tanaka S, Saito Y, Kunisawa J, Kurashima Y, Wake T, Suzuki N, Shultz LD, Kiyono H, Ishikawa F. *Development of mature and functional human myeloid subsets in hematopoietic stem cell-engrafted NOD/SCID/IL2rγKO mice.* J Immunol. 15;188(12):6145-55 **(2012)**

Tervo HM, Goffinet C, Keppler OT. *Mouse T-cells restrict replication of human immunodeficiency virus at the level of integration.* Retrovirology. 8;5:58 **(2008)**

Tervo HM, Keppler OT. *High natural permissivity of primary rabbit cells for HIV-1, with a virion infectivity defect in macrophages as the final replication barrier*. J. Virol. 84, 12300–12314 **(2010)**

Tonomura N, Habiro K, Shimizu A, Sykes M, Yang YG. *Antigen-specific human T-cell responses and T cell-dependent production of human antibodies in a humanized mouse model.*Blood. 111(8):4293-6 **(2008)**

Torten M, Franchini M, Barlough JE, George JW, Mozes E, Lutz H, Pedersen NC. *Progressive immune dysfunction in cats experimentally infected with feline immunodeficiency virus.* J Virol. 65(5):2225-30 **(1991)**

Triboulet R, Mari B, Lin YL, Chable-Bessia C, Bennasser Y, Lebrigand K, Cardinaud B, Maurin T, Barbry P, Baillat V, Reynes J, Corbeau P, Jeang KT, Benkirane M. *Suppression of MicroRNA-silencing pathway by HIV-1 during virus replication.* Science 16;315(5818):1579-82. **(2007)**

Tsurutani N, Yasuda J, Yamamoto N, Choi BI, Kadoki M, Iwakura Y. *Nuclear Import of the Pre-integration Complex Is Blocked upon Infection by HIV-1 in Mouse Cells.* J Virol, 81(2):677-88 **(2007)**

Van der Kuyl AC, Cornelissen M. *Identifying HIV-1 dual infections.* Retrovirology. 24;4:67 **(2007)**

Van Heuverswyn F, Li Y, Neel C, Bailes E, Keele BF, Liu W, Loul S, Butel C, Liegeois F, Bienvenue Y, Ngolle EM, Sharp PM, Shaw GM, Delaporte E, Hahn BH, Peeters M. *Human immunodeficiency viruses: SIV infection in wild gorillas.* Nature 444 (7116): 164 **(2006)**

Van Heuverswyn F, Peeters M. *The origins of HIV and implications for the global epidemic*. Curr. Infect. Dis. Rep. 9 (4): 338-346 **(2007)**

Van Lent AU, Dontje W, Nagasawa M, Siamari R, Bakker AQ. *IL-7 enhances thymic human T cell development in "human immune system" Rag2$^{-/-}$IL-2Rγc$^{-/-}$ mice without affecting peripheral T cell homeostasis.* J Immunol. 15;183(12):7645-55 **(2009)**

Van Rijn RS, Simonetti ER, Hagenbeek A. *A new xenograft, model for graft-versus-host disease by intravenous transfer of human peripheral blood mononuclear cells in RAG2$^{-/-}$ gammac$^{-/-}$ double-mutant mice.* Blood 102:2522–31 **(2003)**

van't Wout AB, Kootstra NA, Mulder-Kampinga GA, Albrecht-van Lent N, Scherpbier HJ, Veenstra J, Boer K, Coutinho RA, Miedema F, Schuitemaker H. *Macrophage-tropic variants initiate human-immunodeficiency-virus type-1 infection after sexual, parenteral, and vertical transmission*. J Clin Invest. 94(5):2060-7 **(1994)**

Varnum-Finney B, Brashem-Stein C, Bernstein ID. *Combined effects of Notch signaling and cytokines induce a multiple log increase in precursors with lymphoid and myeloid reconstituting ability*. Blood 1;101(5):1784-9. **(2003)**

Vogel J, Hinrichs SH, Reynolds RK, Luciw PA, Jay G. *The HIV-1 tat gene induces dermal lesions resembling Kaposi's sarcoma.* Nature 13;335(6191):606-11 **(1988)**

Vormoor J, Lapidot T, Pflumio F. *Immature human cord blood progenitors engraft and proliferate to high levels in severe combined immunodeficient mice*. Blood;83:2489-2497 **(1994)**

Wahl A, Swanson MD, Nochi T, Olesen R, Denton PW, Chateau M, Garcia JV. *Human breast milk and antiretrovirals dramatically reduce oral HIV-1 transmission in BLT humanized mice*. PLoS Pathog. 8(6):e1002732 **(2012)**

Wang HM, Smith KA *The interleukin 2 receptor. Functional consequences of its bimolecular structure*. J Exp Med. 1;166(4):1055-69 **(1987)**

Wang X, Ye L, Hou W, Zhou Y, Wang YJ, Metzger DS, Ho WZ. *Cellular microRNA expression correlates with susceptibility of monocytes/ macrophages to HIV-1 infection*. Blood 113(3):671–674 **(2009)**

Watanabe S, Terashima K, Ohta S, Horibata S, Yajima M, Shiozawa Y, Dewan MZ, Yu Z, Ito M, Morio T, Shimizu N, Honda M, Yamamoto N. *Hematopoietic stem cell-engrafted NOD/SCID/IL2Rgamma null mice develop human lymphoid systems and induce long-lasting HIV-1 infection with specific humoral immune responses*. Blood. 1;109(1):212-8 **(2007)**

Watanabe Y, Takahashi T, Okajima A, Shiokawa M, Ishii N. *The analysis of the functions of human B and T cells in humanized NOD/shi-scid/ gcnull (NOG) mice (hu-HSC NOG mice*) Int Immunol 21: 843–858 **(2009)**

Wege AK, Melkus MW, Denton PW, Estes JD, Garcia JV. *Functional and phenotypic characterization of the humanized BLT mouse model.* Curr. Top. Microbiol. Immunol. 324, 149–165 **(2008)**

Weng X, Priceputu E, Chrobak P, Poudrier J, Kay DG, Hanna Z. *CD4+ T cells from CD4C/HIVNef transgenic mice show enhanced activation in vivo with impaired proliferation in vitro but are dispensable for the development of a severe AIDS-like organ disease.* J Virol. 78(10):5244–57 **(2004)**

Westermann J, Geismar U, Sponholz A. *CD4 T cells of both the nai¨ve and the memory phenotype enter rat lymph nodes and Peyer's*

patches via high endothelial venules: within the tissue their migratory behaviour differs. Eur J Immunol 27:3174–81 **(1997)**

Wheelock EF. *Interferon-like virus inhibitor induced in human leukocytes by phytohemagglutinin*. Science 149:310–11 **(1965)**

Willinger T, Rongvaux A, Takizawa H, Yancopoulos GD, Valenzuela DM. *Human IL-3/GM-CSF knock-in mice support human alveolar macrophage development and human immune responses in the lung*. Proc. Natl. Acad. Sci. USA 108:2390–95 **(2011)**

Wyatt R, Sodroski J. *The HIV-1 envelope glycoproteins: fusogens, antigens, and immunogens*. Science, 280(5371):1884–1888 **(1998)**

Yagi M, Ritchie KA, Sitnicka E, Storey C, Roth GJ, Bartelmez S. *Sustained ex vivo expansion of hematopoietic stemcells mediated by thrombopoietin.* Proc Natl Acad Sci USA. 6;96(14):8126-31 **(1999)**

Yamamoto JK, Barré-Sinoussi F, Bolton V, Pedersen NC, Gardner MB. *Human alpha- and beta-interferon but not gamma–suppress the in vitro replication of LAV, HTLV-III, and ARV-2*. J Interferon Res. 6(2):143-52 **(1986)**

Yonemura Y, Ku H, Lyman SD, Ogawa M. *In vitro expansion of hematopoietic progenitors and maintenance of stem cells: comparison between FLT3/FLK-2 ligand and KIT ligand.* Blood. 15;89(6):1915-21 **(1997)**

Yu X, Yu Y, Liu B, Luo K, Kong W, Mao P, Yu XF. *Induction of APOBEC3G ubiquitination and degradation by an HIV-1 Vif-Cul5-SCF complex*. Science 7;302(5647):1056-60 **(2003)**

Zhang JX, Diehl GE, Littman DR. *Relief of preintegration inhibition and characterization of additional blocks for HIV replication in primary mouse T cells.* PLoS ONE 3(4):e2035 **(2008)**

Zhang Z, Schuler T, Zupancic M, Wietgrefe S, Staskus KA, Reimann KA, Reinhart TA, Rogan M, Cavert W, Miller CJ, Veazey RS, Notermans D, Little S, Danner SA, Richman DD, Havlir D, Wong J, Jordan HL, Schacker TW, Racz P, Tenner-Racz K, Letvin NL, Wolinsky S, Haase AT. *Sexual transmission and propagation of SIV and HIV in resting and activated CD4+ T cells*. Science. 286:1353-1357 **(1999)**

VII. Appendix

a. Plasmid Maps

Expression vector pET15b

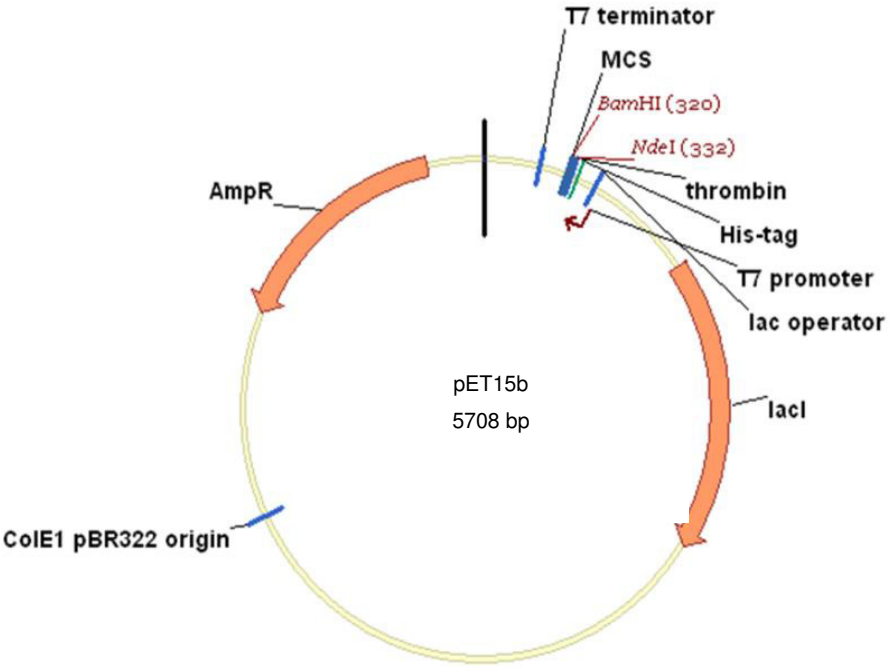

Expression vector pET15b-huBLyS

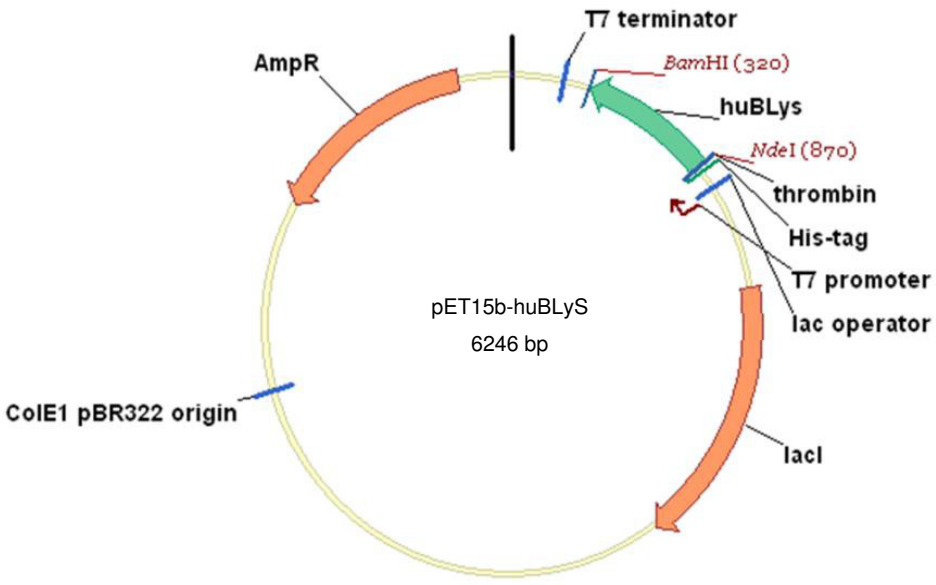

b. Codon-optimized sequence for expression of huBLyS in *E.coli*

5’catatgggcatggccagcatgacaggcggccagcagatgggcagagatctgtacgacgacgatgacaaggac
agatggggcagccacatggccgtgcagggcccagaggaaaccgtgacccaggattgcctgcagctgatcgccga
cagcgagacacccaccatccagaagggcagctacaccttcgtgccctggctgctgagcttcaagagaggcagcgc
cctggaagagaaagaaaacaagatcctcgtgaaagagacaggctacttcttcatctacggccaggtgctgtacacc
gacaagacctacgccatgggccacctgatccagcggaagaaagtgcacgtgttcggcgacgagctgagcctcgtg
accctgttccggtgcatccagaacatgcccgagacactgcccaacaacagctgctacagcgccggaatcgccaag
ctggaagaggggacgaactgcagctggccatccctagagagaacgcccagatcagcctggacggcgacgtgac
ctttttcggcgccctgaagctgctctgaggatcc’3

c. List of abbreviation

Abbreviation	Meaning
°C	Degree Celsius
µg	Microgram
µl	Microliter
aGvHD	Acute graft versus host disease
AIDS	Acquired immunodeficiency syndrome
ALT	Alanine transferase
BLT	Bone marrow-liver-thymus mouse
bp	Base pairs
BRG mouse	Balb/c Rag1$^{-/-}$ $\gamma c^{-/-}$
CCR5	Chemokine CC-receptor 5
cGvHD	Chronic graft versus host disease
Cps/ng	Copies per nanogram
CXCR4	Chemokine CXC-receptor 4
d	Day(s)
DNA	Deoxyribonucleic acid
E.coli	Escherichia coli
ELISA	Enzyme Linked Immunosorbent Assay
FACS	Fluorescence-activated cell sorting
FCS	Fetal calf serum
Fig.	Figure

FSC	Forward scatter
G-CSF	Granulocyte colony-stimulating factor
gp	Glycoprotein
HE	Haematoxylin/eosin
HIV	Human immunodeficiency virus
HLA	Human Leukocyte Antigen
HSC	hematopoietic stem cells
hu	human
huBLyS	Human B-lymphocyte stimulator
i.h.	intrahepatic
i.p.	Intraperitoneal
i.v.	intravenous
IFN	Interferon
Ig	Immunoglobulin
IL	Interleukin
IU/ml	International Unit per milliliter
mg	Milligram
MHC	Major histocompatibility complex
min	Minutes
ml	Milliliter
NRG	NOD Rag1$^{-/-}$ γc$^{-/-}$
ns	Not significant
NSG	NOD scid$^{-/-}$ γc$^{-/-}$
p.r.	Post reconstitution
PBL	Peripheral blood
PBMC	Peripheral blood mononuclear cells
PCR	Polymerase chain reaction
PFA	Paraformaldehyde
PMA	Phorbol myristoyl acetate
qPCR	Quantitative polymerase chain reaction
RT	Room temperature
scid	Severe combined immunodeficiency
SIV	Simian immunodeficient virus
SSC	Sideward scatter

Tab.	Table
$TCID_{50}$	Tissue culture infectious dose 50
TCR	T-cell receptor
TD	T-cell dependent
U/l	Units per liter
w	Week(s)
w/o	Without

d. List of figures

e. List of tables